

University of Nottingham
UK | CHINA | MALAYSIA

In-depth pharmacological investigation of *Lignosus rhinocerotis* which is a local traditional medicinal mushroom

LEE MEI KEE

Thesis submitted to the University of Nottingham for the degree of Doctor of Philosophy

February 2019

Abstract

Lignosus rhinocerotis has been used by the indigenous community within Southeast Asia for centuries to treat a range of health conditions including asthma and chronic cough. Despite this, there is no scientific evidence of the effect of this mushroom on airway patency. Hence, this study was initiated to provide scientific validation of the traditional usage of *L. rhinocerotis* for relieving these airway conditions. The principal aim of this study was to investigate the pharmacological effects and mechanisms of action of *L. rhinocerotis* extract on smooth muscle of different tissues, mainly in airways. The secondary objective was to examine its effect on mast cell degranulation. By using organ bath technique with isolated animal tissues, the effects of hot water extract (HWE), cold water extract (CWE) and methanol extract (ME) on smooth muscle contractility were assessed. CWE exhibited significant relaxation effect on pre-contracted rat airway segments, whilst HWE and ME were devoid of effect. Thus, CWE was chosen for the subsequent investigations.

CWE effectively relaxed carbachol (acetylcholine receptor agonist)- and potassium chloride (KCl; membrane depolarizing agent)-induced pre-contractions in rat and porcine airway segments. Pre-incubation with CWE also attenuated the contractile responses to carbachol, 5-hydroxytryptamine (5-HT; serotonin receptor agonist), and calcium chloride in rat airway segments. Similar relaxant responses were observed in phenylephrine (α_1-adrenoceptor agonist)-pre-contracted rat aorta and U46619 (a thromboxane A_2 receptor agonist)-pre-contracted porcine coronary artery. In the case of determining the mechanisms of action, findings from both airway and vascular smooth muscles strongly suggest that 3′-5′-Cyclic adenosine monophosphate (cAMP) and 3′-5′-Cyclic guanosine monophosphate (cGMP) (via nitric oxide)

pathways, β-adrenoceptors, and K^+ channels are unlikely to be involved. Contractions elicited by the above-mentioned contractile agonists were shown to be mediated via extracellular calcium influx through membrane calcium channels. We therefore deduced that CWE may inhibit extracellular calcium influx through calcium channels. This proposition is supported by the results in calcium imaging assay where CWE significantly inhibited KCl-induced elevation of cytosolic calcium concentration in dorsal root ganglion cells. In contrast, CWE evoked contraction in airway tissues at basal tone but not in vascular tissues, and the contractile response was inhibited by muscarinic receptor antagonist. In electrically stimulated guinea pig ileum, CWE markedly reduced the neurogenic contraction but augmented the basal tone, possibly through modulation of calcium channels and muscarinic receptors, respectively. In an attempt to elucidate the bioactive components responsible for its bronchodilator effect, fractionation of CWE using Sephadex gel permeation chromatography was performed. The high-molecular-weight (HMW) fraction demonstrated significantly higher bronchodilator effects against carbachol-, 5-HT- and calcium-induced contractions compared to CWE and low-molecular-weight fraction. Given that HMW fraction contained highest amount of polysaccharide and proteins, the bioactive components are likely to be polysaccharide-protein complex or proteins.

As for rat basophil leukaemia (RBL-2H3) cells, immunoglobulin E(IgE)/antigen-stimulated degranulation was characterized by increased β-hexosaminidase release and phosphatidylserine externalization, and reduced Alcian blue-stained secretory granules. In unstimulated cells, CWE treatment alone had significantly increased β-hexosaminidase release and phosphatidylserine externalization, but did not affect the amount of stained secretory granules. Conversely, in IgE/antigen-stimulated cells CWE did not significantly affect β-hexosaminidase

release and phosphatidylserine externalization, but had inhibited the reduction of stained secretory granules. In light of this, CWE may be triggering certain degranulation processes i.e. β-hexosaminidase release and phosphatidylserine externalization in unstimulated cells while preventing loss of secretory granules in IgE/antigen-stimulated cells.

To summarize, CWE displayed non-species-specific relaxation effects in many types of smooth muscle tissues. Overall findings strongly suggest that one mechanism by which CWE improves airway patency is via inhibition of extracellular calcium entry through membrane calcium channels.

Publications

1. **Lee, M.-K.**, Lim, K.-H., Millns, P., Mohankumar, S. K., Ng, S.-T., Tan, C.-S., … Ting, K.-N. (2018). Bronchodilator effects of Lignosus rhinocerotis extract on rat isolated airways is linked to the blockage of calcium entry. *Phytomedicine, 42*, 172–179. https://doi.org/https://doi.org/10.1016/j.phymed.2018.03.025

2. **Lee, M.-K.**, Millns, P., Mbaki, Y., Ng, S.-T., Tan, C.-S., Lim, K.-H., … Ting, K.-N. (2018). Data on the Lignosus rhinocerotis water soluble sclerotial extract affecting intracellular calcium level in rat dorsal root ganglion cells. *Data in Brief*, *18*, 1322–1326. https://doi.org/10.1016/j.dib.2018.04.033

3. **Lee, M. K.**, Li, X., Yap, C. S. A., Peter, C. K. C., Tan, C. S., Ng, S. T., … Fung, S. Y. (2018). Airway relaxation effects of water-soluble sclerotial extract from Lignosus rhinocerotis. *Frontiers in Pharmacology*, *9*, 461. https://doi.org/10.3389/fphar.2018.00461

4. Govindaraju, K., **Lee, M. K.**, Mbaki, Y., & Nee, T. K. (2018). Intracellular stored calcium plays a minor role in Gq-coupled receptor-mediated contraction in rat airway smooth muscle. *Life Sciences, Medicine and Biomedicine*, *2*(2), 1–6. https://doi.org/10.3389/fphar.2018.00461

5. **Lee, M. K.**, Tan, C.-S., Ng, S.-T., Lim, K.-H, Ting, K.-N. (2016) *Lignosus rhinocerotis* on Airway Muscle Relaxation. in 'Science and cultivation of edible and medicinal fungi: Mushroom Science IXX', ed. by A.S.M. Sonnenberg & J.J.P. Baars. Proceedings of the 19th Congress of the International Society for Mushroom Science, Amsterdam, the Netherlands, 30 May–2 June 2016. International Society for Mushroom Science. Amsterdam. Volume 19 Part 1 Article 118

Acknowledgements

Firstly, I would like to express my deepest and sincere appreciation to my supervisor a.k.a my boss and role model, Prof. Ting Kang Nee for her wisdom, understanding, patience, motivation, and encouragement, and for being one of the most inspiring people for me. Her constant support and guidance helped me in all time of research and writing this thesis. Thank you for pushing me further than I thought I could go and for giving me many precious opportunities.

Immeasurable appreciation and heartfelt gratitude are also extended to the following persons for contributing to make this study possible:

To my co-supervisor, Prof. Suresh Kumar MohanKumar for his excellent advices and stimulating discussions especially for cell culture work and throughout my PhD study. The helpful feedbacks for this thesis and our publications are also very much appreciated. To Dr. Lim Kuan Hon for his valuable advices and supply of materials for the mushroom extraction and contribution to our publication, to Mr. Premanand Krishnan for helping to run the spectroscopic analysis, and to Dr. Then Sue Mian for the helpful advices on western blot experiments. To Mr. Paul Millns from University of Nottingham UK for providing tremendous technical support and guidance in the analysis of calcium imaging assay.

I am also extremely grateful to my fellow lab colleagues: to Bi Juin for her excellent guidance and company through the hard days in C1B07, to Ms. Asma and Kak Siti for their assistance around in lab, to Kayatri and Fong Kai for the rapports, and to May Zie and Yew Fung for their kind aid in sharing the consumables and also the enjoyable conversations.

I would also like to express my heartfelt gratitude to the University of Nottingham Malaysia for funding my PhD study and the Ministry of Higher Education Malaysia for funding this project.

Most of all, I am fully indebted to my family, especially my mother, for her unconditional support in all means, and to my friends, Ching Yee, Po Yi, Chew Woon, and Jia Xin for the company in down times throughout this PhD journey. I also thank my childhood friend, Kar Lai Pang for supporting me spiritually throughout writing this thesis and my life in general.

Declaration

Ligno Biotech Sdn. Bhd supplied the *Lignosus rhinocerotis* (TM02) sclerotial powder and performed the composition analysis in Section 2.3.3 (**Chapter 2**). Experimental works in Section 3.2.3.6 (**Chapter 3**) and Section 4.2.2.6 (**Chapter 4**), with exception of concentration-response curves to carbachol in the presence of calcium channel blockers and in the absence of external Ca^{2+} (Fig. 4.6C and D), were carried out by Ms. Le Viet Hang in the University of Nottingham UK. Section 4.2.3.1 and 4.2.3.2 (**Chapter 4**) were performed by Mr. Paul Millns from the School of Life Sciences, University of Nottingham UK. All experimental works on porcine coronary arteries (**Chapter 5**) were performed by Mr. Jonathan Mann-Seng Chooi in the University of Nottingham UK. Experimental works in Section 6.2.3 (**Chapter 6**) and **Appendix E** were performed by Dr. Fung Shin Yee and her student, Mr. Alvin Chee Sum Yap, from Department of Molecular Medicine, University of Malaya, whereas Section 6.2.4 and 6.2.5 were performed by Prof. Peter Cheung Chi Keung and his student, Ms. Xiaojie Li, from School of Life Sciences, Chinese University of Hong Kong. Section 6.3.1 and 6.3.2 were analyzed, interpreted and discussed by Dr. Fung Shin Yee and Prof. Peter Cheung Chi Keung, respectively. Results from Section 6.3.1 and 6.3.2 will be included and discussed in this thesis. The *L. rhinocerotis* fractions used in organ bath experiments in Section 6.2.6 to 6.2.8 (**Chapter 6**) were supplied by Dr. Fung Shin Yee. Isolation of guinea pig ileum was performed by Prof. Ting Kang Nee and Dr. Then Sue Mian from the University of Nottingham Malaysia. I declare that all other experimental studies throughout this thesis were carried out by myself.

Abbreviations

2-APB	2-aminoethoxydiphenyl borate
5-HT	5-hydroxytryptamine
AC	Adenylyl cyclase
AM	Acetoxymethyl
ANOVA	Analysis of variance
Anti-DNP IgE	Anti-dinitrophenyl immunoglobulin E
ATP	Adenosine triphosphate
BALF	Bronchoalveolar lavage fluid
BK_{Ca}	Large-conductance Ca^{2+}-activated potassium channel
BSA	Bovine serum albumin
Ca^{2+}	Calcium ion
$[Ca^{2+}]_i$	Cytosolic Ca^{2+} concentration
$CaCl_2$	Calcium chloride
cAMP	3′-5′-Cyclic adenosine monophosphate
cGMP	3′-5′-Cyclic guanosine monophosphate
COPD	Chronic obstructive pulmonary disease
CRAC channels	Calcium release activated calcium channels
CRCs	Concentration-response curves
CWE	Cold water extract
DAG	Diacylglycerol
DNP-HSA	Dinitrophenyl-human serum albumin
DMSO	Dimethyl sulfoxide
DRG	Dorsal root ganglion
EAR	Early asthmatic response
EC_{50}	Half maximal effective concentration
EDRFs	Endothelium-dependent relaxing factors
EDHFs	Endothelium-dependent hyperpolarizing factors
EDTA	Ethylenediaminetetraacetic acid

EFS	Electrical field stimulation
EGTA	Ethylene glycol tetraacetic acid
ELISA	Enzyme-linked immunosorbent assay
E_{max}	Maximum tissue response
EMEM	Eagle's minimum essential medium
FBS	Fetal bovine serum
FcεRI	High-affinity IgE receptors
FITC	Fluorescein isothiocyanate
FRET	Fluoroscence resonance energy transfer
GC	Guanylyl cyclase
GC-MS	Gas chromatography-mass spectroscopy
GECIs	Genetically encoded chemical indicators
GPCR	G protein-coupled receptor
GTP	Guanosine triphosphate
HTS	High throughput screening
HWE	Hot water extract
HMW	High-molecular-weight
Hyp9	1,1'-(2,4,6-Trihydroxy-1,3-phenylene)bis-1-hexanone, 2,4-(bis-1-ketohexyl)phloroglucinol
IBMX	3-isobutyl-1-methylxanthine
IC50	Half maximal inhibitory concentration
ICC	Interstitial cells of Cajal
I_{CRAC}	Ca^{2+}-selective SOCC currents
Ig	Immunoglobulin
IK_{Ca} channel	Intermediate-conductance Ca^{2+}-activated potassium channel
IL	Interleukin
IP_3	Inositol triphosphate
ITS	Internal transcribed spacer
K^+	Potassium ion
K_{ATP} channel	ATP-dependent potassium channel
K_{dr} channel	Ca^{2+}-independent delayed rectifier potassium channel
KCl	Potassium chloride

LAR	Late asthmatic response
L-NAME	N(G)-nitro-L-arginine methyl ester
LMW	Low-molecular-weight
LT	Leukotriene
M	Molar
ME	Methanol extract
MLC	Myosin light chain
MLCK	Myosin light chain kinase
MLCP	Myosin light chain phosphatase
MMW	Medium-molecular-weight
mN	milliNewton
MTT	3-(4,5-Dimethylthiazol-2-yl)-2,5- diphenyltetrazolium bromide
NANC	Non-noradrenergic non-cholinergic
NCX	Na^+/Ca^{2+} exchanger
NO	Nitric oxide
NK	Natural killer
OAG	1-oleoyl-2-acetyl-sn-glycerol
pEC_{50}	Negative logarithm of EC_{50}
PBS	Phosphate-buffered saline
PDE	Phosphodiesterase
PG	Prostaglandin
PGI_2	Prostacyclin
PI	Propidium iodide
PIP_2	Phosphatidylinositol 4,5-bisphosphate
PIPES	Piperazine-N,N'-bis(2-ethanesulfonic acid)
PKA	Protein kinase A
PKC	Protein kinase C
PKG	Protein kinase G
PLC	Phospholipase C
PNAG	4-Nitrophenyl N-acetyl-β-D-gluconide
Pyr3	Ethyl-1-(4-(2,3,3-trichloroacrylamide)phenyl)-5-(trifluoromethyl)-1H-pyrazole-4-carboxylate

RBL	Rat basophil leukaemia
ROCC	Receptor-operated calcium channels
ROCK	Rho-associated protein kinase
rRNA	Ribosomal RNA
SEM	Standard error of mean
SERCA	Sarco/endoplasmic reticulum Ca^{2+} ATPase
SK_{Ca} channel	Small-conductance Ca^{2+}-activated potassium channel
SNP	Sodium nitroprusside
SOCC	Store-operated calcium channels
SR	Sarcoplasmic reticulum
STIM1	Stromal interaction molecule 1
TEA	Tetraethylammonium
Th2	Type 2 T helper
TMM	Tiger Milk's Mushroom
TP receptor	Thromboxane A_2 receptor
TRP	Transient receptor potential
TRPC	canonical transient receptor potential
TRPV1	Transient receptor potential vanilloid 1
VOCC	Voltage-operated calcium channels
WHO	World Health Organization

List of figures and tables

Figures

Figure 1.1: Burden of disease, measured by disability adjusted life years (DALYs) per 100,000 populations attributed to asthma by age group and sex.	1
Figure 1.2: Schematic diagram of the cross-section of airway showing changes that occur with asthma.	4
Figure 1.3: Overview of the signalling pathways involved in the regulation of airway smooth muscle tone.	13
Figure 1.4: The fruiting body of *Lignosus rhinocerotis* consists of pileus (cap) and stipe (stalk) attached to the nutrient-rich sclerotium.	29
Figure 2.1: Schematic diagram of an organ bath set up.	51
Figure 2.2: Representative trace recordings of organ bath procedures prior to the performance of experimental protocols.	58
Figure 2.3: Effect of methanol and cold water extracts on rat airways pre-contracted with carbachol.	64
Figure 2.4: Effect of hot water extract on rat airways pre-contracted with carbachol.	65
Figure 2.5: Concentration- and time-dependent properties of cold water extract on carbachol-pre-contracted rat airways.	67
Figure 2.6: Effect of ipratropium and salmeterol on carbachol-pre-contracted rat airways.	68
Figure 3.1: Effect of cold water extract on rat trachea pre-contracted with different contractile agonists.	96
Figure 3.2: Effect of cold water extract against carbachol- and 5-hydroxytrptamine-induced contractions in rat airways.	98
Figure 3.3: Effect of cold water extract and atropine against 5-hydroxytryptamine-induced contraction in rat trachea.	100
Figure 3.4: Effect of adenosine on rat airways at basal tone and pre-contracted with carbachol.	101
Figure 3.5: Roles of cAMP, cGMP and nitric oxide pathway in cold water extract-induced relaxation in rat trachea.	103
Figure 3.6: Effect of antagonists of β-adrenoceptors and potassium channels against cold water extract-induced relaxation in rat airways.	104
Figure 3.7: Effect of cold water extract on rat airways at basal tone.	107
Figure 3.8: Representative trace recording of cold water extract-induced contraction in rat trachea at basal tone.	108
Figure 3.9: Effect of cold water extract on porcine bronchiole pre-contracted with carbachol.	110

Figure 3.10: Proposed mechanisms involved in cold water extract-mediated airway smooth muscle relaxation.	119
Figure 4.1: Effect of cold water extract against calcium chloride-induced contraction in rat airways.	146
Figure 4.2: The role of calcium in cold water extract-induced relaxation in rat trachea contracted with carbachol.	148
Figure 4.3: Reversibility of the effect of cold water extract against carbachol-induced contraction in rat trachea.	150
Figure 4.4: The role of extracellular calcium in contractions induced by carbachol, 5-hydroxytrptamine, and potassium chloride in rat trachea.	152
Figure 4.5: Effect of calcium channel blockers against carbachol-induced contraction in rat trachea.	155
Figure 4.6: The role of calcium in cold water extract-induced relaxation and carbachol-induced contraction in porcine bronchioles.	158
Figure 4.7: The peak $[Ca_{2+}]_i$ induced by potassium chloride in the presence and absence (control) of cold water extract in DRG cells.	161
Figure 4.8: Complexometric titration test of cold water extract.	162
Figure 5.1: Representative traces of neurogenic responses to electrical field stimulation in guinea pig ileum.	192
Figure 5.2: Effect of cold water extract on phenylephrine-pre-contracted rat aorta.	195
Figure 5.3: The involvement of endothelial nitric oxide pathway in cold water extract-induced relaxation of rat aorta.	196
Figure 5.4: Effect of cold water extract against carbachol-induced relaxation in endothelium-intact rat aorta.	197
Figure 5.5: Effect of cold water extract on U46619-pre-contracted porcine coronary artery.	199
Figure 5.6: Effect of calcium channel blockers against U46619-induced contractions in porcine coronary artery.	200
Figure 5.7: Effect of cold water extract against calcium chloride-induced contractions in porcine coronary artery.	201
Figure 5.8: Effect of cold water extract on basal tension in blood vessels.	202
Figure 5.9: Effect of cold water extract on electrically stimulated guinea pig ileum.	204
Figure 5.10: The involvement of muscarinic receptors in the effects of cold water extract on guinea pig ileum.	205
Figure 5.11: The involvement of α_2- and β-adrenoceptors, opioid receptors and calcium channels in the effects of cold water extract on guinea pig ileum.	207
Figure 6.1: Effect of cold water extract and fractions on rat airways pre-contracted with carbachol.	230
Figure 6.2: Effect of cold water extract and fractions against carbachol- and 5-hydroxytryptamine-induced contractions in rat trachea.	231

Figure 6.3: Effect of cold water extract and fractions against calcium chloride-induced contraction in rat trachea.	233
Figure 7.1: Effect of cold water extract on RBL-2H3 cell viability.	256
Figure 7.2: IgE/antigen-mediated degranulation as measured by β-hexosaminidase release.	258
Figure 7.3: Effect of cold water extract on β-hexosaminidase release.	260
Figure 7.4: IgE/Antigen-induced degranulation characterized by Alcian blue staining.	261-262
Figure 7.5: Effect of cold water extract on degranulation index of IgE/antigen-stimulated cells characterized by Alcian blue staining.	264-265
Figure 7.6: Effect of cold water extract on degranulation index of unstimulated cells characterized by Alcian blue staining.	267
Figure 7.7: Flow cytometric analysis of the effect of cold water extract on cell degranulation.	269
Figure 7.8: Representative density plots of flow cytometric analysis on RBL-2H3 cells stained with FITC-labelled annexin V and propidium iodide.	270
Figure 8.1: Schematic diagram of the proposed mechanisms mediated by cold water extract of *Lignosus rhinocerotis* in airway and vascular smooth muscle relaxation.	289

Tables

Table 1.1: Current available treatment for asthma.	20
Table 1.2: Ethnomedicinal uses of Tiger Milk's Mushrooms (*Lignosus* spp.) by selected tribes of indigenous people in Peninsular Malaysia	31
Table 1.3: Summary of common models used to study airway smooth muscle contraction.	41
Table 1.4: Detection methods in cell-based assays.	45
Table 2.1: Percentage yield of *Lignosus rhinocerotis* extracts.	61
Table 2.2: Summary of the composition analysis of *Lignosus rhinocerotis* sclerotial powder.	63
Table 3.1: Summary of drugs and details.	87
Table 3.2: The maximum response (E_{max}) and pEC_{50} values of carbachol and 5-hydroxytryptamine derived from respective concentration-response curve in the presence of different treatments.	99
Table 3.3: The maximum response (E_{max}) and pEC_{50} values of cold water extract derived from respective concentration-response curve in the presence of propranolol and tetraethylammonium.	105
Table 4.1: Summary of drugs and their details.	131
Table 4.2: The maximum response (E_{max}) and pEC_{50} value of carbachol derived from respective concentration-response curve in the presence of different calcium channel blockers.	156
Table 5.1: The maximum response (E_{max}) and pEC_{50} values of carbachol derived from respective concentration-response curve in the presence of cold water extract.	198
Table 6.1: Chemical composition and monosaccharide profile of cold water extract and its fractions.	228
Table 6.2: The maximum responses (E_{max}) and pEC_{50} values of carbachol and 5-hydroxytryptamine derived from respective concentration response curve in the presence of CWE and fractions.	232
Table 7.1: Degranulation index of RBL-2H3 cells treated with cold water extract.	266

Table of contents

		Page
Abstract		i
Publications		iv
Acknowledgements		v
Declaration		vi
Abbreviations		vii
List of figures and tables		xi
CHAPTER 1.	**General introduction and literature review**……..	1
1.1	Respiratory diseases…….....	3
1.1.1	Pathophysiology and pathogenesis……...……...	3
1.1.2	Smooth muscle…….	6
	1.1.2.1 Structures…….....	6
	1.1.2.2 Mechanisms underlying smooth muscle contraction and relaxation……...	7
	1.1.2.3 Excitation-contraction coupling, secondary messengers, and calcium homeostasis……..	8
	1.1.2.4 Autonomic control and innervations of airway smooth muscle……..……	14
1.1.3	Airway smooth muscle dysfunction and altered calcium signalling……..	15
1.1.4	Immunological aspects…….	16
1.1.5	Drug therapies and their limitations…….	19
1.2	Drug discovery……...…..	22
1.2.1	Natural products as therapeutic agents…….	23
1.2.2	Medicinal mushrooms: Traditional medicinal values and scientific evidence……...….	25
1.3	*Lignosus rhinocerotis*……..……	28
1.3.1	Background……..	28
1.3.2	Ethnomedicinal uses……	30
1.3.3	Medicinal properties…….…..	32
	1.3.3.1 Antiproliferative and cytotoxic properties……	33
	1.3.3.2 Immunomodulatory and anti-inflammatory properties	35
	1.3.3.3 Other biological activities…….	37
1.3.4	Chemical investigations……...……	37

1.4 Research approaches…… 40

1.4.1 Functional studies of smooth muscle……... 40

1.4.2 Organ bath as a pharmacological tool to assess smooth muscle function…… 42

1.4.3 Cell-based assay…….…….. 43

1.5 Research aims……. 46

CHAPTER 2. Extractions of *Lignosus rhinocerotis* and their pharmacological effects on airways……..... 48

2.1 Introduction…….. 48

2.1.1 Organ bath set up……. 49

2.1.2 Rationale for tissue selection in study……. 52

2.1.3 Significance of study……... 53

2.2 Materials and methods……..... 54

2.2.1 Drugs and materials…….…… 54

2.2.2 Extraction……..….. 55

2.2.2.1 Optimization of the solubility of extracts……. 55

2.2.3 Composition analysis of *L. rhinocerotis* sclerotial powder…. 56

2.2.4 Organ bath experiments……... 57

2.2.4.1 Tissue preparation…… 57

2.2.4.2 Preliminary study of *L. rhinocerotis* extracts on airways pre-contracted with carbachol……. 58

2.2.4.3 Effect of the CWE and incubation time on airways pre-contracted with carbachol……. 59

2.2.4.4 Effect of the conventional bronchodilators on airways pre-contracted with carbachol……. 60

2.2.4.5 Statistical analysis…… 60

2.3 Results……..…… 61

2.3.1 Yields from cold water, hot water and methanol extraction… 61

2.3.2 Optimization of the solubility of extracts…… 62

2.3.3 Composition analysis of *L. rhinocerotis* sclerotial powder…. 62

2.3.4 CWE produced most pronounced airway relaxation effect…. 63

2.3.5 Airway relaxation effect of the CWE is concentration- and time-dependent…… 65

2.3.6 Ipratropium and salmeterol relaxed pre-contracted airways... 68

2.4 Discussions……..... 69

CHAPTER 3. Mechanisms of action of *Lignosus rhinocerotis* extract on airways…….. 74

3.1 Introduction…….. 74

3.1.1 Activation of $G_{\alpha q}$ protein-coupled receptors in airways…….. 75

3.1.2 Degradation of cAMP and cAMP by phosphodiesterase enzymes……..…… 78

3.1.3 Potassium channels in airways…… 79

3.1.4 Adenosine in airways…….. 81

3.1.5 Nitric oxide as a potent bronchodilator……... 83

3.1.6 Significance of study……... 85

3.2 Materials and methods……. 86

3.2.1 Drugs and materials……. 86

3.2.2 Tissue preparation…… 88

3.2.3 Experimental protocols ……... 89

3.2.3.1 Effect of CWE on rat trachea pre-contracted with KCl 89

3.2.3.2 Effect of CWE against carbachol- and 5-HT-induced contractions and the role of muscarinic receptors in 5-HT-induced contraction.…….…. 89

3.2.3.3 Effect of adenosine on airways…… 90

3.2.3.4 Effect of inhibitors of PDE enzyme, NO, β-adrenoceptors and potassium channels, and adenylyl cyclase activator on CWE-induced airway relaxation. 91

3.2.3.5 Effect of CWE on rat airways at basal tone……. 92

3.2.3.6 Effect of CWE on porcine airways…….. 93

3.2.4 Statistical analysis……... 94

3.3 Results…….. 95

3.3.1 CWE similarly relaxed pre-contraction by KCl and carbachol…….. 95

3.3.2 CWE attenuated carbachol and 5-HT-induced contractions... 97

3.3.3 Muscarinic receptors were involved with 5-HT-induced contraction……... 100

3.3.4 Adenosine did not affect the tone of rat airways……. 101

3.3.5 CWE potentiated the relaxation effect mediated by cAMP but has no effect on NO/cGMP-mediated responses ……. 102

3.3.6 CWE-induced airway relaxation was not mediated via β-adrenoceptors or potassium channels…….. 104

3.3.7 CWE increased the basal tone of rat airways possibly via muscarinic receptor activation……. 106

3.3.8 CWE exhibited similar responses in porcine bronchiole as in rat airways…… 109

3.4 Discussions…….. 111

CHAPTER 4. The role of calcium underlying the effects of *Lignosus rhinocerotis* extract……. 120

4.1 Introduction……. 120

4.1.1 Calcium entry pathways in airway smooth muscle……. 120

4.1.2 Calcium imaging experiment with dorsal root ganglion cells. 124
4.1.2.1 Calcium imaging technique..……... 124
4.1.2.2 Calcium signalling in dorsal root ganglion cells…….. 126

4.1.3 Metal ion-chelating activity of medicinal mushrooms…… 128

4.1.4 Significance of study……... 130

4.2 Materials and methods…….…… 131

4.2.1 Drugs and materials……. 131

4.2.2 Organ bath experiments…….. 132
4.2.2.1 Tissue preparation…… 132
4.2.2.2 Effect of CWE-induced airway relaxation on extracellular calcium entry in rat airways…… 133
4.2.2.3 Effect of CWE-induced airway relaxation on intracellular calcium mobilization in rat airways……. 134
4.2.2.4 The role of extracellular calcium in smooth muscle contractility mediated by carbachol, 5-HT, and KCl... 134
4.2.2.5 Effect of calcium channel blockers against carbachol-induced contraction in rat airways…..…….. 136
4.2.2.6 The role of calcium mediated by CWE in porcine bronchiole…… 136
4.2.2.7 Statistical analysis…… 138

4.2.3 Calcium imaging experiments……. 139
4.2.3.1 Coverslip preparation and coating…… 139
4.2.3.2 Dorsal root ganglia cell preparation……. 139
4.2.3.3 Fura-2-AM loading…….. 141
4.2.3.4 Calcium imaging experiment……..….. 141
4.2.3.5 Statistical analysis…… 142

4.2.4 Complexometric titration test with CWE…… 143
4.2.4.1 Statistical analysis…… 144

4.3 Results……. 145

4.3.1 Organ bath experiments…….. 145
4.3.1.1 Bronchodilator effect of CWE in airway segments is linked to regulation of calcium entry…….. 145
4.3.1.2 CWE primarily inhibited extracellular calcium influx with little role on intracellular calcium in rat airways. 146

4.3.1.3 Removal of external calcium abolished the contractions to carbachol, 5-HT, and KCl in rat airways…… 151
4.3.1.4 Carbachol-induced contraction was inhibited by calcium channel blockers in rat airways……. 154
4.3.1.5 CWE inhibited extracellular calcium entry in porcine bronchiole…… 157
4.3.2 CWE suppressed the increase in cytosolic calcium levels induced by KCl in dorsal root ganglion cells…….. 160
4.3.3 CWE did not exhibit Ca^{2+}-chelating activity…….. 162
4.4 Discussions……. 163

CHAPTER 5. Pharmacological actions of *Lignosus rhinocerotis* extract on blood vessels and ileum…….. 170

5.1 Introduction……. 170
5.1.1 Blood vessels…….….. 171
5.1.1.1 Vascular contraction and relaxation…… 171
5.1.1.2 Structure and species difference between aorta and coronary artery……. 175
5.1.2 Ileum…… 178
5.1.3 Significance of study……... 182
5.2 Materials and methods……. 184
5.2.1 Drugs and materials……. 184
5.2.2 Tissue preparation…… 184
5.2.3 Effects of CWE on blood vessels…… 187
5.2.3.1 Effect of CWE against pre-contractions induced by phenylephrine and U46619 in rat aorta and porcine coronary artery respectively……. 187
5.2.3.2 Involvement of endothelium and nitric oxide pathway in CWE-induced aortic relaxation…… 188
5.2.3.3 Effect of CWE against carbachol-induced relaxation in rat aorta…… 189
5.2.3.4 Effect of calcium channel blockers on U46619-induced contraction in porcine coronary artery……... 189
5.2.3.5 Effect of CWE on contractile responses to calcium re-introduction…… 190
5.2.3.6 Effect of CWE on blood vessels at resting tension…. 190
5.2.4 Effects of CWE on ileum…….… 191
5.2.4.1 Cumulative concentrations of CWE…… 193
5.2.4.2 Effect of CWE in the presence of atropine, naloxone, rauwolscine, nifedipine or propranolol……..…….…. 193
5.2.5 Statistical analysis…… 194

5.3 Results……. 195

5.3.1 CWE relaxed aorta pre-contracted with phenylephrine…….. 195

5.3.2 CWE-induced aortic relaxation was independent of endothelium and nitric oxide……... 196

5.3.3 CWE did not affect muscarinic receptors in aorta…….……. 197

5.3.4 CWE relaxed porcine coronary artery pre-contracted with U46619…… 199

5.3.5 U46619-induced contraction in coronary artery was inhibited by calcium channel blockers…… 200

5.3.6 Vasorelaxation effect of CWE is linked to the regulation of calcium entry…….. 201

5.3.7 CWE relaxed coronary artery at basal tone…… 202

5.3.8 CWE diminished neurogenic response but augmented basal response in electrically stimulated ileal tissues…….. 203

5.3.9 Treatment with atropine augmented the basal contraction to CWE in ileal tissues……...……. 205

5.3.10 Inhibitory effect of CWE on neurogenic contraction in ileal tissues was slightly recovered by nifedipine…….. 206

5.4 Discussions……. 208

CHAPTER 6. Fractionation of *Lignosus rhinocerotis* extract and the pharmacological effects on airways…….. 216

6.1 Introduction……. 216

6.1.1 Fractionation of natural products…… 219

6.1.2 Significance of study…….. 221

6.2 Materials and methods…… 222

6.2.1 Drugs and materials…… 222

6.2.2 Tissue preparation……... 222

6.2.3 Preparation, extraction and fractionation of CWE……..…. 223

6.2.4 Determination of total carbohydrate and protein contents….. 223

6.2.5 Determination of monosaccharide composition ……. 224

6.2.6 Effect of CWE and fractions on pre-contracted airway segments…….. 224

6.2.7 Effect of CWE and fractions against contractions to carbachol and 5-HT……. 225

6.2.8 Effect of CWE and fractions against calcium-induced contraction…….…….…….…… 225

6.2.9 Statistical analysis…….…….. 226

6.3 Results……. 226

6.3.1 Fractionation of CWE by molecular weight……... 226

6.3.2 Chemical composition of CWE and its fractions…… 227

6.3.3 Unequivocal airway relaxation effects of CWE, HMW and MMW fractions…….…….. 229

6.3.4 HMW fraction markedly prevented carbachol- and 5-HT-induced airway contraction…….…… 231

6.3.5 HMW fraction significantly limited calcium-induced contraction…….. 233

6.4 Discussions……. 234

CHAPTER 7. Effect of *Lignosus rhinocerotis* extract on mast cell degranulation…….. 238

7.1 Introduction……. 238

7.1.1 The suitability of RBL-2H3 cells as a model of degranulation……...… 242

7.1.2 The role of natural products in inhibiting mast cell degranulation……... 243

7.1.3 Significance of study……... 245

7.2 Materials and methods……. 246

7.2.1 Drugs and materials……. 246

7.2.2 Cell culture…….. 247

7.2.3 Cell viability assay…….. 248

7.2.4 Optimization of IgE/antigen-stimulated degranulation using β-hexosaminidase assays…… 249

7.2.5 β-hexosaminidase assays…… 251

7.2.6 Alcian blue staining…… 252

7.2.7 Flow cytometry analysis…… 253

7.2.8 Statistical analysis…….…… 255

7.3 Results…… 256

7.3.1 Concentrations of CWE ≤ 62.5 μg/ml did not affect viability of RBL-2H3 cells…… 256

7.3.2 Concentrations of IgE and antigen for following degranulation assays were optimized…….. 257

7.3.3 CWE triggered β-hexosaminidase release in unstimulated cells…….. 258

7.3.4 CWE decreased degranulation index in IgE/antigen-stimulated cells via Alcian blue staining……. 261

7.3.5 CWE increased phosphatidylserine externalization in unstimulated cells…… 268

7.4 Discussions…….. 271

CHAPTER 8. General discussions……. 279

8.1 Pharmacological effects and mechanisms of action of crude extracts of *L. rhinocerotis*……. 280

8.1.1 Airway smooth muscle…… 280

8.1.2 Vascular smooth muscle……. 284

8.1.3 Ileal smooth muscle…….,…… 286

8.1.4 Summary of findings on smooth muscles……,…….. 287

8.1.5 Effects of CWE on dorsal root ganglion cells and calcium chelation…….,……. 290

8.1.6 Fractionations of CWE and their effects on airways…….. 291

8.2 Effects of CWE on mast cell degranulation…… 292

8.3 Limitations and future studies…….,…… 293

8.4 Concluding statements…… 295

References…… 297

Appendices…… 333

Chapter 1. General introduction and literature review

Asthma is one of the main chronic respiratory diseases characterized by airway obstruction and underlying airway inflammation. According to World Health Organization (WHO)'s estimates in 2016, as many as 235 million people worldwide currently suffer from asthma, accounting for deaths of 383,000 worldwide in 2015. Regardless of the income status of countries, asthma is a global health problem that affects all. Despite the advances in understanding and managing this disease nowadays, asthma is still often underdiagnosed and undertreated, with consequent high morbidity and mortality substantially impairing the quality of life of patients. The economic burden of asthma is considerable, either by the medical cost (long-term therapy) or indirect cost (impaired work ability and premature death) (Nunes, Pereira, & Morais-Almeida, 2017). The disease burden can be clearly seen in Fig. 1.1**,** in which the disability adjusted life years is expressed as the number of lost 'healthy' years due to illness, disability or early death.

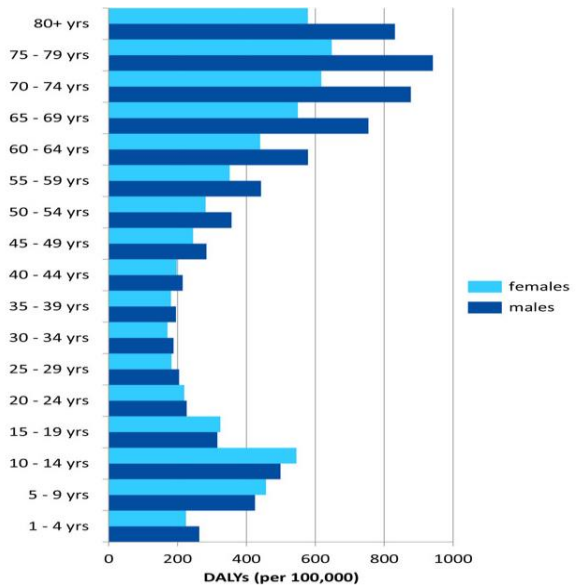

Figure 1.1: Burden of disease, measured by disability adjusted life years (DALYs) per 100,000 populations attributed to asthma by age group and sex. (Adapted from The Global Asthma Report 2014)

On the other hand, cough is an involuntary reflex of respiratory tract to clear the upper airways as a defence mechanism from external stimuli (Chung & Pavord, 2008). There are two categories of cough: acute cough that lasts ≤ 8 weeks, and chronic cough that lasts for ≥ 8 weeks (Faruqi, Murdoch, Allum, & Morice, 2014). A recent systematic review and meta-analysis estimated that the global adult populations affected by chronic cough show as high as 7.9% prevalence (Song et al., 2015). Many chronic respiratory diseases are characterized by chronic cough as one of the major symptoms, for example in asthma and chronic obstructive pulmonary disease (COPD) (Faruqi et al., 2014). Although chronic cough is less recognized than asthma, it can also bring about detrimental impact on quality of life and financial burden to the patients (H & Paramesh, 2018; Song et al., 2015).

At present, the above-mentioned airway conditions face major hurdles, including high epidemiological burden and unmet clinical needs that need to be overcome. In view of this, there is a pressing need for research and development to bring forth more cost-effective therapies to tackle these diseases. In this context, natural products represent a rich source of diverse and biologically active metabolites with exploitable medicinal values providing untapped opportunities in research and development for new therapies. *Lignosus rhinocerotis*, a popular medicinal mushroom, is widely used as a folk medicine among indigenous people in Southeast Asia and Southern China to treat a variety of diseases, mainly for asthma and cough. The cultivated strain of this mushroom has been commercialized in Malaysia and serves as nutraceuticals based on their traditional belief. Despite this, there is a paucity of scientific evidence to date to support its main traditional uses to ameliorate airway conditions.

In the following sections, our primary focus is on asthma as well as chronic cough in relation to the traditional usage of *L. rhinocerotis*. The normal and diseased physiological features of airway smooth muscle and the review of respiratory diseases from various aspects are presented to provide basis for the experimental designs in relation to this project. More detailed description on vascular and ileal smooth muscles will be given in **Chapter 5**.

1.1 Respiratory diseases

1.1.1 Pathophysiology and pathogenesis

Asthma is a chronic inflammatory disorder of respiratory tract involving an array of mediators released from cells in response to various allergens or irritants, including cold air, exercise, respiratory allergens, smoke, and upper respiratory tract viral infection (Erle and Sheppard, 2014). It is characterized by recurrent episodes of widespread and variable airways obstruction, leading to symptoms such as wheezing, breathlessness, chest tightness, and coughing. The asthma attack episodes are normally reversible either spontaneously or with treatment.

The two main airway cell types involved in asthma pathogenesis are epithelial and smooth muscle cells (Erle & Sheppard, 2014). Airway epithelial cells are where inflammation and mucus hypersecretion occur contributing to airway obstruction, whilst airway smooth muscle contraction directly leads to reduction in airway diameter and airway narrowing (Doeing & Solway, 2013). The schematic diagram of airway changes underlying asthma is illustrated in Fig. 1.2. Besides, the chronic inflammatory status in asthma is associated with airway hyperresponsiveness. As one

of the hallmark features of asthma, airway hyperresponsiveness is characterized by augmented contractile responses of smooth muscle with reduced threshold to a variety of contractile stimuli (Doeing & Solway, 2013). In some patients, long term structural changes with hyperplasia and hypertrophy of airway walls can happen, resulting in only partial reversal of airflow limitation. This phenomenon is termed as airway remodelling (Doeing & Solway, 2013).

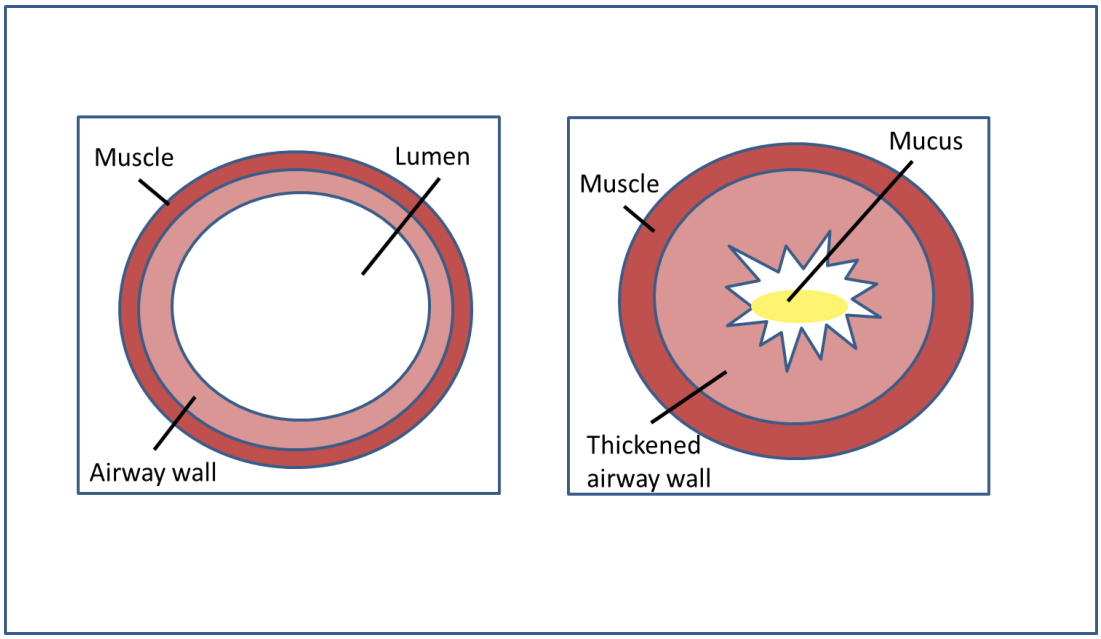

Figure 1.2: Schematic diagram of the cross-section of airway showing changes that occur with asthma. Asthma attack is accompanied by intraluminal mucus hypersecretion and reduced airway lumen diameter due to airway smooth muscle contraction and airway wall inflammation. (Adapted from Doeing & Solway 2013)

Cough is often initiated by inflammation or mechanical changes in airways, or by inhalation of chemical and mechanical irritants. The induction of cough involves a complex reflex arc, in which the signal generated from the stimulation of sensory nerve and chemical receptors is transmitted to the central medullary cough centre via vagal afferent nerves (Polverino et al., 2012). Cough receptors are found in the airways and many parts of the body including trachea, main carina, branching points of large airways, distal smaller airways, and pharynx, just to name a few (Polverino et al.,

2012). Sensory nerve receptors involved in cough reflex pathway responding to the stimuli are categorized based on their conductive properties: rapidly adapting receptors (responding to smoke, bronchoconstriction, mechanical stimuli), slowly adapting receptors (pulmonary stretch receptor) and C-fibre receptors (responding to chemicals such as bradykinin and capsaicin) (Chung & Pavord, 2008). On the other hand, chemical receptors are, for example, ion channels such as sodium ion channel, acid-sensing ion channel, and cationic ion channel, which is the transient receptor potential vanilloid 1 (TRPV1) channel (J. J. Adcock, 2009).

Causes that commonly trigger chronic cough are asthma, eosinophilic bronchitis (presence of eosinophilia in sputum but without airway abnormality as seen in asthma), cough-variant asthma, gastroesophageal reflux disease, and so on (C. E. Brightling, 2011; Chung & Pavord, 2008; Faruqi et al., 2014). Cough variant asthma is a common type of asthma in which the only clinical manifestation is dry, chronic cough; nonetheless, it lacks of other typical symptoms of asthma such as wheezing and breathlessness (Niimi, 2011). Chronic cough is often associated with eosinophilic airway inflammation (C. E. Brightling, 2011). In asthma, cough receptor is triggered by bronchial smooth muscle contraction to constrictor mediators such as histamine (J. J. Adcock, 2009; Chung & Pavord, 2008). Although chronic cough is prevalent, there is little knowledge of the aetiology of the disease. The general consensus is that there is a dysfunction in airway ion channels. Activation of TRPV1 and transient receptor potential ankyrin 1 (TRPA1) channels is known to trigger cough (Birrell et al., 2009), although whether these channels are upregulated in chronic cough remains unclear.

1.1.2 Smooth muscle

1.1.2.1 Structures

Smooth muscle, which is present in several tissues in the body including airways, blood vessels, intestines, gallbladder, stomach and urinary bladder, is responsible for the involuntary movements. These tissues have almost similar structural arrangement with three to four layers surrounding the lumen, an internal hollow space of tissue surrounded by tissue wall (Rang et al., 2015). Each of these layers has different terms in different tissues. For instance in vascular tissues from the most interior layer to the outer layer surrounding tissue lumen, these tunics are termed tunica intima, tunica media, and tunica externa, whereas in airway and bladder tissues, these layers are termed mucosa, submucosa, and adventitia (McCorry, 2009).

Epithelium or endothelium (specialized epithelial cells in vascular tissues), which is in contact with the luminal space, lines the interior mucosa or tunica intima layer respectively. In vascular tissues, the endothelium plays a paramount role in modulating vascular tone by releasing a range of factors including endothelium-dependent relaxing factors (EDRFs) and endothelium-dependent hyperpolarizing factors (EDHFs) (J. A. Hill, Olson, & Griendling, 2012). Hence, endothelium can be removed ("denuded") in functional studies of compounds or drugs to assess the implication of these endothelium-dependent factors. In the substantial middle layer i.e. tunica media or submucosa layer, smooth muscle cells and collagenous fibres predominate (J. A. Hill et al., 2012). Lastly, the outermost layer comprises mainly connective tissues and collagen. On the other hand, the structural arrangement of tissue layers differs slightly in the gastrointestinal tract in which four layers are present, from the lumen outward, i.e. mucosa, submucosa, muscularis externa and adventitia/serosa.

Unlike airway and vascular tissues, the submucosa layer in small intestine, for instance in ileum, merely contains connective tissues which support mucosa and connect to the muscularis externa and serosa (J. A. Hill et al., 2012; McCorry, 2009). Two distinct muscular layers of circular and longitudinal smooth muscle responsible for the gut movement are found within the muscularis externa.

Smooth muscle cells can regulate muscular tone through contraction and relaxation. When smooth muscle contracts, the luminal space they surround narrows resulting in reduced luminal diameter e.g. vasoconstriction or bronchoconstriction. On the contrary, relaxation of smooth muscle increases the luminal diameter, leading to tissue relaxation e.g. vasodilation or bronchodilation. In addition, there is nerve innervation within tissue wall that also partly participates in the modulation of muscular tone. In the following subsections, we mainly focus on the molecular mechanisms of airway smooth muscle in relevance to this thesis.

1.1.2.2 Mechanisms underlying smooth muscle contraction and relaxation

Smooth muscle contraction is resulted by stimulation of actin and myosin, which are the two major contractile protein filaments found in smooth muscle. The generally accepted cross-bridge theory states that smooth muscle contracts due to the interaction between myosin and actin in repetitive cycles of sliding movement (Rang et al., 2015). In airway smooth muscle, calcium ion(Ca^{2+})-binding protein calmodulin binds to enzyme myosin light chain kinase (MLCK), which in turn catalyses phosphorylation of myosin light chain (MLC) to promote binding of myosin to actin filament and initiate contraction. The phosphorylation of MLC can be reversed by myosin light

chain phosphatase (MLCP) via dephosphorylation, leading to smooth muscle relaxation (Girolamo Pelaia et al., 2008). Balance between activities of MLCP and MLCK regulates the smooth muscle tone.

1.1.2.3 Excitation-contraction coupling, secondary messengers, and calcium homeostasis

The excitation-contraction coupling in airway smooth muscle is mainly driven by two mechanisms: Ca^{2+} signalling cascade and the Ca^{2+}-sensitive contractile apparatus. Airway smooth muscle contracts in response to increase in cytosolic Ca^{2+} concentration ($[Ca^{2+}]_i$), where the source can be either extracellular Ca^{2+} entry through membrane voltage-operated calcium channels (VOCC), store-operated calcium channels (SOCC) and receptor-operated calcium channels (ROCC), or mobilization of intracellular Ca^{2+} store i.e. sarcoplasmic reticulum (SR) (reviewed by Billington et al., 2013; Pelaia et al., 2008).

The contraction consists of two phases: an initial transient peak of $[Ca^{2+}]_i$ (phasic response) predominantly induced by intracellular Ca^{2+} release from SR, followed by a sustained rise in $[Ca^{2+}]_i$ (tonic response) which depends largely on extracellular Ca^{2+} influx. To maintain intracellular Ca^{2+} oscillations following the initial Ca^{2+} release, Ca^{2+} influx from the extracellular environment and Ca^{2+} reuptake into SR through sarco/endoplasmic reticulum Ca^{2+}-ATPase (SERCA) are crucial. Another phenomenon is due to enhanced sensitivity of the contractile apparatus of smooth muscle to Ca^{2+}, such as during the application of contractile agonist (Ouedraogo & Roux, 2014). Enhanced Ca^{2+} sensitivity allows for persistent smooth muscle contraction even at minimal increase of $[Ca^{2+}]_i$ above the baseline levels.

Smooth muscle tone can be induced by mechanical or chemical stimulation. In the case of mechanical stimulation, examples of stimulants are stretch receptors (afferent nerve fibre) localized in the airway wall, inhaled irritants, or mucus secretion (Bartlett, Jeffery, Ambrogio, & Wise, 1976). The afferent nerves mediate and trigger cough reflex as a defence mechanism from inflammatory mediators or mechanical stimuli. The autonomic control and innervations of the airways are reviewed in detailed in Section 1.1.2.4.

In this context, chemical stimulation refers to the activation of G protein-coupled receptor (GPCR) upon binding of an agonist (e.g. acetylcholine binding to muscarinic receptors) (Billington & Penn, 2003). In airway smooth muscle, activation of $G_{\alpha q}$ or $G_{q/11}$ protein-coupled receptors, such as muscarinic M_3 receptors, stimulates membrane phospholipase C (PLC) to hydrolyse phosphatidylinositol 4,5-bisphosphate (PIP_2), thus producing two secondary messengers i.e. diacylglycerol (DAG) and inositol triphosphate (IP_3). DAG stimulates protein kinase C (PKC) formation, whereas IP_3 acts on IP_3 receptors on SR stimulating the release of intracellular Ca^{2+} from SR (reviewed by Rang et al., 2015; Wright et al., 2013). Furthermore, Ca^{2+} can be released from SR via ryanodine receptors. Following intracellular Ca^{2+} store depletion, it has been proposed that SOCC will be triggered to allow Ca^{2+} and Na^{+} influx into the cells to sustain a raised $[Ca^{2+}]_i$ for contraction (Siddiqui et al., 2013). Besides, PKC inhibits MLCP to indirectly promote smooth muscle contraction and facilitates additional Ca^{2+} and Na^{+} influx into cells by activating ROCC. The elevation in Na^{+} levels consequent to ROCC and SOCC activation also drives the reverse-mode Na^{+}/Ca^{2+} exchanger (NCX), allowing for more Ca^{2+} influx in exchange of Na^{+} (Berair, Hollins, & Brightling, 2013). Eventually, smooth muscle contraction ensues following increased $[Ca^{2+}]_i$.

In parallel, M_3 receptors are also coupled to $G_{12/13}$ protein, which activates the monomeric G protein Rho A and its downstream effector Rho-associated protein kinase (ROCK) (Yoo et al., 2017). ROCK regulates phosphorylation of MLC through inhibition of MLCP, leading to increased airway smooth muscle contraction (Berair et al., 2013). The PKC and ROCK are also believed to enhance Ca^{2+} sensitivity in airway smooth muscle (Girolamo Pelaia et al., 2008). In general, calcium homeostasis is maintained through negative feedback such that resulting high $[Ca^{2+}]_i$ inactivates the IP_3 receptors, and the SERCA pumps Ca^{2+} back into SR. Consequently, $[Ca^{2+}]_i$ is decreased, causing reactivation of IP_3 receptors to maintain the $[Ca^{2+}]_i$. Proposed candidate for SOCC and ROCC is canonical transient receptor potential (TRPC) channels, and this topic was expanded in **Chapter 4**.

Conversely, airway smooth muscle relaxation is associated with a drop in $[Ca^{2+}]_i$ following cessation of the stimulation of contractile proteins or accumulation of intracellular 3′-5′-cyclic adenosine monophosphate (cAMP) (Billington et al., 2013). β_2-adrenoceptors are probably the most comprehensively studied receptors for mediating cAMP pathway. The dogma is that the activation of G_s-coupled β_2-adrenoceptors located on airway smooth muscle will stimulate adenylyl cyclase (AC) to catalyse the conversion of adenosine triphosphate (ATP) to cAMP and elicit bronchorelaxation (Rang et al., 2015). The cAMP activates protein kinase A (PKA), which in turn inhibits MLCK and phosphoinositide hydrolysis and activates MLCP. It is suggested that PKA could also stimulate NCX to reduce $[Ca^{2+}]_i$ levels and activate large-conductance Ca^{2+}-activated potassium (BK_{Ca}) channels (Barisione, Baroffio, Crimi, & Brusasco, 2010). Additionally, BK_{Ca} channels can be phosphorylated and opened directly by the G_s subunit of β_2-adrenoceptors in airway smooth muscle cells (Barisione et al., 2010). Efflux of potassium ion (K^+) leads to cell membrane

hyperpolarisation at pre- and post-junctional levels, and hence reduction in acetylcholine release and bronchorelaxation. Furthermore, the cAMP/PKA pathway is believed to reduce Ca^{2+} sensitivity of smooth muscle (Billington et al., 2013; Girolamo Pelaia et al., 2008). Overall, the activation of β_2-adrenoceptors by agonist leads to airway smooth muscle relaxation (Barisione et al., 2010; Proskocil & Fryer, 2005; Shore & Moore, 2003). Noteworthy, recent emerging evidence points to ROCC and SOCC, rather than VOCC, as the predominant channels for extracellular Ca^{2+} influx on airway smooth muscle, and β_2-adrenoceptors appear to modulate these channels (Billington et al., 2013).

Aside from cAMP, 3′-5′-cyclic guanosine monophosphate (cGMP) is also recognized as an important second messenger involved in airway relaxation. Guanylyl cyclase (GC) enzyme catalyses the conversion of guanosine triphosphate (GTP) to cGMP, which presumably activates the cGMP-dependent protein kinase G (PKG). Noteworthy, cAMP can cross-stimulate PKG in smooth muscle cells, contributing to bronchodilation (P.J. Barnes, 1998). Studies reported that PKG directly binds MYPT1 subunit of MLCP, inhibits IP_3 receptor, increases MLCP activity, and reduces Ca^{2+} sensitivity of the contractile apparatus (Etter, Eto, Wardle, Brautigan, & Murphy, 2001; Perez-Zoghbi, Bai, & Sanderson, 2010). Nitric oxide (NO) (activates soluble GC) and atrial natriuretic peptide (activates particulate GC) are among the few agents acting through stimulation of cGMP production. The NO has been described as a potent relaxing agent in multiple models and smooth muscles (Azevedo et al., 2014). The roles of NO on airway and vascular smooth muscles are elaborated in **Chapter 3** and **Chapter 5**, respectively.

Excitation-contraction coupling and second messenger system involved in the regulation of airway smooth muscle tone are depicted in Fig. 1.3**.** It is believed that

the excitation-contraction coupling of vascular smooth muscle principally results from membrane depolarization leading to extracellular Ca^{2+} influx through VOCC (Girolamo Pelaia et al., 2008). However, this notion is challenged in airway smooth muscle as evidenced by the poor response of asthmatic patients to VOCC blockers in clinical studies (T. Ahmed, Brot, & Abraham, 1988; Sanderson, Delmotte, Bai, & Perez-Zogbhi, 2008). A number of reviews also outline that the contractile agonist-induced airway contraction primarily relies on intracellular Ca^{2+} release (Ouedraogo & Roux, 2014; Girolamo Pelaia et al., 2008; Sanderson et al., 2008). In the context of airway remodelling in the asthmatic airway, cellular mechanisms along with smooth muscle structure have been altered (Meurs, Gosens, & Zaagsma, 2008).

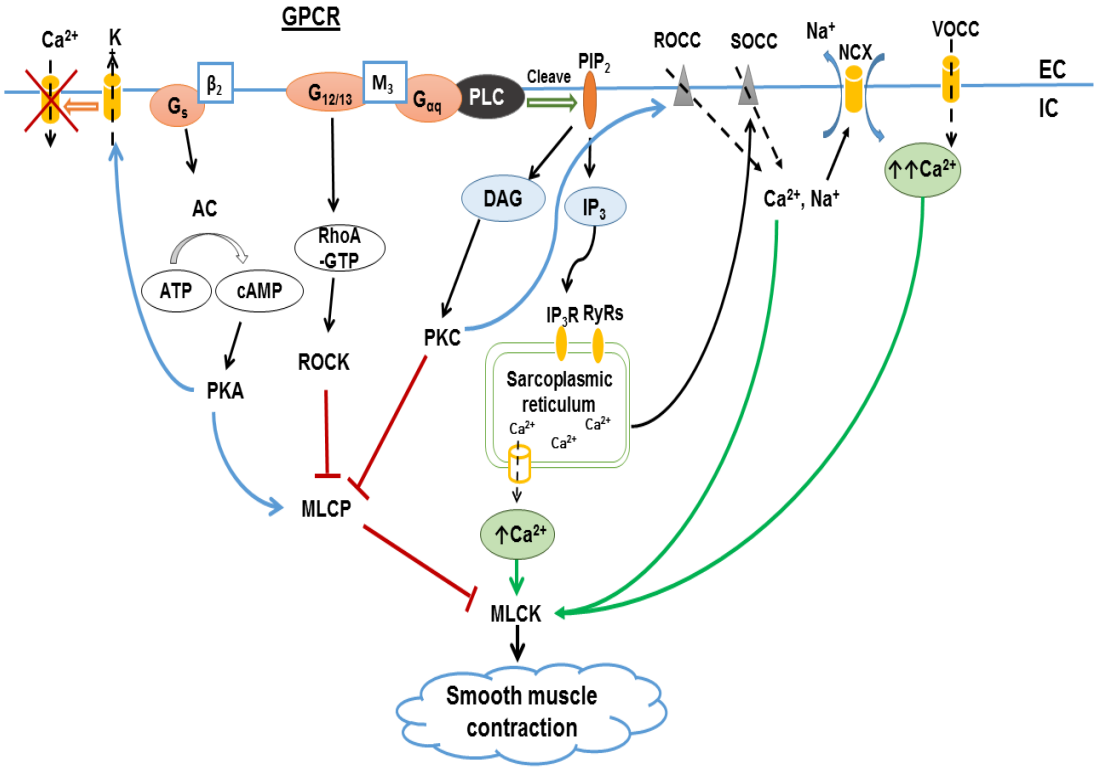

Figure 1.3: Overview of the signalling pathways involved in the regulation of airway smooth muscle tone. Contractile agonists bind to and activate $G_{\alpha q}$ protein-coupled receptor such as muscarinic M_3 receptors, stimulating PLC to cleave PIP_2 into IP_3 and DAG. IP_3 then binds to IP_3R on the surface of sarcoplasmic reticulum and causes the release of Ca^{2+} from internal calcium store. In parallel, RyRs are activated to further release Ca^{2+} from sarcoplasmic reticulum. The entry of Ca^{2+} and Na^{+} into cells through SOCC and ROCC are triggered by depletion of internal calcium store and PKC, which is activated by DAG. PKC also inhibits MLCP causing contraction. The overall rise in intracellular Na^{+} drives extracellular Ca^{2+} entry through reverse mode NCX. VOCC is the main channel through which Ca^{2+} enters into smooth muscle cells upon depolarization. On the other hand, RhoA/ROCK pathway activated by $G_{12/13}$ subunit inhibits MLCP and favours MLCK activity. The general increase in cytosolic Ca^{2+} levels stimulates MLCK to elicit smooth muscle contraction. In contrast, G_s-coupled β_2-adrenoceptors stimulate AC to convert ATP to cAMP. Activated PKA favours MLCP activity over MLCK, as well as stimulates K^{+} efflux to hyperpolarize cell membrane inhibiting extracellular Ca^{2+} influx. Altogether, these lead to smooth muscle relaxation. (Abbreviations: AC = Adenylyl cyclase; ATP = Adenosine triphosphate; cAMP = 3′-5′-cyclic adenosine monophosphate; DAG = Diacylglycerol; EC = Extracellular; IC = Intracellular; IP_3 = Inositol triphosphate; IP_3R = IP_3 receptor; MLCK = Myosin light chain kinase; MLCP = Myosin light chain phosphatase; NCX = Na^{+}-Ca^{2+} exchanger; PIP_2 = Phosphatidylinositol 4,5-bisphosphate; PKA = Protein kinase A; PKC = Protein kinase C; PLC = Phospholipase C; RhoA-GTP = RhoA-GTPase; ROCC = Receptor-operated calcium channels; ROCK = Rho-associated protein serine/threonine kinase; RyRs = Ryanodine receptors; SOCC = Store-operated calcium channels; VOCC = Voltage-operated calcium channels) (Barisione et al., 2010; Berair et al., 2013; Billington et al., 2013)

1.1.2.4 Autonomic control and innervations of airway smooth muscle

Parasympathetic nerves predominate in the autonomic control of human airway smooth muscle. Three subtypes of muscarinic receptors (M_1 - M_3) are expressed in the lungs. Airway epithelium expresses M_1 and M_3 receptors, whilst gland expresses M_3 receptors (Proskocil & Fryer, 2005). M_1 receptors have very low density in airways, mainly facilitating nicotinic neurotransmission. M_2 receptors are inhibitory autoreceptors present in the postganglionic cholinergic nerves, mediating negative feedback on acetylcholine release. The release of acetylcholine from vagus nerves mediates airway smooth muscle contraction by acting on post-junctional muscarinic receptors present on smooth muscle, with M_3 receptors being the most pharmacologically important subtype (Fryer & Jacoby, 1998; Proskocil & Fryer, 2005).

Sympathetic nerves innervate airway blood vessels, glands, and parasympathetic ganglia, but there is no functional evidence for direct sympathetic innervation of airway smooth muscle. Acting on the α_1-adrenoceptors, noradrenaline released from the sympathetic nerves primarily regulates airway blood vessel tone (Peter J Barnes, 2012). Besides, β_2-adrenoceptors are largely present on airway smooth muscle. These receptors are of particular pharmacological interest owing to their regulatory role of smooth muscle tone (Barisione et al., 2010; Proskocil & Fryer, 2005).

Apart from the classical parasympathetic bronchoconstricter and sympathetic bronchodilator nerve systems, a large body of evidence shows that airways are also innervated with non-noradrenergic non-cholinergic (NANC) nerves with substantial variations among species (Peter J Barnes, 1989; Lewis, Short, & Lewis, 2006). It is generally believed that the inhibitory NANC nerves release vasoactive intestinal

peptide and NO to dilate the human airways (Rang et al., 2015). Oppositely, excitatory NANC nerves release neuropeptides including tachykinins substance P and neurokinin A, and possibly peptide calcitonin gene-related peptide to initiate inflammatory response with bronchoconstriction.

1.1.3 Airway smooth muscle dysfunction and altered calcium signalling

In the context of asthma, smooth muscle abnormalities could be the cause or consequence. Exaggerated vagal tone has been associated with chronic airway inflammation and airway hyperresponsiveness. Increasing evidence suggests that overactivation of parasympathetic nerves is likely to account for airway remodelling (Gosens, Zaagsma, Meurs, & Halayko, 2006). In some asthmatic patients, airway remodelling occurs due to chronic inflammatory status in the airways (Siddiqui et al., 2013). Pro-inflammatory mediators are released from epithelial and smooth muscle cells. Eventually, the chronic inflammatory status will lead to progressive thickening of airways associated with physiological changes including fibrosis, angiogenesis and proliferation of smooth muscle (Siddiqui et al., 2013). This process could develop over many years in asthmatic patients, and the exact marker for airway remodelling is yet to be identified. This indicates that besides being a direct target of the asthmatic response, airway smooth muscle also contributes to airway inflammation in the asthma. In addition, the proliferation of airway smooth muscle was shown to be accompanied by increased force and contractility in animal models of asthma (C. Y. Seow, Schellenberg, & Pare, 1998).

Several lines of evidence link the genesis of airway hyperresponsiveness with heightened intracellular Ca^{2+} signalling and Ca^{2+} sensitivity downstream of muscarinic

receptor and Rho A/ROCK pathway activation (Doeing & Solway, 2013; Gosens et al., 2006; Jude, Wylam, Walseth, & Kannan, 2008). Since elevated $[Ca^{2+}]_i$ is fundamental to smooth muscle contraction, it has been postulated that enhanced Ca^{2+} movement or sensitivity is related to airway hyperresponsiveness and increased contractility. Thus, targeting at abnormal Ca^{2+} handling in these aspects should theoretically be beneficial in alleviating airway hyperresponsiveness in asthma.

In contrast, there has been limited investigations on Ca^{2+} signalling associated with cough. Given that chronic cough is a common symptom of asthma, the proposition is that enhanced Ca^{2+} sensitivity should correlate with chronic cough. A previous study by Dubuis et al. (2014) demonstrated that theophylline attenuated cough reflex in guinea pig model via inhibition of Ca^{2+} influx in airway-specific neurons and activation of single C-fibre afferents (Dubuis et al., 2014). Further studies are warranted to understand the role of Ca^{2+} signalling in chronic cough.

1.1.4 Immunological aspects

Allergic asthma is the most common form of asthma triggered by inhaling allergens that cause asthma symptoms. It is characterized by two phases: (1) acute or early asthmatic response (EAR) which occurs within minutes of exposure to allergen and is associated with immediate onset of bronchoconstriction and mast cell degranulation, and (2) late asthmatic response (LAR) which occurs 3-8 hours following the EAR in 50% of patients (O'Byrne, Gauvreau, & Brannan, 2009; Raemdonck et al., 2012). Although LAR is thought to feature eosinophil inflammation, the exact principles underlying LAR are still under investigation.

Asthma is manifested by acute and chronic phases of airway inflammation (Murphy & Byrne, 2010). During the EAR, there is IgE-mediated bronchial smooth muscle contraction with increased airway resistance. Activated CD4 T-lymphocytes recruit leukocytes from bloodstream to airways and direct release of inflammatory mediators from eosinophils, mast cells, and lymphocytes (Robinson, 2010). CD4 type 2 T helper (Th2) cells release interleukin(IL)-4, IL-5 and IL-13. IL-4 together with IL-13 trigger the switching of Ig class from IgM to IgE antibody. Thereafter, IgE-allergen complexes lead to mast cell degranulation and subsequent release of spasmogens from mast cells including histamine, leukotriene(LT)C_4, and prostaglandin(PG)D_2 which directly contract the bronchial smooth muscle and exacerbate airway inflammation (Martinovic, 2013; Murphy & Byrne, 2010).

Other mediators released in the early stage from mast cell degranulation include IL-6, IL-13, tumour necrosis factor-α (TNF-α) and neutral proteases such as tryptase and chymase which have demonstrated range of actions in keeping with airway inflammation and airway hyperresponsiveness (Bradding et al. 2006; Bradding 2007). Additionally, IL-5 could recruit and activate eosinophils. Various chemotaxins and chemokines will recruit leucocytes, especially eosinophils and mononuclear cells into bronchus before proceeding to the LAR. The LAR is a progressive inflammatory process associated with airway hyperresponsiveness, particularly characterized by infiltration of Th2 cells and activation of eosinophils (Holt & Sly, 2007; O'Byrne et al., 2009). Other putative mediators in LAR are induced NO, adenosine, and neuropeptides (Holgate & Polosa, 2006; Rang et al., 2015).

In the context of non-asthmatic chronic cough, some studies showed evidence of its association with airway inflammation, but the underlying mechanisms are not established yet (S. Y. Lee et al., 2001). Previous study revealed that increase in

submucosal mast cells, but not eosinophils or neutrophils, underlies the human airway inflammation (Niimi et al., 2005). Interestingly, airway remodelling, which is characteristic of asthma was also observed in both asthmatic and non-asthmatic cough (Birring, 2011). Besides, patients with eosinophilic bronchitis-associated chronic cough without characteristic of asthma have responded to inhaled corticosteroids, suggesting the role of airway inflammation as a marker in chronic cough (Christopher E Brightling, Ward, Goh, Wardlaw, & Pavord, 1999) .

1.1.5 Drug therapies and their limitations

The current cornerstone treatments for asthma remain to be bronchodilators and corticosteroid. Immediate short-acting and long-acting bronchodilators are prescribed for immediate relief and prevention of bronchoconstriction, respectively, whilst corticosteroids ease airway inflammation. The main drug classes for asthma are described in Table 1.1. The first-line bronchodilator is β_2-adrenoceptor agonists that relieve acute bronchoconstriction in asthmatic attack (Rang et al., 2015). Antimuscarinic drug is indicated as the second-line treatment for uncontrolled asthma, although it is relatively more effective for COPD (I. M. Adcock, Caramori, & Chung, 2008). Other drug classes such as cysteinyl leukotriene receptor antagonists and xanthines are occasionally used to manage uncontrolled asthma, especially in childhood asthma (I. M. Adcock et al., 2008). In the context of airway inflammation, corticosteroid is the most effective and widely used anti-inflammatory treatment for asthma at present (Alangari, 2014). Additionally, the advances in immunobiology of asthma therapy have prompted the development of several other drugs targeted at the cytokines pertaining to pathophysiology of asthma. The potential antiasthmatic agents in development encompass targets on cytokines, interleukins, TNF-α, histamine, PG, chemokine receptors, cell adhesions, transcription factors and kinases, and immunotherapy (Hanania, 2008).

Table 1.1: Current available treatment for asthma. (I. M. Adcock et al., 2008; Hanania, 2008)

Drug Class	Mechanism of actions	Available drugs
β_2-adrenoceptor agonist	• Agonist • Direct bronchodilation • Inhibits mast cell mediator and TNF-α release • Increase mucus clearance	• Salbutamol • Salmeterol • Formoterol
Muscarinic receptor antagonist	• M_3 antagonist • Direct bronchodilation	• Ipratropium
Corticosteroids	• Anti-inflammatory • Inhibits T cell activation, cytokines formation, leukotrienes, eosinophil infiltration and activation, mast cell production	• Beclomethasone • Fluticasone • Prednisolone
CysLT receptor antagonist	• $CysLT_1$: Respiratory mucosa • $CysLT_2$: Inflammatory cells infiltration • Bronchodilation and reduced sputum eosinophilia	• Montelukast • Zafirlukast
Xanthine	• Inhibition of PDE and increases cAMP and cGMP • Bronchodilation	• Theophylline
Anti-IgE antibody	• Monoclonal anti-IgE antibody • Mainly for allergic asthma	• Omalizumab

Abbreviations: cAMP = 3′-5′-Cyclic adenosine monophosphate; cGMP = 3′-5′-Cyclic guanosine monophosphate; CysLT = cysteinyl leukotriene; IgE = Immunoglobulin E; PDE = phosphodiesterase; TNF-α = tumour necrosis factor-α

Despite the mainstay combinatorial treatments that target both inflammatory processes and direct airway relaxation, asthma is still poorly controlled in a considerable population of patients. Various drawbacks of current therapies include tolerance towards β_2-adrenoceptor agonists due to β-adrenoceptor desensitization (Doeing & Solway, 2013), noncompliance towards medications due to fear of long-term side effects (especially corticosteroid) (Dinwiddie & Müller, 2002), poor inhaler technique (a device for administration of some antiasthmatic drugs which requires inspiration-actuation coordination technique), and steroid-resistant asthma in a subset of patients (Brar, 2004). There is a dire need for the development of new therapeutic agents with mechanisms of action different from conventional bronchodilators. The goals of new treatment are to be more patient-friendly and cost-effective, and with less side effects in reducing asthma exacerbations and improving control of asthma.

On the other hand, there is unmet clinical need for effective treatment of chronic idiopathic cough (cough due to unknown causes), which has limited therapeutic options available (Birring, 2011). Recommendations of current guideline focus on treating the coexisting conditions with chronic cough, such as asthma and gastroesophageal reflux (Birring, 2011). Centrally acting antitussive agents including codeine and morphine are not without limitations e.g. central nervous system adverse effects. Therapies targeting the airway transient receptor potential (TRP) ion channels have come into limelight in recent years. TRPV1, TRPA1, and TRP melastin 8 (TRPM8) channels appear to be novel targets for antitussive agents and the investigations of their antitussive potential are ongoing (Andrè et al., 2009; Millqvist, 2016).

1.2 Drug discovery

The lack of efficacy, growing tolerance, as well as vicious side effects of the current medicinal treatments for diseases are the mainspring of drug discovery project, which is initiated based on hypothesis that the activation or inhibition of a pathway or protein will generate therapeutic benefit (Hughes, Rees, Kalindjian, & Philpott, 2011). In new drug discovery, the initial important steps are target identification and validation. A drug target refers to a binding site by which the drug binds to and exerts its action to modulate the biological activities *in vivo* (Gashaw, Ellinghaus, Sommer, & Asadullah, 2011). Drugs, which can 'hit' the targets consist of small-molecular-weight molecule mainly targeting enzymes, extracellular and nuclear receptors, ion channels and transporters, or biologics targeting protein and cell surface receptors. An ideal target should be safe, efficacious, "assayable" to allow for High Throughput Screening (HTS) that screens for a large amount of compounds, and meet clinical and commercial needs. Following the identification, drug target needs to be validated by using various techniques ranging from *in vitro* to *in vivo* models, including literature survey and competitor information, genetics, molecular signalling pathway, cell-based assay, molecular pharmacology, and so on (reviewed by Gashaw et al., 2011; Hughes et al., 2011).

Subsequently, a number of 'hits' (i.e. biological molecules or compounds which show desired activity during screening and confirmed with retesting) are obtained through intensive screening assays (Hughes et al., 2011). The next stage is to refine each hit by generating concentration-response curves in order to compare their potencies through IC_{50} (half maximal inhibitory concentration) and EC_{50} (half maximal effective concentration). Chemistry programme with intensive structure–

activity relationship analysis is run to improve the potency, selectivity, and physiochemical properties of the 'hit', leading to 'lead' development and optimization. Tissue- and cell-based assays will be employed at this stage to examine the functional response of the surviving 'hits' in more intact systems (Hughes et al., 2011).

To optimize the 'lead' and to identify a highly selective candidate for preclinical testing, an array of secondary assays, including safety, toxicity, pharmacokinetics and pharmacodynamics studies, are undertaken. Following preclinical studies, drug candidates go through Investigational New Drug filing and clinical development. Eventually, the new drug is subjected to approval by New Drug Application (NDA) and Food and Drug Administration (FDA) before marketing. The whole drug development pipeline is a lengthy process that commonly takes more than 10 years to produce a safe and efficacious medicinal product after passing numerous rigorous testing and regulatory requirements (reviewed by Hughes et al., 2011). At the present time, drug discovery output is still unable to cope with the need of drug to treat most diseases and to address the current therapy issues in numerous diseases (Harvey, Edrada-Ebel, & Quinn, 2015).

1.2.1 Natural products as therapeutic agents

Natural products sourced from plants, fungi, algae, bacteria, and marine lives have a long history of use by folklore for medicinal purposes in disease prevention and treatment since the ancient time, as far as 2600 B.C., to modern days (reviewed by Dias et al., 2012). Their traditional uses as documented in literature frequently form basis for the primary screening stage of crude extracts and/or fractions from natural

products to guide new drug discovery. One of the examples is theophylline, extracted from the green tea leaf (*Camellia sinensis*), acts as a bronchodilator (Fabricant & Farnsworth, 2001) and has been used as an adjunct treatment for asthma and COPD. Among the new drug developed for antiasthmatic therapies from 1980 to 2010, about 35% of them were indirectly sourced from natural products (Newman & Cragg, 2012). Despite the current trend of drug synthesis towards chemical combinatorial method, there is no doubt natural products will continue to play an imperative role in new drug development.

Indeed, the use of natural products has gained popularity among patients of late to treat various respiratory diseases, especially asthma (T. P. Ng, Wong, Hong, Koh, & Goh, 2003; Rivera, Hughes, & Stuart, 2004). Despite the prevalence of natural product usage among asthmatic patients, poor evaluation of efficacy and safety, and lack of regulation of the use of natural products are worrying as there are risks of potential disease state interaction and adverse events. Hence, there is a need for comprehensive scientific validation of these natural products to minimise adverse events. In view of this, in an effort to harness the potential contribution of natural products to health and to promote safety and effectiveness of natural products through research and development, WHO Traditional Medicine Strategy 2014–2023 is developed to serve as the national policy and guideline in these aspects. Therefore, the exploitation of natural products is worthwhile in the quest for new novel bioactive agents and to facilitate the discovery of 'lead' for drug development. Bioassays with good cost-effectiveness, pharmacological relevance, and reproducibility are required to expedite the early screening process of natural product 'hit'. Some assays of relevance to this project will be discussed in Section 1.4.

1.2.2 Medicinal mushrooms: Traditional medicinal values and scientific evidence

For centuries, macro fungi or medicinal mushrooms have been broadly used by humans as traditional remedies for preventing and treating human diseases, particularly in China, India, Japan and Korea (De Silva, Rapior, Hyde, & Bahkali, 2012). Until today, several drugs have been developed from mushrooms, for instance, krestin obtained from the cultured mycelia of *Coriolus versicolor* (Kobayashi, Matsunaga, & Oguchi, 1995), lentinan derived from *Lentinus edodes* (Ina, Kataoka, & Ando, 2013), and schizophyllan obtained from the liquid cultured broth product of *Schizophyllum commune* (Y. Zhang, Kong, Fang, Nishinari, & Phillips, 2013). Interestingly, these bioactive substances are all mushroom polysaccharides, and are currently in clinical use as anticancer therapy in Japan or China. One of the most established mushrooms in the folk medicine is probably *Ganoderma lucidum*, which is also known as ling zhi in Chinese. *Ganoderma lucidum* is traditionally regarded as a general tonic, along with antiasthmatic, antitussive effects, anti-fatigue, anti-aging, and many other properties (Wachtel-Galor, Yuen, Buswell, & Benzie, 2011). To date, it is still being taken for the aforementioned purposes. Besides, other well-known medicinal mushrooms such as *Cordyceps sinensis*, *Tremella mesenterica*, *Coriolus versicolor*, *Laetiporus sulphurous*, and *Laricifomes officinalis* also have well-documented traditional usage in treating asthma, cough, or tuberculosis (Grienke, Zöll, Peintner, & Rollinger, 2014; Hobbs, 2002; Tuli, Sandhu, & Sharma, 2014).

Macro fungi that encompass the phylum Basidiomycota and some Ascomycota represent a large repertoire of pharmacologically active novel substances, ranging from high-molecular-weight compounds such as polysaccharides, proteins and lipids,

as well as low-molecular-weight metabolites including terpenoids, alkaloids, phenols, lectins, nucleotides, and others (De Silva et al., 2013). These bioactive substances are mostly obtained from the mycelial biomass, fruiting bodies, or supernatants of submerged cultures using bioreactors (Poucheret, Fons, & Rapior, 2006). Crude extracts or fractions of mushrooms have reported lipid-lowering, antioxidant, antitumor, antiproliferative, anti-inflammatory, antidiabetics, and other activities (De Silva et al., 2012; Petrova, Wasser, Mahajna, Denchev, & Nevo, 2005; Poucheret et al., 2006; Z. C. Zhang, Lian, Huang, & Cui, 2009).

Medicinal fungi and their metabolites are notable for immunomodulatory activities (De Silva et al., 2013; Hu, Huang, Wong, & Yang, 2017; Seema Patel & Goyal, 2012; Singh et al., 2015). While most studies link the immunomodulatory properties of these mushrooms to cancer therapy, our focus is on their immunosuppressive properties pertaining to the allergic components in asthma. Triterpenes isolated from *G. lucidum* (Kohda et al. 1985) and aqueous extract of *Phellinus linteus* (Choi et al., 2006) have inhibited the antigen-induced histamine release from rat peritoneal mast cells. Choi et al. (2006) also observed that *P. linteus* extract elevated cAMP levels and inhibited calcium uptake into mast cells, which is requisite for degranulation. Besides, Oh et al. (2011) reported that *Cordyceps militaris* extract inhibited β-hexosaminidase release from RBL-2H3 (rat basophil leukaemia) cells, along with reduced passive cutaneous anaphylaxis response to antigen (bovine serum albumin) challenge in mice. In another study using ovalbumin-challenged mice model, hot water extract of *Ganoderma tsugae* significantly decreased the ovalbumin-induced elevation of serum histamine, PGE_2, and leukocyte infiltration in the bronchoalveolar lavage fluid (BALF) (Lin, Chen, Chiang, & Lin, 2006).

Bronchodilator properties of medicinal mushrooms are also reported. Triterpenoid-rich extract of *G. tsugae* has reduced methacholine-induced airway hyperresponsiveness in ovalbumin-challenged mice model, suggesting that triterpenes are responsible for the antiasthmatic properties (M. L. Chen & Lin, 2007). A herbal medicine intervention therapy, namely ASHMI, containing *G. lucidum* has abolished acetylcholine-induced contraction in tracheal rings from asthmatic and normal murine (T. Zhang et al., 2010). However, this combinatorial herbal therapy contains two other herbs, complicating the identification of the bioactive components. Another study also showed that asthmatic human subjects taking *C. sinensis* capsules have improved lung functions in terms of airway obstruction parameters (N. Wang, Li, Huang, Chen, & Chen, 2016). Taken together, the bronchodilator and anti-inflammatory properties of mushrooms are mostly based on *in vitro* assays and limited to a few mushroom species. Although it appears that medicinal mushrooms may hold the potential to be developed into supporting therapy for asthma, the precise bioactive components and mechanisms of action are still poorly understood.

1.3 *Lignosus rhinocerotis*

1.3.1 Background

Lignosus rhinocerotis, or locally known as Tiger's Milk Mushrooms (TMM), is a popular medicinal mushroom consumed by the indigenous communities in Southeast Asia and Southern China for several centuries. It is mainly distributed in South China, Malaysia, Australia, Africa, Papua New Guinea, Borneo, Philippines, Indonesia, Sri Lanka and Vanuatu (Abdullah et al. 2013;Cui et al. 2011). The history of usage of *L. rhinocerotis* can be dated back to 1664 when it was first recorded in the name of "*Lac Tygridis*" (meaning tiger's milk) by a European government agent who travelled to Southeast Asia (William & Russell, 1907). He described that the local communities used this medicinal fungus to treat incurable diseases. Several others described a fungus species called 'susu rimau' (literally means "tiger's milk") which is used by the Malays to treat "consumption" (or tuberculosis in modern term) and cough (Henry Nicholas Ridley 1890; Burkill 1966). Although TMM is thought to refer to *L. rhinocerotis* collectively, a recent survey suggests that the term TMM used by indigenous communities in Malaysia possibly encompasses other *Lignosus* spp. as well (Lau, Abdullah, Aminudin, Lee, & Tan, 2015). This thesis only focused on *L. rhinocerotis* as it is most used by other researchers, and the local term TMM is generally referred to this particular species.

Belonging to the family of *Polyporaceae* (Basidiomycota), *L. rhinocerotis* consists of two parts: the sclerotium buried underground, and the fruiting body growing above ground with hard and woody stalk (stipe) supporting the cap (pileus). A picture of *L. rhinocerotis* is illustrated in Fig. 1.4. The sclerotium, which is also regarded as the nutrient store of mushroom is initially formed by aggregation of

hyphae (mycelium), then developed into a hard, resting structure (Willetts & Bullock, 1992). The sclerotium can remain dormant for years, and the fruiting body will sprout from it only when the conditions become favourable for growth. The local name TMM was inspired by the whitish appearance of the inside of sclerotium that resembles congealed tiger's milk. On the other hand, *Polyporus rhinocerus*, or hurulingzhi in Chinese, is identified to be taxonomically synonymous of *L. rhinocerotis* (N. L. Huang, 1999). Researchers from Hong Kong have extensively studied on *P. rhinocerus*; nonetheless, molecular analysis has yet to be done to compare the ribosomal RNA (rRNA) between *P. rhinocerus* and *L. rhinocerotis*.

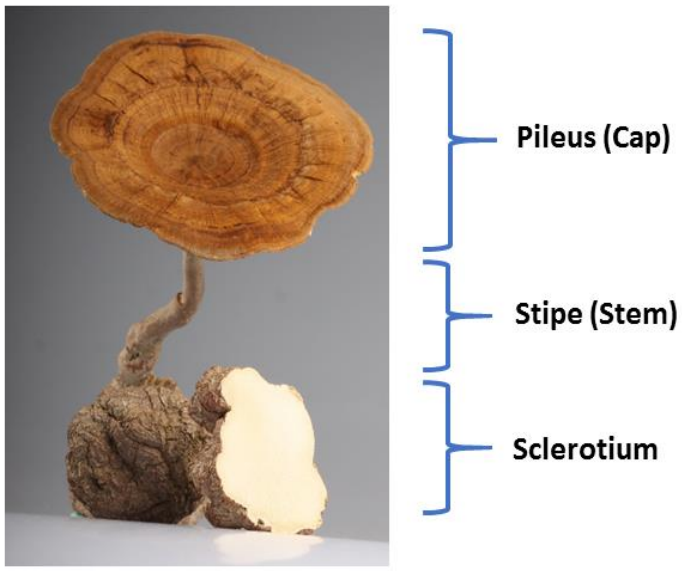

Figure 1.4: The fruiting body of *Lignosus rhinocerotis* consists of pileus (cap) and stipe (stalk) attached to the nutrient-rich sclerotium.

1.3.2 Ethnomedicinal uses

Being hailed as the "national treasure", TMM, in particular *L. rhinocerotis*, is amongst the most important medicinal mushrooms in Malaysia (C. S. Tan et al., 2012). Traditional uses of TMM in Malaysia are well documented in ethnobotanical surveys (Azliza et al., 2012; Chang and Lee, 2004). A survey showed that TMM is the most common macro fungi used by the majority of indigenous communities in Peninsular Malaysia (Su See Lee et al., 2009).

Based on ethnomycological records, the medicinal values of TMM are mostly derived from its sclerotium (Chang and Lee, 2004). Aborigines usually use it to treat cough, asthma, fever, cancer, food poisoning, wound healing, and as a general tonic. It is noted that for the main traditional medicinal uses including asthma, cold and cough, TMM is generally consumed orally by drinking the decoction (boiled alone or with other herbs) or by eaten raw (Azliza et al., 2012; Chang & Lee, 2004; Su See Lee et al., 2009). TMM is also taken by the Mah Meri with *Piper betle* L., *Areca catechu* L. and slaked lime for asthma and breathlessness; whereas in Pahang, TMM is chewed in betel-quid by the Malays to relieve cough (reviewed by Lau et al., 2015). Some of the traditional consumption methods of TMM for various medicinal purposes are summarized in Table 1.2. In China, the sclerotium of *P. rhinocerus* is sold in Chinese herbal shop as a traditional medicine to treat liver cancer, chronic hepatitis and gastric ulcer (N. L. Huang, 1999).

Table 1.2: Ethnomedicinal uses of Tiger Milk's Mushrooms (*Lignosus* spp.) by selected tribes of indigenous people in Peninsular Malaysia. (Adapted from Lau et al., 2015)

Tribes	Location	Part used	Method of preparation/ administration	Ailments treated
Kensiu	Lubuk Ulu Legong, Baling, Kedah	Sclerotium	-Burned and applied on chest -Eaten raw -Shredded, mixed with water, and applied topically	-Asthma -Increased energy -Breast cancer
Temuan	Ulu Kuang, Gombak, Selangor	Sclerotium	-Mixed with *Polyalthia bullata* (Tongkat Ali Hitam) and boiled -Decoction -Eaten raw	-Postpartum -Cough, cold, and asthma -Asthma
	Bukit Lagong, Gombak, Selangor	Sclerotium	-Decoction	-Asthma
	Songkok Village, Hulu Selangor, Selangor	Sclerotium	-Grated, steamed, and mixed with the beak of 'burung lilin' (scientific name not available)	-Asthma
	Sungai Jang, Hulu Selangor, Selangor	Sclerotium	-Eaten raw -Squeezed and applied topically	-Asthma -Lactogogue (increases breast milk)
	Hulu Tamu, Hulu Selangor, Selangor	Sclerotium	-Eaten raw -Decoction	-Tonic for men and women -High fever, headache, overall health
	Sungai Bumbun, Kuala Langat, Selangor	Sclerotium	-Eaten raw	-Enhances body strength and physical fitness

Overall review on the records concludes that TMM has been mainly taken for treating asthma and chronic cough since time immemorial. As previously described, asthma and chronic cough often share similar pathophysiological features and symptoms such as narrowed airways and difficulty in breathing (Section 1.1). Hence, it is likely that the indigenous communities may not be able to explicitly distinguish these two medicinal conditions, and have been using this mushroom to relieve breathing difficulties in general.

1.3.3 Medicinal properties

As *L. rhinocerotis* grows solitarily, it is difficult to locate *L. rhinocerotis* in the jungle, hence deterring the researchers from exploiting its biological activities. There was little research conducted on *L. rhinocerotis* until year 2009, when Tan (2009) reported a successful cultivation of this mushroom in agar, solid and spawn media. Consequently in September 2010, *L. rhinocerotis* was listed in the traditional medicine active ingredient list under the Malaysian National Pharmaceutical Control Bureau. Following this, the supply of *L. rhinocerotis* for pharmacological studies and therapeutic purpose is made possible. In addition, successful cultivation of this mushroom by liquid fermentation techniques was also reported by other researchers (reviewed by Lau et al., 2015).

Studies conducted to date have concentrated on the cultivar of *L. rhinocerotis*, but there are also some that compared the medicinal properties between its wild type (specimen collected from jungle) and cultivar (cultivated for commercial or research purpose). Conventionally, *L. rhinocerotis* is identified by taxonomic classification (by

their morphological characteristics); however, such method is less precise. To allow more accurate authentication of *L. rhinocerotis* specimen, molecular analysis using genetic markers by internal transcribed spacer (ITS) gene region of rRNA was developed (Chon Seng Tan, Ng, Vikneswary, Lo, & Tee, 2010).

The following subsection presents a general overview of the pharmacological activities of *L. rhinocerotis* either directly or indirectly related to their ethnomedicinal uses. Most researchers used aqueous extract in their experiments, as it resembles the traditional aqueous preparations of *L. rhinocerotis* by decoction and maceration.

1.3.3.1 Antiproliferative and cytotoxic properties

Antiproliferative and cytotoxic activities of *L. rhinocerotis* are the most extensively studied to date, partly attributed to the purported anticancer effect of *L. rhinocerotis* in traditional claims. *L. rhinocerotis* extracts have demonstrated cytotoxic activities against solid tumour and leukemic cell lines (Lai et al. 2008; Lee et al. 2012; Zaila et al. 2013; Lau et al. 2013). Lai et al. (2008) was the first group to report the pro-apoptotic and antiproliferative actions of *P. rhinocerus* cultivar obtained from China. Cell viability of HL-60 (acute promyelocytic leukaemia), K562 (chronic myelogenous leukaemia) and THP-1 (acute monocytic leukaemia) cell lines were significantly reduced by the hot water extract of *P. rhinocerus*. The hot water extract was also shown to induce cell cycle arrest at sub G_1 and G_1 phases leading to apoptosis. Nevertheless, the cold alkaline extract was devoid of any antiproliferative effect.

In contrast to the study described above, Lau et al. (2013) reported that the hot water extract of *L. rhinocerotis* cultivar (via solid-substrate fermentation) exhibited

relatively weak cytotoxicity against all cell lines in comparison to cold water extract, which exhibited strong antiproliferative effect against several solid cancer cell lines as well as leukemic cell lines. Similarly, an *in vitro* study by Lee et al. (2012) demonstrated that the cold water extract of *L. rhinocerotis* cultivar (TM02) has decreased cell viability and induced apoptosis of both MCF7 and A549 cell lines. Nonetheless, *L. rhinocerotis* has exhibited selective cytotoxicity towards certain normal human cells (Lau et al., 2013; M. L. Lee et al., 2012; Zaila et al., 2013). In general, several studies proposed that the proteins or polysaccharide-protein complex are the bioactive components accountable for the antiproliferative and apoptotic activities (Lai et al., 2008; M. L. Lee et al., 2012).

When comparing the cytotoxicity between wild type and cultivated strain (or cultivar), cultivated strain appears to have richer nutrient in sclerotium with stronger antioxidant and antiproliferative activities (Y. H. Y. Yap et al., 2013). As a whole, the varied cytotoxic actions of *L. rhinocerotis* observed in different studies may be attributed to the differences in geographical origins, cultivation methods, and postharvest processing protocols. The different harvest stage may also contribute as the cultivated strain is harvested before formation of cap and stipe whilst wild type mushroom is only collected after the emergence of fruiting body from underground (Abdullah et al., 2013; H. Y. Yap et al., 2014). More nutrients are reserved in the sclerotium before formation of cap and stipe, and hence medicinal value may remain in the sclerotium of cultivar.

1.3.3.2 Immunomodulatory and anti-inflammatory properties

Many mushroom polysaccharides are shown to activate host's immune system e.g. macrophages, natural killer (NK) cells, T helper cells, and other effector cells (Jeong, Koyyalamudi, Jeong, Song, & Pang, 2012; Mizuno et al., 2000; Ren, Perera, & Hemar, 2012). These polysaccharides belong mainly to the β-glucan group. Both water-soluble polysaccharide-protein complex and alkaline-soluble β-glucan extracted from *P. rhinocerus* have stimulated an upregulation of Dectin-1 receptors (cell surface β-glucan receptors) on innate immune cells and proliferation of $CD56^+$ NK and normal human spleen monocyte/macrophage cells (Wong, Lai, & Cheung, 2009). The glucans and polysaccharide-protein complex also stimulated proliferation of NK-92MI cells (human IL-2-independent NK cell line derived from NK-92 cells by transfection) with increased expression of cytokines, IL-2 and I-309. The antitumor effect of β-glucan is suggested to be mediated via activation of innate immunity by binding on Dectin-1 receptors (Batbayar, Lee, & Kim, 2012).

Further *in vivo* assays have supplemented the *in vitro* results. Immunostimulatory effects of *P. rhinocerus* were examined by Wong, Lai, & Cheung (2011). Healthy BALB/c mice and athymic nude mice intraperitoneally injected with the sclerotial polysaccharide-protein complex and β-glucan have stimulated serum cytokine profile: β-glucan mainly activated neutrophils, while polysaccharide-protein complex stimulated the functions of a wide range of innate immune cells. Such differences are suggested to attribute to the structural differences between polysaccharide-protein complex and β-glucan. It was concluded in the same study that the sclerotial polysaccharides could activate the innate immune system even without activating the adaptive immune system. Another recent study by Hu et al. (2017a)

investigated the effects of four polysaccharide fractions from *L. rhinocerotis* cultivar, each containing varying compositions of β-D-glucan and proteins. All fractions exhibited protective effects against cyclophosphamide-induced immunosuppression in mice model with increased release of major cytokines, TNF-α and interferon-α.

Aside from immunostimulatory activity, *L. rhinocerotis* also shows anti-inflammatory properties. The methanol, cold water and hot water extracts exhibited significant anti-inflammatory effect, with the highest potency from cold water extract, which significantly reduced *in vivo* carrageenan-induced paw oedema during the three phases of oedema development in Sprague Dawley rat (Sook Shien Lee et al., 2014). In the same study, the high-molecular-weight as well as medium-molecular-weight fractions of cold water extract significantly inhibited TNF-α production in RAW264.7 (murine macrophage cells) cells. In following tests, the protein components of the high-molecular-weight fraction strongly inhibited lipopolysaccharide-induced TNF-α production in RAW264.7 cells. On the contrary, non-protein components were inactive, strongly suggesting that the proteins are accountable for the anti-inflammatory effect (Sook Shien Lee et al., 2014).

Besides, Johnathan et al. (2016) has investigated the effect of *L. rhinocerotis* on inflammatory markers of asthma, including serum IgE levels, cytokine profiles, and inflammatory cells infiltration into lungs. Airway inflammation model of Sprague Dawley rat was induced by ovalbumin sensitization and challenge. Before the ovalbumin challenge, these rats were orally fed with hot water extract of *L. rhinocerotis* for 7 days. Findings revealed that the hot water extract significantly attenuated eosinophil cell infiltration into lung tissues and reduced the levels of serum IgE and Th2 cytokines such as IL-4, IL-5 and IL-13 in BALF. The decrease in these inflammatory markers related to asthma leads to our conjecture that *L. rhinocerotis*

may have antiasthmatic potential, in support of its main traditional usage to alleviate asthmatic symptoms.

1.3.3.3 Other biological activities

Apart from the aforementioned properties, *L. rhinocerotis* has demonstrated a broad spectrum of medicinal properties, including antioxidant (Y. H. Y. Yap et al., 2013), antimicrobial (Mohanarji, Dharmalingam, Kalusalingam, & Science, 2012; Zaila et al., 2013), antiviral (reviewed by Lau et al., 2015), neurite outgrowth stimulation (Eik et al., 2012; Phan, David, Naidu, Wong., & Sabaratnam, 2013; S. L. S. Seow et al., 2015), and fibrinolytic (Ahmad, Noor, & Ariffin, 2013) activities. These properties are demonstrated mainly in preliminary *in vitro* assays and mostly attributed to the aqueous extract. Nevertheless, the exact components or molecular mechanisms contributing to these properties are yet to be delineated.

1.3.4 Chemical investigations

Despite the rising interest in medicinal properties of *L. rhinocerotis*, bioactive compounds accountable for the activities are yet to be isolated and purified. Studies thus far have used crude extracts and fractions obtained by chromatographic separations, and the bioactive components are proposed based on the chemical composition analysis. According to previous studies (Lau et al., 2013; M. L. Lee et al., 2012; Y. H. Y. Yap et al., 2013), the sclerotial aqueous extract of both wild type and cultivar of *L. rhinocerotis* mainly comprises polysaccharides (predominantly β-

glucans), proteins, and polysaccharide-protein complex. These components are suspected to be responsible for the antiproliferative, immunomodulatory and anti-inflammatory activities of the mushroom, in which glucose and mannose appeared to be the important sugar residues in the glycosidic linkage of polysaccharide-protein complex (Lai et al., 2008; Liu, Chen, Chen, Huang, & Cheung, 2016).

Recently, the structural characteristics of an alkaline-soluble polysaccharide obtained from sclerotia of *L. rhinocerotis* cultivar were investigated by Fourier transform infrared spectroscopy, gas chromatography, gas chromatography-mass spectroscopy (GC-MS), 1D and 2D nuclear magnetic resonance spectroscopy (Hu, Huang, Wong, Yang, et al., 2017). The polysaccharide was determined to be a hyperbranched structure with (1→3)-β-D-glucan backbone and adopted compact coil conformation. The structural characteristics of β-D-glucan are believed to play an important role in its biological activities (Wong et al., 2011). Hence, study on the structure-activity relationship of glucan is warranted to facilitate the elucidation of its mechanisms of action.

While the investigations of *L. rhinocerotis* mainly centre on its large-molecular-weight compounds, there are limited phytochemical analysis done, in particular for the secondary metabolites. Phytochemical screening revealed that *L. rhinocerotis* extracts contain alkaloids, phenols, flavonoids, gum and mucilage (Mohanarji et al., 2012; Y. H. Y. Yap et al., 2013; Zaila et al., 2013). Presence of triterpenoids, sugars and their derivatives, fatty acids and their methyl esters, cyclic peptides, sterols, and amides in the mushroom sclerotial and mycelial extract were identified using GC-MS and ultra-high-performance liquid chromatography–electrospray ionization–tandem mass spectrometry (UHPLC-ESI-MS/MS) methods (Lau et al., 2014). In addition to chemical profiling, genome studies also provided

insights into genetic and molecular basis of the medicinal properties of *L. rhinocerotis*. Lectins, cerato-palatanin, and serine proteases are identified to be the three major protein constituents of *L. rhinocerotis* sclerotium by using genome-based proteomic and transcriptomic analysis (H. Y. Y. Yap, Chooi, et al., 2015; H. Y. Y. Yap, Fung, Ng, Tan, & Tan, 2015a, 2015b). The genome of *L. rhinocerotis* also codes for fungal immunomodulatory proteins and sesquiterpenoid (H. Y. Y. Yap, Fung, et al., 2015a; H. Y. Y. Yap et al., 2017). Medicinal properties of *L. rhinocerotis* may be attributed to the aforementioned substances; therefore, there is need to isolate, purify, and characterize these compounds to investigate their bioactivities.

1.4 Research approaches

As mentioned in Section 1.2, generation of drug dose-response relationship is essential in the initial screening stage, whereas cell-based assay is indispensable throughout target identification and validation and lead discovery process. In the following subsections, assays relevant to this thesis are reviewed.

1.4.1 Functional studies of smooth muscle

Smooth muscle contraction is often associated with the pathogenesis of diseases, as well as in health (Brozovich et al., 2016; Doeing & Solway, 2013; Michel, Li, & Lacolley, 2012). A number of *in vivo*, *ex vivo*, and *in vitro* models, from using whole animals, tissues to cells, have been developed to investigate the smooth muscle contractility. However, each model has discrete advantages and limitations that are dependent on the level of integration of multiple cell types and the complexity of the mechanical environment (D. Wright et al., 2012). Models used to study airway smooth muscle function are detailed in Table 1.3.

Table 1.3: Summary of common models used to study airway smooth muscle contraction. (Adapted from Wright et al., 2012)

Model	Advantages	Disadvantages
***In vivo* small animals**	• Assessment of response in fully integrated system • Many ways of developing AHR models	• Cannot directly assess ASM contraction • Questionable relevance for assessing lung mechanics • May not replicate airway wall remodelling
***Ex vivo* airway segments**	• Maintains mechanical properties of airway wall • Maintains integrated multi-cell system • Easy application of dynamic mechanical strain	• Cannot directly assess ASM contraction • Restricted to short term studies due to limited lifespan
Thin cut lung slices	• Maintains integrated multi-cell system • Maintains parenchymal mechanics • Direct visualisation of ASM contraction and signalling events (recordable by using fluorescent dyes)	• Loss of diffusion barriers normally present within the intact lungs • Difficult to isolate source and target of secreted mediators
ASM strip/ring	• Most direct measure of ASM contractility • Easy application of mechanical strain	• Lack of integrated responses and multiple cell types • Restricted to short-medium term studies
***In vitro* cell culture**	• Direct focus on contractile regulatory pathways • Enables very long term studies • Fresh tissue not required	• Progressive loss of contractile phenotype • Lack of integrated responses and multiple cell types • Non-physiological mechanical environment
Engineered tissues	• Reconstruct tissues with single cells • Direct cell function with custom matrices of multiple cell types	• Models are largely unproven

Abbreviation: ASM = Airway smooth muscle; AHR = Airway hyperresponsiveness

1.4.2 Organ bath as a pharmacological tool to assess smooth muscle function

Organ bath is commonly used as a pharmacological tool to assess the effects and elucidate the mechanisms of action of drugs or compounds in various contractile tissues, including airway, blood vessel, bladder, uterine and gastrointestine. *In vitro* preparation of smooth muscle strips or rings could be used in organ bath to construct drug dose–response relationships in target tissues when screening for new drug candidates. The potency and efficacy at tissues of interest, as well as the selectivity of the lead compound could be established before being subjected to *in vivo* pharmacological study (Semenov, Herlihy, & Brenner, 2012). This is crucial in drug discovery during lead optimization process in order to develop new molecules with high selectivity to the target tissues.

Unlike the *in vivo* or *ex vivo* models, which are largely affected by systemic influences from multiple cell types and complex mechanical environment, organ bath provides a direct measurement of smooth muscle contractility in an isolated system (Jespersen, Tykocki, Watts, & Cobbett, 2015). Compared to the intact animal model, this *in vitro* technique is relatively easier to instrument, and the variables, for example drug administration and tissue environment, are more readily controlled by the researchers. With careful dissection, the structures, such as smooth muscle and endothelium/epithelium layers, and innervation of the tissue of interest can be retained to a large extent for functional studies (Fastier & Reid, 1949; Jespersen et al., 2015; Semenov et al., 2012). In light of these advantages of organ bath, this technique was employed in this thesis to investigate the effect of *L. rhinocerotis* on smooth muscle of trachea, bronchus, bronchiole, aorta, coronary artery and ileum. The organ bath set up is elaborated in **Chapter 2**.

1.4.3 Cell-based assay

In recent years, cell-based assay has gained popularity and constitutes a large part of HTS. In comparison to biochemical assay, the outcome of cell-based assay is more relevant to *in vivo* biological responses and it can minimize animal testing. Depending on the research interest, a number of cell-based assays are available with different choices of cells (e.g. cell lines or model organisms), assay approaches and detection methods (An & Tolliday, 2009; Zang, Li, Tang, Wang, & Yang, 2012). When selecting a cell-based assay, a few factors need to be considered: reproducibility, cost, pharmacological relevance and quality of the assay.

First, among the various cell types, immortalized cell lines are most widely used due to the ease of growth and maintenance, low cost, and good reproducibility. However, it is not without shortcoming as immortalized cell lines are homogenous cell population derived from a known tissue type. They may have undergone significant mutation and change in phenotype, and hence the cellular functions are not fully representative of the normal cell type (Zang et al., 2012). On the other hand, primary cells are in closer proximity to normal cells, but not all cell types are available and fresh sample preparation is required. They are also relatively harder to grow and maintain with shorter life span than the immortalized cell lines. Other cell types such as the stem cells represent an evolution to the cell-based assay, but they are also limited by disadvantages (Zang et al., 2012).

Second, cell-based assay approaches include functional assays (e.g. second messenger mobilization after GPCR activation), reporter gene assays (e.g. quantification of GPCR internalization using a GPCR-green fluorescent protein hybrid), and phenotypic assays for cellular processes (e.g. cell migration or cytokinesis)

(An & Tolliday, 2009; Zang et al., 2012). Researchers can make selections based on their research interest.

Last but not the least, the detection methods for examination and quantification of cellular activities comprise electrochemical, colorimetric, luminescent, and fluorescent methods (Szymański, Markowicz, & Mikiciuk-Olasik, 2012; Zang et al., 2012). These methods are briefly described in Table 1.4. Among all, fluorescence detection system is widely used as it provides high sensitivity that facilitates easy-to-operate assay procedure with a wide selection of fluorophores and readout modes.

Table 1.4: Detection methods in cell-based assays. (Szymański et al., 2012; Zang et al., 2012)

Methods	Principle	Example
Electrochemical	• Electrochemical biosensors incorporating biological recognition elements with electrochemical transduction units, based on cellular activity and function, cellular barrier behaviour, and recording/stimulation of electric potential of electrogenic cells	• Amperometric electrochemical methods using a specific enzyme electrode for the determination of pH, dissolved oxygen or glucose
Colorimetric	• Based on colour change upon interaction of cell metabolites and chemical reagents	• MTT or ELISA assay that measures the absorbance
Luminescent	• Luminescent signal in the form of light generated by bioluminescent compound or chemical reaction	• Measurement of gene expression e.g. luciferase gene using reporter gene assays
Fluorescent	• Fluorescent molecule (fluorophore) is excited by light at certain wavelength and emitted light at a longer wavelength	• Measurement of calcium signalling tagged with fluorophores in calcium imaging assay

Abbreviations: ELISA = Enzyme-linked immunosorbent assay; MTT= 3-(4,5-Dimethylthiazol-2-yl)-2,5- diphenyltetrazolium bromide

1.5 Research aims

Although *L. rhinocerotis* is highly regarded in treating airway conditions including asthma and cough, there is no scientific study done to date on its effects on airway function including how the patency of the respiratory tract is affected. So far only one study showed that *L. rhinocerotis* is possibly beneficial in airway inflammation rat model, deduced from the suppression of key inflammatory mediators in asthma and attenuated lung inflammation (Johnathan et al., 2016). Nevertheless, this study was limited to the anti-inflammatory properties, and did not report any direct physiological evidence that the mushroom could relieve obstructed airways. Scientific evidence that could substantiate the usage of *L. rhinocerotis* for medicinal purposes and as nutraceuticals is necessitated.

The rationale of this research is to validate the medicinal uses of *L. rhinocerotis*, to expand knowledge on this mushroom, and to explore its potential as an alternative or adjunct therapy to the conventional bronchodilators for treatment of airway diseases. Given the gap in existing literature, the following research questions are posed in this thesis: (1) What are the effects and mechanisms of action of the crude extracts of *L. rhinocerotis* on airway smooth muscle as well as other smooth muscles (blood vessels and ileum)? (2) How does fractionation of *L. rhinocerotis* extract by molecular weight affect the airway relaxation effect? (3) What are the effects of the crude extract of *L. rhinocerotis* on mast cell degranulation? The principal aim of this research was to investigate the pharmacological actions of *L. rhinocerotis* extract on smooth muscle preparations of different tissues, mainly in airways, and on mast cells to evaluate its antiasthmatic potential.

The objectives of this study were as follows:

(i) To investigate the relaxation effects of the aqueous (hot water and cold water) as well as organic solvent (by methanol) extracts of *L. rhinocerotis*, for the first time, in isolated airway tissues. **(Chapter 2)**

(ii) To elucidate the mechanisms of action of *L. rhinocerotis* extract-induced airway relaxation by using isolated airway tissues. **(Chapter 3)**

(iii) To investigate the influence of *L. rhinocerotis* extract on calcium dynamics by using isolated airway tissues and cell-based assay. **(Chapter 4)**

(iv) To assess the effect of *L. rhinocerotis* extract on other smooth muscles including blood vessels and ileum. This will provide insight into the general effects, mechanisms of action, potential side effects, and selectivity of *L. rhinocerotis* in different smooth muscles. **(Chapter 5)**

(v) To elucidate the bioactive components in *L. rhinocerotis* accounting for the airway relaxation effect. The efficacies of different molecular-weight fractions from the cold water extract are compared. **(Chapter 6)**

(vi) To examine the effect of *L. rhinocerotis* extract on mast cell degranulation by using cell-based assay. **(Chapter 7)**

Chapter 2. Extractions of *Lignosus rhinocerotis* and their pharmacological effects on airways

2.1 Introduction

Preliminary pharmacological screening of the bioactivities using straightforward and reproducible assays is crucial to verify the medicinal properties of natural products claimed in ethnobotanical surveys. Extraction is an important first step to isolate a mixture of potentially bioactive chemical components from natural products for further characterization of their pharmacological activities and purification (Sasidharan, Chen, Saravanan, Sundram, & Yoga Latha, 2011). Popular conventional extraction methods include soxhlet extraction, sonication, hydrodistillation, or maceration in water or organic solvents such as methanol, ethanol, chloroform, and so on (Azmir et al., 2013; Sasidharan et al., 2011). The resultant crude extracts comprise a mixture of chemical compounds of different polarities, and the extraction efficiency highly depends on the choice of solvents. Hence, when choosing the solvent, the polarity of targeted compounds should be the determinant factor. It is well recognized that the extraction method and solvent choice should ideally mimic or follow the traditional methods of preparation if applicable (Fabricant & Farnsworth, 2001).

As mentioned in Section 1.2.1 (**Chapter 1**), traditional uses of natural products often guide 'leads' discovery in drug development pipeline. In light of this, the traditional methods of preparation or administration of natural products should provide clues regarding the identification of potential bioactive components from natural products based on their physiochemical properties e.g. polarity, solubility and heat stability. Various extraction techniques such as aqueous and solvent-based extractions

that mirror the traditional methods could be employed to produce crude extracts for investigation. *L. rhinocerotis* is traditionally consumed by drinking the decoction or by eaten raw to treat asthma and chronic cough. Hence, to replicate these traditional consumption methods, *L. rhinocerotis* was extracted by dissolving the ground sclerotial powder in hot water and cold water in this chapter. In addition to aqueous extraction, methanol extraction was performed to assess the activity of non-aqueous extract. The resultant extracts were then freeze-dried for long-term storage. Thereafter, the extracts were subjected to organ bath experiments to screen for pharmacological activities. The set up of organ bath of relevance to this thesis was briefly described in the following subsection.

2.1.1 Organ bath set up

Isolated tissue bath technique was first introduced by Magnus in 1904, who showed that ileum strip bathed in warm oxygenated modified Ringer's solution retained its spontaneous movement. Two approaches of organ bath have been described. In earlier days, the "immersion" approach by which a drug was added into the bath, muscle response was recorded, and then the contents of organ bath were changed by washing was described. Later in 1949, the perfusion technique was developed in which contents of organ bath were changed intermittently via a constant flow of the bath solution (Fastier & Reid, 1949). This latter technique was then termed "superfusion" by Gaddum (Gaddum, 1953). Since then, the organ bath technique has been modified and improved by scientists over time, but both immersion and superfusion techniques have been commonly used for bioassays with various tissues and purposes (Frigo & Lecchini, 1970; Paton & Vane, 1963; Vane, 1964).

Typically, the organ bath set up is designed as such to mimic the physiological conditions in human, with oxygenation (95% O_2, 5% CO_2) in a temperature-controlled environment (~37°C). The organ bath apparatus normally consists of double-layered water-jacketed glass baths connected to a water bath, which maintains the temperature of glass baths. Tissues isolated from animals or humans are placed into organ baths filled with physiological salt solution, such as the Krebs-Ringer or Krebs-Henseleit bicarbonate solution, to measure the isometric or isotonic force. The use of isotonic or isometric measurement depends on the type of tissue and parameter of interest. Isometric measurement studies the tension of muscle with fixed length, while isotonic measurement measures the length of muscle without change in tension. Neural responses evoked by electrical field stimulation, and contractile or relaxant responses to pharmacological agents or compounds are reflected by the change in the tension of target tissues. As the smooth muscle relaxes or contracts, isometric tension will decrease or increase accordingly, and the resultant change in tension is recorded. Thus, the changes in isometric tension are considered a quantifiable measure representing the relaxant or contractile response of tissues to various stimuli, including drugs and extracts, and will be used throughout this thesis.

When setting up the organ bath, the tissues of interests are excised into rings or strips of fixed lengths. Then, each tissue ring or strip will be mounted to a glass rod, which is connected to the isometric force transducer via a silk thread. The transducer converts the force generated by muscle into an electrical signal to be detected by a data acquisition system (PowerLab software) installed in the laptop, which will then record the tissue response in the unit of tension. In certain experimental protocols, tissues can be mounted to electrical rod instead of glass rod for electrical field stimulation to stimulate the nerves innervating the tissues and release endogenous

neurotransmitters. This aspect was further described in **Chapter 5**. The organ bath set up for isometric measurement is depicted in Fig. 2.1.

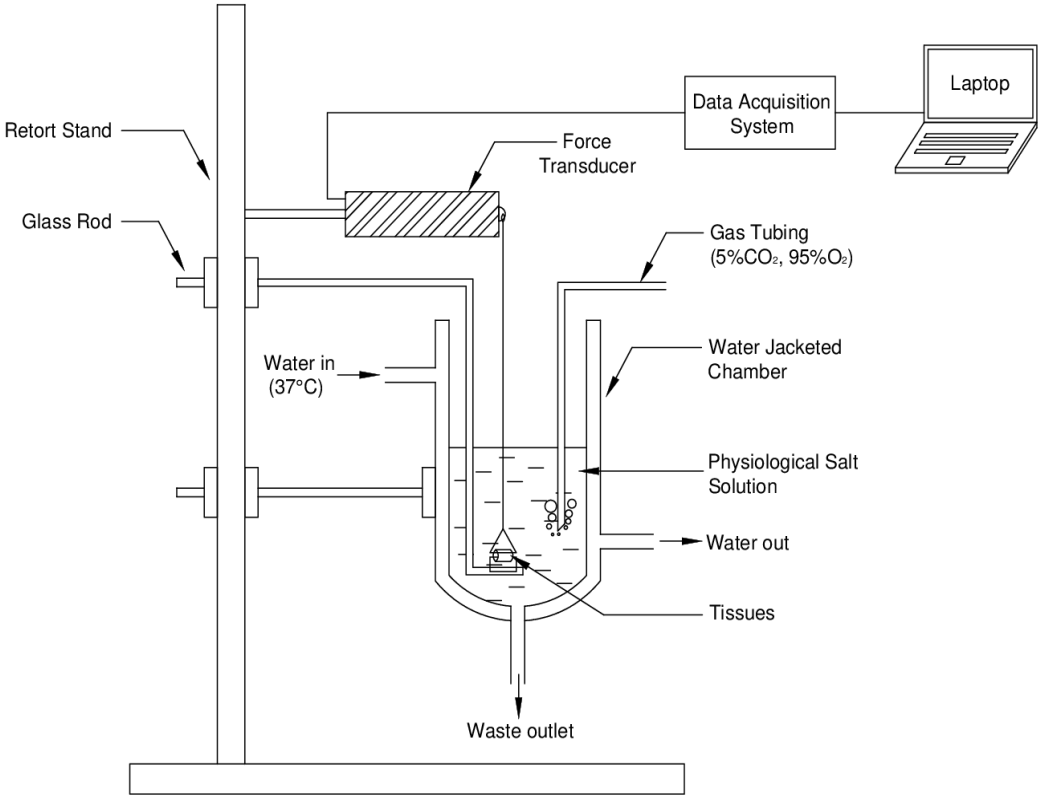

Figure 2.1: Schematic diagram of an organ bath set up. Tissue of interest is connected to the force transducer, which is in turn connected to a data acquisition system installed in the laptop to record the tissue response.

2.1.2 Rationale for tissue selection in study

In the respiratory tract, the upper airway i.e. trachea contains C-shaped rings of cartilage that keep the airways open (Reynolds, Pinkerton, & Mariassy, 2015). Trachea is composed of relatively high cartilaginous structures and low trachealis muscle, a bundle of smooth muscle surrounding the gaps between rings of cartilage. Moving towards the lower airways i.e. bronchus and bronchioles, the amount of cartilage decreases with increasing amount of smooth muscle, hence trachea contains relatively lesser smooth muscle than bronchus.

Asthma causes narrowing mainly of the lower airway i.e. bronchus. Despite that bronchial tissue represents more precise extrapolation of the responses in asthma, tracheal tissues are also commonly used in *in vitro* studies mainly due to the setbacks with using bronchial tissues. The primary concern is that the length of main bronchi that can be isolated from each animal is much shorter than trachea, meaning that more animals are needed to be sacrificed to achieve the desired number of replicates with bronchial tissues compared to tracheal tissues. Secondly, tracheal smooth muscle is perceived to adequately reflect the airway narrowing mediated by bronchial smooth muscle, and therefore is widely used to investigate airway smooth muscle response. Tracheal tissue is also easier to handle and isolate, with reproducible and dependable responses. Hence, both tracheal and bronchial tissues were used in the experiments in this chapter, and in some experiments of the following chapters, only tracheal tissues were used.

2.1.3 Significance of study

Experiments in this chapter aimed to optimize the extraction methods of *L. rhinocerotis* and screen the bioactivity of *L. rhinocerotis* extracts using isolated airway segments. Results derived from this chapter would provide reasonable basis for mechanistic studies in the following chapters. The specific objectives of this chapter were as follows:

(i) To perform cold water, hot water, and methanol extraction of *L. rhinocerotis* sclerotial powder.

(ii) To construct concentration-response curves (CRCs) to the extracts in pre-contracted airway segments using organ bath technique.

(iii) To compare the CRCs of the most active extract under different incubation time.

2.2 Materials and methods

Ground mushroom sclerotial powder (0.2 mm sieve) from *L. rhinocerotis* (TM02 cultivar) was supplied by Ligno Biotech Sdn. Bhd. (Selangor, Malaysia). The TM02 cultivar was identified by the ITS regions of their rRNA (Chon Seng Tan et al., 2010). The mushroom specimen voucher is deposited in the Royal Botanic Garden Kew, K(M)177812. Purified water of Mili-Q quality (18 MΩ) was used throughout the experiment.

2.2.1 Drugs and materials

Standard Krebs-Henseleit bicarbonate solution (abbreviated as "Krebs solution" throughout this thesis) (pH 7.4) was freshly prepared daily or the day before experiment and gassed with 95% O_2, 5% CO_2 for at least 15 minutes prior to use. The composition of Krebs solution is listed in **Appendix A.** Methanol was purchased from Sigma, USA. Carbamycholine chloride or carbachol (Nacalai Tesque, Japan) and ipratropium bromide (Tocris Bioscience, UK) were dissolved in purified water to make stock solution of 0.1 M. Potassium chloride (KCl) was purchased from R & M Chemicals, UK, and dissolved in purified water to make stock concentration of 3 M. Salmeterol xinafoate (Tocris Bioscience, UK) was dissolved in dimethyl sulfoxide (DMSO) (Sigma, USA) 100% to make stock concentration of 0.1 M and further diluted with 75% DMSO (v/v), 50% DMSO (v/v) and distilled water in 10-fold dilutions. The final concentration of DMSO in the baths was up to 0.3%.

2.2.2 Extraction

The extraction methods were adapted from previous paper (Y. H. Y. Yap et al., 2013). All extractions of sclerotial powder were performed with a mass:volume ratio of 1:20 (w/v). For hot water extraction, sclerotial powder was dissolved in water at 95-100°C (not boiling) for 2 hours, whereas for cold water extraction, sclerotial powder was dissolved in water and stirred for 24 hours at 4-7°C. Methanol extraction was performed by suspending the sclerotial powder in methanol at room temperature with 24-hour stirring. Following the extraction, the mixtures were centrifuged at 8000 xg for 15 minutes, and the supernatants were filtered through Whatman No.1 filter paper. Hot water and cold water filtrates were collected and freeze dried for at least 48 hours to produce hot water extract (HWE) and cold water extract (CWE), whereas methanol filtrates were evaporated to dryness at 37°C using rotary evaporator to produce methanol extract (ME). Extracts were collected and kept at -80°C for long-term storage.

2.2.2.1 Optimization of the solubility of extracts

Different vehicles, ranging from purified water to organic solvent i.e. DMSO at different percentages i.e. 50%, 70%, and 100%, were used in a series of tests to dissolve the extracts. There is evidence that DMSO at high concentration possessed interruptive effects in many assays. The goal of this study was to optimize the solubility of the extracts by minimizing the percentage of DMSO in vehicle to avoid these interruptive effects.

2.2.3 Composition analysis of *L. rhinocerotis* sclerotial powder

This subsection was performed and analyzed by Ligno Biotech Sdn. Bhd. The α- and β-glucan analysis of TM02 freeze-dried powder was performed using Megazyme glucan test kit, with pre-treatments using chitinase and alpha-amylase (Sigma-Aldrich, USA). 3'-deoxyadenosine and adenosine analysis was adopted from the method by Furuya et al., (1983). Polysaccharide analysis was performed following hydrolysis in sealed tubes with two transferases MTFA at 100°C for 5 hours. The hydrolysates were evaporated to dryness. The residue was repeatedly evaporated with methanol until the acid had been completely removed. The molar ratios of neutral sugars were determined by converting them to their alditol acetates which were separated and quantified by gas chromatography on a DB-225 fused silica capillary column at 210°C (15 m X 0.25 mm, J&W Scientific). Standard reference materials were obtained from Sigma-Aldrich, USA. Glycoprotein analysis was performed on pre- and post-amylase digested sample (control sample digested with placebo). Free carbohydrate was isolated by dialysis; resultant dialysate was dehydrated and subjected to elemental nitrogen content determined on a Flash 4000 Nitrogen/Protein analyzer. Sample pyrolized at 950°C over palladium/copper catalyst in combustion gases carried by dry helium stream was analyzed by gas chromatography with thermal conductivity detection. Calibration curve from ethylenediaminetetraacetic acid (EDTA) nitrogen was used for quantification. Authentic reference materials were obtained from Thermo Scientific/CE Inc.

2.2.4 Organ bath experiments

2.2.4.1 Tissue preparation

Ethics approval was obtained from the University of Nottingham's Animal Welfare and Ethics Review Body (UNMC#2kn and UNMC12) and the research complied with the European guidelines for laboratory animal use and care (86/609/EEC). Experiments were conducted with male Sprague Dawley rats (260-440 g; 2-3 months old). Animals were purchased from University Putra Malaysia and sacrificed on the day of experiment by cervical dislocation under anaesthesia with diethyl ether. Trachea and bronchus were removed, excised into 2 mm rings, and immediately immersed in Krebs solution. All the methods used in this section were adopted from Loong et al. (2015).

Changes in isometric tension produced by tissue contraction and relaxation were detected by a force transducer (MLTF050/ST, ADInstruments, US). Data was recorded by a PowerLab data acquisition system (LabChart v7.3.4) and laptop (Hewlett-Packard, US). Muscle tension was expressed in the unit of milliNewton (mN). After the application of tension of 9.8 mN (equals to 1 g), tissues were left to equilibrate to bath condition for 30 minutes. Following equilibration, all tissues were exposed to 60 mM KCl twice to assess tissue viability and to provide reference contracture (average of the two peak responses induced by KCl) for subsequent data analysis. Once KCl-induced tissue contraction plateaued (5 to 10 minutes), the baths were washed out with fresh Krebs solution and left to return to basal tone. Fifteen minutes after the washing, second KCl addition and washing were repeated. Following the second washing, tissues were left to return to the resting tension for 15 minutes before the performance of experimental protocols as in following subsections. A

diagram depicting the organ bath procedures prior to the start of experimental protocols is shown in Fig. 2.2.

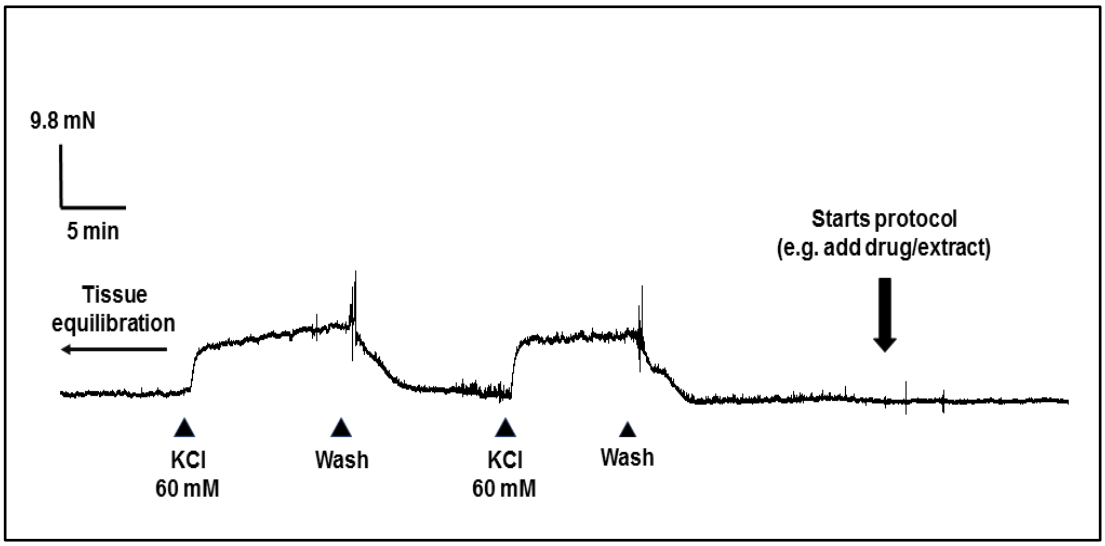

Figure 2.2: Representative trace recordings of organ bath procedures prior to the performance of experimental protocols. Following the tissue equilibration period (~30 minutes), 60 mM KCl was added to induce a tone and left for at least 5 minutes or until response plateaued, followed by washout of bath contents with fresh Krebs solution. Tissues were then left to return to basal tone and stabilize for ~15 minutes prior to second KCl addition and washing steps. Subsequently, tissues were left to return to the resting tension for ~15 minutes before the performance of experimental protocols. Peak responses induced by both KCl additions were averaged to serve as the reference contracture (reference KCl-induced tone) in some experiments. (Abbreviations: KCl = potassium chloride; mN = milliNewton; min = minute)

2.2.4.2 Preliminary study of the effect of *L. rhinocerotis* extracts on airway segments pre-contracted with carbachol

The tone of tracheal and bronchial rings was induced with 1 µM carbachol, a non-selective cholinergic agonist that acts on both nicotinic and muscarinic receptors, to obtain a stable submaximal contraction size between 70% and 80% of the maximum carbachol contraction (Loong et al., 2015). Upon establishing stable contractions,

cumulative CRCs to CWE and ME at time intervals of 1 hour between concentrations (0.5 to 1 mg/ml) were constructed in the preliminary experiments. On the other hand, based on our earlier experiments (**Appendix B**), concentration up to 1 mg/ml of HWE did not exhibit any significant bronchodilator effect on rat bronchial rings. Considering that the traditional usage of *L. rhinocerotis* is mainly by hot water preparation and bronchodilator effect may lie in the HWE, we further tested with higher concentration range of HWE (1 to 8 mg/ml) at time intervals of 30 minutes between concentrations. Vehicle control, either purified water (for CWE and HWE) or the appropriate concentration of DMSO (up to 2% v/v for ME), was carried out. Only one CRC was obtained per tissue. The degree of relaxation was measured as a fraction of the contraction achieved by 1 µM of carbachol and had been expressed as a percentage of carbachol-induced tone.

2.2.4.3 Effect of the CWE and incubation time on airways pre-contracted with carbachol

Cumulative CRCs to CWE were constructed at intervals of 15 minutes between concentrations until full relaxation of the tracheal and bronchial rings pre-contracted with carbachol (1 µM) was fully achieved. In a different set of experiments, cumulative CRCs to CWE were constructed in pre-contracted tracheal and bronchial rings at time intervals of 5, 15 or 30 minutes between concentrations. Vehicle control i.e. purified water was carried out. The degree of relaxation was measured as a fraction of the contraction achieved by 1 µM of carbachol and had been expressed as a percentage of carbachol-induced tone.

2.2.4.4 Effect of the conventional bronchodilators on airways pre-contracted with carbachol

To serve as positive controls, CRCs to ipratropium (non-selective muscarinic receptor antagonist) or salmeterol (β_2-adrenoceptor agonist) were constructed in tracheal and bronchial tissues pre-contracted with 1 µM carbachol. In parallel, CRCs to corresponding vehicle control, DMSO 0.3% v/v, were constructed. The degree of relaxation was measured as a fraction of the contraction achieved by carbachol and had been expressed as a percentage of carbachol-induced tone.

2.2.4.5 Statistical analysis

Data were analysed and graphs were drawn using PRISM v7.0 (Graph pad software). All data were expressed as mean ± standard error of mean (SEM) of n number of animals. Maximum tissue response (E_{max}) and pEC_{50} were derived from nonlinear regression analysis of the obtained CRC. In the event that the E_{max} was not achieved as response has not plateaued, E_{max} was derived from the response generated at the highest concentration tested. In some experiments, responses at each individual concentration were compared with multiple comparison test. The pEC_{50} value was the negative logarithm of EC_{50} where EC_{50} was the concentration of drug/extract that gives 50% of its maximum response. Throughout this thesis, potency was expressed in pEC_{50}. Statistical analyses were performed using two-way Analysis of Variance (ANOVA) followed by multiple comparisons with Bonferroni correction (to assess differences and interactions between concentrations and treatments; Fig. 2.3 to 2.5) and one-way ANOVA (to compare mean differences between groups; Fig. 2.6).

Results were considered statistically significant if p-value was less than 0.05. In the case if the interaction p-value based on two-way ANOVA was < 0.05, this indicated an interaction between treatment groups and concentrations, meaning that difference between treatments were not consistent for different concentrations and thus inferring a concentration-dependent effect of treatment.

2.3 Results

2.3.1 Yields from cold water, hot water and methanol extraction

The CWE and HWE were both in the form of light brownish flakes whilst ME was dark brownish and sticky. The percentage yield of *L. rhinocerotis* extracts were calculated and shown in Table 2.1. Extractions of *L. rhinocerotis* sclerotial powder had produced the highest yield of HWE, 19.0%, which was 2 times higher than CWE, 7.81%, and 9 times higher than ME, 2.26%. This suggests that the sclerotial powder mainly consists of water-soluble compounds.

Table 2.1: Percentage yield of *Lignosus rhinocerotis* extracts.

Extracts	Yield (g)	% Yield relative to *L. rhinocerotis* sclerotial powder (w/w)	% Yield relative to reference (Y. H. Y. Yap et al., 2013)
Hot water	1.901	19.0	95.0
Cold water	0.781	7.81	78.1
Methanol	0.226	2.26	83.7

2.3.2 Optimization of the solubility of extracts

The aqueous extracts of *L. rhinocerotis* including HWE and CWE were moderately soluble in purified water at stock concentration of 100 mg/ml. For HWE, sonication for about 10 minutes at 40°C was done to aid the solubility in water. For CWE, sonication did not improve the solubility significantly, and therefore this step was not carried out. While for ME, the minimum concentration of DMSO required to fully dissolve ME was 100% and the concentration of stock solution was 50 mg/ml. Vehicle controls in the following organ bath studies corresponded to the final concentration of the vehicle of each extract in the bath.

2.3.3 Composition analysis of *L. rhinocerotis* sclerotial powder

The composition analysis of *L. rhinocerotis* freeze-dried sclerotial powder is summarized in Table 2.2. The powder material contained largely β-glucans, polysaccharides, and glycoproteins. It also contained trace amount of adenosine and its derivatives including adenine, 3'-deoxyadenosine, ethyl- and hydroxyethyl-adenosine.

Table 2.2: Summary of the composition analysis of *Lignosus rhinocerotis* sclerotial powder.

Analytes	Contents (mg/g)	% relative to total amount
Total polysaccharides	401.4	44.30
β-1,3/1,6-glucan	286.8	31.65
Glycoprotein	186.1	20.54
α-glucan	29.91	3.30
3'-deoxyadenosine	0.873	0.09
Ethyl-adenosine	0.399	0.04
Adenosine	0.282	0.03
Hydroxyethyl-adenosine	0.268	0.03
Adenine	0.024	0.002

2.3.4 CWE produced most pronounced airway relaxation effect

In order to detect any relaxation induced by the extracts, carbachol was used to pre-contract the airway segments. Preliminary results showed that ME failed to exhibit any significant relaxation effect in both tracheal (T) and bronchial (B) rings (E_{max}: T: 49.82 ± 12.03%, B: 62.37 ± 9.15%%; both $p > 0.9999$) compared to vehicle control (E_{max}: T: 52.39 ± 2.47%, B: 59.75 ± 4.88) (Fig. 2.3A and B). CWE produced significant relaxation in bronchial rings compared to vehicle control at 0.5 mg/ml (21.94 ± 1.24% vs 7.51 ± 1.11%, $p = 0.0051$) and 1.0 mg/ml (48.12 ± 5.88% vs 14.72 ± 1.21%, $p < 0.0001$) (Fig. 2.3D). In contrast, CWE failed to relax the tracheal rings up to 1.0 mg/ml compared to vehicle control (19.51 ± 5.53% vs 10.53 ± 7.04%, $p = 0.4744$) (Fig. 2.3C).

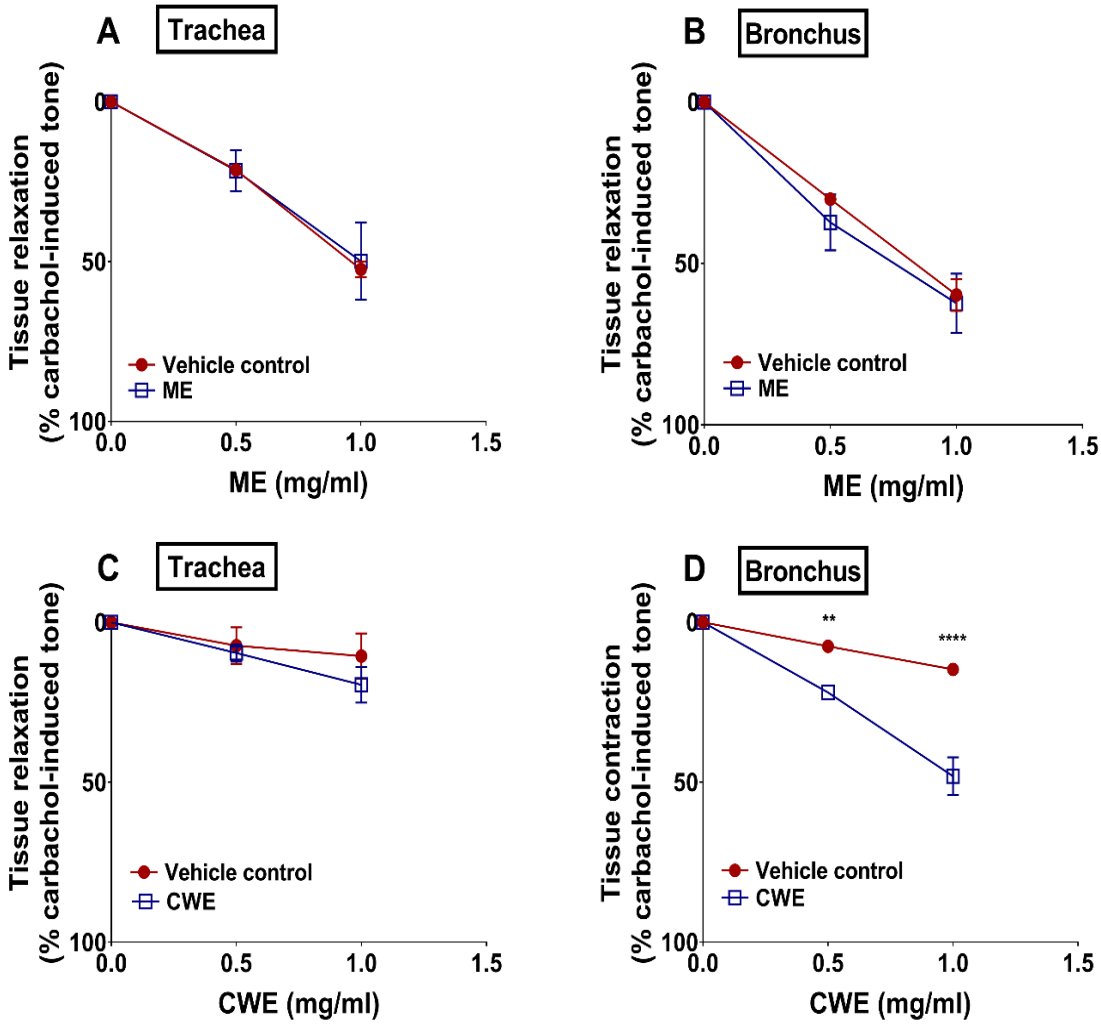

Figure 2.3: Effect of methanol and cold water extracts on rat airways pre-contracted with carbachol. Concentration response curves to (A),(B) ME and (C),(D) CWE in tracheal and bronchial rings pre-contracted with 1 µM carbachol. Tissue relaxation was expressed as a percentage of carbachol-induced contraction. Data were shown as means ± SEM of 3 to 4 animals. Two-way ANOVA with Bonferroni correction was made between treatment and vehicle control: $^{**}p < 0.01$, $^{****}p < 0.0001$. (Abbreviations: CWE = Cold water extract; ME = Methanol extract)

Similarly, Fig. 2.4 shows that HWE was devoid of significant relaxation effect in both tracheal (T) and bronchial (B) rings (E_{max}: T: 35.18 ± 3.33%, B: 78.00 ± 5.01%; both $p > 0.9999$) compared to vehicle control (E_{max}: T: 43.28 ± 14.93%, B: 84.01 ± 13.16%). Based on these results, we had used the most bioactive extract i.e. CWE for the subsequent experiments in this thesis.

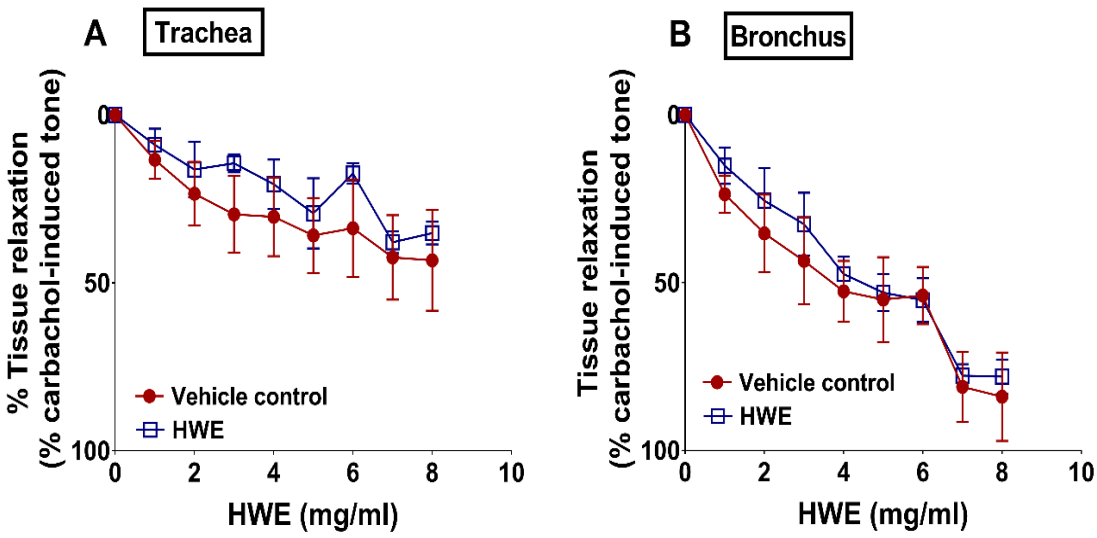

Figure 2.4: Effect of hot water extract on rat airways pre-contracted with carbachol. Concentration-response curves to HWE in (A) tracheal and (B) bronchial rings pre-contracted with 1 µM carbachol. Tissue relaxation was expressed as a percentage of the carbachol-induced contraction. Data were shown as means ± SEM of 3 animals. (Abbreviations: HWE = Hot water extract)

2.3.5 Airway relaxation effect of the CWE is concentration- and time-dependent

To investigate the impact of concentration and incubation time, CWE was added to the tissues every 0.25 mg/ml until full relaxation of tissues (relative to carbachol-induced tone) were achieved. Results showed that CWE produced significant relaxation in both tracheal and bronchial rings (Fig. 2.5A). In trachea, tissue was significantly relaxed from 2.50 mg/ml to 3.75 mg/ml, while in bronchus, tissue was significantly relaxed from 2.0 mg/ml to 2.5 mg/ml, when compared to vehicle control. The extract fully relaxed the tracheal rings (E_{max}: 106.10 ± 4.69%; $p < 0.0001$) at 3.75 mg/ml and bronchial rings (E_{max}: 106.45 ± 8.50%; $p < 0.0001$) at 2.5 mg/ml. The relaxation effects of vehicle control in both tracheal (E_{max}: 6.33 ± 3.21%) and

bronchial rings (E_{max}: 24.34 ± 14.92%) were negligible. On the basis that 100% relaxant response was achieved in both tracheal and bronchial rings, the respective pEC_{50} values of CWE CRC were -0.43 ± 0.02 and -0.13 ± 0.10**.** Fig. 2.5B shows the trace recording of the relaxation effect of CWE on pre-contracted bronchial segment. Two-way ANOVA results showed an interaction between treatments and concentrations ($p < 0.0001$), indicating that these factors are interdependent.

Next, tissues were exposed to CWE at varying time intervals of 5 minutes, 15 minutes, and 30 minutes between concentrations. The results demonstrated that at the same highest concentration used in tracheal rings, which is CWE 2.75 mg/ml, the magnitude of tissue relaxation increased with incubation duration (E_{max}: 5-minute: 11.92 ± 3.21%; 15-minute: 61.31 ± 15.79%; 30-minute: 118.19 ± 7.93%) (Fig. 2.5C). Similar finding was observed in bronchial rings at CWE 2.0 mg/ml (E_{max}: 5-minute: 21.49 ± 11.66%; 15-minute: 72.04 ± 10.05%; 30-minute: 116.25 ± 9.78%) (Fig. 2.5D). The effect of vehicle control was negligible and therefore not shown in Fig. 2.5C and D. Maximum responses of all incubation times were statistically significant among each other in tracheal and bronchial rings ($p < 0.0001$). Overall, the findings suggest that the longer the tissues were exposed to the extract, a greater relaxant response was observed. Two-way ANOVA results also showed an interaction between treatments and concentrations ($p < 0.0001$), indicating that these factors are interdependent.

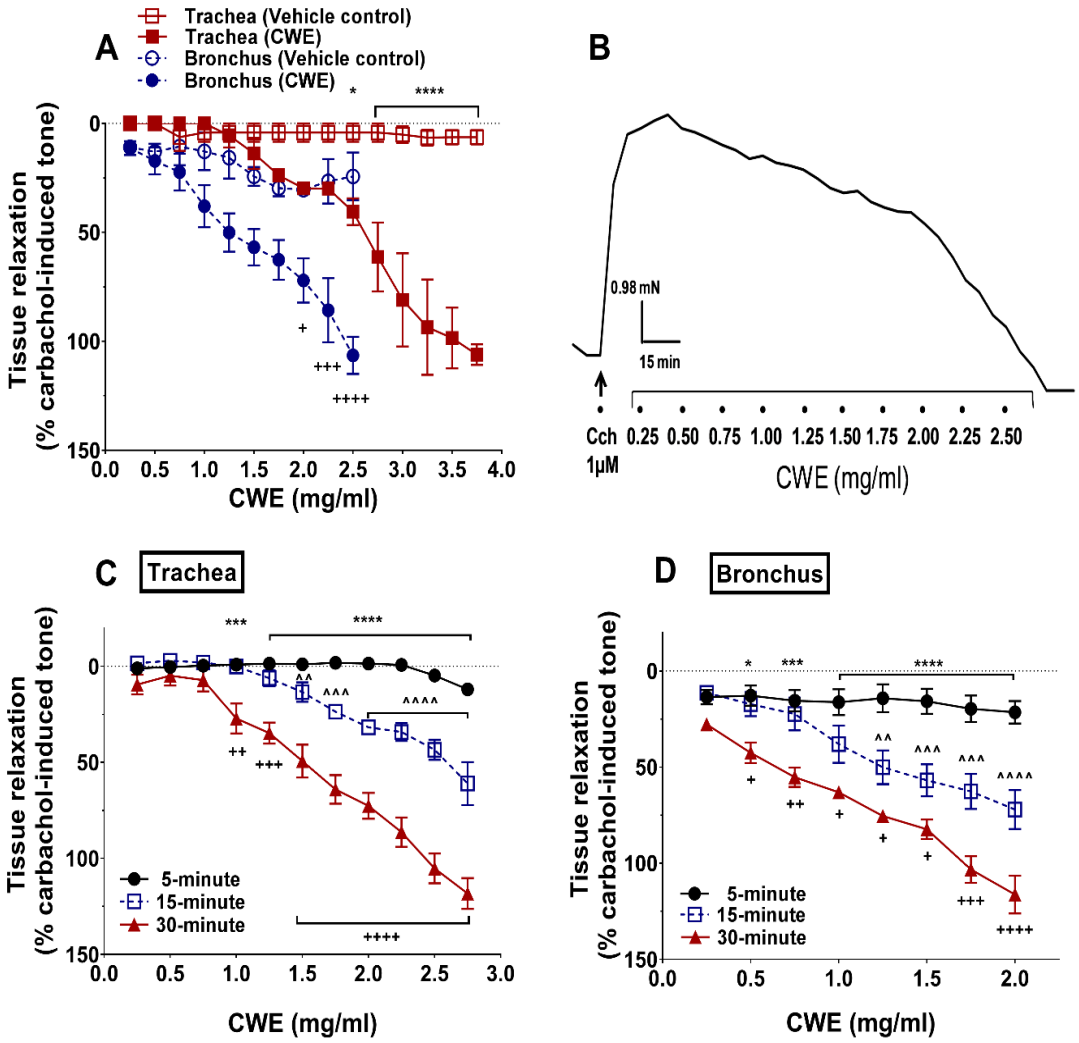

Figure 2.5: Concentration- and time-dependent properties of cold water extract on carbachol-pre-contracted rat airways. (A) Concentration-response curves to CWE at time intervals of 15 minutes between concentrations on tracheal and bronchial rings pre-contracted with 1 μM carbachol. (B) Representative trace recording of the relaxation effect of CWE on bronchial rings pre-contracted with carbachol. Effect of different time intervals between concentrations of CWE i.e. 5-, 15- and 30-minute against carbachol-pre-contracted (C) tracheal and (D) bronchial rings. Tissue response was expressed as a percentage of carbachol-induced contraction. Data were shown as means ± SEM of 3 to 5 animals. Two-way ANOVA with Bonferroni correction was made between treatment and vehicle control: for (A) trachea: $^{*}p < 0.05$, $^{****}p < 0.0001$; bronchus: $^{+}p < 0.05$, $^{+++}p < 0.001$, $^{++++}p < 0.0001$; for (C) and (D) 15-min vs 30-min: $^{*}p < 0.05$, $^{***}p < 0.001$, $^{****}p < 0.0001$, 5-min vs 15-min: $^{+}p < 0.05$, $^{++}p < 0.01$, $^{+++}p < 0.001$, $^{++++}p < 0.0001$, 5-min vs 30-min: , $^{\wedge\wedge}p < 0.01$, $^{\wedge\wedge\wedge}p < 0.001$, $^{\wedge\wedge\wedge\wedge}p < 0.0001$. (Abbreviations: Cch = Carbachol; CWE = Cold water extract)

2.3.6 Ipratropium and salmeterol relaxed pre-contracted airways

Subsequent experiment tested the airway relaxation effect of positive controls. In airways pre-contracted with carbachol, ipratropium effectively relaxed the tracheal (T) rings (E_{max}: 117.80 ± 6.22%; p = 0.0004) (Fig. 2.6A) and bronchial (B) rings (E_{max}: 113.40 ± 1.64%; p = 0.0031) (Fig. 2.6B) compared to vehicle control (E_{max}: T: 31.42 ± 4.73%, B: 26.95 ± 13.48%). Salmeterol showed a significant relaxation in bronchial rings but minimal effect in tracheal rings (E_{max}: T: 41.67 ± 14.85%, p > 0.05; B: 104.40 ± 16.33%, p = 0.0104) compared to respective vehicle control (E_{max}: T: 41.26 ± 4.80%, B: 31.92 ± 10.13%) (Fig. 2.6A and B). The relaxation effect of vehicle control in both airway segments was negligible.

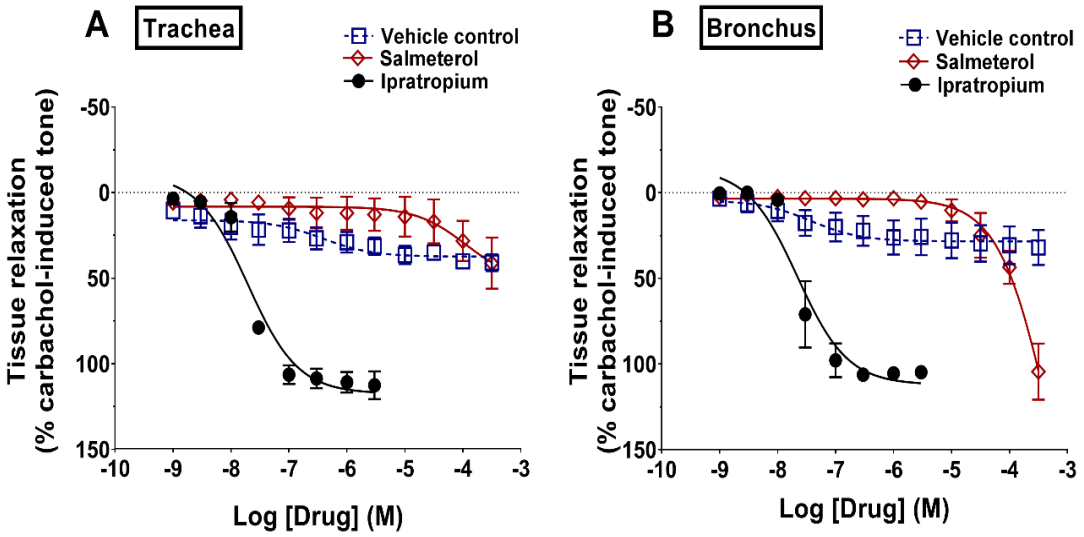

Figure 2.6: Effect of ipratropium and salmeterol on carbachol-pre-contracted rat airways. Concentration-response curves to ipratropium and salmeterol in (A) tracheal and (B) bronchial rings pre-contracted with 1 µM carbachol. Tissue response was expressed as the percentage of carbachol-induced tone. Data were shown as means ± SEM of 3 to 4 animals.

2.4 Discussions

The composition analysis of *L. rhinocerotis* sclerotial powder in this study revealed the presence of 79% of total polysaccharides (predominantly β-glucan) and 20% of glycoprotein. This is in agreement with a previous study by Y. H. Y. Yap et al. (2013) where sclerotial powder of *L. rhinocerotis* TM02 cultivar and wild type contained highest amount of carbohydrates and insignificant amount of proteins. We also identified adenosine and a series of its derivatives in TM02 cultivar.

The higher yields of aqueous extracts, HWE and CWE, compared to ME also indicate that *L. rhinocerotis* sclerotium contains more water-soluble compounds with higher polarity. Previous chromatographic analysis of the chemical constituents of *L. rhinocerotis* by Lau et al. (2013) revealed that the aqueous extract mainly contains relatively polar compounds, which supports our findings. The slight differences in the percentage yields relative to other researchers (Yap et al., 2013) may be attributed to the different instrumental setting in different laboratories and slight adaptation to the extraction methods.

To our knowledge, this is the first study to demonstrate that CWE displayed direct bronchodilator properties in rat airways, in support of its traditional claims for relieving asthma and chronic cough. Our study showed that a longer incubation period of CWE enhanced the bronchorelaxant response in the airway rings. In contrast, both ME and HWE did not show any significant difference in carbachol-induced pre-contraction compared to respective vehicle control i.e. DMSO and water in the airway segments.

Unexpectedly, the HWE was lack of airway relaxation effect when one of the traditional applications of *L. rhinocerotis* for asthma and cough is mainly by decoction (Azliza et al., 2012; Chang & Lee, 2004). One of the possible reasons is that the therapeutic effect in traditional preparation comes from synergistic effect with other herbs rather than *L. rhinocerotis* alone. Another possibility is that the active constituents contributing to the airway relaxation effect may be heat-labile, such as the proteins. In fact, in some of the tribes in Malaysia, *L. rhinocerotis* sclerotium is eaten raw for asthma (Lau et al., 2015), and this might explain the bronchodilator effect of CWE in this study. Besides, ME did not exhibit any relaxation effect, indicating that water-soluble polar compounds, which are not soluble in methanol are most likely to be responsible for the bronchodilator properties.

Polysaccharides isolated from natural products demonstrated *in vivo* bronchodilator effect in mice (Pi, Wang, Lu, Lu, & Chen, 2014). The carbohydrates could form complex with proteins to become large-molecular-weight glycoproteins. In addition, the carbohydrate contents of CWE, HWE and ME obtained from *L. rhinocerotis* TM02 cultivar were reported to be 68.4%, 92.2% and 12.8%, respectively, while the protein contents were found to be 2.0%, 0.2% and 0.2%, respectively (Sook Shien Lee et al., 2014). Given that CWE contained highest amount of proteins, we speculate that the proteins or glycoproteins are accountable for the airway relaxation effect.

Large-molecular-weight polysaccharide-protein complex is less likely to penetrate tissues directly (El Enshasy & Hatti-Kaul, 2013; T. F. Schmidt et al., 2009). Therefore, we propose that the observed time-dependent effects of CWE are modulated by cell surface receptors (G. D. Brown & Gordon, 2003; El Enshasy & Hatti-Kaul, 2013). The longer response time observed may be linked to time required

for these large molecules to adsorb and bind to these surface proteins/receptors. In an earlier study, a polysaccharide isolated from a marine filamentous fungus *Phoma herbarum* exhibited time-dependent binding to macrophages, possibly via Toll-like receptors or complement CR3 receptors which led to significant activation of P38 kinase (S. Chen et al., 2009). Polysaccharide isolated from *Terminalia chebula* aqueous extract also exhibited time-dependent antitussive effect on citric acid-induced cough in guinea pig (Nosalova et al., 2013). The enhanced potency of CWE with prolonged incubation observed herein is somewhat resembling the findings in these studies. Hence, it is plausible that the large polysaccharides, proteins or polysaccharide-protein complex may partly contribute to the time-dependent properties of the mushroom's airway relaxant effect.

The time-dependent properties of CWE in relaxing pre-contracted airway segments suggest that instead of providing immediate bronchodilator effect for acute asthma attack, *L. rhinocerotis* may have potential benefit by preventing and relieving airway obstruction that takes place in the LAR of asthma, COPD and chronic cough. The direct airway relaxation effect of CWE corroborates the *in vivo* inhibitory effects of *L. rhinocerotis* on ovalbumin-induced airway inflammation, therefore substantiating its antiasthmatic potential (Johnathan et al., 2016).

Bronchodilators such as β_2-adrenoceptor agonists (salmeterol) and muscarinic antagonists (ipratropium) are often used as reliever in asthma and COPD. Results from Section 2.3.5 and 2.3.6 clearly showed that the efficacy of CWE was comparable to ipratropium, and better than salmeterol in relaxing airway contraction. Both CWE and ipratropium successfully relaxed tracheal and bronchial rings for more than 100%. In our study, salmeterol exhibited less pronounced airway relaxation effect in trachea compared to ipratropium. One possible explanation is that the upper airway may

possess lower abundance of β_2-adrenoceptors. The density of β_2-adrenoceptors was shown to increase from the upper to lower airways using radioligand binding assays in guinea pig (Carswell and Nahorski, 1983). Higher abundance of β_2-adrenoceptor mRNA was also identified in the lower airway smooth muscle of human and rat (Hamid et al., 1991).

Taken together, the results in this chapter led us to postulate a few pathways that may be mediated by *L. rhinocerotis*. Firstly, given that CWE relaxed carbachol-induced contraction, inhibition of $G_{\alpha q}$-coupled signalling pathway may be implicated. Secondly, direct regulation of $[Ca^{2+}]_i$ may be involved. Thirdly, the main signalling pathway involved in airway smooth muscle relaxation is activation of β_2-adrenoceptors coupled to cAMP pathway and potassium channel activation, these components may therefore be affected. Fourthly, a number of studies showed that lectin (El Enshasy & Hatti-Kaul, 2013) and polysaccharides (Mizuno et al., 2000) isolated from mushroom can activate macrophage cells and stimulate the production of NO, which is known as a relaxing factor. Hot water extract of *P. rhinocerus* was shown to activate macrophage and increase NO production in murine macrophage cells (Guo, Wong, & Cheung, 2011). Therefore, NO and the downstream cGMP pathway are also likely to be involved.

In summary, CWE-induced airway relaxation effect was concentration- and time-dependent, and the efficacy was comparable to conventional bronchodilators in rat isolated airways. Both isolated trachea and bronchus were fully relaxed by CWE with similar efficacy, albeit the potency was higher in bronchus. In light of the above findings, subsequent mechanistic studies to elucidate the bronchodilator effect of CWE were carried out mainly in tracheal tissues with optimized time intervals of 15 minutes between concentrations (**Chapter 3 and 4**). A few airway relaxation

pathways that might be implicated by CWE were hypothesized and subsequently tested in **Chapter 3**. The cold water extract of *L. rhinocerotis* was termed as "CWE" throughout this thesis.

Chapter 3. Mechanisms of action of *Lignosus rhinocerotis* extract on airways

3.1 Introduction

Findings in **Chapter 2** unequivocally demonstrated the relaxation effect of CWE in rat airways. Airways of small rodents are widely used in pharmacological studies for new drug testing due to their reproducibility, relatively higher cost-effectiveness and ease of handling. However, it should be noted that they are not without limitations as there are appreciable differences in lung sizes and anatomy, and airway responses to stimuli or mediators as compared to human (Meurs et al., 2008). Porcine lung anatomy, size, and physiology closely resemble those of human, making it an ideal non-rodent animal choice for translational research (Judge et al., 2014). In light of this, we hypothesized that there may be different responses elicited by CWE on rat and porcine airways due to interspecies differences.

In addition, given that CWE relaxed airway contraction to carbachol, we proposed that CWE may directly block muscarinic receptors in causing airway relaxation. CWE is also likely to affect the signalling pathways downstream of muscarinic receptor activation, regulation of $[Ca^{2+}]_i$, and activation of cAMP and NO/cGMP pathways. The insights on cAMP and cGMP pathways associated with airway smooth muscle relaxation were provided in Section 1.1.2.3, **Chapter 1**. In the following subsections, other mechanisms to be examined in this chapter were reviewed.

3.1.1 Activation of $G_{\alpha q}$ protein-coupled receptors in airways

Excessive release of acetylcholine, causing overactivation of muscarinic receptors, has been implicated in the pathophysiology of asthma and COPD (Erle & Sheppard, 2014). Airway smooth muscle contraction can be induced by acetylcholine released from parasympathetic nerves, or by histamine and CysLT released from mast cells and basophils, particularly in asthmatic subjects but less so in individuals without compromised respiratory function. The underlying mechanisms of contractile agonist-induced airway smooth muscle contraction are activation of predominant $G_{\alpha q}$-coupled muscarinic M_3 receptors by acetylcholine. On the other hand, histamine is believed to exert its bronchoconstrictor effect via activation of $G_{\alpha q}$-coupled histamine H_1 receptors expressed on airway smooth muscle (Togias, 2003).

Serotonin or 5-hydroxytryptamine (5-HT) is another important neurotransmitter that triggers the same second messenger pathway as muscarinic receptor activation via the $G_{\alpha q}$ protein. Activation of 5-HT receptors on airway smooth muscle has caused smooth muscle contraction, relaxation or biphasic responses in different species in different studies. The role of 5-HT in constricting human airways remains controversial due to discrepant responses, probably mediated via different receptor subtypes and coupling pathways. Further complicating the matter is that 5-HT may indirectly modulate the acetylcholine levels leading to muscle contraction (Cazzola, Matera, D'Amato, & Rossi, 1995).

Studies revealed that 5-HT induced sustained weak contraction in mice tracheal segments *in vitro* (Adner et al., 2002) and increased pulmonary resistance in guinea pig *in vivo* (Buckner, Dea, Liberati, & Krell, 1991). The contractile response to 5-HT is believed to be mainly mediated via 5-HT_2 subtype, but mixed findings are

reported. In rat, evidence shows that the airway contraction was mediated through activation of 5-HT_{2A} receptors located on airway smooth muscle (Cazzola & Matera, 2000). The 5-HT-induced contraction, transforming growth factor-β1 release, and human bronchial smooth muscle cell proliferation were attenuated by 5-HT_2 antagonists in mice precision-cut lung slices (Löfdahl, Wenglén, Rydell-Törmänen, Westergren-Thorsson, & Larsson-Callerfelt, 2018). Potent 5-HT_2 receptor antagonists also antagonized 5-HT-evoked bronchoconstriction in guinea pig (Selig, Bloomquist, Cohen, & Fleisch, 1988), implicating the involvement of 5-HT_2 subtype. Conversely, a recent *in vivo* study demonstrated that in ovalbumin-induced airway inflammation mice model, inhalation of 5-HT_{2A} agonist was beneficial in preventing the airway hyperresponsiveness (Nau et al., 2015). Eosinophil levels in the BALF, lung tissue inflammation, mucus production, and mucus cell hyperplasia were decreased in the treated group. In some species including human bronchi (Goldie, Paterson, & Wale, 1982) and guinea pig trachea (Campos-Bedolla et al., 2008), 5-HT induced biphasic responses (initial contraction and subsequent relaxation). Campos-Bedolla et al. (2008) reported that the biphasic responses of 5-HT in guinea pig tracheal rings were possibly mediated by the activation of 5-HT_{2A} receptors through Na^+/K^+-ATPase pump and Ca^{2+}-activated potassium channels. Besides, Dupont et al. (1999) showed that 5-HT enhanced the electrical field stimulation-induced contraction of human bronchial tissue, which is inhibited by 5-HT_3 and 5-HT_4 antagonists, suggesting a role of these receptor subtypes.

In addition, there has been a positive correlation between 5-HT level and asthmatic symptoms. For instance, 5-HT plasma levels were raised in asthmatic patients, in which free 5-HT was found to positively correlate with the asthma severity (Lechin, Van Der Dijs, Orozco, Lechin, & Lechin, 1996). Dürk et al. (2013) performed

a segmental allergen provocation (with 10-fold higher doses of rye pollen, birch pollen, or house dust mite allergen that caused 20% fall in forced expiratory volume in one second, FEV_1) in patients with mild allergic asthma. As a result, the allergen-provoked patients had decreased serum 5-HT levels but increased BALF 5-HT levels, supporting a positive link between free 5-HT levels with allergic asthma. In the same study, BALF 5-HT levels were also elevated in asthmatic patients without allergen provocation compared to healthy subjects (Dürk et al., 2013). Despite these, inhaled 5-HT did not affect the airway obstruction parameters in both asthmatic and non-asthmatic patients (Cushley, Wee, & Holgate, 1986). While several studies above described that 5-HT can provoke airway smooth muscle contraction, its role in asthma remains controversial due to contradicting reports from various studies.

Contractile agonists such as carbachol, 5-HT, and histamine are commonly used to elicit airway contraction in pharmacological experiments. However, rat and porcine isolated airways were unresponsive and did not respond consistently to exogenous histamine, respectively, in our earlier experiments (data not shown). This may be explained by *in vitro* evidence that rat is relatively insensitive to histamine compared to guinea pig (Dürk et al., 2013) and human (Dürk et al., 2013) in causing airway contraction. In rat, allergen-induced bronchoconstriction was mainly mediated by 5-HT, but less so by histamine, thromboxane and leukotrienes (Wohlsen, Uhlig, & Martin, 2001), whist the opposite was observed in human and guinea pig (Wohlsen et al., 2003). In this chapter, our experiments mainly centre on 5-HT- and carbachol-induced contractions to investigate the role of $G_{\alpha q}$-coupled pathways in responses elicited by CWE.

3.1.2 Degradation of cAMP and cAMP by phosphodiesterase enzymes

The cyclic nucleotides cAMP and cGMP molecules are amongst the important second messengers in modulation of airway smooth muscle tone apart from DAG and IP_3 (Section 1.1.2.3, **Chapter 1**). Both molecules are hydrolysed by a family of enzymes, termed phosphodiesterase (PDE). The PDE enzymes exist in several isoforms: PDE3, PDE4, PDE7, and PDE8 inhibit cAMP degradation, PDE5, PDE6, and PDE9 inhibit cGMP degradation, and PDE1, PDE2, PDE10, and PDE11 inhibit the degradation of both cAMP and cGMP (Azevedo et al., 2014). Owing to the regulatory role of cAMP and cGMP in airway tone as well as structural alterations, PDE enzyme inhibitors that prevent the breakdown and augment the levels of these molecules are therefore beneficiary in treatment of airway diseases (Siddiqui et al., 2013). For instance, theophylline, a non-selective PDE inhibitor, and roflumilast, a PDE4 inhibitor, are approved for asthma and COPD management, respectively. A study carried out by Perez-Zoghbi et al. (2010) revealed that the inhibition of PDE5 has sustained NO-induced relaxation of mouse airway smooth muscle, inferring that PDE5 reduces cGMP levels and dampens NO-mediated bronchodilation. Despite that, preclinical studies of PDE4 inhibitor suggest that it rather acts as an anti-inflammatory agent than bronchodilator in respiratory diseases (Page & Spina, 2012).

The earlier PDE inhibitors such as theophylline and 3-isobutyl-1-methylxanthine (IBMX) bind non-selectively to all PDE enzymes. More recently developed PDE isoform-selective inhibitors, for instance rolipram and roflumilast (PDE4-selective), nimodipine (weakly PDE1-selective), and sildenafil (PDE5-selective), prove to be important pharmacological tool to further characterize the functional role of the cGMP and cGMP molecules (Azevedo et al., 2014).

3.1.3 Potassium channels in airways

Cell membrane of airway smooth muscle and nerves contains a variety of potassium channels. Changes in the gating of these channels will result in membrane hyperpolarization, modulating the muscle tone. In resting membrane potential, potassium channels act as a strong outward rectifying current that stabilizes the membrane potential and counteracts the tendency to depolarization, maintaining the basal tone of smooth muscle (G Pelaia et al., 2002). Potassium channels of relevance to airway smooth muscle are identified to be: (1) Ca^{2+}-dependent potassium channels including large-conductance Ca^{2+}-activated potassium (BK_{Ca}) channel, intermediate-conductance Ca^{2+}-activated potassium (IK_{Ca}) channel, small-conductance Ca^{2+}-activated potassium (SK_{Ca}) channel, (2) voltage-gated Ca^{2+}-independent delayed rectifier potassium (K_{dr}) channel, and (3) ATP-dependent potassium (K_{ATP}) channel (G Pelaia et al., 2002).

The predominant potassium channel in airway smooth muscle is BK_{Ca} channel, which is modulated by contractile and relaxant agent that inhibits and promotes the opening of channel respectively. The activation of BK_{Ca} channel is by direct stimulation of either AC or G_s subunit of GPCR in response to membrane depolarization or increase in $[Ca^{2+}]_i$ (Barisione et al., 2010). Therefore, it counteracts the actions of depolarizing stimuli and contractile agents that promote intracellular Ca^{2+} store release or extracellular Ca^{2+} entry. Iberiotoxin as well as charybdotoxin are well known BK_{Ca} channel blockers effective at nanomolar concentration in smooth and skeletal muscles (Meera, Wallner, & Toro, 2000). Unlike iberiotoxin, which selectively blocks BK_{Ca} channel, charybdotoxin also blocks IK_{Ca} channel. Other pharmacological agents such as apamin and glibenclamide selectively block SK_{Ca} and

K_{ATP} channels, respectively. Voltage-gated potassium channels, including K_{dr} and A-type potassium channels (voltage-gated Ca^{2+}-independent potassium channel; no evidence of existence in airway smooth muscle), are sensitive to 4-aminopyridine and tetraethylammonium (TEA) (Harding et al., 2018). Additionally, TEA is capable of blocking the BK_{Ca} channel and inhibiting outward rectification in cells at concentrations of 10 and 30 mM (Kotlikoff, 1993).

Supposedly, the opening of potassium channels that induces smooth muscle cell membrane hyperpolarization should evoke bronchodilation. In fact, potassium channel openers have been proposed to be a potential therapeutic target for treatment of asthma and COPD. This is supported by finding that blockade of potassium channels by TEA (10 to 30 mM) has initiated myogenic response via enhanced electrical and contractile activity in airway smooth muscle (Imaizumi & Watanabe, 1981). However, clinical studies revealed that potassium channel openers are less than satisfactory treatment for asthma and COPD. The possible use of K_{ATP} channel openers, which are powerful vasodilators, is limited in asthma treatment, partly due to the lack of tissue selectivity and unwanted cardiovascular side effects such as hypotension (G Pelaia et al., 2002). Besides, relatively few modulators of BK_{Ca} channel have been identified to date, with some examples including triterpenes (dehydrosoyasaponin I, soyasaponin I, soyasaponin III) and benzimidazolone compounds (NS 004 and NS 1619) (G Pelaia et al., 2002). When compared to isoprenaline (β-adrenoceptor agonist), the potassium channel opener, cromakalim, induced almost equal relaxation of spontaneous tone in the airway smooth muscle (Arch et al., 1988). These small molecule potassium channel activators have demonstrated variable degree of bronchodilator actions *in vitro* and *in vivo*, especially in hyperresponsive airways (G Pelaia et al., 2002). However, there are contradicting

results on their effectiveness in relaxing cholinergically induced contraction (J. L. Black & Barnes, 1990). The benefit of potassium channel openers in alleviating respiratory diseases remains to be determined.

3.1.4 Adenosine in airways

Adenosine receptors are implicated in some asthmatic features including bronchoconstriction, mucus secretion, and airway inflammation (Burnstock, Brouns, Adriaensen, & Timmermans, 2012). The nucleoside adenosine has been one of the important mediators of purinergic signalling pathway that elicits a wide range of pharmacological effects in human and animals (Burnstock et al., 2012). Adenosine stimulates cell surface adenosine receptors including A_1, A_{2A}, A_{2B}, and A_3 subtypes. A_{2A} and A_{2B} subtypes are coupled to G_s protein whilst A_1 and A_3 subtypes are coupled to G_i protein (Rang et al., 2015). Accumulating evidence delineates the role of adenosine in pathogenesis of asthma and drives research interest into adenosine receptors as potential therapeutic target for asthma therapy (R. Brown, Spina, & Page, 2008).

Due to the expression of different receptor subtypes on almost all cell types in airways, there are discrepant reports of adenosine-induced bronchoconstrictor and bronchorelaxant responses. This is further complicated by the conflicting responses among different species used in the experimental models. Previous studies showed that adenosine contracted the airways via A_1 and A_{2B} receptors in rat and mice, and via A_3 receptors in rat, guinea pig, and mice (reviewed by Spicuzza et al., 2006). In contrast, carbachol-pre-contracted guinea pig trachea was relaxed by adenosine

(Darmani & Broadley, 1986; Losinski & Alexander, 1995) and its analogues (Brackett & Daly, 1991). There is also *in vivo* evidence that adenosine-induced bronchoconstriction is possibly mediated via stimulation of mast cell degranulation (Spicuzza et al., 2006). Selective activation of A_{2A} receptor appeared to inhibit neutrophil recruitment and release of pro-inflammatory mediators including histamine and tryptase from mast cells (reviewed by Wilson et al., 2009), whereas activation of A_{2B} receptor was shown to induce mast cell degranulation and elevate cytokine release (Spicuzza et al., 2006). Hence, it is noteworthy that these proposed mechanisms are not conclusive given the contradicting and limited studies described above (reviewed by Wilson et al., 2009).

Currently, theophylline is one of the few therapeutic agents in the market that affects the adenosine receptors. However, it remains elusive whether the bronchodilator effect of theophylline for asthma treatment is relevant to the antagonism of adenosine receptors (Burnstock et al., 2012). In addition, the relaxation effects of theophylline and enprofylline (both are xanthine derivatives) are independent of adenosine antagonism (Darmani & Broadley, 1986). A few selective agents acting on A_1 and A_2 receptors have been developed, and some are under ongoing pre-clinical and clinical trials presently. The role of A_3 receptors remains to be elucidated due to opposing effects elicited by the activation of this receptor subtype (R. Brown et al., 2008).

To explore the role of adenosine receptors, some nonselective adenosine receptor agonists, such as 5'-N-ethylcarboxamidoadenosine (NECA) and adenosine, selective adenosine receptors agonists, N6-cyclopentyladenosine (CPA) for A_1 receptor, or nonselective adenosine receptor antagonists, for example caffeine and theophylline, are available for use in pharmacological experiments.

3.1.5 Nitric oxide as a potent bronchodilator

The NANC system exists in the airways of animals and human to mediate contraction (excitatory NANC) or relaxation (inhibitory NANC) (see Section 1.1.2.4, **Chapter 1**). Evidence points to the role of nitric oxide (NO) released from peripheral nerve endings as the main neurotransmitter for the inhibitory NANC system (Ricciardolo, 2003). NO is synthesized from the amino acid L-arginine by NO synthase, which exists in isoforms of constitutive endothelial NO synthase, constitutive neural NO synthase and inducible NO synthase (Ricciardolo, 2003). Constitutive NO synthase induces Ca^{2+}-dependent NO release upon stimulation by agonist such as acetylcholine and bradykinin (Forstermann et al., 1991), whereas inducible NO synthase participates in Ca^{2+}- independent pro-inflammatory NO release (Morris & Billiar, 1994). The action of NO was first discovered for being a potent vasodilator; thereafter, the relaxing effect of NO is confirmed in many other tissues including airways (Ricciardolo, 2003).

The NO is well characterized to exert its effect by activating the GC enzyme and increasing the cGMP levels. The bronchodilator effect of NO is believed to be mainly mediated by NO released from the epithelial cells, as removal of airway epithelium has potentiated the response of smooth muscle to contractile agonists (Di Maria, Spicuzza, Mistretta, & Mazzarella, 2000). Studies showed that cGMP is the final mediator of the bronchodilator effect elicited by NO, which activates intracellular kinases and/or opens membrane BK_{Ca} channel (Di Maria et al., 2000). Recent study demonstrated that NO relaxed mice lung slices by inhibiting Ca^{2+} release from SR through IP_3 receptors and reducing the frequency of contractile agonist-induced Ca^{2+} oscillations (Perez-Zoghbi et al., 2010).

Additionally, evidence supports that endogenous NO confers crucial bronchoprotective role in airway hyperresponsiveness. Several studies reported the ability of NO to influence allergen-induced airway hyperresponsiveness mediated by different agents, such as histamine in animal models (Di Maria et al., 2000; Ricciardolo, 2003). Inhibition of inducible NO synthase-derived NO also showed modulatory role on allergen-induced airway hyperresponsiveness (Prado, Martins, & Tibério, 2011). Besides, inhibition of neural NO synthase has provoked cholinergically induced bronchoconstriction without influencing the endogenous acetylcholine release from neural pathway (Ward et al., 1993) and histamine-induced bronchoconstriction *in vitro* and *in vivo* (Nijkamp, Linde, & Folkerts, 1993).

The role of NO can be studied pharmacologically using known pharmacological agents such as the NO donor and NO synthase inhibitor. A number of L-arginine analogues, serving as substrates of NO synthase to inhibit NO production, are important pharmacological tool to unravel the physiological roles of NO. Among the NO synthase inhibitors, N(G)-monomethyl-L-arginine (L-NMMA) and N(G)-nitro-L-arginine methyl ester (L-NAME) are the most commonly used.

3.1.6 Significance of study

Core objective of this chapter was to elucidate the molecular mechanisms by which *L. rhinocerotis* CWE elicited bronchodilator effect using organ bath set up. The specific objectives focussed within this chapter are as follows:

(i) To construct CRCs to CWE on rat airways contracted by carbachol, KCl, and 5-HT.

(ii) To construct CRCs to adenosine on pre-contracted rat airways and at basal tone.

(iii) To compare the efficacies of CWE-induced relaxation in the presence of inhibitors of β-adrenoceptors, PDE enzymes and potassium channels in pre-contracted rat airways.

(vi) To compare the efficacies of CWE-induced relaxation in the presence of NO synthase inhibitor and NO donor in pre-contracted rat airways.

(v) To construct CRCs to CWE on rat airways at basal tone (without pre-contraction) and to elucidate the mechanisms.

(vi) To construct CRCs to CWE on pre-contracted porcine bronchiole tissues and at basal tone.

3.2 Materials and methods

3.2.1 Drugs and materials

CWE was prepared as described in Section 2.2.2 (**Chapter 2**). Krebs solution was prepared as per **Appendix A**. Details on drugs including brands, solvents, stock solutions, and final concentrations of DMSO (in the bath) used in this chapter are listed in Table 3.1. The preparation of carbachol, ipratropium and KCl followed Section 2.2.1 (**Chapter 2**). Ten-fold serial dilutions using purified water or 50% DMSO were made for all stock solutions to produce respective working solutions. The final concentration of each drug was reported in Section 3.2.3.

Table 3.1: Summary of drugs and details.

Drugs	Company, Country	Solvent	Stock solution (mM)	Final DMSO concentration in bath (%, v/v)
5-hydroxytryptamine hydrochloride/ Serotonin hydrochloride	Nacalai Tesque, Japan	Purified water	100	-
Adenosine	Tocris Bioscience, UK	DMSO 100%	100	0.15
S-(-)-propranolol hydrochloride	Santa Cruz, USA	DMSO 100%	100	0.15
Tetraethylammonium (TEA) chloride	Sigma, USA	DMSO 100%	5000 (5 M)	0.2
Rolipram	Tocris Bioscience, UK	DMSO 100%	10	0.1
Forskolin	Sigma, USA	DMSO 100%	100	0.05
3-isobutyl-1-methylxanthine (IBMX)	Tocris Bioscience, UK	DMSO 100%	100	0.075
***N*^{G}-Nitro-L-Arginine methyl ester (L-NAME) hydrochloride**	ChemSln, USA	Purified water	100	-
Sodium nitroprusside (SNP)	ChemSln, USA	Purified water	100	-
Atropine sulfate	Tocris Bioscience, UK	Purified water	100	-

3.2.2 Tissue preparation

Experiments were conducted with male Sprague Dawley rats (218-480 g; 2-3 months old) purchased from University Putra Malaysia or porcine lungs obtained from local abattoir in Nottingham, UK. Ethics approval for rat was obtained from the University of Nottingham's Animal Welfare and Ethics Review Body (UNMC#2kn and UNMC12). Rats were sacrificed either by carbon dioxide or by cervical dislocation under anaesthesia with diethyl ether. Tracheal and bronchial rings were isolated and immediately immersed in Krebs solution. Porcine bronchioles were isolated from the lungs and stored in Ficoll solution at 4°C overnight. All tissues were cleaned of their connective tissues. Then, porcine bronchioles were excised into 2 to 4 mm rings while rat trachea and bronchus were excised into 2 mm rings, and immediately immersed in standard Krebs solution.

Tissues were mounted to organ bath set up and left to equilibrate to bath condition for 30 minutes after the application of tension of 9.8 mN (rat airways) or 19.6 mN (porcine bronchiole). Subsequently, steps were repeated as in Section 2.2.4.1 (**Chapter 2**) where tissues were exposed to 60 mM KCl twice to obtain the average reference contracture, followed by performance of experimental protocols below.

3.2.3 Experimental protocols

3.2.3.1 Effect of CWE on rat trachea pre-contracted with KCl

To investigate the effect of CWE on different contractile agents, the tone of rat tracheal rings was induced with KCl (60 mM) or carbachol (1 µM) to obtain a stable contraction. Upon establishing stable contractions, cumulative CRCs to CWE at time intervals of 15 minutes between concentrations were constructed. Vehicle control i.e. purified water was performed. Corresponding to the agonist used to pre-contract the tissues, the degree of relaxation was measured as a fraction of the contraction achieved by KCl or carbachol and had been expressed as a percentage of KCl- or carbachol-induced tone.

3.2.3.2 Effect of CWE against carbachol- and 5-HT-induced contractions and the role of muscarinic receptors in 5-HT-induced contraction

Rat tracheal and bronchial rings were pre-incubated with CWE (3.5 mg/ml) or purified water (vehicle control) for at least 30 minutes, prior to the construction of cumulative CRCs to carbachol. Tissue contraction to carbachol had been expressed as a percentage of reference KCl-induced tone. In a separate protocol, tracheal and bronchial segments were pre-incubated with CWE (3.5 mg/ml), ipratropium (30 µM), or purified water (vehicle control) for at least 30 minutes, prior to the construction of cumulative CRCs to 5-HT. This concentration of CWE was chosen based on the results from earlier experiments to ensure maximal relaxation in all airway segments (data not shown). Carbachol and 5-HT were added at intervals of 5 minutes or until

response plateaued. Tissue contraction to carbachol and 5-HT was measured as a fraction of change from basal tension and expressed as a percentage of reference KCl-induced tone.

To rule out the involvement of muscarinic receptors in 5-HT-mediated contraction, tracheal segments were pre-incubated with atropine (1 µM; Harding et al., 2018) simultaneously with CWE (3.5 mg/ml), or atropine (1 µM) simultaneously with purified water (vehicle control), or vehicle control alone for 30 minutes prior to construction of cumulative CRCs to 5-HT. Tissue contraction to 5-HT had been expressed as a percentage of reference KCl-induced tone.

3.2.3.3 Effect of adenosine on airways

As *L. rhinocerotis* sclerotial powder contains adenosine and its derivatives (Section 2.3.3, **Chapter 2**), hence the effect of adenosine on airway tone was examined herein. First, the tone of tracheal and bronchial rings was induced with 1 µM carbachol to obtain a stable contraction. Upon establishing stable contractions, cumulative CRCs to adenosine were constructed. Purified water was added to different bath as vehicle control. The degree of relaxation was measured as a fraction of the contraction achieved by carbachol and had been expressed as a percentage of carbachol-induced tone. In a different protocol, adenosine was added into the preparations in a cumulative manner to tracheal and bronchial rings at basal tone. Adenosine were added at intervals of 5 minutes or until response plateaued. Purified water was added to different bath as vehicle control. The degree of contraction was measured as a fraction of change from tissue basal tone and had been expressed as a percentage of reference KCl-induced tone.

3.2.3.4 Effect of inhibitors of PDE enzyme, NO, β-adrenoceptors and potassium channels, and adenylyl cyclase activator on CWE-induced airway relaxation

As pre-incubation with some drugs below significantly reduced subsequent carbachol-induced tone, concentration of carbachol at 1 to 3 µM was applied to achieve a stable submaximal pre-contraction (~100 to 200% relative to KCl-induced contraction). To investigate the involvement of cAMP and cGMP pathways, rat tracheal rings were pre-incubated with forskolin (10 µM; Mizuta et al., 2012), an AC activator, rolipram (10 µM; Harding et al., 2018), a PDE4 inhibitor, or IBMX (10 µM; Ma, Venkatachalam, Parys, & Gill, 2002), a non-selective PDE inhibitor, for at least 30 minutes, prior to the addition of carbachol (concentration range from 1 to 3 µM) to achieve a stable submaximal contraction (~100 to 200% relative to KCl-induced contraction). Then, cumulative CRCs to CWE were constructed.

In a different set of experiments, rat tracheal segments were pre-incubated with L-NAME (100 µM; Rameshrad, Babaei, Azarmi, & Fouladi, 2016), an inhibitor of NO synthase, or sodium nitroprusside (SNP) (3 µM; concentration that causes ~70% inhibition of carbachol-induced tone from earlier experiment), a NO donor, for at least 30 minutes, prior to pre-contraction with carbachol as mentioned in paragraph above. This was followed by construction of cumulative CRCs to CWE. Given that all drugs had final DMSO concentration of less than 0.1%, DMSO 0.1% v/v was used as the vehicle control in this experiment.

In another set of experiments, to examine the roles of β-adrenoceptors and potassium channels in CWE-induced bronchorelaxation effect, rat tracheal rings were pre-incubated with propranolol (30 µM; fArrieta et al., 2010), a non-selective β-adrenoceptor antagonist, or TEA (10 mM; Kotlikoff, 1993), a non-specific potassium

channel blocker, or DMSO 0.2% (vehicle control) for 30 minutes. Then, pre-contraction with 1 µM carbachol and construction of cumulative CRCs to CWE were carried out.

For all protocols described in this subsection, the degree of relaxation was measured as a fraction of the contraction achieved by carbachol and had been expressed as a percentage of carbachol-induced tone.

3.2.3.5 Effect of CWE on rat airways at basal tone

Earlier experiments in our lab had shown that at basal tone of tissues (tissues not pre-contracted with any contractile agent), cumulative CRCs of CWE (0.25 mg/ml to 5.0 mg/ml) in rat tracheal rings did not induce any significant response (data not shown). Therefore, a different protocol was planned for construction of non-cumulative CRCs to CWE in rat tracheal and bronchial rings. Between each concentration of CWE once the response plateaued, the bath content was washed out and replaced with fresh Krebs buffer. Tissues were left to return to basal tone for about 15 minutes before the next concentration of CWE was added. Purified water was added as the vehicle control in different preparations. The degree of contraction was measured as a change from tissue basal tone and expressed as a percentage of reference KCl-induced tone.

In a different set of experiments, 4 mg/ml of CWE was first added to the tracheal rings. Bath content was then washed out and replaced with fresh Krebs solution. Tissues were left to return to basal tone for about 15 minutes. Subsequently, some tissues were pre-incubated either with or without atropine (1 µM), a non-selective muscarinic receptor antagonist, for at least 30 minutes before the second

addition of 4 mg/ml CWE. This concentration of CWE was derived from non-cumulative CRCs to CWE that has induced submaximal contraction in rat tracheal rings. The degree of contraction induced by CWE was measured as a change from basal tone. CWE-induced tone during the second addition was expressed as a percentage normalized to CWE-induced tone during the first addition.

3.2.3.6 Effect of CWE on porcine airways

To rule out if the effect of CWE is species- and tissue- specific, experiments were conducted in porcine bronchiole rings. The tone of bronchiole rings was induced with 1 µM carbachol to obtain a stable contraction prior to cumulative CRCs to CWE at time intervals of 15 minutes between concentrations were constructed. Vehicle control i.e. purified water was performed. In parallel, cumulative CRCs to ipratropium were performed in different tissues. The degree of relaxation was measured as a fraction of the contraction achieved by carbachol and had been expressed as a percentage of carbachol-induced tone. In a different set of experiments, non-cumulative CRCs to CWE were constructed in porcine isolated bronchiole rings at basal tone. Methods as described in first paragraph of Section 3.2.3.5 were repeated.

3.2.4 Statistical analysis

Data were analysed and graphs were drawn using PRISM v7.0 (Graph pad software). All data were expressed as mean ± SEM of n number of animals. Concentrations of drugs were presented in graph in logarithm of doses in molar (M). Due to the tight concentration range used for CWE, concentrations of CWE were shown in mg/ml instead of logarithm. Maximum tissue contraction or relaxation response (E_{max}) and pEC_{50} values were derived from nonlinear regression analysis of the obtained CRC. In the event that the E_{max} is not achieved as response has not plateaued, E_{max} would be derived from the response generated at the highest concentration tested. In some experiments, responses at each individual concentration were compared with multiple comparison test. Statistical analyses were performed using one-way ANOVA with Dunnett correction (Fig. 3.2C and D, 3.3, 3.5 and 3.6), two-way ANOVA followed by multiple comparisons with Bonferroni correction (Fig. 3.1, 3.7A, 3.9B and C), and Student's unpaired t-test (Fig. 3.2A and B, 3.4, 3.7B, 3.9A). One-way ANOVA was used to compare the mean differences, whereas two-way ANOVA was used to compare the differences and to analyse the interactions between concentrations and treatments. Results were considered statistically significant if p-value was less than 0.05. In the case if the interaction p-value based on two-way ANOVA was < 0.05, this indicated an interaction between treatment groups and concentrations, meaning that difference between treatments were not consistent for different concentrations and thus inferring a concentration-dependent effect of treatment.

3.3 Results

3.3.1 CWE similarly relaxed pre-contraction by KCl and carbachol

Results demonstrated that CWE significantly relaxed KCl-induced pre-contraction (E_{max} of CWE: 124.65 ± 12.48%, vehicle control: 84.01 ± 6.15%; $p = 0.0081$) (Fig. 3.1A). The difference in responses between CWE treatment and vehicle control was statistically significant at concentrations 4.0 to 4.5 mg/ml. Two-way ANOVA results showed that there was an interaction between treatments and concentrations ($p = 0.0019$), indicating that these factors are interdependent. CWE-induced relaxant responses were similar for both carbachol- and KCl-induced pre-contractions, with no significant difference in the maximum responses ($p > 0.999$) (Fig. 3.1B). It was also observed that the vehicle control in KCl-induced pre-contraction was less sustained than that in carbachol-induced pre-contraction (Section 2.3.5, **Chapter 2**). Altogether, the results suggest that CWE relaxes airway smooth muscle either via inhibition of the contractile mechanisms mediated by both KCl and carbachol or via activation of different relaxing pathway.

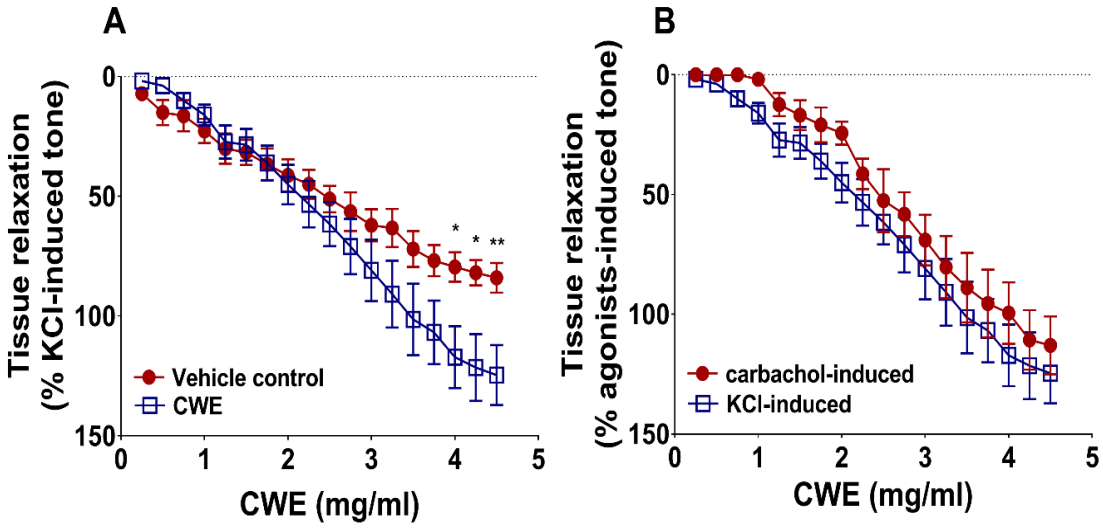

Figure 3.1: Effect of cold water extract on rat trachea pre-contracted with different contractile agonists. (A) CRCs to CWE or vehicle control in tracheal rings pre-contracted with 60 mM KCl. (B) CRCs to CWE in tracheal rings pre-contracted with 1 µM carbachol or 60 mM KCl. Tissue response was expressed as a percentage of KCl- or carbachol-induced contraction corresponding to the agonists used to pre-contract the tissues. Data were shown as means ± SEM of 4 to 6 animals. Two-way ANOVA with Bonferroni correction where comparison of means was made between treatment group and vehicle control: *$p < 0.05$, **$p < 0.01$. (Abbreviations: CWE = Cold water extract; CRCs = Concentration-response curves)

3.3.2 CWE attenuated carbachol and 5-HT-induced contractions

Fig. 3.2A shows that pre-incubation of tracheal tissues with CWE significantly suppressed the E_{max} of carbachol-induced contraction compared to vehicle control. In addition, CWE significantly shifted the potency of carbachol-induced contraction to the left by ~8.7-fold. Likewise in bronchial tissues (Fig. 3.2B), CWE also evidently suppressed the E_{max} of carbachol-induced contraction in comparison to vehicle control. Potency of carbachol CRC was not affected by CWE treatment in the bronchus. The E_{max} and pEC_{50} values are recorded in Table 3.2.

Similarly, maximum response of 5-HT-induced contraction was significantly reduced by CWE pre-incubation in tracheal rings (Fig. 3.2C) and almost completely abolished in bronchial rings (Fig. 3.2D) (Table 3.2). In Section 2.3.6 (**Chapter 2**), ipratropium, as a positive control, relaxed carbachol-induced pre-contraction in tracheal and bronchial rings. Fig. 3.2C and 3.2D show that ipratropium also significantly suppressed 5-HT-induced contraction in both tracheal and bronchial tissues when compared to vehicle control. It was also observed that 4 out of 9 bronchial tissues with 5-HT-induced contraction were relatively less or not responsive to CWE treatment and these values had been factored into the graph to display the average (Fig. 3.2D). CWE did not affect the pEC_{50} values of 5-HT curve in both tracheal and bronchial rings (Table 3.2).

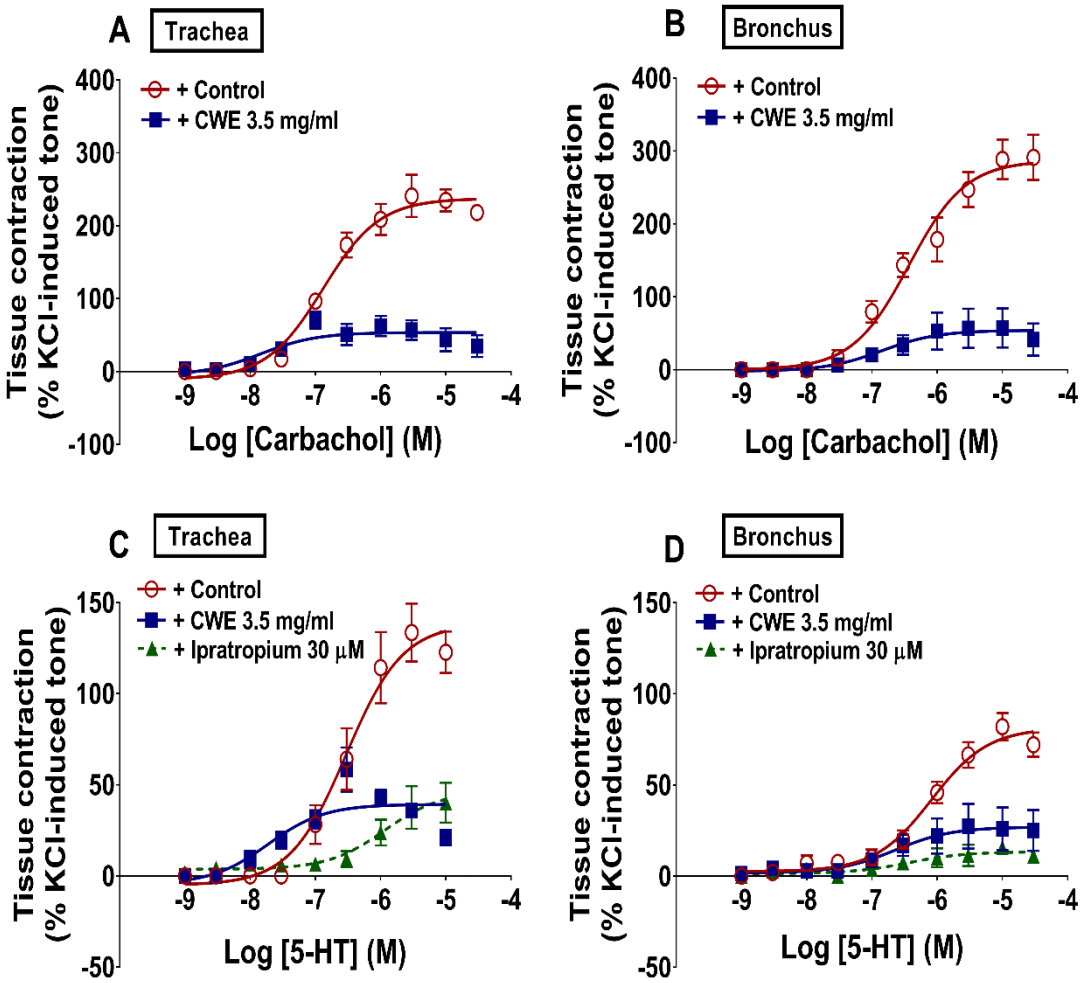

Figure 3.2: Effect of cold water extract against carbachol- and 5-hydroxytrptamine-induced contractions in rat airways. Effect of pre-incubations with CWE or vehicle control (purified water) for 30 minutes on CRCs to carbachol in (A) tracheal and (B) bronchial rings. Effect of pre-incubations with CWE, ipratropium, or vehicle control (purified water) for 30 minutes on CRCs to 5-HT in (C) tracheal and (D) bronchial rings. Tissue response was expressed as a percentage of KCl-induced tone. Data were shown as means ± SEM of 3 to 9 animals. (Abbreviations: 5-HT = 5-hydroxytryptamine; CRCs = Concentration-response curves; CWE = Cold water extract)

Table 3.2: The maximum response (E_{max}) and pEC_{50} values of carbachol and 5-hydroxytryptamine derived from the respective concentration-response curve in the presence of different treatments. Unpaired T-test (carbachol) or one-way ANOVA with Dunnett correction (5-HT) where comparison of means were made between vehicle control and treatment groups (**p < 0.01; ***p < 0.001). Individual p-value was stated. Data represented the means ± SEM of 3 to 9 animals.

Compound	Treatment	Trachea		Bronchus	
		E_{max} (%)	pEC_{50}	E_{max} (%)	pEC_{50}
Carbachol	**+ Vehicle (water)**	237.50 ± 17.99	6.88 ± 0.10	286.80 ± 28.43	6.42 ± 0.11
	+ CWE 3.5 mg/ml	53.46 ± 13.21** (p = 0.0012)	7.82 ± 0.66*** (p = 0.0005)	54.97 ± 26.04*** (p = 0.001)	7.03 ± 0.32 (p = 0.0865)
5-HT	**+ Vehicle (water)**	139.70 ± 13.20	6.49 ± 0.13	83.37 ± 7.36	6.19 ± 0.16
	+ CWE 3.5 mg/ml	53.46 ± 7.60** (p = 0.0083)	7.37 ± 0.18 (p = 0.458)	27.41 ± 12.59** (p = 0.0014)	7.01 ± 0.92 (p = 0.103)
	+ Ipratropium 30 µM	50.91 ± 13.84** (p = 0.0029)	6.32 ± 0.51 (p = 953)	16.00 ± 0.46** (p = 0.0052)	6.10 ± 0.57 (p = 0.981)

Abbreviations: 5-HT = 5-hydroxytryptamine; CWE = Cold water extract

3.3.3 Muscarinic receptors were involved with 5-HT-induced contraction

The involvement of muscarinic receptors on 5-HT-induced contraction was investigated. Fig. 3.3 shows that in vehicle control tissues, 5-HT CRCs achieved a maximum response of 139.70 ± 13.20%. Simultaneous pre-incubation of tracheal rings with atropine and vehicle control significantly decreased the maximum response (E_{max}: 47.05 ± 9.81%, $p < 0.0001$). Combinatorial pre-incubation with atropine and CWE 3.5 mg/ml had additive effect that further reduced the maximum response of 5-HT-induced contraction (E_{max}: 19.61 ± 6.53%, $p = 0.0002$). The potencies of 5-HT CRC were not affected by all treatments. These results suggest that the relaxation effect of CWE involves pathway other than that downstream of muscarinic receptors, and post-junctional cholinergic activation may have a role in 5-HT-induced airway contraction.

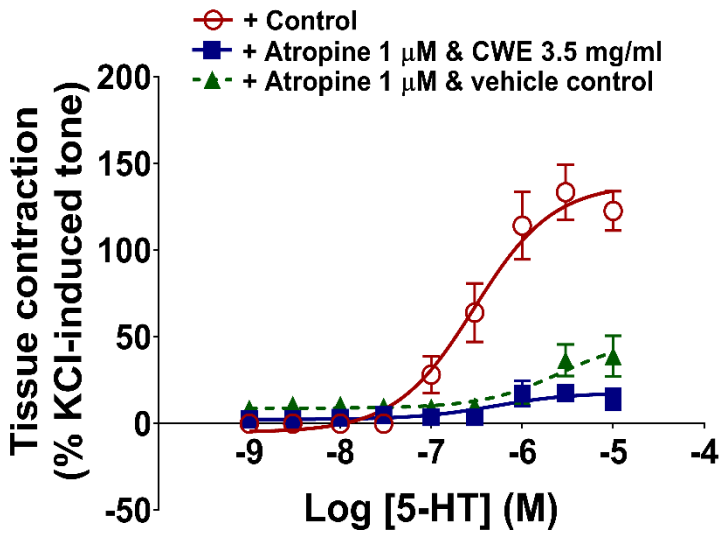

Figure 3.3: Effect of cold water extract and atropine against 5-hydroxytryptamine-induced contraction in rat trachea. CRCs to 5-HT in tissues pre-incubated with atropine and CWE, atropine and vehicle control, or vehicle control alone (purified water) for 30 minutes. Tissue response was expressed as a percentage of KCl-induced tone. Data were shown as means ± SEM of 3 to 5 animals. (Abbreviations: 5-HT = 5-hydroxytryptamine; CRCs = Concentration-response curves; CWE = Cold water extract)

3.3.4 Adenosine did not affect the tone of rat airways

Fig. 3.4A and B show that adenosine was devoid of any effect in tracheal (T) and bronchial (B) rings pre-contracted with carbachol (E_{max}: T: $p = 0.9628$; B: $p = 0.0918$). At basal tone, adenosine also did not exhibit any significant effect on both tracheal and bronchial rings (E_{max}: T: $p = 0.7767$; B: $p = 0.1414$). These results indicated that adenosine did not affect the tone of rat isolated airways.

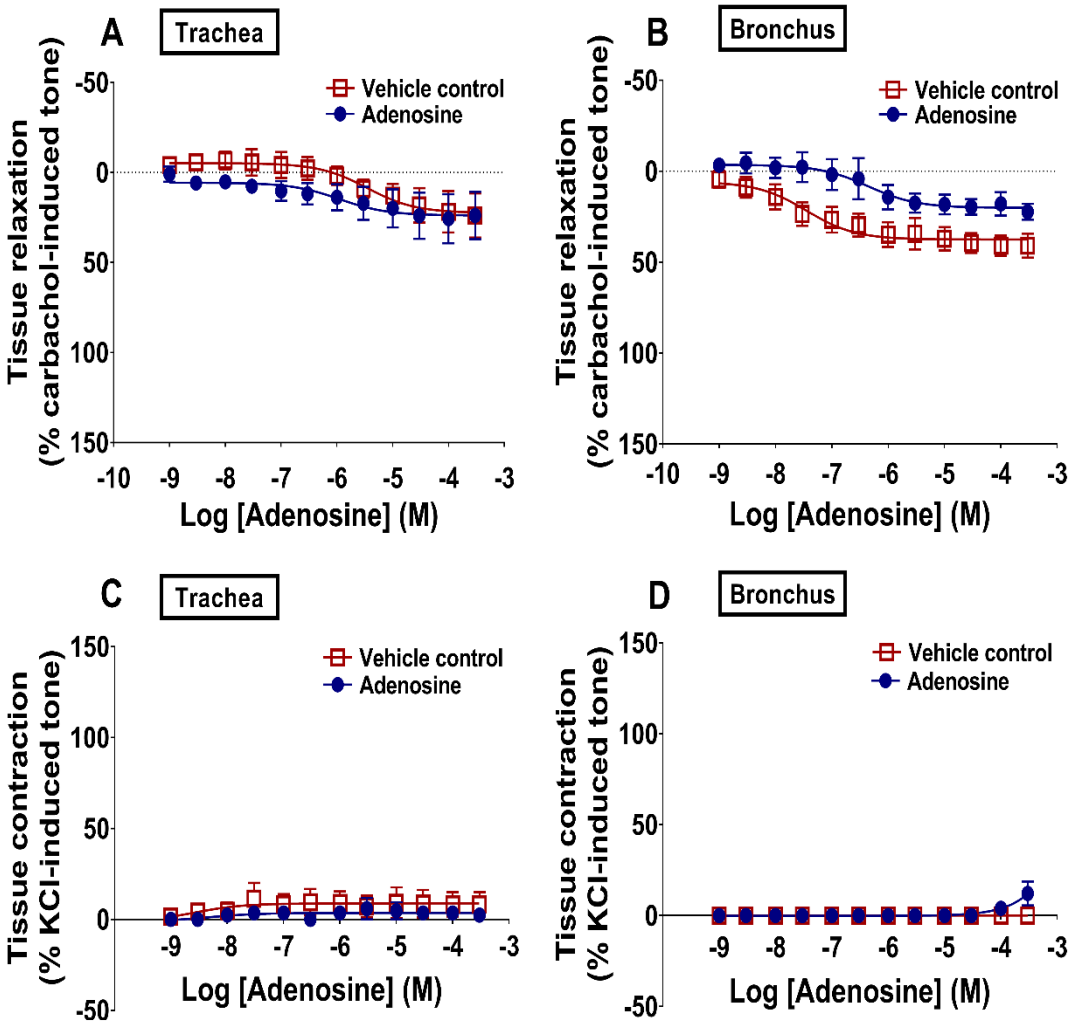

Figure 3.4: Effect of adenosine on rat airways at basal tone and pre-contracted with carbachol. Concentration-response curves (CRCs) to adenosine in (A) tracheal and (B) bronchial rings pre-contracted with 1 µM carbachol. CRCs to adenosine in (C) tracheal and (D) bronchial rings at basal tone. Tissue response was expressed as a percentage of (A),(B) carbachol or (C),(D) KCl-induced tone. Data were shown as means ± SEM of 3 animals.

3.3.5 CWE potentiated the relaxation effect mediated by cAMP but has no effect on NO/cGMP-mediated responses

The roles of cAMP, cGMP and NO pathways were examined by pre-incubating the tracheal rings with a series of drugs, and their effects on CRCs to CWE were assessed. The maximum response of CWE CRCs in vehicle control tissues was 103.21 ± 11.87%, and the maximum responses were not significantly different in the presence of forskolin, rolipram, IBMX, SNP and L-NAME as all of the tissues had achieved full relaxation (> 100%) at the highest concentration tested ($p > 0.05$) (Fig. 3.5A and B). Since the CRCs to CWE had not plateaued, to compare the potency of each curve pEC_{50} value was estimated as the concentration that produced 50% relaxation by constraining the maximum response to 100% for all groups. Fig. 3.5A demonstrates that in vehicle control tissues, the pEC_{50} value of CWE CRCs is -0.31 ± 0.05. The pre-incubation with forskolin significantly increased the potency of CWE CRC by ~3.2-fold (pEC_{50}: 0.20 ± 0.08; $p = 0.0017$). IBMX also slightly increased the potency by ~2.2-fold (pEC_{50}: 0.045 ± 0.10; $p = 0.0189$). In contrast, rolipram did not affect the potency of CWE CRC (pEC_{50}: -0.12 ± 0.11; $p = 0.3227$). This potentiation effect by forskolin on CWE-induced relaxation suggests that CWE may either activate components upstream of cAMP or act via mechanism different from cAMP pathway.

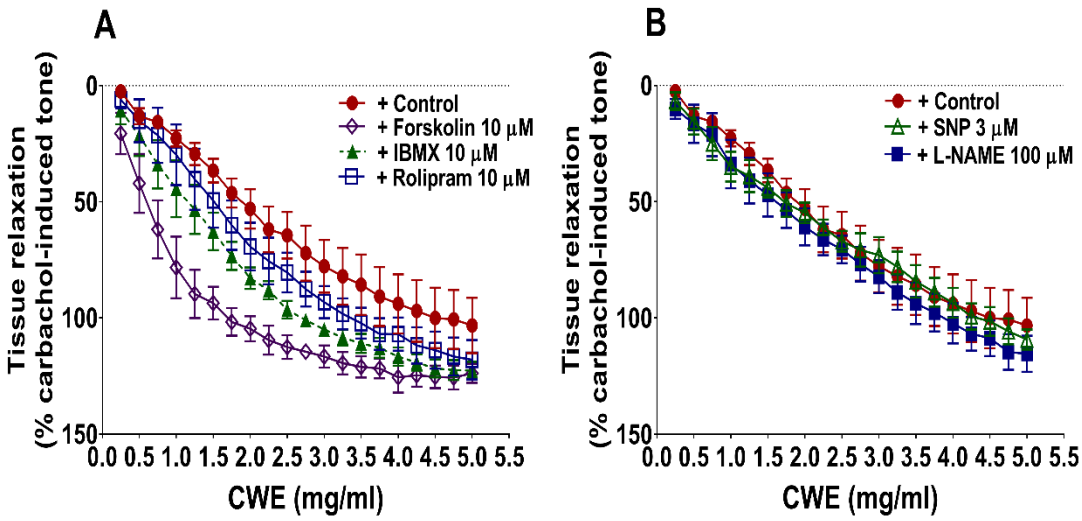

Figure 3.5: Roles of cAMP, cGMP and nitric oxide pathway in cold water extract-induced relaxation in rat trachea. (A) Tracheal rings were pre-incubated with forskolin, IBMX, or rolipram for 30 minutes prior to pre-contraction with 1 µM carbachol, followed by construction of CRCs to CWE. Similar procedure was performed for (B) except that tracheal rings were pre-incubated with L-NAME or SNP instead. The vehicle control i.e. DMSO 0.1% was added in different preparations prior to CRCs to CWE. Tissue response was expressed as a percentage of carbachol-induced tone. Data were shown as means ± SEM of 5 to 6 animals. (Abbreviations: cAMP = 3'-5'-Cyclic adenosine monophosphate; cGMP = 3'-5'-Cyclic guanosine monophosphate; CRCs= concentration-response curves; CWE = cold water extract; IBMX = 3-isobutyl-1-methylxanthine; L-NAME = N^G-Nitro-L-Arginine methyl ester; SNP = Sodium nitroprusside)

Besides, Fig. 3.5B demonstrates that pre-incubations with SNP and L-NAME did not affect the potency (pEC50: SNP: -0.17 ± 0.09, p = 0.385; L-NAME: -0.1797 ± 0.1, p = 0.422) of CWE CRCs when compared to vehicle control. Hence, the results strongly suggest that the bronchodilator effect of CWE is not mediated via NO/cGMP pathway.

3.3.6 CWE-induced airway relaxation was not mediated via β-adrenoceptors or potassium channels

Pre-incubation of tissues with propranolol and TEA did not significantly affect the E_{max} and pEC_{50} values induced by CWE in both tracheal (Fig. 3.6A) and bronchial (Fig. 3.6B) rings. The E_{max} and pEC_{50} values are summarized in Table 3.3. As the response had not plateaued at the highest concentration, pEC_{50} values were obtained by constraining the maximum responses to 100%. These findings suggest that β-adrenoceptors or potassium channels did not participate in CWE-induced airway relaxation.

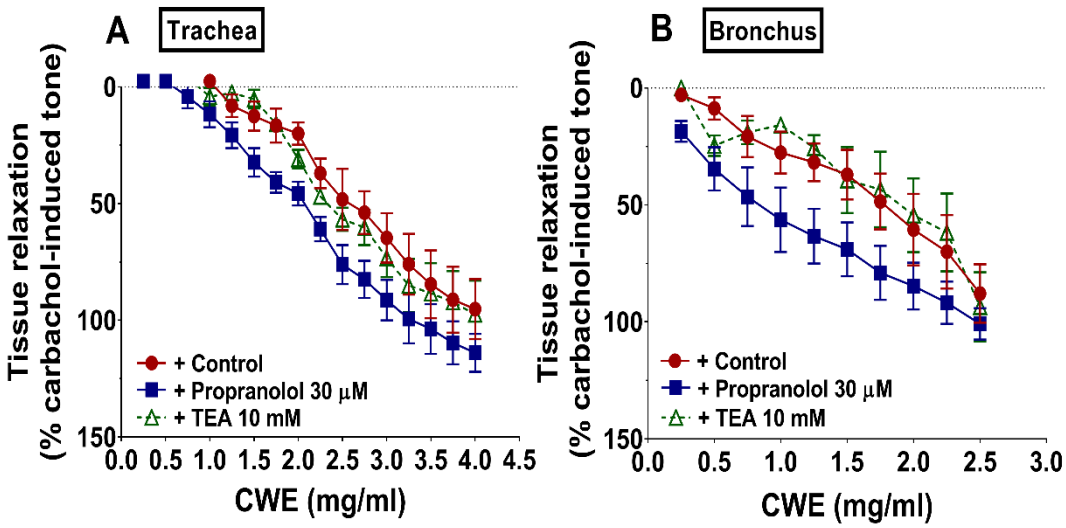

Figure 3.6: Effect of antagonists of β-adrenoceptors and potassium channels against cold water extract-induced relaxation in rat airways. (A) Trachea and (B) bronchial tissues were pre-incubated with propranolol or TEA for at least 30 minutes prior to pre-contraction with 1 µM carbachol, followed by construction of concentration-response curves to CWE. Tissue response was expressed as a percentage of carbachol-induced tone. Data were shown as means ± SEM of 3 to 6 animals. (Abbreviations: CWE = Cold water extract; TEA = Tetraethylammonium)

Table 3.3: The maximum response (E_{max}) and pEC_{50} values of cold water extract derived from the respective concentration-response curve in the presence of propranolol and tetraethylammonium. One-way ANOVA with Dunnett correction where comparison of the means were made between vehicle control and the treatment groups. Individual p-value was stated. Data represented the means ± SEM of 3 to 6 animals.

Treatments	Trachea		Bronchus	
	E_{max} (%)	pEC_{50}	E_{max} (%)	pEC_{50}
+ Vehicle (purified water)	99.52 ± 12.80	-0.22 ± 0.21	87.80 ± 12.43	-0.24 ± 0.27
+ Propranolol 30 µM	118.20 ± 8.03 (*p* = 0.390)	-0.28 ± 0.04 (*p* = 0.923)	100.80 ± 6.65 (*p* = 0.553)	0.06 ± 0.11 (*p* = 0.096)
+ TEA 10 mM	101.80 ± 14.40 (*p* = 0.987)	-0.35 ± 0.01 (*p* = 0.783)	93.47 ± 14.41 (*p* = 0.915)	-0.28 ± 0.07 (*p* = 0.958)

Abbreviations: CWE = Cold water extract; TEA = tetraethylammonium

3.3.7 CWE increased the basal tone of rat airways possibly via muscarinic receptor activation

Non-cumulative CRCs to CWE had induced significant contractions in both rat tracheal (from 4 to 6 mg/ml) and bronchial (from 2 to 4 mg/ml) tissues at basal tone (Fig. 3.7A). In tracheal rings, the maximum response induced by CWE at 5 mg/ml was 70.92 ± 15.58% compared to vehicle control, 3.49 ± 1.79% ($p = 0.0014$). In bronchial rings, CWE elicited a maximum response at 3 mg/ml (E_{max} of CWE: 106.47 ± 3.64%, vehicle: 0%; $p < 0.0001$), which was by ~1.6-fold lower concentration and ~1.5-fold higher response compared to tracheal rings. Interestingly, after the achievement of maximum response, CWE-induced tone gradually declined with increasing concentrations of CWE, suggesting a desensitization of the response has taken place. Two-way ANOVA results also showed an interaction between treatments and concentrations in tracheal ($p = 0.0399$) and bronchial ($p < 0.0001$) tissues, indicating that these factors are interdependent.

Subsequent experiments assessed if CWE-induced airway contraction was mediated by muscarinic receptors. Results demonstrated that the second CWE-induced tone was significantly attenuated by pre-incubation with atropine (E_{max}: 26.46 ± 10.98%; $p = 0.0039$) compared to vehicle control (E_{max}: 95.96 ± 6.18%) (Fig. 3.7B), suggesting that CWE-induced contraction is mediated by muscarinic receptor activation.

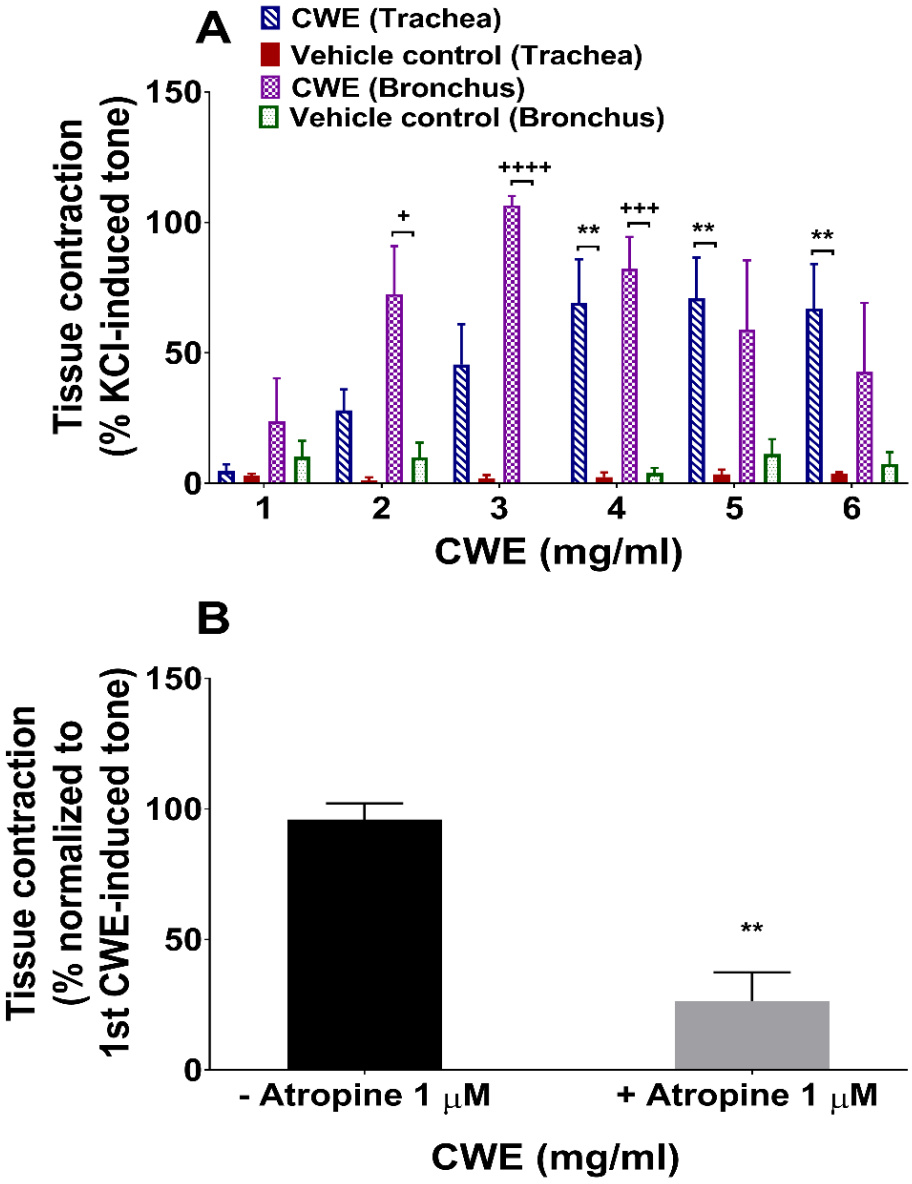

Figure 3.7: Effect of cold water extract on rat airways at basal tone. Non-cumulative concentration-response curves to cold water extract (CWE) in (A) tracheal and bronchial rings at the basal tone (without pre-contraction). Tissue response was expressed as a percentage of KCl-induced tone. (B) In tracheal rings, CWE was first added to induce a tone, and then washed out with fresh Krebs solution. Subsequently, tissues were pre-incubated either with (+) atropine 1 µM for 30 minutes or without (-) atropine, followed by the second addition of CWE. Tissue response induced by second CWE addition was normalized to the response induced by first CWE addition (represents 100%). Data were shown as means ± SEM of 3 to 5 animals. For (A), two-way ANOVA with Bonferroni correction was done between treatment group and vehicle control in trachea: $^{**}p < 0.01$; in bronchus: $^{+}p < 0.05$, $^{+++}p < 0.001$, $^{++++}p < 0.0001$; for (B), unpaired T-test was done between treatment group and vehicle control: $^{**}p < 0.01$.

Fig. 3.8 depicts the representative trace recording in which at the basal tone of tracheal tissue, CWE induced initial transient peak of contraction, followed by a slightly lower sustained contraction in the later phase. Nevertheless, the pattern of contraction was not consistent as for some tissues, the degree of CWE-induced contraction was lower in general and not sustained in the later phase. Pre-incubation with atropine had lowered the initial peak as well as the sustained contraction induced by CWE.

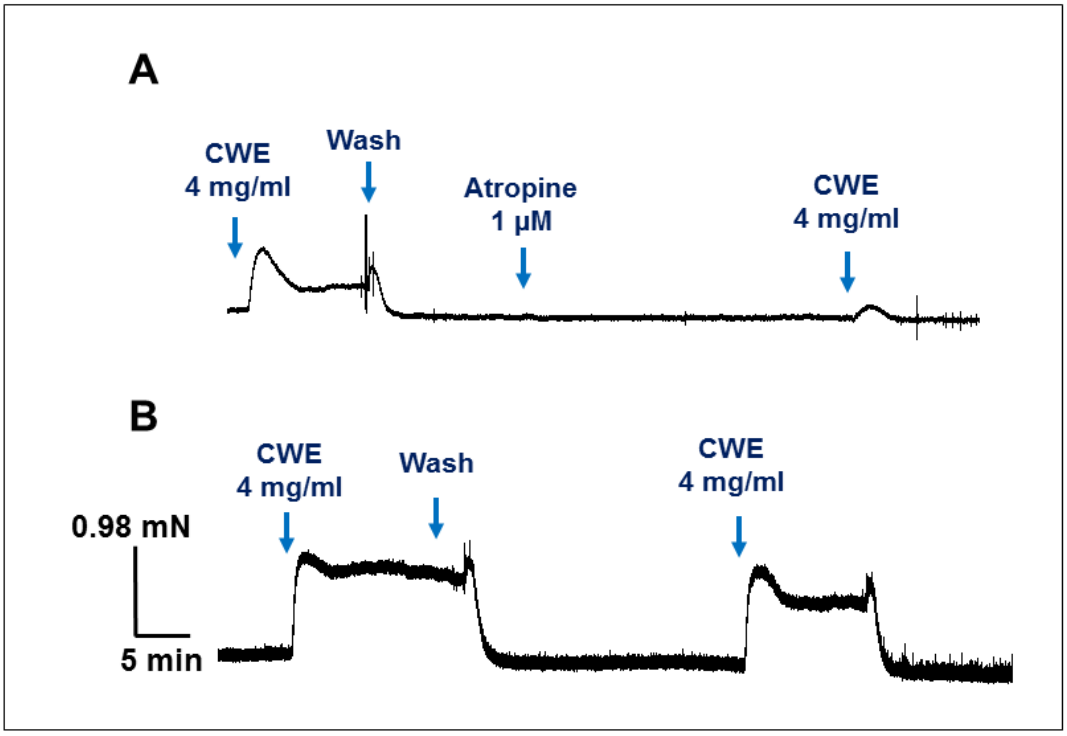

Figure 3.8: Representative trace recording of cold water extract-induced contraction in rat trachea at basal tone. Following the first CWE addition, tissues were washed out with fresh Krebs solution, and then pre-incubated (A) with or (B) without atropine before the second CWE addition. (Abbreviations: CWE = cold water extract; min = minute; mN = milliNewton)

3.3.8 CWE exhibited similar responses in porcine bronchiole as in rat airways

Our results showed that carbachol pre-contracted porcine bronchiole rings were significantly relaxed by the positive control, ipratropium (E_{max} of ipratropium: 141.70 ± 8.62%, vehicle: 39.83 ± 20.09%, p = 0.0096) (Fig. 3.9A). Besides, Fig. 3.9B demonstrates that CWE also significantly relaxed bronchiole rings pre-contracted with carbachol at concentrations 0.316 to 5.62 mg/ml (E_{max} of CWE: 90.69 ± 3.69%, vehicle: 48.45 ± 2.48%, $p < 0.0001$). By constraining the maximum response of CWE CRCs to 100%, the potency of CWE was 0.216 ± 0.229. Two-way ANOVA results also showed an interaction between treatments and concentrations (p = 0.0008), indicating that these factors are interdependent.

In porcine bronchiole rings at the basal tone, non-cumulative addition of CWE from 4 to 7 mg/ml had induced significantly higher tissue contraction than vehicle control. Maximum contractile response to CWE was achieved at 5 mg/ml (E_{max} of CWE: 39.74 ± 7.50%, vehicle: 0.57 ± 0.33%; $p < 0.0001$) (Fig. 3.9C). Of note is that the maximum contractile response to CWE in porcine bronchiole rings was lower than those in rat airways at the same concentration, while the potency of CWE-induced relaxation was slightly higher in pre-contracted porcine bronchioles compared to rat airways. Two-way ANOVA results also showed an interaction between treatments and concentrations (p = 0.0002), indicating that these factors are interdependent. These results indicated that other than rat species, CWE also exhibited concentration-dependent airway relaxation and contraction in pig.

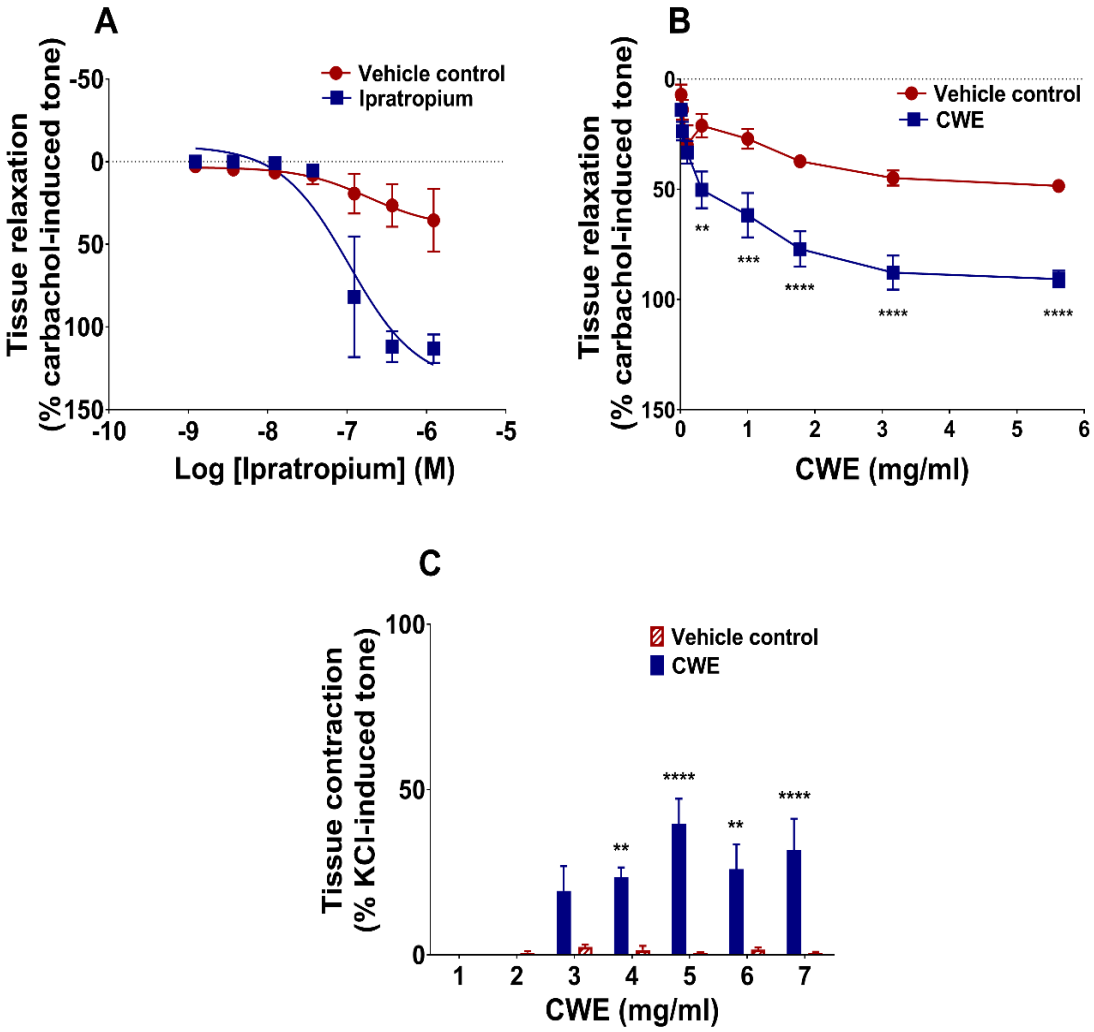

Figure 3.9: Effect of cold water extract on porcine bronchiole pre-contracted with carbachol. Cumulative concentration-response curves (CRCs) to (A) ipratropium and (B) cold water extract (CWE) in bronchioles rings pre-contracted with 1 µM carbachol. Tissue response was expressed as a percentage of carbachol-induced contraction. (C) Non-cumulative CRCs to CWE were constructed in bronchiole rings at basal tone. Tissue response was expressed as a percentage of KCl-induced tone. Data were shown as means ± SEM of 3 to 5 animals. Two-way ANOVA with Bonferroni correction was done to compare means between CWE treatment and vehicle control: $^{**}p < 0.01$, $^{***}p < 0.001$, $^{****}p < 0.0001$.

3.4 Discussions

Our results demonstrated that CWE significantly relaxed both porcine and rat airways pre-contracted with carbachol, indicating that the airway relaxation effect of CWE is not selective to species, and therefore rejecting our hypothesis. The relaxant response to CWE was comparable to ipratropium, which also fully relaxed the pre-contracted rat and porcine airways; however, CWE required relatively longer incubation time to achieve a full relaxation compared to ipratropium.

The possible mechanisms by which CWE exhibited bronchodilator effect were elucidated herein. It is noted that pre-treatment with CWE possessed non-competitive antagonistic effects on airway contractions induced by carbachol and 5-HT, as deduced from the marked reduction in maximum responses that were not reversed by increasing concentrations of the agonists. This implies that instead of providing immediate bronchodilator effect for acute bronchoconstriction, regular application of *L. rhinocerotis* may have potential benefit in preventing and relieving acute and chronic airway obstructions that take place in EAR and LAR.

5-HT is a non-selective agonist of 5-HT receptors. Our earlier results showed that 5-HT-induced airway contraction was inhibited by metergoline, an antagonist for various 5-HT receptors including subtype 1, 2, 5, 6, and 7, indicating that the contraction was mediated by activation of one or more of these receptor subtypes (data not shown). In this study, blockade of muscarinic receptors with ipratropium and atropine pre-incubation had largely attenuated 5-HT-evoked contraction, indicating that post-junctional cholinergic activation may have a role in 5-HT-mediated airway contraction. This finding is in agreement with previous study (Szarek, Zhang, & Gruetter, 1995), which suggests that aside from directly activating 5-HT_2 receptors

located on airway smooth muscle, 5-HT also indirectly activates 5-HT_2 receptors on cholinergic nerve endings to elicit contraction of rat airways. Combinatorial treatment of CWE with atropine had further reduced 5-HT-induced maximum contractile response by 30% lower than treatment with atropine alone. This additive effect suggests that CWE is likely to affect other components besides muscarinic receptors, leading to hypothesis that the effect of CWE is not mediated by direct blockade of muscarinic receptors.

Activation of both M_3 and 5-HT_2, especially 5-HT_{2A}, receptors are presumably coupled to $G_{\alpha q}$ protein subunit (Hazelwood & Sanders-Bush, 2004; Kurrasch-Orbaugh, Parrish, Watts, & Nichols, 2003), leading to an overall increase in the $[Ca^{2+}]_i$ levels and hence airway smooth muscle contractions. The similar inhibitory effects of CWE on both carbachol and 5-HT infer that the airway relaxation effect may be mediated via regulation of Ca^{2+} signalling pathway downstream of $G_{\alpha q}$-coupled receptors. There have been mixed findings about the pools of Ca^{2+} utilized by carbachol and 5-HT for contraction. $G_{\alpha q}$-coupled receptor activation by agonists has been associated with stimulation of intracellular Ca^{2+} release which in turn triggers extracellular Ca^{2+} influx through membrane calcium channels, especially ROCC and SOCC. In comparison, extensive reviews indicate that the role of VOCC is relatively less significant in contractile agonist-induced contraction, supported by the finding that L-type calcium channels blockers failed to ameliorate asthmatic symptoms and lacked effectiveness in inhibiting airway smooth muscle contraction induced by contractile agonists and inflammatory mediators (Girolamo Pelaia et al., 2008). This is probably due to insufficient extent of depolarization induced by the agonists to activate VOCC (Sanderson et al., 2008). Evidence shows that intracellular Ca^{2+} may be the

predominant Ca^{2+} source for contraction mediated by activation of $G_{\alpha q}$-coupled receptors by agonists (Girolamo Pelaia et al., 2008; Sanderson et al., 2008).

Moreover, our results demonstrated that CWE produced similar degree of relaxation on airway segments pre-contracted with KCl and carbachol. In view of this, we deduced that CWE may either act via a direct relaxation mechanism e.g. cAMP and cGMP pathways, or via inhibition of the mechanism affected by both KCl and carbachol. KCl is known to depolarize smooth muscle cell membrane and predominantly open VOCC, especially L-type calcium channels, resulting in an influx of extracellular Ca^{2+} (Sanderson et al., 2008). Hence, CWE may block extracellular Ca^{2+} influx through membrane calcium channels, possibly L-type calcium channels. Gathered observations from the relaxation effects of CWE on carbachol-, 5-HT- and KCl-induced contractions suggested two possibilities: Firstly, CWE may block membrane calcium channels, in particular L-type calcium channels, and hence carbachol, 5-HT, and KCl may depend on extracellular Ca^{2+} to elicit contraction. The calcium mechanisms of these contractile agents were elucidated in **Chapter 4** to validate this hypothesis. Secondly, CWE may activate mechanisms independent of $G_{\alpha q}$-coupled pathways and membrane calcium channels, possibly through cAMP or cGMP pathway. The latter hypothesis was discussed in the following paragraphs. Furthermore, given that CWE blocked contractions induced by different contractile agonists, we deduced that the bronchodilator effect of *L. rhinocerotis* is not mediated via direct blockade of muscarinic receptors, rejecting our hypothesis.

To rule out the involvement of β_2-adrenoceptors, propranolol that non-selectively blocks β-adrenoceptors was used. Our results showed that propranolol did not affect the CRCs to CWE, inferring CWE does not act via β_2-adrenoceptor activation. In support of this, pre-contracted rat tracheal tissues poorly responded to

salmeterol (Section 2.3.6, **Chapter 2**), indirectly supporting that the main relaxing effect of CWE is not mediated via β_2-adrenoceptors. On the other hand, BK_{Ca} channel is the predominant potassium channel in airway smooth muscle that opens in response to cAMP or directly coupled to β_2-adrenoceptors via G_s protein, and TEA was shown to inhibit this channel (Harding et al., 2018). In this study, CWE-induced relaxation was unaffected by inhibition of TEA-sensitive potassium channels. This implies that CWE does not relax airway smooth muscle through opening of these potassium channels. Thus, these findings indicate that β_2-adrenoceptors and its downstream potassium channel opening which presumably couple to cAMP pathway are not implicated by CWE.

Moving on to the second messengers, forskolin is an established AC activator that rapidly potentiates cAMP generation and elevates intracellular cAMP levels. Marked potentiating effect of forskolin on CWE-induced bronchorelaxation was observed in this study. There are two possible explanations for this effect: Firstly, CWE may prevent the breakdown of cAMP by inhibiting the PDE enzyme. Secondly, CWE may act through cAMP-independent pathway, leading to the additive effect with forskolin. The first hypothesis complements the previous results where CWE-induced relaxation was not affected by propranolol, leading to proposition that CWE is unlikely to affect cAMP pathway downstream of β_2-adrenoceptors. In support of this, the inhibition of PDE4, which selectively breaks down cAMP, by rolipram was devoid of effect on CWE-induced relaxation, indicating that the components upstream of cAMP pathway (AC and β_2-adrenoceptor activation) are not likely to be affected. Subsequent findings showed that pre-treatment with IBMX, a broad range inhibitor of PDE enzymes, has slightly augmented the relaxant response to CWE, suggesting that either cAMP or cGMP pathway may play a minor role. The scope of current study does not

allow for interpretation of the cellular cAMP level, and further test is warranted to address this aspect. Functional evidence up to this point indicate that cAMP pathway is possibly not involved, hence we hypothesized that NO/cGMP pathway may be affected by CWE.

Subsequently, the role of CWE on NO/cGMP pathway was studied with L-NAME and SNP. The lack of effect of L-NAME on CWE-induced relaxation suggests that CWE does not activate the NO/cGMP pathway. Moreover, SNP, which should directly elevate the NO levels and stimulate cGMP production, failed to potentiate CWE-induced relaxation in this study. Our results, however, do not agree with the previous study by Guo et al. (2011) where hot water extract of *L. rhinocerotis* was shown to stimulate murine macrophage cells and induce NO production. We attribute the discord to the different cell types and extracts used by Guo et al. (2011) and ours. The NO synthase located in airway epithelial cells may not be activated by CWE in our study. As such, these results strongly suggest that NO/cGMP pathway is not implicated, rejecting our previous hypothesis.

Next, we assessed the possibility of exogenous adenosine as a bronchodilator component of CWE. The present study showed that cumulative CRCs to adenosine did not have any effect on rat airway segments pre-contracted with carbachol as well as at basal tone. A previous study showed that in Brown Norway rats, only sensitized and ovalbumin-challenged airways responded to adenosine and adenosine receptor agonists (Hannon et al., 2002). Similar to our findings, Hannon et al. (2002) did not observe any response to exogenous adenosine in non-sensitized rats (control). This is in accordance with other researchers where adenosine-induced bronchoconstriction (Spicuzza et al., 2006) and bronchodilation (Cushley, Tattersfield, & Holgate, 1983) were more pronounced in asthmatics patients than healthy subjects. It was also found

that the expression of A_1 receptors on bronchial tissue was higher in ovalbumin-challenged Wistar rats compared to control rats (Alfieri et al., 2012). It is therefore plausible that the lack of response to adenosine in our experiments is because the airways segments were obtained from non-sensitized and non-ovalbumin-challenged rats. This might also be partly explained by changes in the contractile properties of sensitized airway smooth muscle. Indeed, altered responses to contractile agents including histamine, carbachol, and KCl in sensitized human airway smooth muscle were reported by Black et al. (1989), who suggested that Ca^{2+} handling mechanisms may be different for sensitized airways. Similarly, contractile responses of sensitized airway smooth muscle to other substances such as substance P and neurokinin A (Ben-Jebria, Marthan, Rossetti, & Savineau, 1993) and leukotriene C4 (D. Schmidt, Ruehlmann, Branscheid, Magnussen, & Rabe, 1999) were augmented, inferring that sensitized airways have altered contractile properties. Taken together, we excluded the possibility of adenosine being the bioactive component for bronchodilator properties of *L. rhinocerotis*. However, as crude extract is a mixture of various components, we cannot discount the possibility of synergistic effect from multiple constituents causing the bronchorelaxation effect.

Interestingly, we also observed that at the basal tone, non-cumulative CRCs to CWE had induced significant contraction in rat and porcine airway segments. The rat bronchus was more susceptible to the contraction at a lower concentration (2 to 4 mg/ml), compared to rat trachea (4 to 6 mg/ml) and porcine bronchioles (4 to 7 mg/ml). This is in line with the finding that lower concentration was required to achieve full relaxation in rat bronchial tissues relative to other tissues. We postulate that this may be due to the higher amount of smooth muscle present in bronchus where relaxation or contraction takes place. It is also noted that in the airway tissues, CWE-induced

contraction progressively decreased with increasing concentrations, probably due to desensitization of the cellular targets or the bronchodilator effect may predominate at higher concentrations. Looking at the trace recording, CWE induced a sharp initial peak of contraction, followed by a lower sustained phase of contraction (Fig. 3.8). We postulate that these different phases of contraction may attribute to the utility of different Ca^{2+} pools by CWE, such that an increase in intracellular Ca^{2+} release in initial phase followed by calcium channel opening in the sustained phase.

Unexpectedly, the bronchoconstricter effect of CWE was shown to be mediated by muscarinic receptor activation as pre-incubation with atropine largely suppressed the contraction induced by CWE. This finding appears to contrast with the antagonistic effect of CWE on carbachol-induced contraction. One possible explanation is that the relaxation effect of CWE may not be mediated through direct blockade of muscarinic receptors, supporting our previous hypothesis. Secondly, different components in the CWE may account for the bronchodilator and bronchoconstricter effects, complicating the result interpretation. It is possible that the bronchodilator effect of CWE overcomes the bronchoconstricter effect in the presence of contractile agonist. In line with this, cumulative CRCs to CWE at basal tone did not induce any pronounced contraction (data not shown) as compared to noncumulative CRCs. This infers that bronchodilator effect is able to override the bronchoconstricter effect gradually with cumulative addition of CWE. By contrast, in noncumulative CRCs, a high concentration of CWE was added at one point, and therefore the bronchodilator effect may fail to exert immediate effect to counteract the bronchoconstricter effect.

Another interesting speculation is, assuming that there is only one bioactive component in CWE causing the relaxation and contraction of airway smooth muscle,

this bioactive component may act as a partial agonist that activates the muscarinic receptors in the absence of muscarinic agonist and inhibits muscarinic receptors in the presence of muscarinic agonist. The agonistic and antagonistic effects of a partial agonist are produced at the same concentration range with full agonist at low concentrations (Mailman and Boyer et. al., 1997). The similar concentration range of CWE that produced the bronchodilator and bronchoconstricter effect appears to coincide with this nature of partial agonist. However, a partial agonist should be competitive in nature with full agonist. Our results showing that CWE non-competitively blocked carbachol-induced contraction did not seem to agree with this aspect and this is unable to be explained with the current experiments. Similar muscarinic receptor-mediated tracheal contraction, which involves Ca^{2+} mobilization, was seen in the aqueous extract of *Pleurotus ostreatus* (Schachter et al., 2005). However, the effect of this mushroom on pre-contracted airways was not evaluated.

The postulated mechanisms of action implicated by CWE-induced bronchorelaxation are depicted in Fig. 3.10 below. We emphasize that these propositions are based on functional data, and thus the involvement of a certain mechanism cannot be completely ruled out. However, the evidence strongly suggests that β-adrenoceptors, potassium channels, cAMP and NO/cGMP pathways, and adenosine are not contributing to the bronchodilator effect elicited by CWE. Overall results indicate that CWE possibly affects the $G_{\alpha q}$-coupled signalling pathway and inhibits membrane calcium channels, particularly L-type calcium channels and others including ROCC and SOCC (proposed candidates of TRPC channels). Based on this, experiments conducted in **Chapter 4** were designed to underpin the role of Ca^{2+} underlying CWE-induced relaxation and contraction as well as carbachol-, 5-HT, and KCl-induced contraction in relation to the effect of CWE.

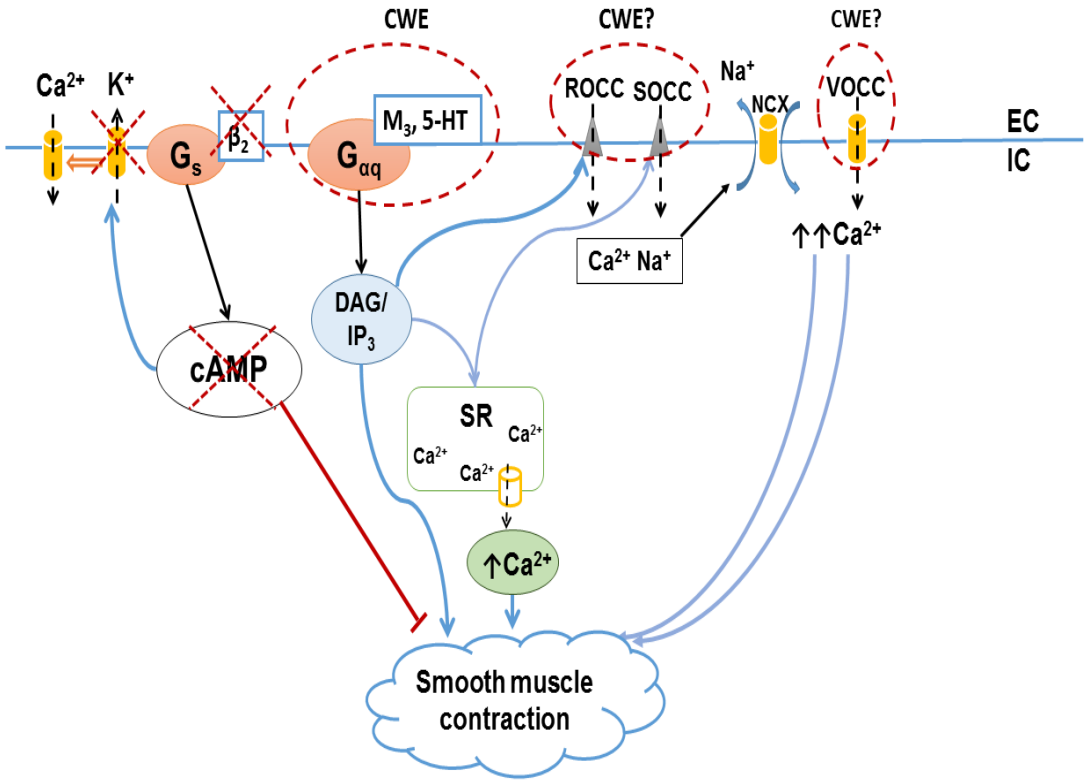

Figure 3.10: Proposed mechanisms involved in cold water extract-mediated airway smooth muscle relaxation. Pathways that are unlikely and likely to be affected by CWE are represented by red broken cross and red broken circle, respectively. (Abbreviations: 5-HT = 5-hydroxytryptamine; cAMP = 3′-5′-cyclic adenosine monophosphate; CWE = Cold water extract; DAG = Diacylglycerol; EC = Extracellular; IC = Intracellular; IP_3 = Inositol triphosphate; NCX = Na^+-Ca^{2+} exchanger; ROCC = Receptor-operated calcium channel; ROCK = Rho-associated protein serine/threonine kinase; SOCC = Store-operated calcium channel; SR = Sarcoplasmic reticulum; VOCC = Voltage-operated calcium channel)

Chapter 4. The role of calcium underlying the effects of *Lignosus rhinocerotis* extract

4.1 Introduction

As an extension to the results in **Chapter 2 and 3**, we sought to elucidate the calcium dynamics affected by CWE as well as contractile agents in the present chapter. Isolated airway tissues continued to be employed in organ bath experiments to complement the results from previous chapters. Calcium imaging experiments with dorsal root ganglion cells were performed to measure the effect of CWE on depolarization-induced rise in $[Ca^{2+}]_i$ to support the findings from organ bath experiments. Complexometric titration was conducted to investigate the Ca^{2+}-chelating properties of CWE in relation to its bronchodilator effect. Backgrounds of the aforementioned subjects of relevance to this chapter were elaborated in the following subsections.

4.1.1 Calcium entry pathways in airway smooth muscle

It has been proposed that a number of extracellular Ca^{2+} entry pathways, including VOCC, SOCC, ROCC, and NCX, contribute to the contraction of airway smooth muscle (S. Hirota & Janssen, 2007; Girolamo Pelaia et al., 2008; Salido, Sage, & Rosado, 2009; Kartik Venkatachalam, van Rossum, Patterson, Ma, & Gill, 2002). The general idea is that blockade of VOCC should attenuate the airway smooth muscle contraction induced by membrane depolarization. L-type calcium channels are the predominant VOCC in airway smooth muscle (K. Hirota, Hashiba, Yoshioka, Kabara,

& Matsuki, 2003). These channels are modulated by three classes of calcium channel antagonists binding to separate binding sites: dihydropyridine (nifedipine, nitrendipine), phenylalkylamine (verapamil, gallopamil), and benzodiazepines (diltiazem). These antagonists mainly exert their effects by binding to the α_1 subunit in S5-S6 pores of the L-type calcium channels (Striessnig et al., 1998).

A number of studies have put forth evidence for the participation of L-type calcium channels in Ca^{2+} influx related to SR Ca^{2+} refilling for sustained acetylcholine-induced contractions in airway smooth muscle of bovine (S. Hirota & Janssen, 2007), guinea pig (Flores-Soto, Reyes-García, Sommer, & Montaño, 2013), pig (Dai, Kuo, Leo, van Breemen, & Lee, 2006) and human (Dai et al., 2007). On the contrary, increasing evidence also denotes the minor role of membrane depolarization and VOCC in maintaining airway smooth muscle contraction and that Ca^{2+} influx through other channels including SOCC and ROCC may play a more crucial role (Sanderson et al., 2008).

The depletion of internal Ca^{2+} store, whether consequent to IP_3 receptor activation or not, is a stimulating factor of SOCC in an effort to refill the store and is pivotal in maintaining the calcium homeostasis in airway smooth muscle (Smyth et al., 2010). Thus far, two currents have been recorded for this pathway in airway smooth muscle: non-selective SOCC currents (I_{SOC}), and Ca^{2+}-selective SOCC currents (I_{CRAC}) which is mediated by calcium release activated calcium (CRAC) channels (Siddiqui et al., 2013). At present, one of the identified candidate molecular components of SOCC is TRPC channels, as all of them are coupled to PLC activation (K Venkatachalam & Montell, 2007). Other recently discovered components of SOCC i.e. stromal interaction molecule 1 (STIM1), Ca^{2+} sensor on SR membrane, and Orai-

1, which are localized on cell membrane, are proposed to activate the CRAC through communication between these two components (Stathopulos et al., 2013).

TRPC channels are Ca^{2+}-permeable cation channels. To date, the TRPC subfamily identified comprises TRPC1 to TRPC7, which are further divided into three subgroups by their sequence homology: TRPC1/C4/C5, TRPC3/C6/C7, and TRPC2 (Alexander et al., 2015). TRPC1 channel forms heteromeric channels with TRRPC4 or TRPC5, and this subgroup is expressed in the brain, heart, lung, liver, spleen, and testis (L. Wu, Sweet, & Clapham, 2010). TRPC7 is highly expressed in heart and lung of mouse but in human, it is expressed mainly in central nervous system and peripheral tissues such as pituitary gland and kidney (Riccio et al., 2002). TRPC3 and TRPC6 are widely expressed in the neuronal, epithelial, smooth muscle, and cardiac muscle cells (Abramowitz & Birnbaumer, 2009). The molecular expression of TRPC proteins also differs among species. In the context of airway smooth muscle, the expression and functional role of TRPC proteins remain to be identified. TRPC1 protein is expressed in rat airway smooth muscle (Sweeney et al., 2002)**,** while TRPC1, TRPC3 (possibly with TRPC6 and TRPC7), and TRPC4 proteins are detected in porcine airway smooth muscle (Ay, Prakash, Pabelick, & Sieck, 2004). The proteins and mRNA of TRPC1 and TRPC3 are also detected in C57/B6 mice (Xiao, Zheng, Liao, & Wang, 2010). In human, TRPC1, TRPC3, TRPC4, and TRPC6 channels are expressed in airway smooth muscle (Corteling et al., 2004).

The TRPC channels are generally believed to be activated through PLC pathway downstream of $G_{\alpha q}$-coupled receptors, or receptor tyrosine kinases. A large body of evidence suggests its contribution to ROCC and SOCC activated by depletion of intracellular Ca^{2+} stores, although the data are not very consistent for some channel subtypes (Salido et al., 2009). TRPC1 channel is probably the most established and

widely studied for its role as a subunit of SOCC. The TRPC1-SOCC was shown to be regulated by STIM1 mediating Ca^{2+} influx upon store depletion (Zeng et al., 2008). TRPC2 channel is a pseudogene in human and is of least research interest. TRPC3 to TRPC7 channels are activated through muscarinic M_3 receptor stimulation in HEK293 (human embryonic kidney) cells (Abramowitz and Birnbaumer, 2009). Besides, TRPC4 and TRPC5 subgroups are shown to be activated by the stimulation of $G_{\alpha q}$-coupled receptors and receptor tyrosine kinases, which are coupled to PLC_β and PLC_γ, respectively (Plant & Schaefer, 2003). TRPC3/C6/C7 can be directly activated by DAG in a PKC-independent manner (Harteneck & Gollasch, 2011; Okada et al., 1999). Although the activation of all TRPC subgroups are frequently related to store depletion, controversy still exists to the role of these TRPC channels as SOCC due to contradicting reports from different cell lines, sources, and approaches (Alexander et al., 2015; Plant & Schaefer, 2003; Salido et al., 2009).

In an effort to elucidate the pharmacological role of these TRPC channels, several selective- and non-selective antagonists of TRPC channels are being developed. Non-selective TRPC channel inhibitors including 2-aminoethoxydiphenyl borate (2-APB), SKF96365, N-(p-amylcinnamoyl) anthranilic acid (ACA), and W-7 (Alexander et al., 2015) are synthesized, whilst Pyr3 was synthesized as the first TRPC3-selective inhibitor (Kiyonaka et al., 2009). Hyperforin, a natural compound isolated from St John's Wort extract, and Hyp9, a simplified derivative of hyperforin, are selective agonists of TRPC6 channel (Alexander et al., 2015). The membrane-permeable analogue of DAG, 1-oleoyl-2-acetyl-sn-glycerol (OAG), is frequently used to activate TRPC3/C6/C7 channels (Inoue et al., 2001; Kiyonaka et al., 2009; Okada et al., 1999). Selective and non-selective inhibitors of TRPC channels are employed in this chapter to assess their role in carbachol-induced contraction.

4.1.2 Calcium imaging experiment with dorsal root ganglion cells

4.1.2.1 Calcium imaging technique

Calcium imaging technique has been used to explore Ca^{2+} signalling and quantify $[Ca^{2+}]_i$ in living cells. In order to detect the $[Ca^{2+}]_i$, a range of fluorescent Ca^{2+} indicators are developed to fulfil the research needs, for example the ease of use, cost-effectiveness, sensitivity, reliability, and reproducibility. In early 1980s, the development of chemical indicators with their acetoxymethyl (AM) groups, for instance Quin-2-AM, Fura-2-AM, and Indo-1-AM, represented a breakthrough in the calcium imaging technology (Meldolesi, 2004; Price, 1985). Later, the technology has moved on to genetically encoded chemical indicators (GECIs) i.e. FIP-CB_{SM} (Romoser, Hinkle, & Persechini, 1997) and cameleon with improved expression (Miyawaki, Griesbeck, Heim, & Tsien, 1999). Both GECIs rely on binding of calmodulin to MLCK of smooth muscle. Thereafter, the cameleon-based GECIs have been greatly improved in terms of Ca^{2+} binding, pH stability, folding effciency, and fluoroscence resonance energy transfer (FRET) change (Palmer, Qin, Park, & McCombs, 2011). Further improvement strategies were made to GECIs by development of Troponin C-based GECIs (Heim & Griesbeck, 2004), and also reengineer of the binding interface between calmodulin and target peptide to create wider range of Ca^{2+} affinities and to reduce perturbation by endogenous calmodulin (Palmer et al., 2006).

The development of chemical Ca^{2+} indicators was paralleled by the development of various dye loading approaches. The choice of loading method depends on the type of Ca^{2+} indicators, the cell/tissue preparation, research question, and location of interest (Grienberger & Konnerth, 2012). One of the most common

methods is by coupling the indicator dyes, which are normally hydrophilic in nature, to hydrophobic AM group to facilitate passive diffusion into cells. Subsequently, the AM group is cleaved off by unspecific esterases, leaving the membrane-impermeable Fura-2 trapped inside the cells (Meldolesi, 2004). Other loading methods include invasive micro- and macro-injection, diffusion from patch pipettes or through gap junctions, ATP-induced permeabilization, hyposmotic shock treatment, gravity, and sample loading (Takahashi, Camacho, Lechleiter, & Herman, 1999).

Apart from dye loading, optical imaging devices are important features for calcium imaging to visualize and record the cellular Ca^{2+} dynamics. So far, two different approaches for the measurement of fluorescence signal have been described: (a) non-radiometric indicator with single fluorescent protein, and (b) radiometric indicator with a pair of fluorescent protein engineered for FRET (Heim & Griesbeck, 2004). The main types of imaging instrumentation include wide-field microscopy using photodiode array or charged coupled detector camera, laser scanning microscopy using confocal or two photon microscopy, and more recently microendocscopic approaches or portable head-mounted microscopes used for recordings in freely moving animals (Grienberger & Konnerth, 2012). Wide-field microscopy and confocal microscopy are frequently used for *in vitro* imaging such as neuronal cell culture or brain slices at superficial layer, whilst two-photon microscopy can be used to visualize deeper brain tissues *in vivo*, providing high resolution and high sensitivity imaging (Grienberger & Konnerth, 2012).

The major advantages of chemical indicators are broad range of Ca^{2+} affinities and also needlessness for transfection of cells as with GECIs (Paredes, Etzler, Watts, Zheng, & Lechleiter, 2008). Being non-invasive and easily loaded to isolated cells from vertebrae organism, chemical indicators can also target certain subcellular

compartments by using low-affinity indicators (Paredes et al., 2008). However, chemical indicators are not without their own limitations; it is difficult to target specific intracellular location, and the dye in AM form will compartmentalize into membrane bound vacuoles in experiments longer than 30 minutes or an hour, depending on the cell type and temperature (Paredes et al., 2008). In comparison, GECIs have several advantages over chemical indicators such as enhanced specificity of subcellular targeting, stability in long experimental duration, expression within intact tissues, and unnecessary dye loading step (Heim & Griesbeck, 2004; Pérez Koldenkova & Nagai, 2013). However, a longer time of preparation, ranging from weeks to months, is required for transfection of cells using GECIs.

4.1.2.2 Calcium signalling in dorsal root ganglion cells

Dorsal root ganglion (DRG) is a cluster of sensory neurons lying at the dorsal root of spinal nerves. They are composed of afferent neurons and ensheathing satellite glial cells that form functional unit together for bidirectional communication (Hanani, 2005), as well as connective tissue cells. These neurons are responsible for transmitting neuronal information via action potential generation and transmission from the periphery to central nervous system in response to mechanical, thermal, and chemical stimuli by generating and transmitting.

Isolating and culturing the somata (round-shaped cell bodies located on side branch of main axon) from DRG cells have been relatively easy and a standard technique for monitoring Ca^{2+} dynamics in neuronal cells. Following somata isolation, various means can be employed to activate the neurons such as membrane

depolarization using increased bath K^+ concentration or electrical field stimulation, or agonist binding to receptor (Gemes et al., 2010). Approaches such as microelectrode or electroporation are being adapted in an effort to load the calcium dye and to record the responses from single somata (Y. Chen & Huang, 2017; Gemes et al., 2010).

The DRG neurons express a variety of ion channels, for instance, hyperpolarization-activated cyclic nucleotide–gated, sodium, potassium, chloride and calcium channels that participate in the modulation of membrane potential and generation of action potential (Moraes, Kushmerick, & Naves, 2017). Intracellular Ca^{2+} is an important second messenger in sensory neurons that regulates diverse events such as neuronal differentiation, gene expression, neurotransmitter release, excitability, and apoptosis (Gemes et al., 2010). In mammalian neurons, source of extracellular Ca^{2+} influx includes VOCC, ionotropic glutamate receptors, nicotinic acetylcholine receptors, and TRPC channels, whilst intracellular Ca^{2+} is released from internal store via IP_3 and ryanodine receptors (Grienberger & Konnerth, 2012).

The VOCC is classified into high- and low-voltage activated channels based on their pharmacological properties and voltage-dependent activation, which are then subclassified into high-voltage L-, N-, P/Q-, and R-types as well as low-voltage T-type that have been identified in rat DRG (Fang, Hwang, Kim, Jung, & Oh, 2010; Park & Luo, 2010; Scroggs & Fox, 1992; Z. Wu, Chen, & Pan, 2004). In light of this, besides being a widely used model to study the sensory neuron properties (Todorovic and Jevtovic-Todorovic, 2011), DRG cells are also frequently used to assess the calcium channel properties in various studies involving other cell types, such as blood vessels (Fujii et al., 1997, Todorovic and Jevtovic-Todorovic, 2011) and mammalian eggs (Currie et al., 1992). Sustained membrane depolarization induced by K^+ application mainly opens the L-type and N-type calcium channels in rat DRG cells

(Fuchs, Rigaud, Sarantopoulos, Filip, & Hogan, 2007). Given that, this cell type is of interest in this thesis to investigate the effect of CWE on L-type calcium channels.

4.1.3 Metal ion-chelating activity of medicinal mushrooms

Metal ions are essential for many important chemical processes in the human body, especially in the central nervous system, by binding to biological molecules such as nucleic acids, enzymes and proteins (Burdette & Lippard, 2003). These metal ions include spectroscopically silent ions such as K^+, Na^+, Ca^{2+}, Mg^{2+}, and Zn^{2+}, and spectroscopically accessible ions including Fe^{2+}, Cu^+, Mn^{2+}, and so on (Crichton, 2008). Chelating agents such as ethylenediaminetetraacetic acid (EDTA) and ethylene glycol tetraacetic acid (EGTA) are commonly used to chelate divalent ions as they can form stable complexes with metal ions. Compared to EDTA, EGTA has a higher affinity for Ca^{2+} and therefore is useful when preparing buffer solution (M Takemoto, Takagi, Ogino, & Tomita, 1998), for instance, addition into Krebs solution to specifically remove Ca^{2+} in organ bath experiments.

Mushroom extracts from *L. rhinocerotis* (Y. H. Y. Yap et al., 2013), *Cordyceps militaris* (Tuli et al., 2014), *Lentinus edodes*, *Pleurotus eous* (Boonsong, Klaypradit, & Wilaipun, 2016) and many others, have been reported to possess chelating activities on metal ions, especially Fe^{2+}, contributing to their well-known antioxidant properties (Tuli et al., 2014). The Fe^{2+}-chelating effect of mushroom extracts is believed to be mainly attributed to the phenols and flavonoids, as well as polysaccharides, polysaccharide-protein complex and ascorbic acid to lesser extent (Barros, Cruz, Baptista, Estevinho, & Ferreira, 2008; Cör, Knez, & Hrnčič, 2018). The structure of

cordycepin, which is found in *C. militaris*, is hypothesized to be able to chelate metal ions in the form of di-, tri- and tetra-dentate ligands (Tuli et al., 2014). While many studies focussed on their antioxidant properties, there is little study of mushroom extracts or its components on their Ca^{2+}-chelating effect. The Ca^{2+}-chelating activities are, however, reported for some of the secondary metabolites such as phenols and terpenoids present in *L. rhinocerotis*. There is evidence that plant phenols (Z. Zhao, Vavrusova, & Skibsted, 2018) and terpenoids (Abramov, Zamaraeva, Hagelgans, Azimov, & Krasilnikov, 2001) can form complex with Ca^{2+}. To our knowledge, there is no study to date that directly examines the Ca^{2+}-chelating activity of CWE of *L. rhinocerotis*.

4.1.4 Significance of study

In light of the findings from **Chapter 3**, we hypothesized that one plausible mechanism of action of CWE is by blocking membrane calcium channels in airway smooth muscle, especially L-type calcium channels. Therefore, the present chapter aimed to elucidate the Ca^{2+} dynamics affected by CWE, as well as contractile agents to substantiate the findings related to CWE. The specific objectives of this chapter were as follows:

(i) To examine the response of CWE in the presence and absence of extracellular Ca^{2+} on isolated airways contracted with calcium chloride (equals to introduction of Ca^{2+}) using organ bath set up.

(ii) To construct CRCs to carbachol, 5-HT, and KCl in the presence and absence of extracellular Ca^{2+} on isolated airways using organ bath set up.

(ii) To examine the contraction elicited by carbachol in the presence of a number of calcium channel blockers using organ bath set up.

(iii) To monitor KCl-induced calcium dynamics in DRG cells in the presence of CWE using calcium imaging technique.

(iv) To assess the Ca^{2+}-chelating effect of CWE using complexometric titration.

4.2 Materials and methods

4.2.1 Drugs and materials

The CWE was extracted as described in Section 2.2.2, **Chapter 2**. Details on drugs including brands, solvents, stock solutions, and final concentrations of DMSO (in the bath) used in this chapter are listed in Table 4.1. Ten-fold serial dilutions were made for all stock solutions to produce respective working solutions. EGTA (Sigma, US) was dissolved in purified water to make stock of 0.1 M and the pH was adjusted to 8.0. The preparation of carbachol, 5-HT and KCl followed Section 2.2.1 (**Chapter 2**) and Section 3.2.1 (**Chapter 3**). Ten-fold serial dilutions were made for all stock solutions to produce respective working solutions.

Table 4.1: Summary of drugs and their details.

Drugs	Company, Country	Solvent	Stock solution (mM)	Final DMSO concentration in bath (%, v/v)
Thapsigargin	Santa Cruz, USA	DMSO 100%	10	0.05
SKF96365	Sigma, USA	DMSO 100%	100	0.1
2-aminoethoxydiphenyl borate (2-APB)	Santa Cruz, USA	DMSO 100%	100	0.1 to 0.3
Nifedipine	Nacalai Tesque, Japan	DMSO 100%	100	0.05
Pyr3	Sigma, USA	DMSO 100%	100	0.15

As for calcium imaging experiments, all chemicals and reagents were purchased from Sigma-Aldrich, UK unless stated otherwise. The composition of superfusion buffer is listed in **Appendix A**. Buffer was kept at 37°C constantly during use. Fura-2-AM was dissolved in anhydrous DMSO to make a stock concentration of 5 µM. CWE was dissolved in purified water to make stock concentration of 100 mg/ml prior to the experiment. Nifedipine was dissolved in DMSO 100% to make stock concentration of 100 mM (Final DMSO concentration is 0.033% v/v).

With regards to complexometric titration, Eriochrome Black T 0.5% was purchased from Sigma, USA, while EDTA disodium dihydrate was purchased from First Base, Singapore.

4.2.2 Organ bath experiments

4.2.2.1 Tissue preparation

In the following subsections, experiments were conducted with male Sprague Dawley rats (235-440 g; 2-3 months old) or pig. Sprague Dawley rats were purchased from Universiti Putra Malaysia and Universiti Kebangsaan Malaysia, while porcine lungs were obtained from a local abattoir in Nottingham, UK. The method of sacrifice and tissue isolation were repeated as per Section 3.2.2 (**Chapter 3**). In some experiments of this chapter, "calcium-free Krebs" solution (without Ca^{2+}), containing all ingredients as listed for standard Krebs solution (**Appendix A**) except calcium chloride ($CaCl_2$), was used to create a calcium-free environment for the tissues. Therefore, to differentiate this from the standard Krebs solution (containing 1.26 mM Ca^{2+}), the standard and calcium-free Krebs solutions were given different terms as

"normal Krebs" and "calcium-free Krebs" solutions, respectively, throughout this chapter. In some experiments, EGTA was added to calcium-free Krebs solution to chelate the external Ca^{2+} in the buffer. Tissues were left to equilibrate to bath condition for 30 minutes after the application of tension of 9.8 mN (rat airways) or 19.6 mN (porcine bronchiole). Following equilibration, all tissues were exposed twice to 60 mM KCl to assess tissue viability and to provide reference contracture for subsequent data analysis. After the KCl was washed out and a stable basal tone was re-established, experiments were carried out as in following sections.

4.2.2.2 Effect of CWE-induced airway relaxation on extracellular calcium entry in rat airways

In order to investigate the role of extracellular Ca^{2+} in CWE-induced airway relaxation, a Ca^{2+}-free environment was created by immersing the airway segments in calcium-free Krebs solution. Then, rat tracheal and bronchial rings were pre-incubated with CWE (3.5 mg/ml), nifedipine (10 µM; determined in preliminary experiments) or DMSO 0.05% v/v (vehicle control) for at least 30 minutes. Nifedipine, a L-type calcium channel blocker, served as the positive control. Then, 60mM KCl was added to the tissues to induce depolarization for about 10 minutes prior to the construction of cumulative CRCs to $CaCl_2$. This experimental method was adapted from previous study (Hosoe et al., 2006). The degree of contraction was measured as a fraction of the contraction from basal tension and had been expressed as a percentage of reference KCl-induced tone.

4.2.2.3 Effect of CWE-induced airway relaxation on intracellular calcium mobilization in rat airways

To assess if CWE blocks intracellular Ca^{2+} release, rat tracheal rings were pre-incubated either with CWE (3.5 mg/ml) or purified water (vehicle control) in calcium-free Krebs solution, or with purified water (vehicle control) in normal Krebs solution for at least 30 minutes. Then, a single concentration of carbachol (300 µM) was added to induce tone and tissues were left in bath for 1 hour. The degree of contraction was measured as a fraction of the contraction from basal tension at 0, 0.5, and 1.0 hour after carbachol addition. Data had been expressed as a percentage of reference KCl-induced tone.

In a different set of experiments, rat tracheal rings were pre-incubated with CWE (3.5 mg/ml) or purified water (vehicle control) in normal Krebs solution for at least 30 minutes, prior to the first addition of carbachol (300 µM). Subsequently, tissues were washed out with fresh normal Krebs solution and left to equilibrate for at least 15 minutes. A second addition of carbachol (300 µM) was then added to the tissues to induce contraction. The degree of contraction was taken at the point of maximal carbachol-induced contraction and measured as a fraction of contraction from basal tension. Data was expressed as a percentage of reference KCl-induced tone.

4.2.2.4 The role of extracellular calcium in smooth muscle contractility mediated by carbachol, 5-HT, and KCl

The role of extracellular Ca^{2+} mediated by contractile agonists was examined by comparing their contractions induced in normal Krebs and calcium-free Krebs

solutions. Rat tracheal rings were first immersed in normal Krebs solution. Cumulative CRCs to carbachol, 5-HT, or KCl were constructed. When the contraction induced by the last concentration of drugs plateaued, tissues were washed out with fresh calcium-free (containing EGTA 1 mM) or normal Krebs solution (control). Then, a second cumulative CRC to the same contractile agonist i.e. carbachol, 5-HT, or KCl was constructed in respective tissue. Only two CRCs to the same contractile agonist were obtained per tissue.

In another set of experiments, rat tracheal rings were first immersed in calcium-free Krebs solution (containing EGTA 1 mM). Thapsigargin (1 µM, Govindaraju et al., 2018), a non-competitive inhibitor of SERCA, or DMSO 0.05% (vehicle control) was added to the tissues and incubated for at least 40 minutes. Carbachol (30 µM; the concentration derived from E_{max} of carbachol CRCs) was then added to tissues and incubated for 30 minutes to release the Ca^{2+} from intracellular store, while EGTA served to buffer the released Ca^{2+}. Following that, tissues were washed out with fresh normal Krebs solution and thapsigargin (1 µM) was added again to ensure continuous inhibition of SERCA. Once tissues stabilized, cumulative CRCs to 5-HT or carbachol were constructed. The SERCA pumps Ca^{2+} across the SR membrane to replete the depleted intracellular Ca^{2+} store, and thapsigargin can prevent this, hence maintaining minimal intracellular Ca^{2+} store level after carbachol has induced the release of most Ca^{2+} from SR. In this circumstance, any contraction induced by 5-HT or carbachol should be primarily induced by extracellular Ca^{2+}. The degree of contraction in the experiments described above was measured as a fraction of the contraction from basal tension and had been expressed as a percentage of reference KCl-induced tone.

4.2.2.5 Effect of calcium channel blockers against carbachol-induced contraction in rat airways

Rat tracheal rings were pre-incubated with calcium channel blockers, including nifedipine (10 µM), pyr3 (30 µM,; selective inhibitor of TRPC3 channel, Harding et al., 2018), SKF96365 (10 µM; TRPC channel and SOCC blocker, M Takemoto et al., 1998), 2-aminoethoxydiphenyl borate (2-APB) (100 µm; TRPC channel and SOCC blocker, Harding et al., 2018), CWE (3.5 mg/ml), or DMSO 0.15% (vehicle control) for at least 30 minutes. Then, cumulative CRCs to carbachol were constructed. The degree of contraction was measured as a fraction of the contraction from basal tension and had been expressed as a percentage of reference KCl-induced tone.

4.2.2.6 The role of calcium mediated by CWE in porcine bronchiole

To investigate the effect of CWE on extracellular Ca^{2+} entry in porcine bronchioles, bronchiole rings were first immersed in calcium-free Krebs solution before being incubated with CWE (1.8, 3.2, or 5.6 mg/ml which induced 50%, 70%, or 100% relaxation of carbachol pre-contraction respectively) or purified water (vehicle control) for at least 30 minutes. Then, 60mM KCl was added to the tissues to induce depolarization for about 10 minutes prior to the construction of cumulative CRCs to $CaCl_2$. The degree of contraction was measured as a fraction of the contraction from basal tension and had been expressed as a percentage of reference KCl-induced tone. The experiment described in this subsection was performed by Ms. Le Viet Hang in the University of Nottingham, UK.

In a different set of experiments, bronchiole rings were first immersed in normal Krebs solution, and cumulative CRCs to carbachol were constructed. Once the contractile response has plateaued, bath content was washed out and replaced with fresh calcium-free Krebs solution (containing EGTA 1 mM) or normal Krebs solution (control). Tissues were left to return to basal tone for 15 minutes prior to construction of second cumulative CRCs to carbachol. Only two CRCs were obtained per tissue.

To investigate the effect of calcium channel blockers and CWE against carbachol-induced contraction, porcine bronchiole rings were pre-incubated with 5.6 mg/ml of CWE (concentrations which induced 100% relaxation against carbachol pre-contraction), SKF96365 (100 µM), 2-APB (300 µM), nifedipine (10 µM), or DMSO 0.3% (vehicle control). Then, cumulative CRCs to carbachol were constructed. In all above experiments, the degree of contraction was measured as a fraction of the contraction from basal tension and had been expressed as a percentage of reference KCl-induced tone.

4.2.2.7 Statistical analysis

Data were analysed and graphs were drawn using PRISM v7.0 (Graph pad software). All data were expressed as mean ± SEM of n number of animals. Maximum tissue contraction or relaxation response (E_{max}) and pEC_{50} were derived from nonlinear regression analysis of the obtained CRC. In the event that the E_{max} was not achieved as response has not plateaued, E_{max} was derived from the response generated at the highest concentration tested. In some experiments, responses at each individual concentration were compared with multiple comparison test. Statistical analyses were performed using one-way ANOVA with Dunnett correction (to compare the mean differences among groups, Fig. 4.1, 4.4A and B, 4.5, 4.6A, B and D, 4.7), two-way ANOVA followed by multiple comparisons with Bonferroni correction (to compare the mean differences among groups and analyse the interactions between treatments and concentrations, Fig. 4.2 and 4.3), and Student's unpaired t-test (Fig. 4.4C and 4.6C). Results were considered statistically significant if p-value was less than 0.05.

4.2.3 Calcium imaging experiments

The following Section 4.2.3.1 and 4.2.3.2 were performed by Mr. Paul Millns from the School of Life Sciences, University of Nottingham.

4.2.3.1 Coverslip preparation and coating

Glass coverslips were sterilized in the following steps: Coverslips were washed in 10% Decon solution for at least 2 hours, rinsed for five times with double distilled water (ddH_2O), soaked in 4.0 M concentrated hydrochloric acid for at least 30 minutes, rinsed again for five times with ddH_2O, and finally autoclaved before coating. To coat the coverslips, 100 µl of poly-L-Lysine was added to the centre of the coverslips and left for at least 40 minutes at room temperature. The coverslips were then washed with ddH_2O and allowed to dry. 10 µl of Laminin was added, followed by drying for at least 45 minutes. Coverslips were washed again with ddH_2O and allowed to dry before use.

4.2.3.2 Dorsal root ganglia cell preparation

Adult male Sprague Dawley rats were purchased from Charles River, UK. The initial weight range was 200–250 g. Studies were carried out in accordance with the UK Home Office Animals (Scientific Procedures) Act (1986). The use of the animals was approved by the University of Nottingham (UK) Animal Welfare and Ethical review Body (approval reference number 000100). Rats were group housed at the Bio Support

Unit, University of Nottingham, in open cages and fed ad libitum. The rats were sacrificed by concussion of brain, followed by cervical dislocation. Spinal column and the DRG neurons were isolated from Sprague Dawley rats following the previously described method (Lindsay, 1988).

The isolated DRG neurons were put into Dulbecco's calcium- and magnesium-free phosphate-buffered saline (PBS) solution and washed once by gravity. Then, 3.5 ml of Collagenase solution, comprising Neurobasal media 90% (Invitrogen, UK); Horse serum 10%; Collagenase, was added to the DRG neurons and incubated for 90 minutes at 37°C. The DRG neurons were washed gently in PBS solution for three times by gravity. Following the addition of trypsin solution 0.25% to DRG neurons, the neurons were then gently pipetted up and down to partly disrupt the ganglia. Subsequently, the neurons were incubated for 10 minutes at 37°C. One ml of bovine serum albumin (BSA) solution (16% w/v in Hanks' Balanced Salt Solution-HEPES) was added to the DRG neurons and triturated more firmly so as to totally dissociate the DRG cells. The cell suspension was then carefully layered on top of 3 mls of the BSA solution, followed by centrifugation at 1600 rpm for 6 minutes. The supernatant solution was carefully removed and the cell pellet was gently resuspended in 170 µl of the complete neurobasal media. 20 µl of cells were pipetted onto each coverslip and incubated at 37°C, 5% CO_2. After 15-20 minutes of incubation, once cells had attached, 130 µl of complete neurobasal media was added to the coverslip and cells were incubated overnight.

4.2.3.3 Fura-2-AM loading

In order to visualize the calcium dynamics, a fluorescent calcium dye, Fura-2-AM, was loaded into the cells. Coverslip with cells was removed from the incubator and rinsed with superfusion buffer for three times. Immediately, cells were incubated in 300 µl of 5 µM Fura-2-AM solution for 30 minutes in dark. Then, cells were washed three times with superfusion buffer and left for 15 minutes prior to imaging experiment. Fura-2 has a maximal absorption peak range of 335 (maximal $[Ca^{2+}]_i$) to 363 nm (minimal $[Ca^{2+}]_i$), and an emission peak of 500 nm (Takahashi et al., 1999). Radiometric measurement of $[Ca^{2+}]_i$ of this dye is normally taken at dual excitation wavelength (340 and 380 nm).

4.2.3.4 Calcium imaging experiment

Coverslips with DRG cells were fixed on a Perspex chamber using vacuum grease. DRG cells were superfused with superfusion buffer at 2 ml/min continuously. The first 30 mM KCl (represented as the initial KCl response) was added to induce a rise in $[Ca^{2+}]_i$ to serve as the reference response. This was followed by a 20-minute washout period with superfusion buffer. Then, 30 mM KCl was added again to the same preparation to evoke a second KCl-induced peak response in the control set (without any treatment). Similar experiments were repeated for the treatment sets, where cells were pre-incubated with CWE (3.5 mg/ml) or nifedipine (30 µM; Yokogawa, Kim, Krieger, & Puil, 2001) for 30 minutes prior to the second 30 mM KCl addition. As

DMSO less than 0.1% was devoid of interruptive effect in earlier experiments (data not shown), vehicle control was therefore not carried out.

4.2.3.5 Statistical analysis

Images were taken using a Leica DM-IRB and DM-IL microscope (Leica microsystems, Germany) equipped with QImaging Retiga-EXi camera. The $[Ca^{2+}]_i$ of individual neuron was measured as the change in the ratios of peak fluorescence intensities (measured at 500 nm) at excitation wavelengths of 340 and 380 nm, respectively. The average 340/380 nm ratio represented the $[Ca^{2+}]_i$, whilst the changes in $[Ca^{2+}]_i$ induced by the second KCl exposure were expressed as the percentage of the first KCl-induced response. Neurons that displayed < 10% of $[Ca^{2+}]_i$ to KCl were treated as non-responsive and excluded from analysis. Data were expressed in mean values ± SEM with *n* number of neuron cells tested. Independent experiments were done in triplicate. Statistical analysis was performed using one-way ANOVA with Dunnett correction. Results were considered statistically significant if p-value was less than 0.05.

4.2.4 Complexometric titration test with CWE

To examine if CWE complexes and chelates Ca^{2+} present in the normal Krebs solution, a method called complexometric titration was used to compare Ca^{2+} concentration in the sample with and without CWE. The concept of this approach is to titrate the Ca^{2+} present in sample with EDTA. A dye called Eriochrome Black T 0.5%, which appears blue in protonated form and red when complexes with Ca^{2+}, is used as the indicator. This indicator is initially added to the sample solution to form Ca^{2+}-indicator complex, which is less stable than Ca^{2+}-EDTA complex, and turns the sample red. When the solution is titrated with EDTA, Ca^{2+} will dissociate from the indicator and form stronger complex with EDTA. The endpoint occurs when Ca^{2+}-indicator complex is completely replaced by Ca^{2+}-EDTA complex, returning the solution into blue colour.

The EDTA solution was prepared by first drying the EDTA disodium dihydrate in oven at 80°C for 4 hours, then the dried EDTA powder was transferred to a volumetric flask and dissolved in purified water to make 0.01 M EDTA solution. On the other hand, NaOH solution was prepared by dissolving the powder in purified water to make 1.0 M NaOH. The pH of NaOH solution was adjusted to 12 and was added to the sample in order to precipitate magnesium ions, forming $Mg(OH)_2$. The solution was allowed to sit for 5 minutes for the precipitate to form, turning the solution cloudy. As EDTA can bind to both Ca^{2+} and Mg^{2+}, addition of NaOH served to remove Mg^{2+} and to ensure that EDTA only complexed with Ca^{2+} in the following titration step. Sample solution was prepared by mixing 20 ml normal Krebs solution, 3 ml of 1.0 M NaOH, 3.5 mg/ml of CWE, and 8 drops of Eriochrome Black T 0.5%. In parallel, control was prepared by replacing the CWE with purified water in corresponding volume. The sample solution initially appeared in red colour due to

Eriochrome Black T. Then, the sample solution was then titrated slowly with 0.01M EDTA solution and swirled continuously to dissolve the indicator, until the last red tinges disappeared and solution turned blue. The titration was repeated for three times with fresh sample and the average of the titres was taken. The degree of change in Ca^{2+} content in CWE-treated samples was measured as a percentage relative to Ca^{2+} content in control samples (represents 100%).

4.2.4.1 Statistical analysis

The volumes of EDTA solution were calculated from the triplicate of titre readings. The moles of EDTA solution required to chelate the Ca^{2+} was obtained. The following ratio was used to calculate the concentration of Ca^{2+} in the sample solution:

$$Ca^{2+}: EDTA = 1 : 1$$

Student's unpaired t-test was performed to compare the mean values between vehicle control and CWE-treated group.

4.3 Results

4.3.1 Organ bath experiments

4.3.1.1 Bronchodilator effect of CWE in airway segments is linked to regulation of calcium entry

To assess the influence of extracellular Ca^{2+} in airway contraction, we removed extracellular Ca^{2+} source during pre-incubation with CWE or nifedipine and subsequently contracted the tissues with re-introduction of $CaCl_2$. Pre-incubation of rat tracheal rings with CWE (E_{max}: 16.21 ± 7.93%; $p < 0.0001$) and nifedipine ($E_{max:}$ 40.87 ± 10.96%; $p < 0.001$) had significantly suppressed $CaCl_2$-induced contraction compared to vehicle control (E_{max}: 101.88 ± 9.10%) (Fig. 4.1A). Similarly in rat bronchial rings, CWE (E_{max}: 92.01 ± 14.13%; $p < 0.01$) and nifedipine (E_{max}: 31.31 ± 8.76%; $p < 0.0001$) also significantly attenuated $CaCl_2$-induced contraction compared to vehicle control (E_{max}: 144.51 ± 8.23%) (Fig. 4.1B). These observations suggest that one possible mechanism of CWE-induced airway relaxation is via blockade of membrane calcium channels. The representative trace recordings for these observations are included in **Appendix C**.

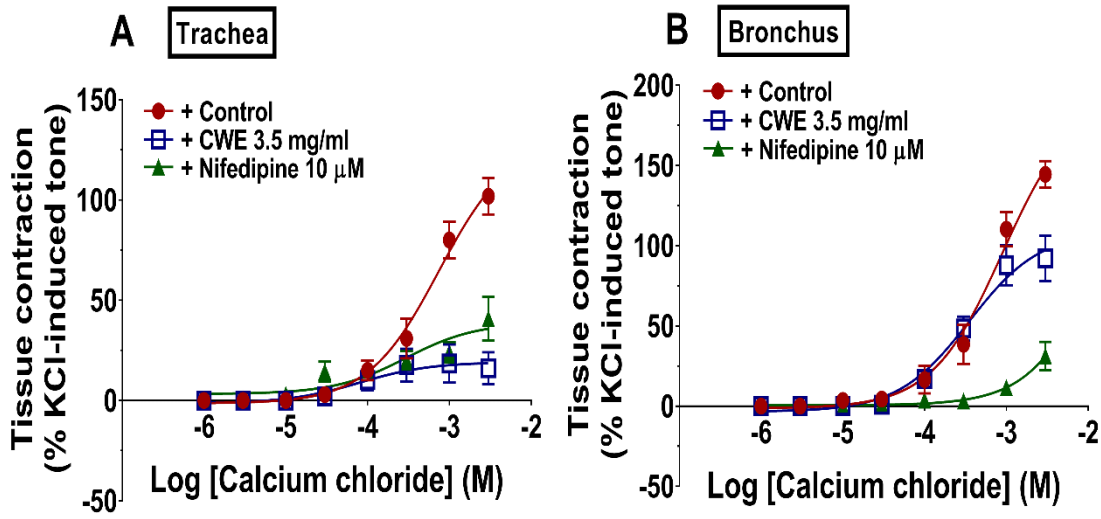

Figure 4.1: Effect of cold water extract against calcium chloride-induced contraction in rat airways. In the absence of external Ca^{2+}, (A) tracheal and (B) bronchial tissues were pre-incubated with CWE, nifedipine, or purified water (vehicle control) for 30 minutes. Then, 60 mM KCl was added to depolarize the tissue prior to addition of increasing concentrations of calcium chloride to induce contraction. Tissue response was expressed as a percentage of reference KCl-induced tone. Data were shown as means ± SEM of 4 to 7 animals.

4.3.1.2 CWE primarily inhibited extracellular calcium influx with little role on intracellular calcium in rat airways

Tracheal rings were immersed in calcium-free Krebs solution to assess the effect of CWE on intracellular Ca^{2+} mobilization induced by carbachol. Fig. 4.2A shows that in vehicle control (immersed in calcium-free Krebs solution), carbachol induced a tone that slowly decreased over the time (0 hour: 58.32 ± 9.04%, 0.5 hour: 48.94 ± 9.06%, 1 hour: 20.65 ± 15.49%). Pre-incubation with CWE (in calcium-free Krebs solution) was not significantly different from vehicle control in terms of the initial peak of carbachol-induced contraction (0 hour: 48.48 ± 9.01%; $p > 0.9999$) (Fig. 4.2A). These observations suggest that CWE does not affect the mechanism, most probably

intracellular Ca^{2+} release from store, involved in the initial peak contraction induced by carbachol. Subsequently at 0.5 hour after carbachol addition, the contraction was significantly reduced in CWE-treated tissues (0.5 hour: 5.47 ± 9.47%; $p = 0.0292$), meaning that carbachol-induced contraction was less sustained compared to vehicle control. At 1 hour after the addition of carbachol, the contraction had largely decreased for both CWE treatment (1 hour: -11.34 ± 11.22%) and vehicle control, however, there was no significant difference between both groups ($p = 0.149$) (Fig. 4.2A). The differences in the responses between CWE and vehicle control at 0 and 0.5 hour were ~1.2-fold and ~9-fold, respectively. The fold of change at 1.0 hour was unable to be determined as the response for CWE treatment has dropped below 0%. Representative trace recordings are shown in Fig. 4.2B and C. Two-way ANOVA results showed that there was no interaction between the treatments and duration ($p = 0.313$), indicating that these factors are independent of each other. These observations suggest that CWE does not affect the initial phase of peak contraction, but does inhibit the Ca^{2+} signalling involved in the sustained phase of carbachol-induced contraction.

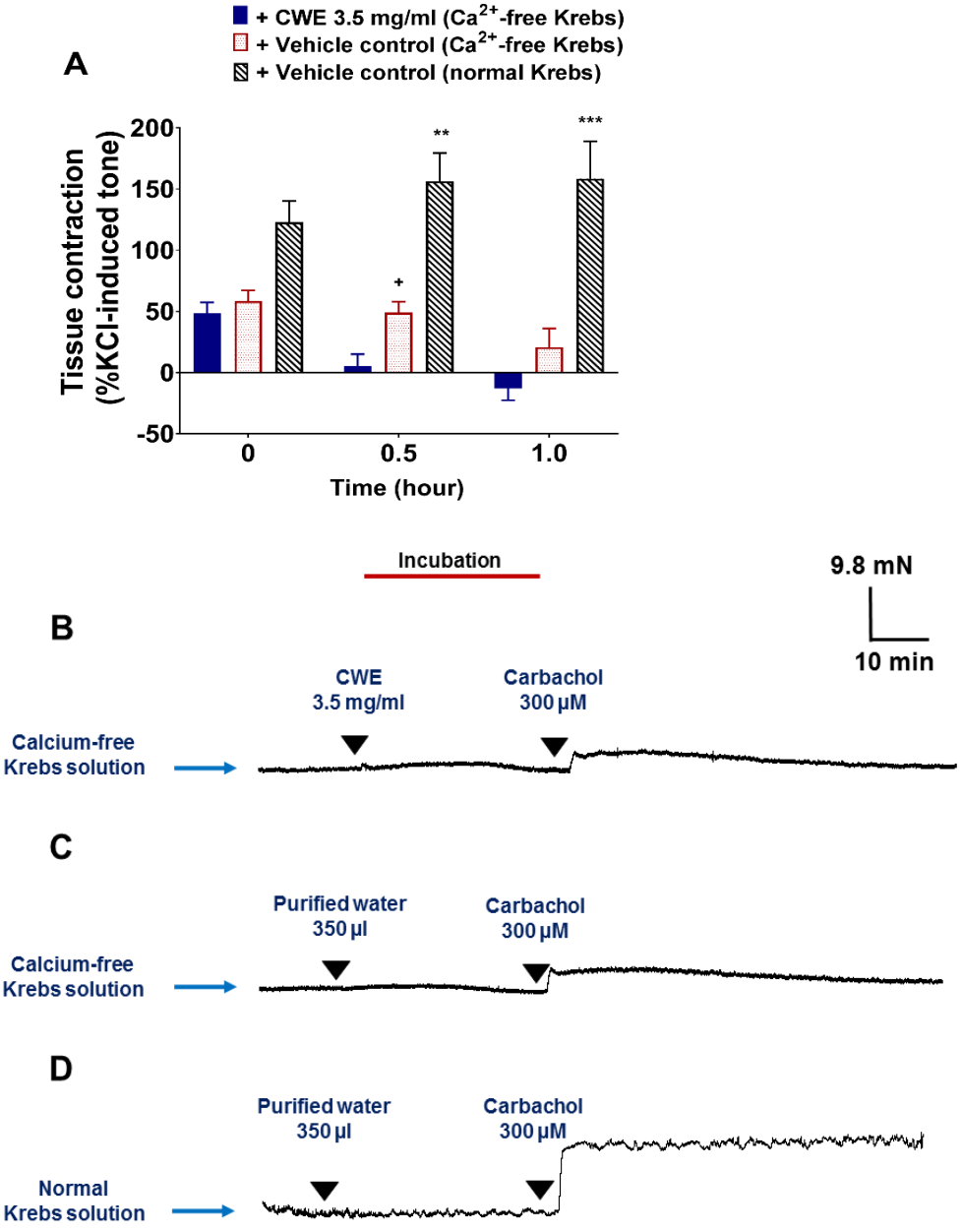

Figure 4.2: The role of calcium in cold water extract-induced relaxation and carbachol-induced contraction in rat trachea. (A) In calcium-free Krebs solution, tissues were pre-incubated with cold water extract (CWE) 3.5 mg/ml or purified water (vehicle control) for 30 minutes, whereas in normal Krebs solution, tissues were pre-incubated with purified water (vehicle control) for 30 minutes. Then, 300 µM carbachol was added into the bath to induce contraction. The contractile response was measured at 0, 0.5 and 1 hour after addition of carbachol and was expressed as a percentage of reference KCl-induced tone. Data were shown as means ± SEM of 3 to 8 animals. Representative trace recordings of pre-incubation with (B) vehicle control or (C) CWE in calcium-free Krebs solution, or with (D) vehicle control in normal Krebs solution in tracheal rings contracted with carbachol. Two-way ANOVA with Bonferroni correction was performed for differences between CWE and vehicle control (Ca^{2+}-free Krebs): $^{+}p < 0.05$; between vehicle controls of Ca^{2+}-free Krebs and normal Krebs: $^{**}p < 0.01$, $^{***}p < 0.001$.

On the other hand, the role of extracellular and intracellular Ca^{2+} in carbachol-induced contraction was investigated by comparing the magnitude of contractile response between normal (with extracellular Ca^{2+}) and calcium-free (without extracellular Ca^{2+}) Krebs solution. In normal Krebs solution, the initial peak contraction induced by carbachol (at 0 hour) in vehicle control were up to 122.93 ± 17.38%, which was nonsignificantly higher than that in calcium-free Krebs solution, 58.32 ± 9.04% (p = 0.0561) (Fig. 4.2A, C and D). Carbachol-induced sustained contraction in normal Krebs solution had gradually increased after the addition (0.5 hour: 156.27 ± 23.12%, 1 hour: 158.51 ± 30.51%) (Fig. 4.2D), and there was a significant difference from those in calcium-free Krebs solution (0.5 hour: 48.94 ± 9.06%, p = 0.0016; 1 hour: 20.65 ± 15.49%, p = 0.0001) (Fig. 4.2C). The difference in carbachol-induced contraction between normal Krebs and calcium-free Krebs solution was heightened over time, by ~2-fold at 0 hr, ~3.2 fold at 0.5 hr and ~7.7 fold at 1.0 hr.

Taken together, we observed that carbachol-induced contraction was less sustained and had lower initial peak of contraction in the absence of external Ca^{2+}. This showed that both intracellular and extracellular Ca^{2+} contributed to initial phase of peak contraction. Extracellular Ca^{2+} plays predominant role in the sustained phase while intracellular Ca^{2+} only has a minor role. This also indicates that CWE may have little effect on intracellular Ca^{2+} mobilization (initial contraction), and primarily act by inhibiting the extracellular Ca^{2+} influx (sustained contraction).

Additionally, the reversibility of CWE-induced relaxation was examined in a different set of experiments. In normal Krebs solution, pre-incubation with CWE had significantly reduced the initial peak contraction induced by first carbachol addition compared to vehicle control (CWE: 78.70 ± 18.36%, vehicle control: 170.54 ± 0.91%;

p = 0.0037) (Fig. 4.3). This was dissimilar with the observation in Fig. 4.2A and B where CWE did not affect the initial phase of carbachol-induced contraction in calcium-free Krebs solution. This implies that CWE is likely to affect the influx of extracellular Ca^{2+} in normal Krebs solution. When tissues were washed out with fresh normal Krebs solution and the second carbachol was added again, carbachol-induced contraction did not recover. This suggests that the effect of CWE is likely to be irreversible. Two-way ANOVA showed that there was no interaction between the different treatment groups (p = 0.1108).

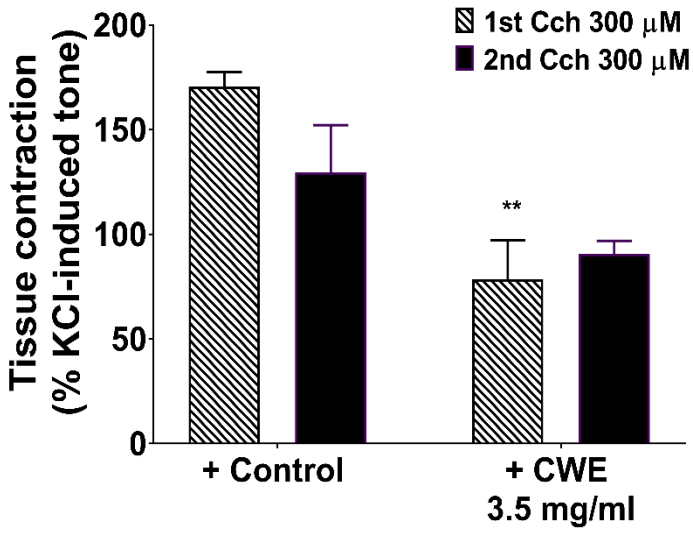

Figure 4.3: Reversibility of the effect of cold water extract against carbachol-induced contraction in rat trachea. In normal Krebs solution, tracheal rings were pre-incubated with cold water extract (CWE) or purified water (vehicle control) for 30 minutes prior to the addition of first carbachol (1st Cch, 300 μM). Tissues were then washed out with fresh normal Krebs solution and left to equilibrate for 15 minutes before adding the second carbachol (2nd Cch, 300 μM). Tissue response was expressed as a percentage of reference KCl-induced tone. Data were shown as means ± SEM of 6 to 8 animals. Two-way ANOVA with Bonferroni correction where comparison of means of 1st carbachol-induced response between CWE treatment and vehicle control was made: $^{**}p < 0.01$.

4.3.1.3 Removal of external calcium abolished the contractions to carbachol, 5-HT, and KCl in rat airways

To assess the role of extracellular Ca^{2+} in contractions induced by carbachol, 5-HT, and KCl, contractile responses of tissues immersed in calcium-free Krebs (with EGTA) and normal Krebs solution were compared. Fig. 4.4A, B and C show that contractile responses to carbachol, 5-HT, and KCl were almost completely abolished in the absence of external Ca^{2+} (E_{max}: carbachol: 5.99 ± 4.99%, p = 0.0011; 5-HT: 9.61 ± 2.50%, p = 0.0019; KCl: 9.91 ± 8.61%, p = 0.0061) when compared to the presence of external Ca^{2+} (E_{max}: carbachol: 180.50 ± 28.83%; 5-HT: 125.10 ± 8.95%; KCl: 136.70 ± 23.38%). In addition, the potency of 5-HT CRC was increased by ~4.4-fold in the absence of external Ca^{2+} (pEC_{50} in normal Krebs: 6.15 ± 0.05 vs calcium-free Krebs: 6.79 ± 0.16, p = 0.0162) (Fig. 4.4B). The potency of carbachol CRC was not significantly affected by the external Ca^{2+} (p = 0.4598) (Fig. 4.4A). It was unable to calculate the pEC_{50} of KCl CRC in normal Krebs solution as the response had not plateaued at the highest concentration tested (Fig. 4.4C).

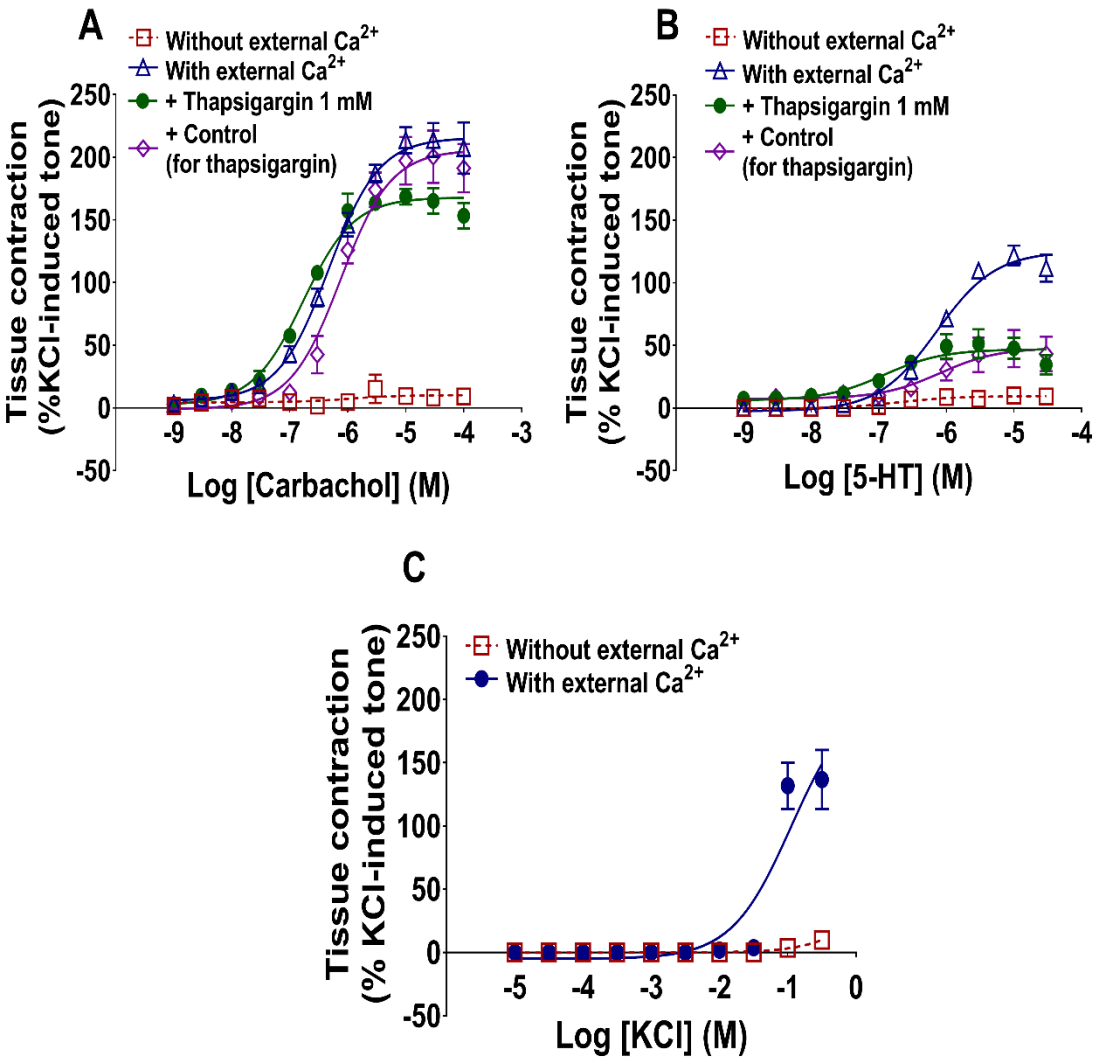

Figure 4.4: The role of extracellular calcium in contractions induced by carbachol, 5-hydroxytrptamine, and potassium chloride in rat trachea. Tissues were immersed in calcium-free Krebs solution (represented by broken line, without external Ca^{2+}) or normal Krebs solution (represented by solid line, with external Ca^{2+}) prior to construction of cumulative concentration-response curves to (A) carbachol, (B) 5-HT, or (C) KCl. In (A) and (B), additional set of experiments were conducted where tissues were pre-incubated with thapsigargin or vehicle control (DMSO 0.05%) prior to the additions of carbachol or 5-HT. Tissue response was expressed as a percentage of reference KCl-induced tone. Data were shown as means ± SEM of 3 to 8 animals. (Abbreviations: 5-HT = 5-hydroxytryptamine; KCl = Potassium chloride)

Additional set of experiments was carried out in Fig. 4.4A and B. Emptying of intracellular Ca^{2+} store was promoted with carbachol and thapsigargin, which prevented Ca^{2+} refill of SR, in calcium-free Krebs solution. Subsequently, CRCs to carbachol were constructed in normal Krebs solution. Results showed that thapsigargin-treated tissues did not significantly affect the maximum response of carbachol (E_{max} of thapsigargin: 163.60 ± 8.53% vs vehicle control: 166.80 ± 20.53%; p = 0.89) (Fig. 4.4A). However, thapsigargin had slightly increased the potency of carbachol by ~3-fold (pEC_{50} of thapsigargin: 6.81 ± 0.025 vs vehicle control: 6.32 ± 0.12; p = 0.0078) (Fig. 4.4A). Besides, the maximum response of 5-HT-induced contraction was not affected by thapsigargin when compared to vehicle control (E_{max}: 42.14 ± 8.70% vs vehicle control: 38.81 ± 13.55%; p = 0.89) (Fig. 4.4B). Similarly, the potency of 5-HT CRC was also not affected by thapsigargin (p = 0.65).

Taken together, the results above strongly suggest that the contractions to carbachol, 5-HT, and KCl primarily rely on extracellular Ca^{2+} influx as the removal of external Ca^{2+} almost completely attenuated their contractile responses. The role of intracellular Ca^{2+} was nearly insignificant, as supported by the unchanged responses of carbachol and 5-HT before and after depletion of intracellular Ca^{2+} store.

4.3.1.4 Carbachol-induced contraction was inhibited by calcium channel blockers in rat airways

To examine the membrane calcium channels by which carbachol affects, carbachol-induced contraction was examined in the presence of blockers targeting various calcium channels. Fig. 4.5 shows that pre-incubation with a series of calcium channel blockers significantly suppressed carbachol-induced contractions. The E_{max} and pEC_{50} values are summarized in Table 4.2. Pre-treatment with nifedipine, SKF96365, and 2-APB had significantly attenuated the maximum response of carbachol CRC when compared to vehicle control. Nifedipine also decreased the potency of the curve by ~2.6-fold. Similarly, CWE had significantly suppressed the maximum response, but conversely increased the potency of carbachol CRC by ~12.9-fold. These results infer that VOCC, SOCC and TRPC channels are possibly implicated in carbachol-induced contraction. On the other hand, the presence of Pyr3 did not affect the contraction compared to vehicle control, suggesting that TRPC3 channel is not involved in carbachol-induced contraction. The effects of these calcium channel blockers appear to be non-competitive, which was similar to CWE, as increasing agonist concentration did not restore the contractile response to carbachol.

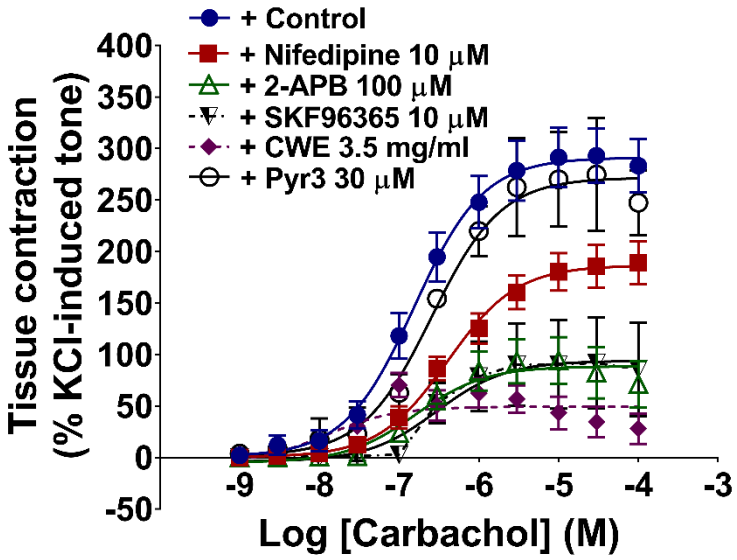

Figure 4.5: Effect of calcium channel blockers against carbachol-induced contraction in rat trachea. Tracheal rings were pre-incubated with nifedipine, 2-APB, SKF96365, CWE, Pyr3, or DMSO 0.15% (vehicle control) for 30 minutes prior to CRCs to carbachol. Tissue response was expressed as a percentage of reference KCl-induced tone. Data were shown as means ± SEM of 3 to 6 animals. (Abbreviations: 2-APB = 2-aminoethoxydiphenyl borate; CWE = cold water extract; CRCs = Concentration-response curves)

Table 4.2: The maximum response (E_{max}) and pEC_{50} value of carbachol derived from the respective concentration-response curve in the presence of different calcium channel blockers. One-way ANOVA with Dunnett correction where comparison of the means was made between vehicle control and treatment groups (*p < 0.05; ***p < 0.001; ****p < 0.0001). Individual p-value was stated. Data represented the means ± SEM of 3 to 6 animals.

Treatments	Trachea	
	E_{max} (%)	pEC_{50}
+ Vehicle (DMSO 0.1%)	291.90 ± 27.76	6.81 ± 0.11
+ CWE 3.5 mg/ml	49.46 ± 13.37**** (p = 0.0001)	7.92 ± 0.06**** (p = 0.0001)
+ Nifedipine 10 µM	188.20 ± 19.11* (p = 0.0255)	6.39 ± 0.11* (p = 0.0379)
+ 2-APB 100 µM	89.51 ± 23.16**** (p = 0.0001)	6.78 ± 0.10 (p = 0.999)
+ SKF96365 10 µM	94.33 ± 45.49*** (p = 0.0005)	6.64 ± 0.12 (p = 0.7849)
+ Pyr3 30 µM	272.20 ± 26.58 (p = 0.9822)	6.60 ± 0.09 (p = 0.6518)

Abbreviations: 2-APB = 2-aminoethoxydiphenyl borate; CWE = cold water extract

4.3.1.5 CWE inhibited extracellular calcium entry in porcine bronchiole

This section examined the role of calcium mediated by CWE and carbachol in porcine bronchiole tissues. Fig. 4.6A shows that in vehicle control tissues, addition of KCl only evoked a maximum response of 20.94 ± 5.03%. Conversely, in the presence of CWE, KCl evoked significant contraction prior to CRCs to $CaCl_2$ in calcium-free Krebs solution (E_{max} of CWE 1.8 mg/ml: 66.06 ± 8.03%, p = 0.0006; CWE 3.2 mg/ml: 71.47 ± 8.02%, p = 0.0002; CWE 5.6 mg/ml: 85.10 ± 9.95%, p = 0.0001). The contraction was reflected in Fig. 4.6B, showing that the tissue tone prior to addition of $CaCl_2$ was higher in tissues pre-treated with CWE compared to vehicle control (untreated). This was in marked contrast from rat airway segments where no significant KCl-induced contraction was observed in CWE pre-treated tissues (Section 4.3.1.1).

In Fig. 4.6B, increasing concentrations of $CaCl_2$ had evoked contraction in control tissues with a maximum response of 151.31 ± 14.26%. Although the tissues pre-incubated with CWE had higher initial tone due to KCl-evoked contraction, the tissue tone did not increase significantly following addition of $CaCl_2$. The maximum response of $CaCl_2$-induced contraction in CWE-treated tissues was significantly lower than the control tissue (E_{max} of CWE 1.8 mg/ml: 101.66 ± 13.91%, p = 0.0446; CWE 3.2 mg/ml: 93.84 ± 15.52%, p = 0.012; CWE 5.6 mg/ml: 79.00 ± 17.24%, p = 0.0007) (Fig. 4.6B). The representative trace recordings for these observations are shown in **Appendix C**. These results imply that CWE may prevent extracellular Ca^{2+} entry through membrane calcium channels.

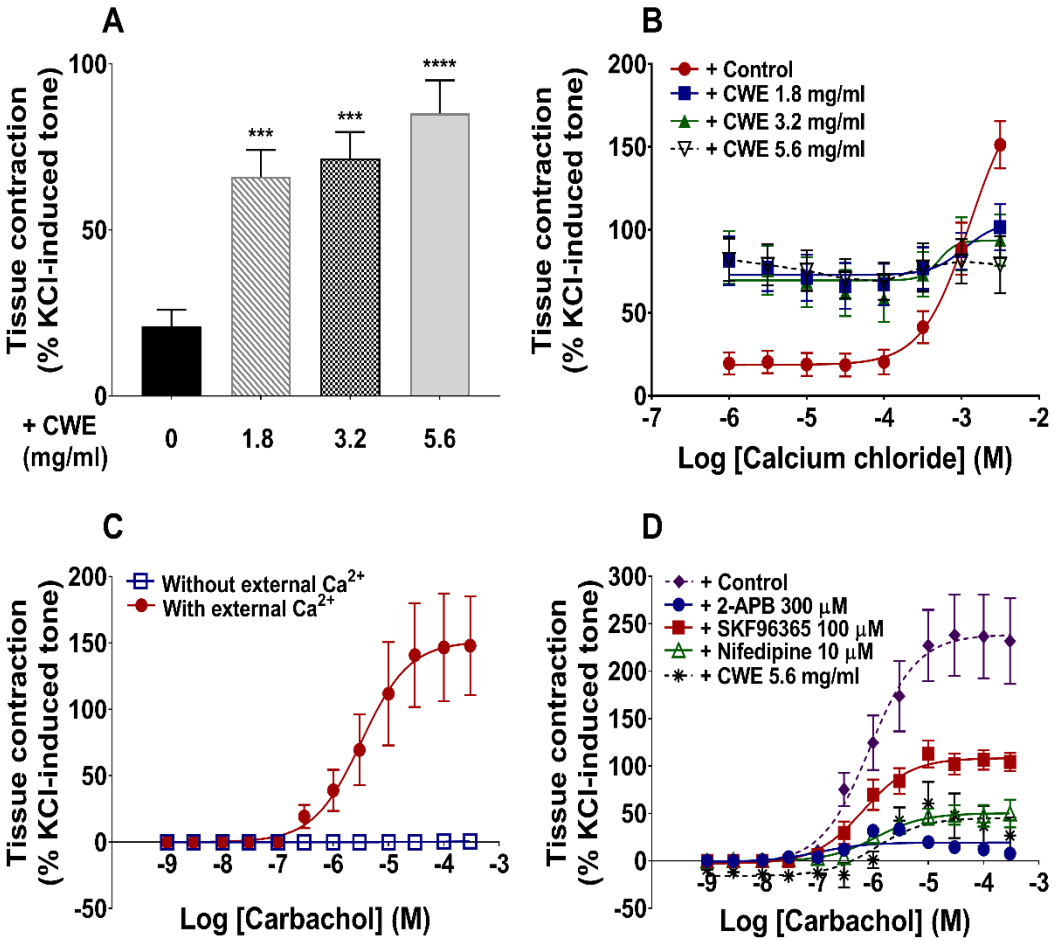

Figure 4.6: The role of calcium in cold water extract-induced relaxation and carbachol-induced contraction in porcine bronchioles. (A),(B) Bronchiole rings were immersed in calcium-free Krebs solution and pre-incubated with CWE or vehicle control for at least 30 minutes. Then, KCl (60mM) was added to tissues to induce depolarization, followed by CRCs to calcium chloride. (A) represents tissue contraction induced by KCl added before the CRCs to calcium chloride. (B) represents the subsequent tissue contraction induced by calcium chloride. (C) CRCs to carbachol in calcium-free Krebs solution (without external Ca^{2+}) or normal Krebs solution (with external Ca^{2+}). (D) CRCs to carbachol in tissues pre-incubated with nifedipine, 2-APB, SKF96365, CWE, or DMSO (vehicle control). Data were shown as means ± SEM of 3 to 10 animals. Tissue response was expressed as a percentage of reference KCl-induced tone. One-way ANOVA with Dunnett correction where comparison of means was made between vehicle control and CWE-treated groups: ***$p < 0.001$, ****$p < 0.0001$. (Abbreviations: 2-APB = 2-aminoethoxydiphenyl borate; CRCs = cumulative concentration-response curves; CWE = cold water extract)

Subsequent experiments investigated the role of extracellular Ca^{2+} mediated by carbachol in porcine bronchioles. Fig. 4.6C shows that removal of external Ca^{2+} (E_{max}: 1.43 ± 1.43%; p = 0.006) had significantly suppressed carbachol-induced contraction compared to the presence of external Ca^{2+} (E_{max}: 154.70 ± 38.74%). The potency of carbachol was not significantly affected by removal of external Ca^{2+} (p = 0.2883). Besides, Fig. 4.6D demonstrates that maximum response of carbachol was significantly suppressed by the treatments with CWE (E_{max}: 46.61 ± 21.45%; p = 0.0001), 2-APB (E_{max}: 19.53 ± 4.39%; p = 0.0001), SKF96365 (E_{max}: 109.50 ± 11.49%; p = 0.0072), and nifedipine (E_{max}: 50.55 ± 11.07%; p = 0.0002) when compared to vehicle control (E_{max}: 239.40 ± 43.74%). In addition, 2-APB had increased the potency of the curve by ~10-fold (pEC_{50} of 2-APB: 7.023 ± 0.166 vs vehicle control: 6.054 ± 0.111; p = 0.0021).

4.3.2 CWE suppressed the increase in cytosolic calcium levels induced by KCl in dorsal root ganglion cells

In calcium imaging experiments, addition of KCl served to depolarize the DRG neuronal cells, producing a reproducible and reversible peak. In the control set, second KCl peak response (without treatment) remained similar to the first KCl peak (Fig. 4.7A and 4.7D). Pre-incubation with CWE had significantly attenuated the elevated $[Ca^{2+}]_i$ evoked by second KCl exposure (p = 0.0001) (Fig. 4.7B and 4.7D). This observation was mirrored in nifedipine treatment group (p = 0.0001) (Fig. 4.7C and 4.7D). These results suggest that CWE blocks membrane calcium channels, especially L-type calcium channels, to inhibit the rise in $[Ca^{2+}]_i$ induced by KCl. In Fig. 4.7B, we observed a depression in the ratio of fluorescence intensities throughout the incubation period of CWE, which is believed to be due to interference from CWE as a result of wavelength overlap. The intensity ratio had restored to the basal $[Ca^{2+}]_i$ levels once CWE was removed prior to the application of second KCl.

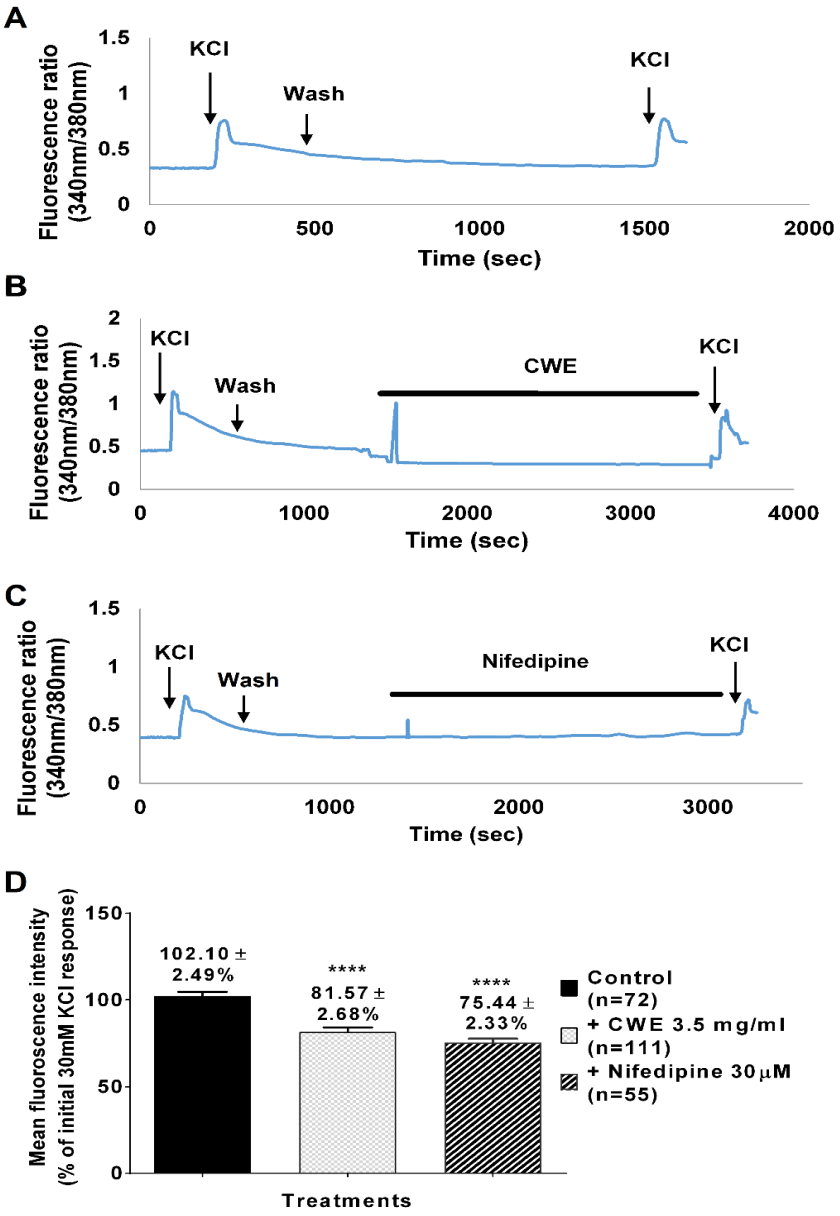

Figure 4.7: The peak $[Ca^{2+}]_i$ induced by potassium chloride in the presence and absence (control) of cold water extract in DRG cells. Representative calcium imaging traces of $[Ca^{2+}]_i$ induced by KCl in (A) control-, (B) CWE- and (C) nifedipine-treated rat dorsal root ganglion cells. Trace (A) shows similar magnitude of increase in Ca^{2+} transients following the first and second 30 mM KCl application. The second KCl peak was attenuated by treatment with (B) CWE and (C) nifedipine (incubation period shown by thick bar). Artefact spikes were observed at 1500 sec in trace (B) and (C) slightly after the start of compound infusion. (D) Treatment with CWE and nifedipine significantly reduced the $[Ca^{2+}]_i$ levels induced by second KCl peak. Data represented the mean values ± SEM of n number of neurons. Mean fluorescence intensity of second KCl peak was expressed as a percentage of the first KCl (30 mM) peak which served as a reference. One-way ANOVA with Dunnett correction where comparison of mean was performed between control and treatment groups, ****p < 0.0001. (Abbreviations: $[Ca^{2+}]_i$ = cytosolic calcium; CWE = cold water extract; DRG = Dorsal root ganglion; KCl = potassium chloride)

4.3.3 CWE did not exhibit Ca^{2+}-chelating activity

To rule out if the bronchodilator effect of CWE attributes to its Ca^{2+}-chelating ability, calcium titration test was conducted. Fig. 4.8 shows that Ca^{2+} concentration in the sample containing CWE (103.40 ± 3.84%, p = 0.426) did not differ significantly from the sample containing vehicle control (which represents 100%). This suggests that CWE does not complex with Ca^{2+}.

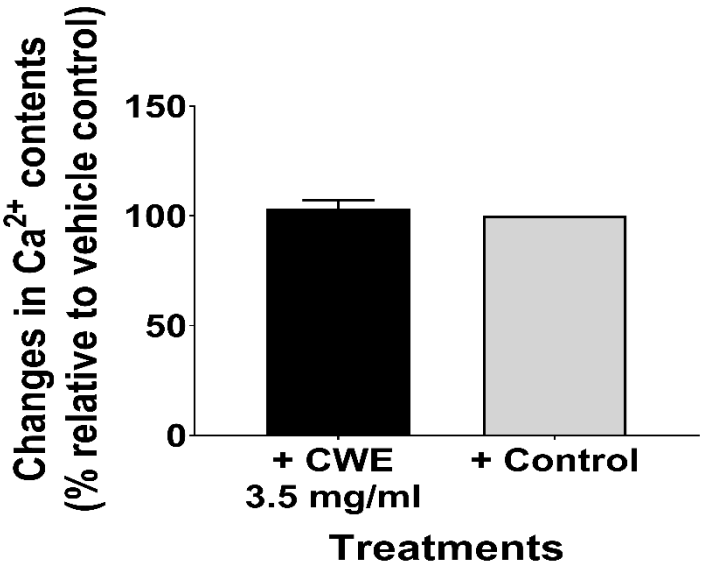

Figure 4.8: Complexometric titration test of cold water extract. Experiments were performed in triplicates. The degree of change in Ca^{2+} contents in cold water extract-treated samples was measured as a percentage relative to the Ca^{2+} contents in vehicle control samples (represents 100%). (Abbreviations: CWE = Cold water extract)

4.4 Discussions

In the present chapter, we had elucidated the roles of extracellular and intracellular Ca^{2+} mediated by CWE in airways. We also characterized the Ca^{2+} influx mechanisms participating in contractions elicited by carbachol, 5-HT, and KCl. The entry of Ca^{2+} in response to KCl in smooth muscle is known to be mainly due to cell membrane depolarization, which induces extracellular Ca^{2+} influx through VOCC, especially L-type calcium channels (Sanderson et al., 2008). Our observation shown herein is in line with other researchers as nifedipine substantially suppressed $CaCl_2$-induced contraction in KCl-depolarised rat airway segments (Fig. 4.1). This showed that KCl-induced depolarization triggered extracellular Ca^{2+} influx through opening of L-type calcium channels which were presumably blocked by nifedipine. This inhibitory effect was mirrored by CWE, suggesting that CWE could also prevent extracellular Ca^{2+} entry through blockade of membrane calcium channels. These results corroborate the inhibitory effects of CWE and nifedipine on KCl-induced elevation of $[Ca^{2+}]_i$ in DRG cells using calcium imaging technique (Fig. 4.7).

In support of our findings, the exposure of rat DRG cells to KCl was shown to induce cell depolarization and increase calcium transients, which depend mostly on extracellular Ca^{2+} influx through L-type and N-type calcium channels in other studies (Fuchs et al., 2007; L. Zhao et al., 2016). This notion was substantiated by evidence that removal of extracellular Ca^{2+} had attenuated the elevation of $[Ca^{2+}]_i$ induced by depolarization, indicating the predominant role of Ca^{2+} influx in contributing to the transient peak of $[Ca^{2+}]_i$ (Azmir et al., 2013; Gerevich et al., 2004; Ouyang et al., 2005). We, however, could not determine if $[Ca^{2+}]_i$ is changed during the incubation period of CWE due to spectroscopic interference.

A similar inhibition of calcium-induced contraction by CWE in KCl-depolarised airways was also observed in porcine bronchiole tissues (Fig. 4.6B), supporting the results in rat airways. Interestingly, pre-incubation with CWE had increased the tone of porcine bronchiole tissues upon addition of KCl (prior to $CaCl_2$ CRC) in a calcium-free environment (Fig. 4.6A). This potentiating effect increased with higher concentrations of CWE. It is intriguing as this response was not observed in rat airway segments despite that CWE had induced significant airway contraction at basal tone in both species (**Chapter 3**). It is unlikely that this contraction was caused by an immediate increase in $[Ca^{2+}]_i$ as the contraction did not occur during pre-incubation period, but only occurred upon KCl addition. Instead, we speculate that CWE might increase the Ca^{2+} sensitivity of bronchioles. This speculation coincides with our findings in Fig. 3.7B (**Chapter 3)** in which tissues exposed to atropine had attenuated CWE-induced contraction. We deduce that CWE may activate muscarinic receptors at tissue basal tone, which subsequently stimulates the downstream PKC pathway leading to enhanced Ca^{2+} sensitivity of the contractile apparatus.

The other possibility is that CWE may mobilize intracellular Ca^{2+} store along with extracellular Ca^{2+} influx upon KCl addition. Although this experiment was conducted in the absence of external Ca^{2+}, there might be traces amount of Ca^{2+} remaining in the calcium-free Krebs solution that could enter the cells upon depolarization. Nevertheless, whether the traces of external Ca^{2+} are sufficient to evoke a contraction is doubtable. Subsequent observations in the same protocol where KCl-induced tone did not increase further with increasing concentrations of $CaCl_2$ in CWE-treated tissues infer that pre-treatment with CWE may protect against calcium-induced contractions. Moreover, based on the results of complexometric titration, we ruled out that CWE-induced relaxation is attributed to its Ca^{2+}-chelating activity.

Additional evidence of CWE inhibiting membrane calcium channels was gathered by elucidating the Ca^{2+} dynamics mediated by carbachol. In Fig. 4.2, removal of external Ca^{2+} greatly reduced the sustained contraction (by ~7.7-fold at 1 hr) induced by carbachol, but reduced the initial peak of contraction to a lesser extent (by ~2-fold at 0 hr). These results suggest that carbachol utilizes both intracellular and extracellular Ca^{2+} for the initial phase of contraction but depends predominantly on extracellular Ca^{2+} influx for the sustained contraction. Extracellular Ca^{2+} influx via SOCC is pivotal in repletion of intracellular Ca^{2+} store to maintain a sustained elevated $[Ca^{2+}]_i$ in smooth muscle (Siddiqui et al., 2013). It is strongly likely that the sustained contraction induced by carbachol in normal Krebs solution also depends on extracellular Ca^{2+} influx. Furthermore, the same experiment showed that in the absence of external Ca^{2+}, CWE significantly suppressed the sustained contraction induced by carbachol but failed to reduce the initial peak of contraction. We thus deduce that the effect of CWE is largely mediated via blockade of extracellular Ca^{2+} entry during the sustained contraction, at the same time preventing repletion of Ca^{2+} store. CWE may have little effect on intracellular Ca^{2+} mobilization, as evidenced by its lack of inhibitory effect on the initial phase of carbachol-induced contraction. This proposition is supported by the suppression of carbachol-induced contraction by CWE in normal Krebs solution (Fig. 4.3).

To substantiate the above findings, subsequent experiments were conducted to assess the role of extracellular Ca^{2+} mediated by carbachol, 5-HT and KCl in rat airway segments (Fig. 4.4). EGTA was added into the bath solution to ensure complete elimination of external Ca^{2+}. Results showed that contractions induced by carbachol, 5-HT and KCl were almost completely abolished in the absence of external Ca^{2+}, suggesting that extracellular Ca^{2+} plays predominant role in contraction induced by

these agents. Similar observation was found in porcine bronchiole tissues where removal of external Ca^{2+} also totally attenuated the contractile response to carbachol (Fig. 4.6C), corroborating our findings in rat airways.

In spite of this, the above results seem to contradict with general findings by some researchers where *in vitro* acetylcholine or carbachol primarily relies on Ca^{2+} release from intracellular store to elicit contraction in isolated trachea of guinea pig (F. Ahmed, Foster, Small, & Weston, 1984) and cat (Yushi Ito & Itoh, 1984). Our results also disagree with the general consensus where intracellular Ca^{2+} release predominates over extracellular Ca^{2+} influx following receptor-activated airway smooth muscle contraction (Girolamo Pelaia et al., 2008). We, however, found our observations in line with a report by Baba et al. (1985) in which removal of external Ca^{2+} quickly abolished the sustained contraction induced by carbachol, leaving only a small maintained tension in guinea pig trachea, thus suggesting that the transient contraction is triggered by limited intracellular Ca^{2+} store.

Furthermore, other studies had demonstrated that carbachol only induced transient contraction in calcium-free Krebs solution, indicating that extracellular Ca^{2+} influx is important for the maintenance of sustained contraction in guinea pig trachea (Baba, Satake, Takagi, & Tomita, 1986; Masamori Takemoto, Ito, Takagi, Ogino, & Tomita, 1998). Another study by Black et al. (1986) also showed that carbachol-induced contraction was completely abolished in calcium-free Krebs solution, while KCl-induced contraction was only partially reduced in human bronchial spirals, in contrast with our finding.

Further evidence points to the significant role of extracellular Ca^{2+} in contributing to $G_{\alpha q}$-coupled contraction. In Fig. 4.4A and B, intracellular Ca^{2+} was emptied by EGTA and carbachol, and repletion of Ca^{2+} store through SERCA was

inhibited by thapsigargin. In such environment, cumulative CRCs to carbachol and 5-HT were not affected, indicating that mobilization of intracellular calcium store plays an insignificant role. We thus postulate that extracellular Ca^{2+} is the sole source for $[Ca^{2+}]_i$ spike in maintenance of airway contraction induced by CRCs to carbachol and 5-HT. This is, however, dissimilar from the previous results where addition of a single high concentration of carbachol (300 μM) was capable to trigger a transient peak of contraction (Fig. 4.2A). This may be explained by the evidence that intracellular Ca^{2+} contributes significantly to the contraction induced by higher concentration of carbachol (Masamori Takemoto et al., 1998).

We proposed several reasons that may contribute to the discrepancies. Firstly, carbachol may use different calcium pools when added in single concentration and in cumulative concentrations. Similar responses were observed in studies by Black et al. (1986) and Baba et al. (1986) where cumulative CRCs and single concentration of carbachol were applied respectively. Secondly, there may be interference from EGTA. EGTA, when incubated in calcium-free Krebs solution for sufficiently long period, may destabilize the cell membrane and sequester away loosely bound Ca^{2+} at cytoplasm or cell membrane as well as intracellular Ca^{2+} from the SR store (Guan, Kwan, & Daniel, 1988; Kanae, Takagi, & Hotta, 1977). It is likely that EGTA could immediately sequester the intracellular Ca^{2+} released during cumulative additions of carbachol, and hence the $[Ca^{2+}]_i$ levels are not sufficiently high to evoke a contraction. Thirdly, we postulate there may be species difference. There is little study on the calcium roles of carbachol, 5-HT and KCl in rat airways, and thus this piece of evidence complements the knowledge.

In addition, carbachol-induced contraction was sensitive to pre-treatment with 2-APB and SKF96365 (non-selective blockers of TRPC channels, Alexander et al.,

2015), and nifedipine in rat and porcine airways (Section 4.3.1.4 and 4.3.1.5). This implies that carbachol-induced contraction is likely to involve extracellular Ca^{2+} influx through TRPC and L-type calcium channels. Nevertheless, it is noted that 2-APB has complex pharmacological properties; in addition to direct inhibition of TRPC channels (Harding et al., 2018), it also exhibited dose-dependent stimulation ($\leq$ 20 μM) and inhibition ($\geq$ 30 μM) of I_{CRAC} and SOCC (DeHaven, Smyth, Boyles, Bird, & Putney, 2008). Moreover, contradictory effects of 2-APB on intracellular calcium dynamics are reported with different concentrations. At low concentration, 2-APB elicited stimulatory effect on Ca^{2+} influx through SOCC (10 μM; Ma, Venkatachalam, Parys, & Gill, 2002), whereas at high concentration, 2-APB inhibited intracellular Ca^{2+} release induced by methacholine and thapsigargin (100 μM; Lievremont et al., 2005). Such Ca^{2+}-releasing activity may partly explain the increased potency of carbachol by 2-APB (Fig. 4.6D).

Despite the possible implication of TRPC channels, TRPC3 channel is probably not affected or only play a minor role as pre-treatment with Pyr3, a TRPC3-selective inhibitor, did not significantly affect carbachol-induced contraction. Intriguingly, the potency of carbachol was slightly increased by CWE, in contrast to nifedipine which decreased the potency of carbachol in rat tracheal tissues. This implies that CWE may potentiate carbachol-induced contraction at low concentrations of carbachol, possibly due to increased Ca^{2+} sensitivity of smooth muscle, partially supporting our previous hypothesis. Another possibility is that CWE acts as partial agonist by activating muscarinic receptors in the absence or low concentration of muscarinic receptor agonist, in support of the inference deduced from **Chapter 3**. Besides, the pEC_{50} value may be shifted to the left as CWE has achieved the maximum response at a lower concentration.

To summarize, evidence gathered from the mechanistic experiments indicates that extracellular Ca^{2+} entry plays a more important role than intracellular Ca^{2+} release in airway smooth muscle contraction induced by carbachol, 5-HT, and KCl. Both extracellular and intracellular Ca^{2+} contributes to the initial phase of carbachol-induced contraction, whereas extracellular Ca^{2+} is probably the primary source for sustained contraction elicited by carbachol. Collectively, these data strengthen the view that CWE mainly blocks extracellular Ca^{2+} entry through membrane calcium channels in airway smooth muscle, supporting our hypothesis. Elevation of $[Ca^{2+}]_i$ evoked by membrane depolarization in DRG cells was blocked by CWE, further corroborating the inhibitory role of CWE on L-type calcium channels. We cannot completely preclude the effect of CWE on intracellular Ca^{2+} mobilization, but our results strongly suggest that the role of intracellular Ca^{2+} is relatively minor. In following **Chapter 5**, the effect of CWE on vascular and ileal smooth muscles was examined to further understand the mechanisms of action of CWE and to support the findings in airway smooth muscle.

Chapter 5. Pharmacological actions of *Lignosus rhinocerotis* extract on blood vessels and ileum

5.1 Introduction

Experiments in this thesis so far had used rat airway smooth muscle to examine the pharmacological effects of CWE. To date, there is no scientific evidence of the effect of CWE on other smooth muscles such as blood vessels and ileum. Notably, there exist structural and mechanistic similarities and differences between these tissues and airways. For instance, when compared to airway smooth muscle, it is well established that extracellular Ca^{2+} influx is mainly mediated via VOCC in vascular smooth muscle such that calcium channel blockers are effective therapies for hypertension and other vascular diseases (Brozovich et al., 2016).

A number of plants were reported with similar relaxation effects on different types of smooth muscles (Khazdair & Boskabady, 2015). Both *Nigella sativa* and *Ferulla asafoetida* exhibited similar relaxant responses on different smooth muscle tissues (airways, blood vessels, gastrointestinal and urogenital tracts) (Keyhanmanesh, Gholamnezhad, & Boskabady, 2014; Khazdair & Boskabady, 2015). Mechanistic studies of *N. sativa* on various smooth muscles are complementary with each other and lead to conjecture that the relaxation effects are generally mediated through blockade of calcium channels or opening of potassium channels (Keyhanmanesh et al., 2014). Besides, *Viscum album*, or mistletoe, possessed inhibitory effects on smooth muscle contraction of both aorta and jejunum. The relaxant responses are possibly mediated through blockade of VOCC, as supported by observations in both smooth

muscle preparations (Khan et al., 2016). Thus, this shows that certain mechanisms in different tissues could complement with each other.

In view of this, the present chapter intended to explore if CWE exhibits similar relaxant response in other smooth muscles. Such information is important for further characterization of the mechanisms of actions of CWE. Additionally, investigating CWE in animal species other than rat, either rodent or non-rodent, would be useful to rule out species-specific effect of CWE. The following subsections provided an overview of the tissues, including blood vessels and ileum, to be tested in the present chapter.

5.1.1 Blood vessels

5.1.1.1 Vascular contraction and relaxation

The tone of vascular smooth muscle is important to regulate the blood flow through blood vessels, and therefore maintaining an optimal blood circulation and pressure in the body. Similar to airway smooth muscle, vascular smooth muscle will contract and relax, with altered vascular luminal size occurring to reflect vasoconstriction and vasorelaxation respectively. Activities of vascular smooth muscle are dependent on the levels of $[Ca^{2+}]_i$. Smooth muscle contraction is initiated by an increase in $[Ca^{2+}]_i$ and Ca^{2+} sensitivity of the contractile apparatus; this can be induced by activation of GPCR (G_q, $G_{12/13}$, G_i) and/or opening of calcium channels (Rang et al., 2015). Elevation of $[Ca^{2+}]_i$ then triggers the phosphorylation of MLC by MLCK, resulting in the binding of myosin to actin filament to elicit smooth muscle contraction (Brozovich et al., 2016). On the other hand, vascular smooth muscle relaxes when $[Ca^{2+}]_i$ is

decreased following termination of contractile stimuli or mechanisms. This could be achieved by the activation of G_s-coupled receptors, release of EDRFs, blockade of Ca^{2+} channels, and opening of K^+ channels.

Activation of G_q protein-coupled receptors triggers PLC to stimulate the downstream second messengers DAG and IP_3, which in turn activates PKC and IP_3 receptor respectively. The PKC is known to induce extracellular Ca^{2+} entry through cation channels and possibly TPRC channels. IP_3 receptor activation could lead to mobilization of intracellular Ca^{2+} store, and hence elevation of $[Ca^{2+}]_i$. Examples of G_q-coupled receptors on vascular smooth muscle are α_1-adrenoceptors, thromboxane A_2 receptors (TP), histamine H_1 receptor, and serotonin 5-HT_2 receptors (Bastin & Heximer, 2011). On the other hand, G_i-coupled receptors inhibit AC to decrease intracellular cAMP levels whilst $G_{12/13}$-coupled receptors activate the RhoA/Rho kinase pathway, both leading to vascular contraction. A number of agonists of these receptors can be applied to evoke contraction in blood vessels for examination and characterization of the pharmacological effects of agents of interest. For instance, phenylephrine and U46619, coupled to the $G_{\alpha q}$ protein, are commonly used contractile agents of blood vessels.

Besides, vascular relaxation can be achieved via stimulation of G_s-coupled receptors that activate AC enzyme and elevate cAMP levels. One of the examples is isoprenaline that induces vasorelaxation by binding to G_s-coupled β-adrenoceptors. Several subtypes of muscarinic receptors are expressed on the endothelium and smooth muscle of airways and blood vessels. As M_3 receptors are $G_{\alpha q}$-coupled, activation of these receptors on smooth muscle by agonists generally lead to smooth muscle contraction via increased $[Ca^{2+}]_i$ such as in airways (Rang et al., 2015). Despite that, paradoxical effect is observed in blood vessels as activation of endothelial M_3

receptors causes increased synthesis of NO and vascular smooth muscle relaxation. When endothelium of blood vessels is disrupted, acetylcholine is unable to elicit vasorelaxation due to removal of endothelial M_3 receptors, and by contrast, vasoconstriction occurs due to activation of M_3 receptors located on smooth muscle (Furchgott, 1999).

Vascular relaxation can be endothelium-dependent or –independent. The endothelium plays a key role in balancing the vascular smooth muscle tone by releasing EDRFs and endothelium-dependent contracting factors in response to neurotransmitters, platelet-derived products, hormones, and shear stress (Vanhoutte, 1989). As of today, EDRFs are known to include NO, prostacyclin (PGI_2) and EDHFs (Kang, 2014). In vascular tissues, it is well established that the NO mainly released from constitutive NO synthase in endothelium diffuses to adjacent smooth muscle to activate the soluble GC and increase cGMP levels, which in turn activates PKG to cause smooth muscle relaxation (Lincoln, 1989).

On the other hand, PGI_2 synthesis is synthesized from breakdown of arachidonic acid by phospholipase A_2 enzyme and subsequent conversion to PGH_2 by cyclooxygenase-1 enzyme (Mitchell, Ali, Bailey, Moreno, & Harrington, 2008). Then, PGI_2 synthase and thromboxane A_2 synthase enzymes catalyse the formation of PGI_2 and thromboxane A_2 from PGH_2 in vascular endothelium and platelet, respectively. The opposing effects of PGI_2 (vasodilator) and thromboxane A_2 (vasoconstrictor) render the balance between productions of these two hormones to be crucial in maintaining the vascular tone (Majed & Khalil, 2012). PGI_2 selectively binds to rhodopsin-like prostacyclin receptors expressed on vascular smooth muscle to stimulate AC and the downstream cAMP/PKA pathways. Both NO synthesis and phospholipase A_2 activation are Ca^{2+}-dependent steps (Mitchell et al., 2008).

Compared to NO, PGI_2 contributes relatively lesser to the endothelium-dependent relaxation in large vessels including rat aorta and proximal mesenteric arteries (Shimokawa et al., 1996). The role of PGI_2 increases with smaller blood vessels such as small resistance rat mesenteric arteries and human gastroepiploic arteries (Majed & Khalil, 2012).

Besides, EDHFs which are thought to regulate NO- and PGI_2-independent vasorelaxation can activate potassium channels, in particular Ca^{2+}-activated potassium channels, and hyperpolarize smooth muscle cells (Félétou & Vanhoutte, 2000). Other proposed candidates of EDHFs include gap junctions, epoxyeicosatrienoic acids (a product of cytochrome P450), and hydrogen peroxide (Fisslthaler et al., 1999; Tudor M. Griffith, 2004). Eichler et al. (2003) revealed that the activation of both small- and intermediate-conductance Ca^{2+}-activated potassium channels contributes largely to vascular smooth muscle cell hyperpolarization and EDHF-mediated response. In addition, potassium ion (K^+) itself is also proposed as a EDHF as K^+ efflux via endothelial Ca^{2+}-activated potassium channels may induce hyperpolarization by activating inwardly rectifying potassium (K_{ir}) channel on smooth muscle endothelial cells (Edwards, Dora, Gardener, Garland, & Weston, 1998)

As with other smooth muscles, the source of Ca^{2+} in vascular tissues can be either intracellular Ca^{2+} release from SR, or extracellular Ca^{2+} influx through membrane ion channels. Intracellular Ca^{2+} was released from SR into cytosol through ryanodine and IP_3 receptors, whilst extracellular Ca^{2+} is believed to enter into the cells primarily through L-type calcium channels in vascular smooth muscle. Other ion channels including voltage-dependent T-type Ca^{2+} channels, non-selective cation channels (ROCC/SOCC), NCX, and Ca^{2+}-permeable ligand-gated cation channels are also permeable to Ca^{2+} influx across the plasma membrane (Amberg & Navedo, 2013).

In recent years, interest is gaining for the role of TRPC channels in both vascular smooth muscle and endothelial cells. TRPC channel mRNA and/or proteins are identified in various species and vascular tissues including aorta and arteries (Firth, Remillard, & Yuan, 2007; Inoue et al., 2006). The Ca^{2+} influx through TRPC channels plays an important role in contributing to endothelium-dependent vasodilation, vascular wall permeability, and angiogenesis in vascular endothelial cells (Earley & Brayden, 2015). In vascular smooth muscle, agonists-induced vasoconstriction and mitogen-mediated smooth muscle cell proliferation are related to TRPC channel opening (Firth et al., 2007). Increased expression of TRPC channels is also associated with vasoconstriction via Ca^{2+} influx through SOCC in rat pulmonary artery (Kunichika et al., 2004; L. C. Ng & Gurney, 2001).

5.1.1.2 Structure and species difference between aorta and coronary artery

Aorta is the main artery in human body that originates from the left ventricle of the heart supplying oxygenated blood to the body. Coronary arteries comprise left and right coronary arteries branching off the ascending aorta. The left and right coronary arteries then branch off into smaller arteries to supply oxygenated blood to the left and right side of myocardium (atrium and ventricle) respectively. Coronary circulation is therefore vital for the cardiac function.

Both aorta and coronary arteries belong to the large vessels. However, they do possess difference in terms of their structures, size and calcium requirements for contraction. Notably, coronary artery is smaller than aorta in size. Also, aorta is elastic artery whilst coronary artery is muscular artery (Waller et al., 1992). The presence of

endothelium exerted greater inhibition on contractions induced by histamine, phenylephrine, 5-HT, and acetylcholine in coronary artery compared to aorta (T. M. Griffith, Henderson, Edwards, & Lewis, 1984). In a previous study, coronary smooth muscle cells differed from non-coronary smooth muscle cells by showing highly differentiated phenotypes, with lower proliferation, adhesion, and collagen synthesis (Sachin Patel et al., 2000).

A number of animal species including rats, mice, dogs, pigs, and monkeys have been used in the cardiovascular research. Among these species, small rodents are the most commonly used in pharmacological studies for cardiovascular system due to relatively lower cost and ease of handling. Rat aorta has been extensively used in preclinical *in vitro* and *in vivo* assays, with particular emphasis on the mechanisms underlying vasodilation, vasoconstriction, and angiogenesis (Rameshrad et al., 2016). Despite the advantages of rodent tissues, the distinct differences in heart sizes and pathophysiological features exist between humans and rodents, and therefore the results should be interpreted with caution (Camacho, Fan, Liu, & He, 2016).

As for non-rodent animal species choice, pig has become one of the popular models for cardiovascular research besides monkey and dog (Crick, Sheppard, Ho, Gebstein, & Anderson, 1998). One of the reasons is because the heart of pig closely resembles that of human in terms of anatomic and physiologic features, with similar sizes in heart and blood vessels (Swindle, Makin, Herron, Clubb, & Frazier, 2012). Furthermore, pig shares almost identical distribution of coronary arterial blood supply with human, and the right coronary artery is also the dominant artery in both species (Reese, Mikawa, & Bader, 2002; Rodrigues, Silva, Águas, & Grande, 2005; Sahni, Kaur, Harjeet, & Jit, 2008). Based on these literatures, as far as the coronary arteries

are concerned, pig is therefore considered a suitable animal species for translational research to extrapolate the data in animals to humans.

Cationic channels are expressed in aortic and coronary arterial smooth muscle. Many pieces of evidence support the existence of high-voltage-activated (L-, N-, P-, Q-, R-type) and low-voltage-activated (T-type) calcium channels in these vascular smooth muscle by using corresponding calcium channel antagonists. The L-type and T-type (Andreasen et al., 2006; Ganitkevich & Isenberg, 1990; Kuga et al., 1990), and P- and Q-type (Andreasen et al., 2006) Ca^{2+} currents, which are sensitive to calcium channel antagonists, were detected in rat aortic, guinea pig coronary arterial and mesenteric arterial smooth muscle cells. Besides, proteins or mRNA of TRPC channels are reportedly present in aorta of rat and mouse in isoforms of TPRC1 to TRPC7 (Earley & Brayden, 2015; Firth et al., 2007). Proteins of TRPC1, TRPC3, TRPC4, TRPC5, and TRPC6 are also identified in human coronary arteries (Firth et al., 2007). Considering the mechanisms of action of CWE deduced from previous chapters, we focussed on studying the involvement of TRPC and L-type calcium channels in this chapter.

5.1.2 Ileum

Smooth muscle of gastrointestinal tissues contracts due to direct action on muscle fibre or indirect action through the excitation of intrinsic network of nerves. In gastrointestinal tissues, the muscular layer consists of circular and longitudinal smooth muscle. The peristaltic movement of the gut is modulated by repeated cycles of contraction and relaxation of these muscles. It was initially proposed that during "preparatory phase" of peristalsis when the intestinal lumen is distended by content, the longitudinal muscle contracts, causing shortening of intestinal segment (Bennett, 1997). Subsequently during "emptying phase" of peristalsis, the longitudinal muscle relaxes while circular muscle contracts to propel the food content towards the direction of anal. This idea is contrasted by later study which showed that preparatory phase is not necessary during peristalsis, although the peristaltic wave generally depends on the muscle tone and contraction (Spencer, Smith, & Smith, 2001). The general notion is that Interstitial cells of Cajal (ICC) generates and propagates slow waves that modulates the peristaltic movement in the gastrointestinal tract.

The gastrointestinal tract receives extensive excitatory and inhibitory inputs from a complex network of enteric nervous system, namely myenteric plexus and submucous plexus. Preganglionic parasympathetic fibres synapse with the postganglionic neurons, mainly cholinergic and excitatory, causing stimulating effect on gastrointestinal smooth muscle activity (Rang et al., 2015). As cholinergic nerves are activated, acetylcholine is released from the nerve terminals and triggers smooth muscle contraction. On the other hand, the sympathetic fibres play a crucial role in the relaxation of gastrointestinal smooth muscle. The sympathetic fibres are mainly postganglionic, and may inhibit acetylcholine release at the nerve terminals by acting

on α_2-adrenoceptors through presynaptic inhibition while activation of postsynaptic α_1-adrenoceptors contributes to smooth muscle relaxation (Rang et al., 2015). The presence of functional β-adrenoceptors (β_1, β_2, and β_3 subtypes) were reported in guinea pig ileum, and upon stimulation, it leads to smooth muscle relaxation (Horinouchi & Koike, 2000; Nasser, Ho, & Sharkey, 2006). Of all subtypes, β_1-adrenoceptors are found to be the predominant adrenoceptors in both mice (Hutchinson, Evans, & Summers, 2001) and guinea pig ileum (Grassby & Broadley, 1984).

It is also well documented that morphine depresses gastrointestinal motility. Three subtypes of opioid receptors, namely μ, κ, and δ, are expressed in the cholinergic neurons of intestine (Galligan & Akbarali, 2014). It has been suggested that μ and κ receptors negatively regulate acetylcholine release evoked by electrical stimulation in guinea pig ileal longitudinal muscle (Kojima, Takahashi, Fujina, & Owyang, 1994). The κ receptor activation is associated with blockade of VOCC resulting in reduced extracellular Ca^{2+} entry (Kojima et al., 1994), while μ receptor activation increases K^+ conductance. Morphine and encephalin were shown to activate the resting K^+ conductance of myenteric neurons and cause dose-dependent hyperpolarization, especially in low extracellular Ca^{2+} concentration (Morita & North, 1982). Subsequent study suggests that the hyperpolarization effect induced by morphine is possibly linked to its inhibitory effect on acetylcholine release (Cherubini, Morita, & North, 1985). This is further supported by evidence that activation of μ and δ receptors increases K^+ conductance (Cherubini & North, 1985; North, Williams, Surprenant, & Christie, 1987) whereas κ receptor directly inhibits Ca^{2+} entry into nerve terminals (Cherubini & North, 1985), therefore inhibiting the release of endogenous acetylcholine. In guinea pig ileal preparations, inhibitory effect of endogenous opioids

on acetylcholine release was shown to be modulated via μ receptor, but not κ and δ receptors (Nishiwaki, Saitoh, Nishio, Takeuchi, & Hata, 1998).

Other than adrenaline and acetylcholine, the enteric neurons also secrete a number of neuropeptides and transmitters such as NO, 5-hydroxytrptamine, purines, and many others, which mediate the excitatory and inhibitory NANC systems that stimulates and inhibits gastrointestinal motility, respectively. It is believed that the inhibitory NANC nerves upon stimulation release a few neurotransmitters, including NO, ATP, carbon monoxide, and vasoactive intestinal peptide, whereas the excitatory NANC nerves release tachykinins such as substance P, neurokinin A, and neurokinin B through stimulation of tachykinin receptors (Bennett, 1997).

In ileal smooth muscle, M_2 and M_3 muscarinic receptor subtypes are preferentially expressed, with preponderance of M_2 subtype (Clague, Eglen, Strachan, & Whiting, 1985; Eglen, Hegde, & Watson, 1996). The general notion is that the activation of G_i-coupled M_2 receptors reduces cAMP levels while $G_{\alpha q}$-coupled M_3 receptors activates the DAG/IP_3/PKC pathway, with both leading to smooth muscle contraction. Nonetheless, functional studies using carbachol to elucidate the role of muscarinic receptors showed that the contractile response of ileum was mediated exclusively by M_3 subtype, whilst the role of M_2 subtype is not entirely clear (Eglen & Harris, 1993). Recent studies showed that M_2 receptors are suggested to play an important functional role by directly inducing contraction in ileal (Matsui et al., 2002; Toshihiro Unno et al., 2005) and gastric smooth muscle (Stengel & Cohen, 2003). Acetylcholine mediated nonselective cationic channels in guinea pig ileums, in which the cationic channels are gated primarily by M_2 receptor activation which is in turn regulated by M_3 receptor (Zholos & Bolton, 1997). In mouse ileum, neurogenic cholinergic contraction is entirely attributed to M_2 and M_3 receptors, with the latter

playing a predominant role in wild type mice and with exogenously applied agonists (T. Unno et al., 2006). Although M_2 receptor activation by agonist produced less pronounced contraction of gut smooth muscle, it demonstrated marked contraction when stimulated by endogenous acetylcholine release upon neurogenic stimulation. Apart from M_2 and M_3 subtypes, the presence of other muscarinic receptor subtypes (M_1, M_4 and M_5) is also suggested in guinea pig gastric smooth muscle in a study by So et al. (2003), but their roles are less clear.

There are two routes by which neurogenic acetylcholine-induced contraction involves muscarinic receptor activation. Firstly, acetylcholine directly activates the smooth muscle cell M_2 and M_3 receptors, which possibly triggers the opening of L-type calcium channels and SOCC allowing for extracellular Ca^{2+} influx and intracellular Ca^{2+} mobilization (Wegener et al., 2006). Another proposed route is by direct activation of M_3 receptors on ICC, a pacemaker cell, to induce contraction via electromechanical coupling to adjacent smooth muscle cells, as seen in mouse ileum and jejunum (Hirst & Ward, 2003; Wegener et al., 2006). The electrical activity of ICC appears to arise from IP_3-dependent internal Ca^{2+} store mobilization, chloride channels, and VOCC (Hirst & Ward, 2003). The electromechanical coupling between smooth muscle and ICC was decreased by L-type calcium channel blocker, suggesting that this channel may be activated (Wegener et al., 2006).

There is evidence of presynaptic muscarinic autoreceptors that negatively regulate acetylcholine release from nerve terminals (Fosbraey & Johnson, 1980; Nishiwaki et al., 1998; Takeuchi et al., 2005). In support of this, the role of presynaptic muscarinic receptors acting as autoinhibition of acetylcholine release has been suggested to be regulated via M_1 and M_2 receptors in guinea pig stomach (Ogishima, Kaibara, Ueki, Kurimoto, & Taniyama, 2000), M_3 receptors in longitudinal muscle of

guinea pig ileum (Soejima, Katsuragi, & Furukawa, 1993), and M_1 receptors in circular muscle of guinea pig ileum (Dietrich & Kilbinger, 1995). Therefore, when compared to exogenous muscarinic agonists directly applied to organ bath preparations, endogenous acetylcholine released from parasympathetic nerve terminals are subject to modulation by muscarinic autoinhibition as well as degradation by cholinesterase.

Owing to the extensive enteric nervous system and secretion of a range of transmitters, guinea pig ileum has been a useful model system in pharmacological studies. Electrical field stimulation (EFS) of gastrointestinal smooth muscle has been broadly used in studies to induce release of endogenous acetylcholine through parasympathetic nerve stimulation (Kojima et al., 1994; Matsui et al., 2002; Nishiwaki et al., 1998; T. Unno et al., 2006). Drugs or unknown compounds can be applied to electrically stimulated tissues to assess their effects on parasympathetic nerves and endogenous acetylcholine release.

5.1.3 Significance of study

The present chapter aimed to unravel the effects of CWE on vascular and ileal smooth muscles to further the understanding on the general effects, mechanisms of action, potential side effects, and selectivity of CWE in different tissues. The outcome also served to support the findings in airways. The usage of different animal species and tissues would confirm if the relaxant and contractile responses to CWE are tissue- or species-specific. In vascular tissues, contractile agonists were applied to induce smooth muscle contraction, whereas in ileal tissues, neuronal release of acetylcholine

was induced using electrical field stimulation. We hypothesized that CWE could relax vascular smooth muscle contraction through blockade of extracellular Ca^{2+} entry, but independent of NO/cGMP pathway. It was also hypothesized that CWE could relax ileum via similar Ca^{2+} entry inhibition. The specific objectives of this chapter were as follows:

(i) To construct CRCs to CWE on rat aorta and porcine coronary artery pre-contracted with phenylephrine and U46619, respectively.

(ii) To construct CRCs to CWE in aorta pre-contracted with phenylephrine by removing the endothelium and exposing tissues to NO synthase inhibitor.

(iii) To assess the effect of calcium channel blockers on contractile agents-induced contractions and re-introduction of calcium in Ca^{2+}-free Krebs solution in aorta and coronary artery.

(iv) To construct cumulative CRCs to CWE on neurogenic contraction induced by EFS of guinea pig ileum.

(v) To construct cumulative CRCs to CWE in the presence of antagonists of muscarinic, β-adrenergic, opioid and α_2-adrenergic receptors in ileal tissues.

5.2 Materials and methods

5.2.1 Drugs and materials

CWE was prepared as described in Section 2.2.2, **Chapter 2**. Standard Krebs solution was prepared as per **Appendix A**. L-NAME, SNP, nifedipine, SKF96365, and carbachol were prepared as per Section 3.2.1 and 4.2.1, **Chapter 3 and 4**. Atropine sulfate, naloxone hydrochloride, phenylephrine, U46619, and SKF96365 were purchased from Sigma, USA. Isoproterenol hydrochloride (isoprenaline) was purchased from Tokyo Chemical Industry, Japan. Rauwolscine hydrochloride was purchased from Tocris Bioscience, UK. All drugs were dissolved in purified water except nifedipine and SKF96365. Nifedipine and SKF96365 were dissolved in 100% DMSO (Sigma-Aldrich, USA) respectively to make stock solutions. Ten-fold serial dilutions were made for all stock solutions to produce respective working solutions. The working concentration for nifedipine was 10 mM for blood vessels (final DMSO concentration in bath is 0.05% v/v) and 100 µM for ileum (final DMSO concentration in bath < 0.01% v/v), and 100 mM for SKF96365 (final DMSO concentration in bath is 0.3% v/v).

5.2.2 Tissue preparation

Ethics approval was obtained from the University of Nottingham's Animal Welfare and Ethics Review Body for rat (UNMC#2kn and UNMC12). In following Section 5.2.3, the experiments were conducted either with male Sprague Dawley rats (240-400g; 2-3 months old) or with pig. Sprague Dawley rats were purchased from

Universiti Putra Malaysia and Universiti Kebangsaan Malaysia. Rats were sacrificed by carbon dioxide or cervical dislocation under anaesthesia with diethyl ether. The thoracic aorta was isolated and used immediately on the day of the experiment. On the other hand, porcine hearts were obtained from a local abattoir in Nottingham, UK. The anterior coronary artery was isolated from the hearts and stored in Ficoll solution at 4°C overnight. All tissues were cleaned of their connective tissues. On the next day, the coronary artery was excised into 4 mm rings and immediately immersed in standard Krebs solution.

The aorta and coronary artery were mounted to organ bath set up as mentioned in Section 2.2.2.1 (**Chapter 2**). In Section 5.2.3.5, "calcium-free Krebs" solution (without Ca^{2+}), containing all ingredients as listed in **Appendix A** except calcium chloride, was used to create a calcium-free environment for the tissues. After tissues were mounted, they were left to equilibrate to the organ bath for 30 minutes after the application of 19.6 mN tension (aorta) or 98 mN (coronary artery) to achieve a steady baseline tone. Following equilibration, steps were repeated as in Section 2.2.4.1 (**Chapter 2**) where tissues were exposed to 60 mM KCl for two times to obtain the average reference contracture for vascular tissues. After the KCl was washed out and a stable resting tension was re-established, experiments were carried out as in the organ bath section below. In some experiments of Section 5.2.3.2, the endothelium of aortic rings was removed mechanically ("denuded") by rubbing the internal surface with the teeth of the forceps tip. The denudation was deemed successful if 1 µM carbachol failed to elicit > 20% relaxation response of 100 nM phenylephrine-induced contraction (Loong et al., 2015). Experiments in all sections were performed with intact endothelium unless specified.

Dunken Hartley guinea pig (360-720g; 3-4 months old) was collected from Monash University Malaysia on the day of experiment. Ethics approval for guinea pig was obtained from the University of Nottingham's Animal Welfare and Ethics Review Body (UNMC13). Guinea pigs were sacrificed by carbon dioxide, ileum was isolated and the contents inside were washed out with Krebs solution. Ileal tissues were then cut into several sections with length of approx. 4 cm long before stored in standard Krebs solution. For ileal preparations, all organ bath experiments were performed under conditions of "high calcium" Krebs solution (containing two times higher calcium concentration than standard Krebs solution). The preparations were mounted vertically, whereby one end of tissue was attached to an electrode (ileal segment wrapping around the platinum electrode) while the other end was attached to the force transducer via a silk thread. The changes in tissue tension along the longitudinal muscle were therefore recorded by the transducer. The tension changes recorded in some tissues were slightly affected by the concurrent spontaneous tone occurring in the circular smooth muscle.

A tension of 4.9 mN was applied to the ileal tissue. Tissues were then left to equilibrate for 30 minutes in high-calcium Krebs solution for at least 30 minutes or until basal tension was stable before stimulation response was carried out. Electrical stimuli were generated with a stimulator that delivers electrical pulses to the tissues via the electrode. Submaximal voltage for EFS (electrical field stimulation) was determined by the following steps:

a. All parameters were fixed except amplitude: Frequency: 0.1Hz; Duration: 2 minutes; Train pulse: 0.5 ms

b. Experiment was started with amplitude of 5V and increasing by 5V every 2 minutes until the maximum response was obtained.

c. The submaximal voltage which gave second highest contraction response (5 to 15V, depending on tissues) was taken and used subsequently throughout the experiments.

5.2.3 Effects of CWE on blood vessels

All experimental works on porcine coronary arteries were performed by Mr. Jonathan Mann-Seng Chooi in the University of Nottingham, UK.

5.2.3.1 Effect of CWE against pre-contractions induced by phenylephrine and U46619 in rat aorta and porcine coronary artery respectively

The tone of aortic rings was induced with 100 nM phenylephrine, a selective α_1-adrenoceptor agonist, to obtain a stable submaximal contraction size between 70% and 80% of the maximum phenylephrine-induced contraction (Loong et al., 2015). Upon establishing stable contractions, cumulative concentrations of CWE were added in aortic rings every 5 minutes or until the relaxation response plateaued. Purified water was added into different tissue preparations to serve as the vehicle control. Tissue relaxation was expressed as a percentage of phenylephrine-induced tone. Our earlier experiments (data not shown) showed that the concentration range of CWE used in airways did not produce any significant relaxation in aorta, and therefore we had used higher concentrations of CWE in blood vessels.

Phenylephrine produced poor contractility in porcine coronary arterial tissues, achieving only 30% of KCl-induced tone in our earlier experiment, hence a TP

receptor agonist, U46619 (10 to 30 nM), was used to pre-contract the arterial rings (Ting et al., 2000). Once stable tone was achieved, cumulative CRCs to CWE were constructed at 5 minute intervals between concentrations or until the relaxation plateaued. Corresponding vehicle control was carried out in a different set of tissues. Tissue relaxation to CWE was measured as a fraction of the contraction achieved by U46619 and expressed as a percentage of U46619-induced tone.

5.2.3.2 Involvement of endothelium and nitric oxide pathway in CWE-induced aortic relaxation

The tone of the aortic rings was induced with 100 nM phenylephrine. Upon establishing stable contractions, cumulative CRCs to CWE were constructed in denuded aortic rings to assess the role of CWE on EDRFs. Purified water was added into different tissue preparations to serve as the vehicle control. In a different set of experiments, endothelium-intact aortic rings were pre-incubated with L-NAME (100 µM) or purified water (vehicle control) for 30 minutes prior to pre-contraction with 100 nM phenylephrine. Then, cumulative CRCs to CWE were constructed. Tissue relaxation was measured as a fraction of the contraction achieved by phenylephrine and was expressed as a percentage of phenylephrine-induced tone.

5.2.3.3 Effect of CWE against carbachol-induced relaxation in rat aorta

We hypothesized that CWE may activate muscarinic receptors by acting as a partial agonist in inducing airway contraction and relaxation (see discussion in **Chapter 3 and 4**). Therefore, in this subsection we had examined if the presence of CWE could affect the CRC to carbachol in aorta. CWE at a final concentration of 6, 12, or 21 mg/ml (concentrations that induced appx. 50%, 70%, and 100% relaxation of aorta) was added into the bath for at least 30 minutes before aortic rings were pre-contracted with phenylephrine (100 nM to 1 μM, to induce a contractile response ~100-200% relative to KCl-induced tone). Upon establishing a stable contraction, cumulative CRCs to carbachol were constructed. Tissue relaxation was measured as a fraction of the contraction achieved by phenylephrine and was expressed as a percentage of phenylephrine-induced tone.

5.2.3.4 Effect of calcium channel blockers on U46619-induced contraction in porcine isolated coronary artery

In coronary arterial rings, 10 μM SKF96365 or 10 μM nifedipine was added into the bath for at least 30 minutes before construction of cumulative CRCs to U46619. DMSO 0.1% was added into different tissue preparations to serve as vehicle control. Tissue contraction to U46619 was measured as a change from basal tension and was expressed as a percentage of reference KCl-induced tone.

5.2.3.5 Effect of CWE on contractile responses to calcium re-introduction

We previously found that CWE inhibited Ca^{2+} entry via membrane calcium channels in airway segments, thus we hypothesized that CWE may exert similar mechanism in vascular smooth muscle. Higher concentrations of CWE (10 to 16 mg/ml) were initially tested, but these concentrations had completely suppressed the contraction elicited by $CaCl_2$ in the following protocol. Therefore, lower concentrations of CWE were applied to demonstrate a clearer difference in inhibitory effects. In calcium-free Krebs solution, CWE (3, 6, or 7 mg/ml) or purified water (vehicle control) was added to porcine coronary arterial rings for at least 30 minutes before 60 mM KCl was added to induce membrane depolarization. This was followed by the construction of cumulative CRCs to $CaCl_2$. Tissue contraction to $CaCl_2$ was measured as a change from basal tension and was expressed as a percentage of reference KCl-induced tone.

5.2.3.6 Effect of CWE on blood vessels at resting tension

Cumulative CRCs to CWE were constructed in porcine coronary arterial and rat aortic rings at basal tone. Tissue relaxation was expressed as the percentage of reference KCl-induced tone.

5.2.4 Effects of CWE on ileum

Fig. 5.1 illustrates the representative traces of EFS-induced responses in guinea pig ileum, and the way in which measurements were taken. Each tissue was electrically stimulated with pre-determined parameters to evoke submaximal contraction. The last three twitch responses prior to addition of drug/extract were averaged and served as the reference contracture for neurogenic contraction whilst the basal tension prior to addition of drug/extract served as the reference contracture for basal contraction. Once the twitch responses stabilized (~3 minutes), protocols were performed and CWE was added under repetitive EFS of ileal tissues. In all the following protocols, CWE was added into the baths every 5 minutes or until response plateaued. Neurogenic contractile response to treatment was expressed as a percentage of corresponding reference contracture. Basal contraction was measured as a fraction of change from corresponding reference contracture and expressed in mN. The measurement methods of neurogenic and basal contraction stated herein will apply to the following Section 5.2.4.1 to 5.2.4.2.

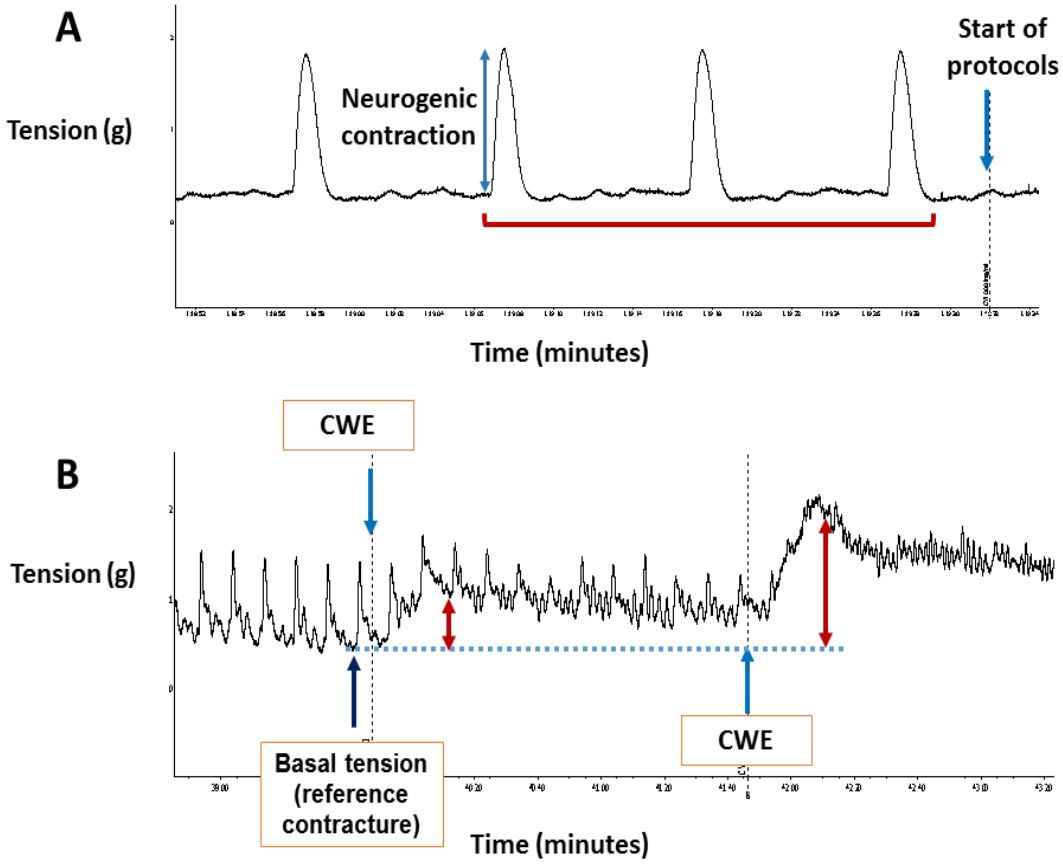

Figure 5.1: Representative traces of neurogenic responses to electrical field stimulation in guinea pig ileum. (A) Twitch responses generated by repetitive stimulation under submaximal parameters prior to treatments. EFS-induced neurogenic contraction was measured as the difference between trough to peak of tension. The red bar represents the last three twitches prior to addition of drug/extract that were averaged and served as the reference contracture for neurogenic contraction. Neurogenic contraction was expressed as a percentage of reference contracture. (B) Twitch responses stimulated under submaximal parameters with treatments (CWE or vehicle control). The red arrow represents the basal contraction that was measured as a difference from the reference contracture at basal tension. Basal contraction was measured in muscle tension, gram (g), and converted to milliNewton (mN). (Abbreviations: CWE = Cold water extract; EFS = Electrical field contraction)

5.2.4.1 Cumulative concentrations of CWE

Cumulative CRCs to CWE or purified water (vehicle control) were constructed in the ileal tissues. The concentration range of CWE was from 0.001 mg/ml to 1.0 mg/ml. Addition of CWE > 1 mg/ml was restricted by the bath volumes.

5.2.4.2 Effect of CWE in the presence of atropine, naloxone, rauwolscine, nifedipine or propranolol

To investigate the involvement of muscarinic receptors, opioid receptors, β- and α_2-adrenoceptors in CWE-induced response, ileal tissues were initially exposed to atropine (30 nM, Kerr et al., 1995; non-selective muscarinic antagonist), naloxone (30 nM, Morita and North, 1982; a non-selective opioid receptors antagonist), rauwolscine (300 nM, Scheibner et al., 2002; a α_2-adrenoceptor antagonist), nifedipine (30 nM, Mitchelson and Ziegler, 1984) or propranolol (3 μM, Hutchinson et al., 2001; a non-selective β blocker) for 30 minutes. This was followed by cumulative CRCs to CWE. In the control tissues, CRCs to CWE were performed in the absence of the above-mentioned drugs.

5.2.5 Statistical analysis

Due to the wide concentration range of CWE tested in blood vessels and ileum, the x-axis of graph was expressed as concentration of CWE in logarithm throughout this chapter. Data were analysed and graphs were drawn using PRISM v7.0 (Graph pad software). All data were expressed as mean ± SEM of *n* number of animals (aorta and coronary artery) or *n* number of preparations (ileum). Maximum tissue contraction or relaxation response (E_{max}) was derived from nonlinear regression analysis of the constructed CRCs or as an average response generated from the highest concentration tested (if relaxation response has not plateaued). In some experiments, responses at each individual concentration were compared with multiple comparison test. Statistical analyses were performed using one-way ANOVA with Dunnett correction (to compare the mean differences; Fig. 5.2B, 5.4, 5.5B, 5.6 and 5.10), two-way ANOVA followed by multiple comparison tests with Bonferroni correction (to compare the mean differences and to analyse the interaction between concentrations and treatments; Fig. 5.2A, 5.5A, 5.7 and 5.8), and Student's unpaired t-test (Fig. 5.3, 5.9 and 5.11). Results were considered statistically significant if p-value was less than 0.05. In the case if the interaction p-value based on two-way ANOVA analysis was < 0.05, this indicated an interaction between treatment groups and concentrations, meaning that effect of the treatments was different with concentrations.

5.3 Results

5.3.1 CWE relaxed aorta pre-contracted with phenylephrine

Fig. 5.2 shows that CWE significantly relaxed pre-contracted aortic rings from 6 mg/ml onwards. The maximum response of CWE, 97.70 ± 5.21%, was significantly higher than vehicle control, 58.99 ± 2.93% ($p < 0.0001$). The pEC_{50} value of CWE CRC was -0.68 ± 0.12 by constraining the maximum response to 100%. Two-way ANOVA results also showed an interaction between treatments and concentrations ($p < 0.0001$), indicating that these factors are interdependent. The above findings indicated that CWE possessed vasorelaxant activity.

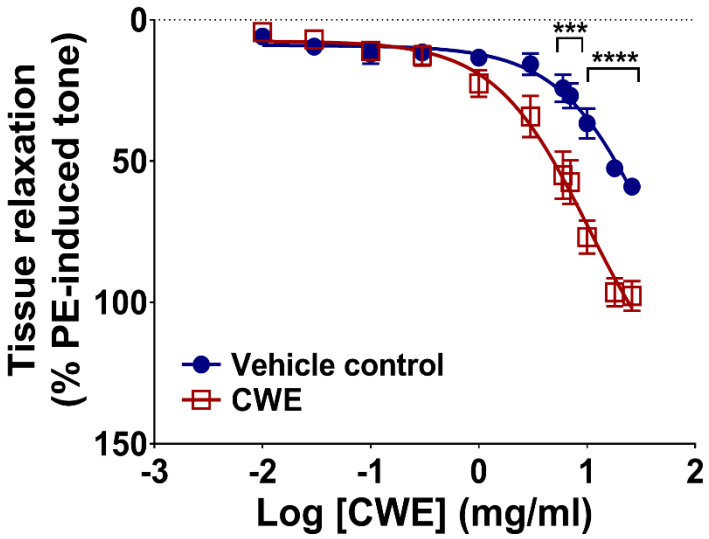

Figure 5.2: Effect of cold water extract on phenylephrine-pre-contracted rat aorta. Concentration-response curves to CWE or vehicle control (purified water) were constructed in aortic rings pre-contracted with 100 nM PE. Tissue response was expressed as a percentage of PE-induced tone. Data were shown as means ± SEM of 5 animals. Two-way ANOVA with Bonferroni correction compares the means between CWE and vehicle control: ***$p < 0.001$, ****$p < 0.0001$. (Abbreviations: CWE = cold water extract; PE = Phenylephrine)

5.3.2 CWE-induced aortic relaxation was independent of endothelium and nitric oxide

To determine whether EDRFs are implicated, CWE-induced relaxation was compared between endothelium-denuded and endothelium-intact aortic rings. Endothelium removal did not alter the maximum response of CWE-induced relaxation ($p = 0.4592$; Fig. 5.3A). Subsequently, the effect of CWE on NO was ruled out as the presence of L-NAME did not affect CWE-induced relaxation in aortic rings ($p > 0.9999$) (Fig. 5.3B). These results indicated that vasorelaxation elicited by CWE was independent of endothelium and NO.

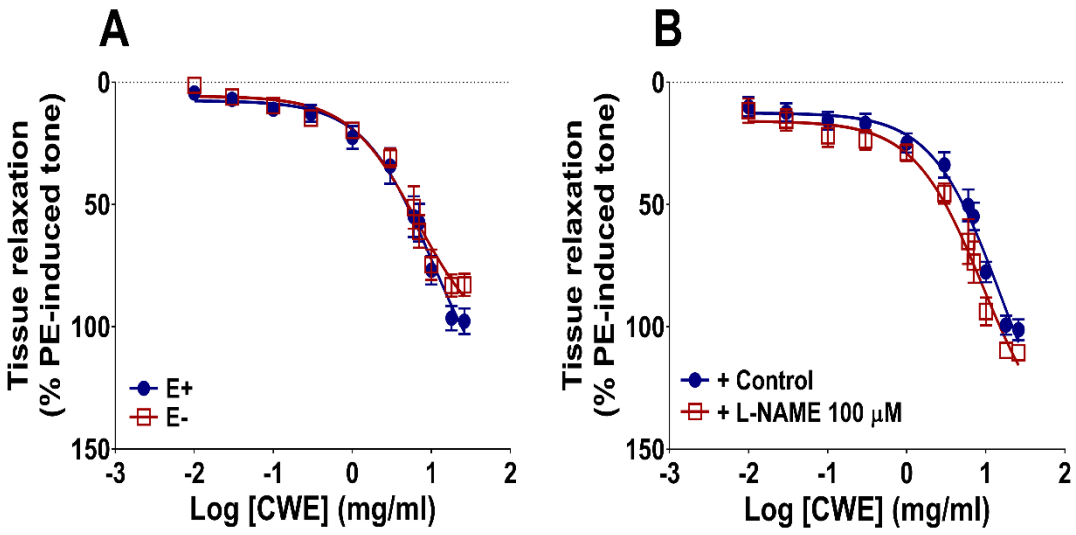

Figure 5.3: The involvement of endothelial nitric oxide pathway in cold water extract-induced relaxation of rat aorta. (A) CRCs to CWE or vehicle control (purified water) were constructed in endothelium-intact (E+) or endothelium-denuded (E-) rat aortic rings pre-contracted with 100 nM PE. (B) Aortic rings were pre-incubated with L-NAME or vehicle control (purified water) for 30 minutes prior to pre-contraction with 100 nM PE, followed by construction of CRCs to CWE. Tissue response was expressed as a percentage of PE-induced tone. Data were shown as means ± SEM of 4 to 7 animals. (Abbreviations: CWE = Cold water extract; CRCs = concentration-response curves; L-NAME = N(G)-nitro-L-arginine methyl ester; PE = Phenylephrine)

5.3.3 CWE did not affect muscarinic receptors in aorta

Pre-treatment with CWE did not affect the maximum response and potency of carbachol-induced relaxation in isolated aorta (Fig. 5.4). The E_{max} and pEC_{50} values are summarized in Table 5.1. These findings exclude the involvement of muscarinic receptors as a site of action for CWE.

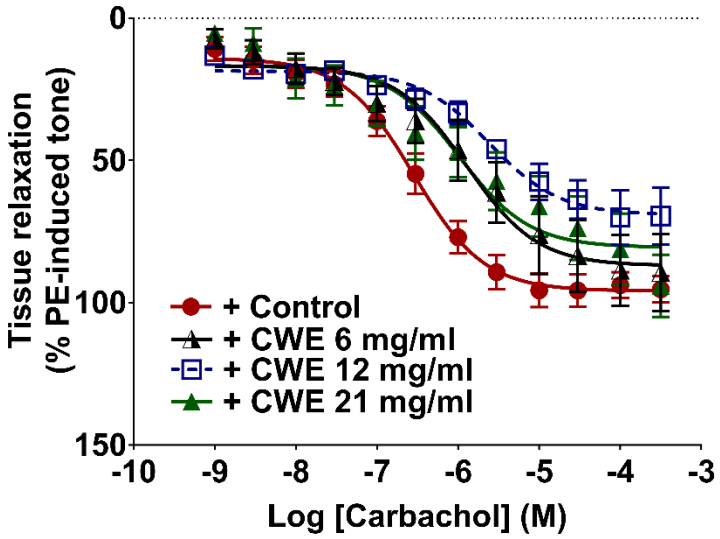

Figure 5.4: Effect of cold water extract against carbachol-induced relaxation in endothelium-intact rat aorta. Aortic rings were pre-incubated with various concentrations of CWE or vehicle control (purified water) for 30 minutes prior to pre-contraction with 100 nM PE, followed by concentration-response curves to carbachol. Tissue response was expressed as a percentage of PE-induced contraction. Data were shown as means ± SEM of 4 to 6 animals. (Abbreviations: CWE = Cold water extract; PE = Phenylephrine)

Table 5.1: The maximum response (E_{max}) **and pEC_{50} values of carbachol derived from the respective concentration-response curve in the presence of cold water extract.** One-way ANOVA with Dunnett correction where comparison of the means of maximum response and pEC_{50} were performed between vehicle control and the treatment groups, and p-values were shown. Data represented the means ± SEM of 4 to 6 animals.

Treatments	E_{max} (%)	p-value	pEC_{50}	p-value
+ Vehicle (purified water)	96.01 ± 6.26	-	6.55 ± 0.08	-
+ CWE 6 mg/ml	86.71 ± 13.26	0.851	6.10 ± 0.32	0.361
+ CWE 12 mg/ml	69.34 ± 9.61	0.221	5.72 ± 0.21	0.059
+ CWE 21 mg/ml	81.01 ± 9.82	0.567	5.94 ± 0.20	0.136

Abbreviations: CWE = Cold water extract

5.3.4 CWE relaxed porcine coronary artery pre-contracted with U46619

In porcine coronary arterial tissues, CWE produced significantly higher relaxation from 1 mg/ml onwards with maximum response of 121.70 ± 6.67% compared to vehicle control, 34.78 ± 7.10% ($p < 0.0001$) (Fig. 5.5). Interestingly, following the maximum relaxation response at 12.88 mg/ml, a subsequent rebound contraction of 16.90%, albeit not significant, was seen at 19 mg/ml. Two-way ANOVA results showed an interaction between treatments and concentrations ($p < 0.0001$), indicating that these factors are interdependent.

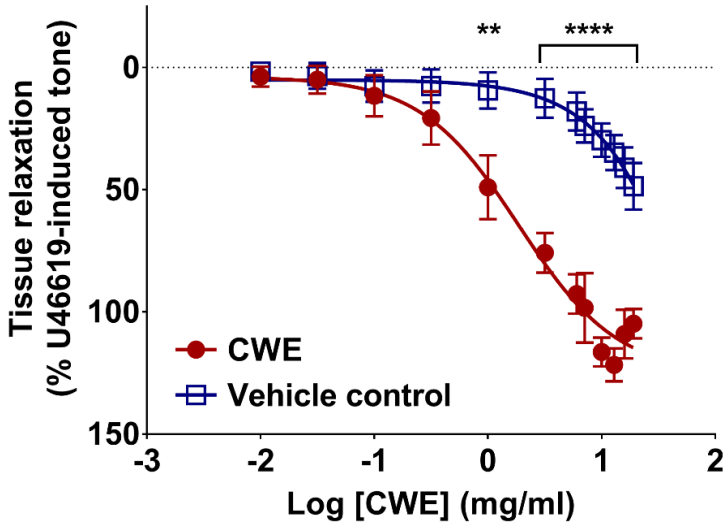

Figure 5.5: Effect of cold water extract on U46619-pre-contracted porcine coronary artery. Concentration-response curves to cold water extract (CWE) in arterial rings pre-contracted with U46619 (100 to 300 nM). Tissue response was expressed as a percentage of U46619-induced contraction. Data were shown as means ± SEM of 5 animals. Two-way ANOVA with Bonferroni correction was done to compare mean differences between CWE and vehicle control: $^{**}p < 0.01$, $^{****}p < 0.0001$.

5.3.5 U46619-induced contraction in coronary artery was inhibited by calcium channel blockers

Nifedipine and SKF96365 had attenuated the contractile responses to U46619 in coronary arterial tissues (E_{max} of nifedipine: 39.37 ± 1.84%, p = 0.0021; SKF96365: 52.33 ± 9.44%, p = 0.0075) compared to vehicle control (E_{max}: 97.38 ± 7.26%) (Fig. 5.6). The potency of U46619 CRC was also shifted to the right by nifedipine (pEC_{50}: 7.11 ± 0.11; p = 0.0013) and by SKF96365 (pEC_{50}: 7.38 ± 0.09; p = 0.024), which were ~5.5-fold and ~3-fold lower than vehicle control (pEC_{50}: 7.85 ± 0.004), respectively. This suggests that the contractile response to U46619 in porcine coronary artery is mediated by external Ca^{2+} influx.

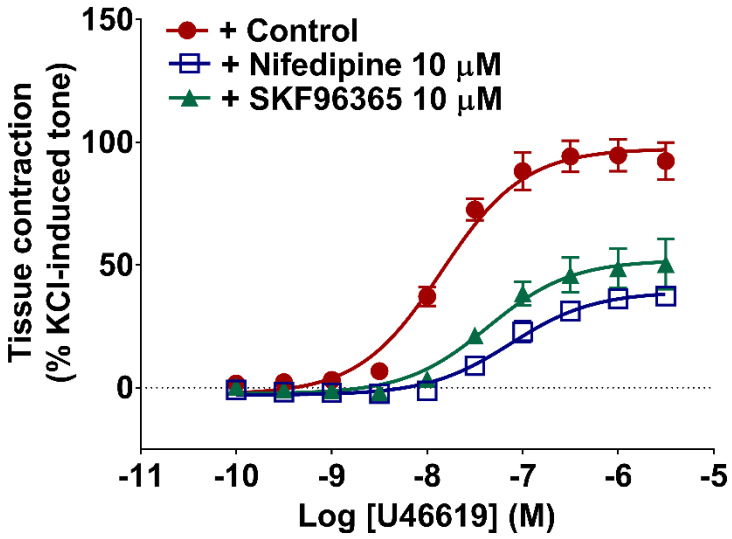

Figure 5.6: Effect of calcium channel blockers against U46619-induced contractions in porcine coronary artery. Tissues were pre-incubated with nifedipine, SKF96365, or vehicle control (DMSO 0.1%) for 30 minutes prior to concentration-response curves to U46619 in arterial rings. Tissue response was expressed as a percentage of reference KCl-induced contraction. Data were shown as means ± SEM of 3 animals.

5.3.6 Vasorelaxation effect of CWE is linked to the regulation of calcium entry

In calcium-free Krebs solution, pre-incubation with CWE significantly inhibited the contractile response to $CaCl_2$ (E_{max} of CWE 3 mg/ml: 63.28 ± 8.76%, $p = 0.001$; CWE 6 mg/ml: 28.48 ± 9.38%, $p < 0.0001$; CWE 7 mg/ml: 33.73 ± 4.73%, $p < 0.0001$) compared to vehicle control (E_{max}: 110.20 ± 5.25%) (Fig. 5.7). This suggests that CWE blocks extracellular Ca^{2+} influx through membrane calcium channels.

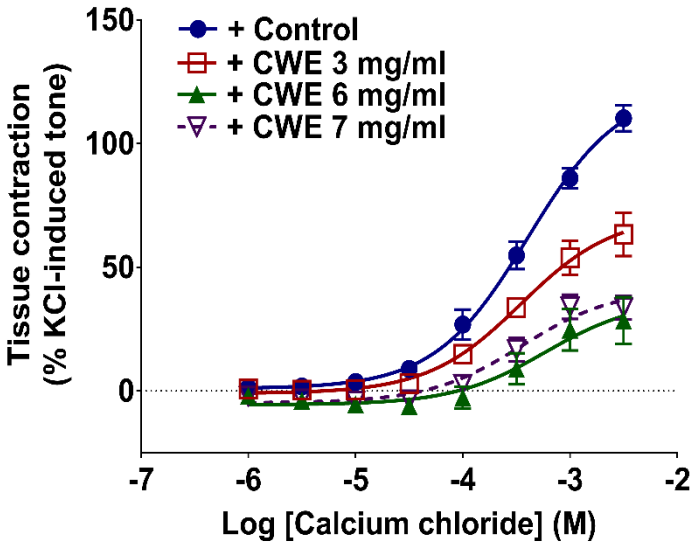

Figure 5.7: Effect of cold water extract against calcium chloride-induced contractions in porcine coronary artery. Arterial rings were pre-incubated with various concentrations of cold water extract (CWE) or vehicle control (purified water) for 30 minutes in calcium-free Krebs solution Then, 60 mM KCl was added to depolarize the tissue prior to addition of increasing concentrations of calcium chloride to induce contraction. Tissue response was expressed as a percentage of reference KCl-induced contraction. Data were shown as means ± SEM of 5 animals.

5.3.7 CWE relaxed coronary artery at basal tone

Treatment with CWE did not have significant effect on the basal tension in rat aortic rings (p = 0.6381) (Fig. 5.8A), but had significantly relaxed porcine coronary arterial rings at basal tension (at 7.08 mg/ml, p = 0.0097; from 10.00 mg/ml to 19.05 mg/ml, p < 0.0001) with E_{max} of 34.78 ± 4.01% compared to vehicle control, E_{max}: -6.14 ± 5.13% (Fig. 5.8B).

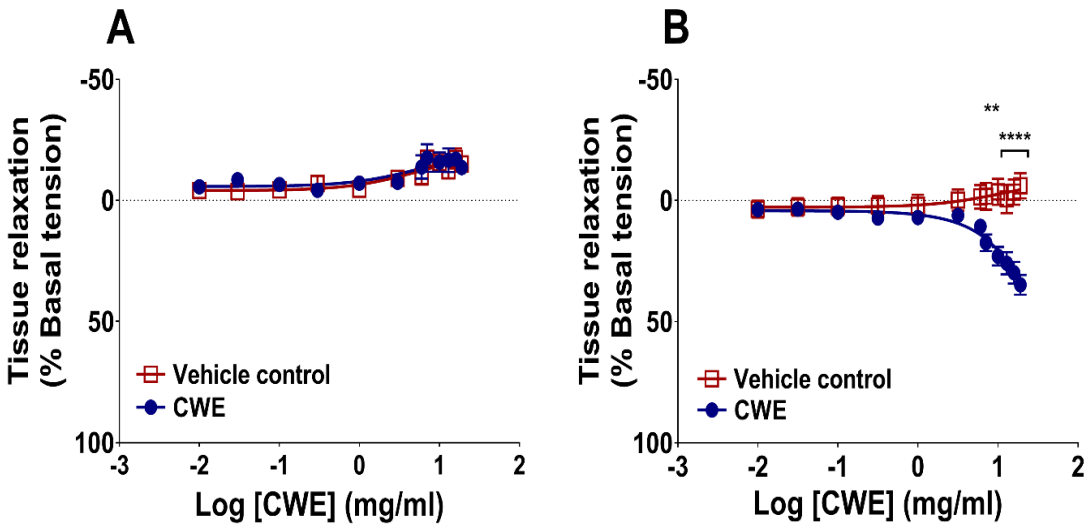

Figure 5.8: Effect of cold water extract on basal tension in blood vessels. Concentration-response curves to cold water extract in (A) rat aortic rings and (B) porcine coronary arterial rings at basal tone. Tissue response was expressed as a percentage of basal tension. Data were shown as means ± SEM of 4 to 5 animals. Two-way ANOVA with Bonferroni correction was done to compare the mean differences between CWE and vehicle control: **p < 0.01, ****p < 0.0001.

5.3.8 CWE diminished neurogenic response but augmented basal response in electrically stimulated ileal tissues

In EFS-stimulated ileal tissues, Fig. 5.9A demonstrates that CWE at 0.3 and 1.0 mg/ml significantly reduced the neurogenic contraction (E_{max} of CWE: 17.96 ± 8.89%, vehicle: 100.18 ± 1.42%; $p < 0.0001$). In contrast, basal tension of the ileal tissue was transiently augmented by CWE 1.0 mg/ml (E_{max} of CWE: 8.79 ± 1.15 mN, vehicle: -0.42 ± 0.17 mN; $p < 0.0001$) (Fig. 5.9B). The neurogenic and basal contractions for vehicle control remained constant throughout the experiment.

The representative traces illustrated in Fig. 5.9C show that from CWE 0.1 mg/ml onwards, there was an immediate reduction in the neurogenic contraction upon the addition of CWE, followed by a gradual recovery of neurogenic contraction, although not to the full extent. At CWE 1 mg/ml, in 4 out of 8 preparations the neurogenic contraction was masked by noises and not identifiable, and therefore we considered that the responses for these tissues were fully abolished (i.e. 0%). In the remaining preparations, there was minimal neurogenic contraction observed. On the other hand, the basal tension of ileal tissue was transiently and rapidly elevated following the application of CWE 1.0 mg/ml, followed by gradual decline that did not recover towards the end of experiment. Two-way ANOVA results showed an interaction between treatments and concentrations for both neurogenic and basal contraction ($p < 0.0001$), indicating that these factors are interdependent.

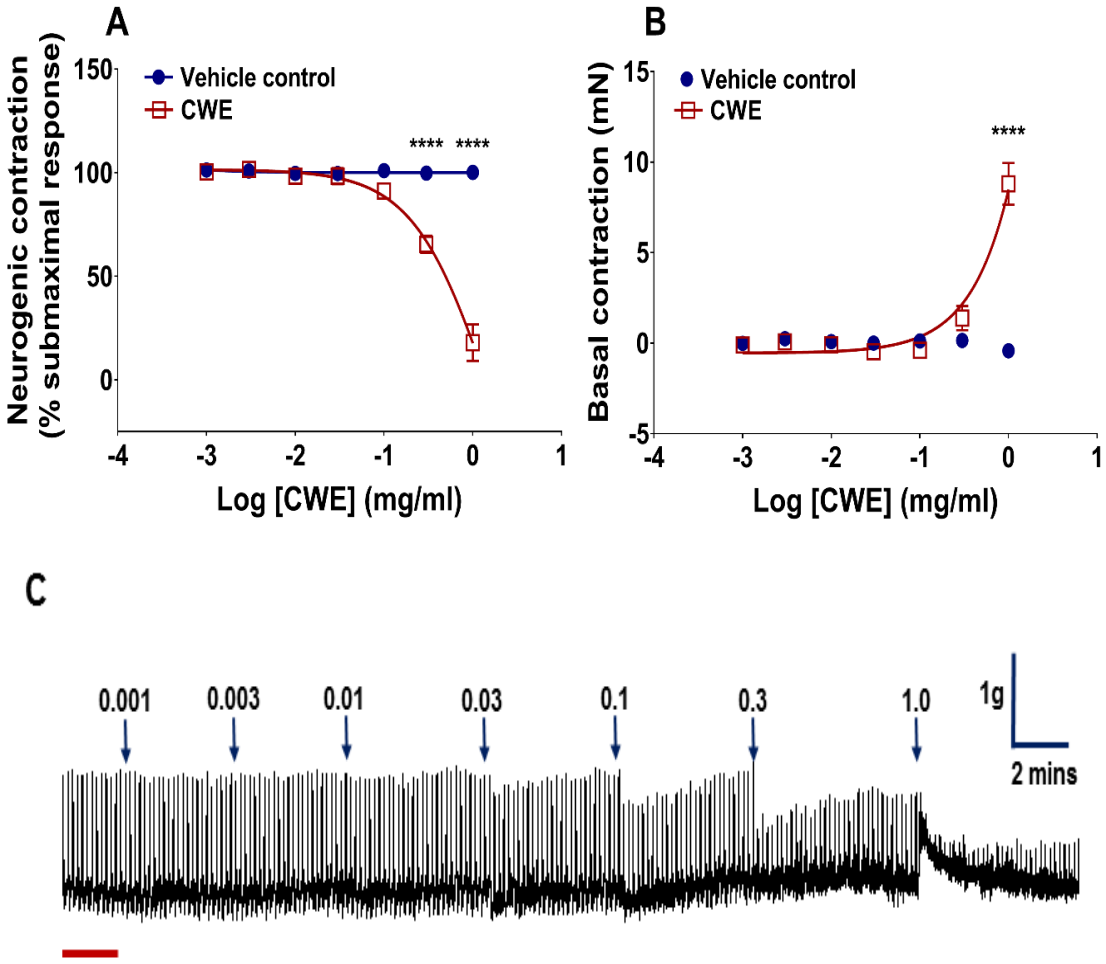

Figure 5.9: Effect of cold water extract on electrically stimulated guinea pig ileum. Concentration-response curves to cold water extract (CWE) or vehicle control were constructed in ileal tissues. (A) Neurogenic contraction in response to treatment was expressed as the percentage of neurogenic contraction at reference contracture. (B) Basal contraction relative to basal tension at reference contracture was expressed as muscle tension in milliNewton (mN). The nonlinear curve was unable to be constructed for vehicle control in (B) due to non-converged points. (C) Representative trace of concentration-response curve to CWE in ileal tissue. The neurogenic response was diminished but basal tension was transiently augmented with increasing concentrations of CWE. The red bar represents the reference contracture whilst arrows represent cumulative concentrations of CWE applied to the tissue (in mg/ml). Data were shown as means ± SEM of 8 preparations. Two-way ANOVA with Bonferroni correction where comparison of means was made between CWE and vehicle control: ****$p < 0.0001$.

5.3.9 Treatment with atropine augmented the basal contraction to CWE in ileal tissues

Fig. 5.10A demonstrates that the pre-treatment with atropine did not significantly affect the neurogenic contraction reduced by CWE (E_{max} of atropine: 53.85 ± 8.44%, control: 22.83 ± 13.99%; p = 0.1655). On the other hand, we observed that the presence of atropine has augmented the basal contraction evoked by CWE with maximum response of 19.60 ± 1.62 mN compared to control, 7.93 ± 1.97 mN (p = 0.0067) (Fig. 5.10B). These results suggest that CWE may exert inhibitory effect by binding to muscarinic receptors.

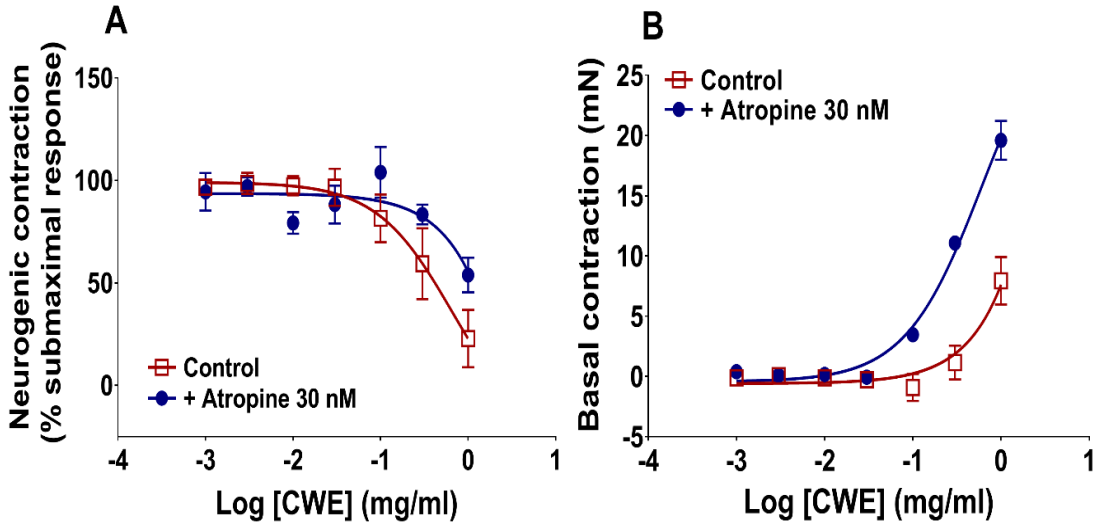

Figure 5.10: The involvement of muscarinic receptors in the effects of cold water extract on guinea pig ileum. Ileal tissues were exposed to atropine for 30 minutes, prior to construction of concentration-response curves to CWE under electrical field stimulation. (A) Neurogenic response was expressed as a percentage of neurogenic contraction relative to reference contracture. (B) Basal response relative to reference contracture was expressed as muscle tension in milliNewton (mN). Data were shown as means ± SEM of 4 to 5 preparations.

5.3.10 Inhibitory effect of CWE on neurogenic contraction in ileal tissues was slightly recovered by nifedipine

Fig. 5.11 shows that in control tissues, maximum response of neurogenic contraction and basal contraction were 17.96 ± 8.89% and 8.80 ± 1.15 mN, respectively. Pre-treatment of ileal tissues with rauwolscine, naloxone and propranolol did not significantly affect the neurogenic responses of electrically stimulated ileal tissues (E_{max} of rauwolscine: 25.66 ± 5.11%, $p = 0.8664$; naloxone: 31.80 ± 9.07%, $p = 0.4988$; propranolol: 17.51 ± 6.33%, $p = 0.9999$) (Fig. 5.11A). Similarly, the basal contraction was unaffected by rauwolscine and naloxone (E_{max} of rauwolscine: 4.49 ± 1.54 mN, $p = 0.063$; naloxone: 7.33 ± 1.21 mN, $p = 0.702$; propranolol: 10.95 ± 0.78 mN, $p = 0.485$) (Fig. 5.11B). Hence, these observations suggest that both α_2-adrenoceptors and opioid receptors are not likely to participate in CWE-mediated effects in ileal tissues.

Interestingly, Fig. 5.11C demonstrates that CWE-evoked decrease in neurogenic contraction was slightly recovered in ileal tissues exposed to nifedipine compared to control (E_{max} of nifedipine: 52.56 ± 4.67%; $p = 0.027$). In contrast, the basal contraction elicited by CWE was not significantly affected by nifedipine (E_{max} of nifedipine: 4.99 ± 2.63 mN; $p = 0.149$) (Fig. 5.11D). These results indicated that the basal tension elevated by CWE is probably not mediated via Ca^{2+} influx through L-type calcium channels.

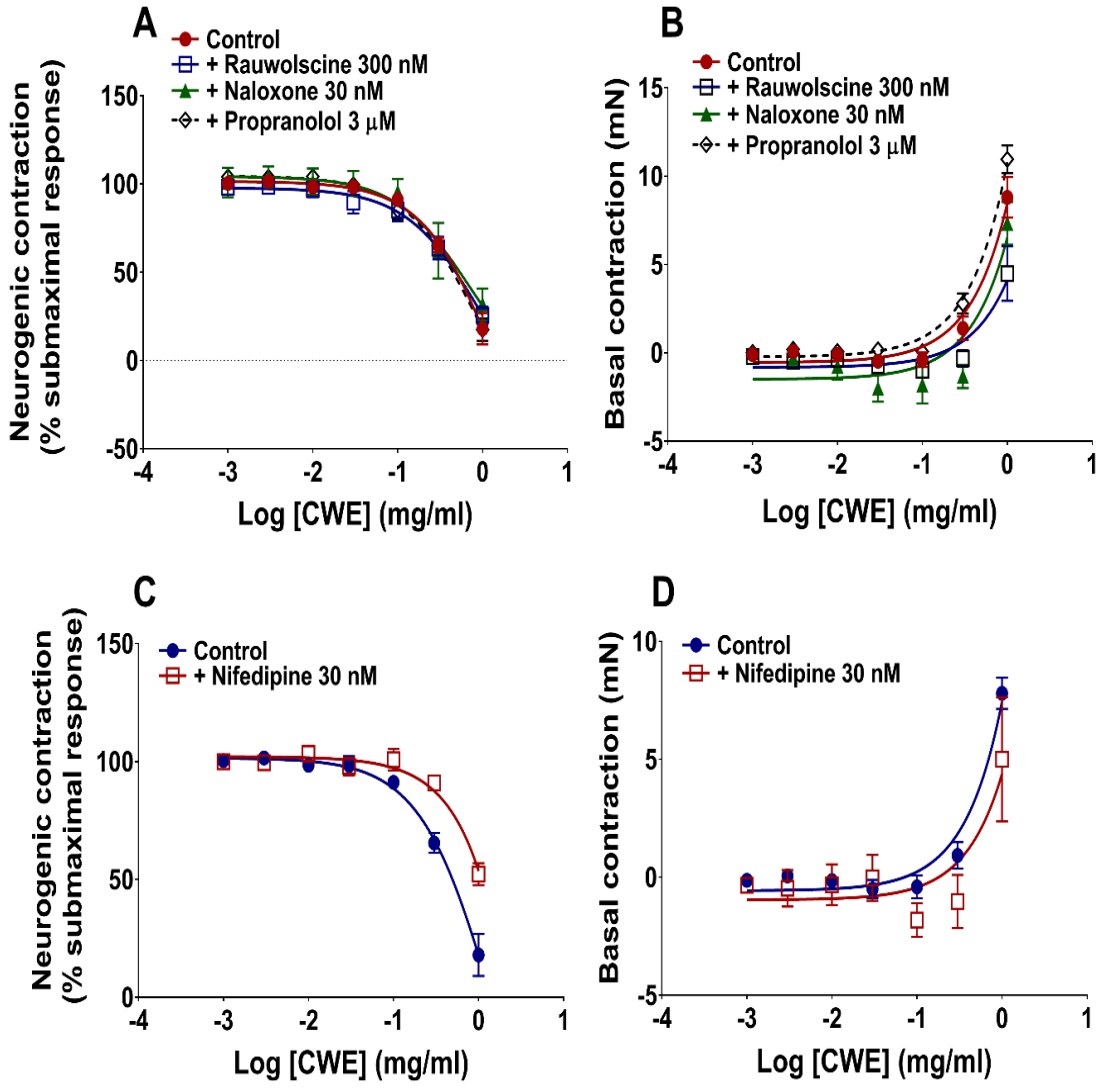

Figure 5.11: The involvement of α_2- and β-adrenoceptors, opioid receptors and calcium channels in the effects of cold water extract on guinea pig ileum. Ileal tissues were exposed to (A),(B) rauwolscine, naloxone, propranolol, or (C),(D) nifedipine for 30 minutes, prior to construction of concentration-response curves to CWE under electrical field stimulation. (A),(C) Neurogenic response was expressed as the percentage of neurogenic contraction relative to reference contracture. (B),(D) Basal response was expressed as muscle tension in milliNewton (mN) relative to the reference contracture. Data were shown as means ± SEM of 4 to 8 preparations.

5.4 Discussions

In the present chapter, CWE demonstrated *in vitro* vasorelaxation activities, in support of our hypothesis. Vascular relaxation was shown in both rodent and non-rodent mammals, indicating that it is not species-specific. Regardless of the animal species, CWE relaxed pre-contracted smooth muscles of different vascular tissues, which were the aorta and coronary artery in this study.

In this study, CWE reduced contractile responses to both phenylephrine and U46619 in aorta and coronary artery, respectively, indicating that the mechanisms mediated by these two contractile agonists are blocked by CWE. Phenylephrine and U46619 are known to activate $G_{\alpha q}$ protein-mediated DAG/IP_3 pathways along with PKC and SOCC/ROCC activation. Entry of extracellular Ca^{2+} is essential for the contractions to both agonists in vascular smooth muscle cells (Ding & Muray, 2005). In previous study, phenylephrine-induced intracellular Ca^{2+} oscillations were sensitive to nifedipine and SKF96365, suggesting that TRPC and L-type calcium channels are implicated (C. H. Lee et al., 2001). This was confirmed in our earlier study in which phenylephrine-induced contraction in rat isolated aorta was sensitive to SKF96365 and nifedipine, supporting that extracellular Ca^{2+} influx through TRPC and L-type calcium channels are involved (Govindaraju et al., 2018). We also revealed that although the presence of external Ca^{2+} was essential for phenylephrine-induced contraction, removal of external Ca^{2+} did not completely abolish the contraction, and the emptying of intracellular Ca^{2+} store by thapsigargin also significantly decreased the contractile response, indicating that intracellular Ca^{2+} may also play a role (Govindaraju et al., 2018).

U46619-induced contraction was shown to be decreased by nifedipine in different vascular tissues, for instance in bovine coronary artery (Ding & Muray, 2005) and canine pulmonary veins (Drummond & Cocks, 1996). Conversely, in rat pulmonary artery rings, U46619-induced contraction was blocked by SKF96365 (McKenzie, MacDonald, & Shaw, 2009), but was insensitive to nifedipine; however, the concentration of nifedipine used was 1 μM, which was lower than other studies. OAG-stimulated Ca^{2+} entry is sensitive to SKF96365 (He et al., 2017). As U46619 can activate DAG, it is therefore reasonable to speculate that U46619 also activates TRPC channels. Based on these reports, we therefore hypothesized that U46619-induced contraction in porcine coronary artery may be partly mediated by Ca^{2+} entry through TRPC and L-type calcium channels. To confirm this, our results revealed that pre-incubation with nifedipine and SKF96365 had reduced U46619-induced contraction, which is in agreement with previous studies. Thus, this suggests that TRPC and L-type calcium channels participate in contractions induced by U46619 as per phenylephrine.

Since phenylephrine and U46619-induced contractions are linked to opening of membrane calcium channels, we went on to test if CWE could affect extracellular Ca^{2+} entry into cells. In this study, 7 mg/ml of CWE was shown to completely abolished $CaCl_2$-induced contraction in coronary artery, indicating that one possible mechanism of CWE is by blocking permeation of extracellular Ca^{2+} through membrane calcium channels. This corroborates the relaxation effects of CWE on phenylephrine- and U46619-evoked contractions above, implying that CWE may inhibit TRPC and L-type calcium channels.

We previously deduced that CWE may act as a partial agonist on muscarinic receptors (**Chapter 3 and 4**). However, this proposition is discounted by the results

herein that CWE did not affect carbachol-induced relaxation in aortic rings. Subsequently, our findings showed that CWE-induced vasorelaxation was not affected by endothelium removal. This was further validated by the evidence that CWE-induced vasorelaxation was unaffected in the presence of L-NAME, a NO synthase inhibitor. Taken together, these findings ruled out the implication of EDRFs by CWE.

Besides, CWE significantly relaxed coronary artery at resting tension but was devoid of effect in aorta. This implies that the coronary artery, but not aorta, has a spontaneous contraction at resting tension contributing to the basal tone. Although both aorta and coronary artery belong to the large elastic vessels, they do possess differences in respect of their structure, such that the coronary artery has a greater endothelium-smooth muscle ratio than aorta (T. M. Griffith et al., 1984). The regulation of basal tone in blood vessels has been reported in several studies (Ginsburg, Bristow, Harrison, & Stinson, 1980; Merkus et al., 2003; Rubanyi & Paul, 1985). Rubanyi and Paul (1985) reported that porcine coronary artery possesses spontaneous tone and proposed that the maintenance of basal tone in artery is ascribed to continuous release of vasoconstrictor cyclooxygenase products (Rubanyi & Paul, 1985). By contrast, isolated aorta from normotensive Sprague Dawley rats did not display any active basal tone (Dellipizzi, Pucci, Mosny, Deseyn, & Nasjletti, 1997; Pucci, Tong, Miller, Guan, & Nasjletti, 1995). Intriguingly, the lack of contractile effect of CWE on blood vessels at basal tone does not converge with earlier observations in airways where CWE has induced concentration-dependent contraction at basal tone.

The antihypertensive and vasorelaxation effects of medicinal mushrooms have been attributed to their proteins and polysaccharide fraction (Chiou, Chang, Chou, & Chen, 2000; Yahaya, Rahman, & Abdullah, 2014), and lectins (Singh et al., 2015). The bioactive compound accountable for the vasorelaxant effect is unknown yet, but

there is good reason to speculate that the proteins, polysaccharide-protein complex or lectins present in *L. rhinocerotis* possibly contribute to the vasorelaxant response. We also cannot exclude the possibility that the vasorelaxation effect of CWE may be due to synergistic effect from several active constituents in the crude extract. The active components underlying the vasorelaxation effect of CWE remain to be elucidated.

Other than the regulation of extracellular Ca^{2+} influx, several pathways are potentially mediated by CWE in relaxing vascular smooth muscles. Potential mechanisms include inhibition of RhoA/Rho kinase cascade, activation of β-adrenoceptors or the opening of K^+ channels to cause vasorelaxation. Despite that the effect of TP receptors activated by U46619 is more known to be related to $G_{\alpha q}$ protein, TP receptors are also coupled to another G protein i.e. $G_{12/13}$. Stimulation of $G_{12/13}$ protein mainly leads to activation of RhoA/ROCK-mediated pathway and smooth muscle contraction. Activation of $G_{12/13}$ pathway by U46619 is evidenced by the impaired contractile responses to TP receptor agonist in $G_{12/13}$-knockout mice (Wirth et al., 2008). Activation of α_1-adrenoceptors by phenylephrine is, however, exclusively associated with $G_{\alpha q}$ protein. Besides, Ding and Muray (2005) demonstrated that several proteins including PKC, tyrosine kinases and rho-kinase were involved in U46619-mediated contraction. Hence, we cannot completely rule out the effect of CWE on the RhoA/ROCK pathway. Nevertheless, evidence from our previous experiments (**Chapter 3**) precluded the involvement of TEA-sensitive potassium channels and β-adrenoceptors in CWE-induced bronchorelaxation. The current experiments do not allow for further interpretation but we postulate that these sites are similarly not affected by CWE in blood vessels.

As for ileal smooth muscle, our preliminary experiments showed that electrically evoked contraction was abolished by atropine, indicating that the

neurogenic contraction is likely to be due to enhanced acetylcholine release from cholinergic nerve terminals that activates muscarinic receptors on smooth muscle (data not shown). Nonetheless, evidence shows that electrical field stimulation can also stimulate noradrenergic nerves, induce release of prostaglandin-like substances and encephalin, or directly stimulate of smooth muscle, if parameter of high frequencies (≥ 2 Hz), long pulse duration (≥ 1 ms), or high voltage (≥ 60 V) is used (Baumgarten et al., 1982). Relatively low parameters (0.1 Hz, 5 to 10 V, 0.5 ms) are used in the present study, hence supporting the sole contribution of cholinergic nerve to the elicited neurogenic contractions.

In the present study, our hypothesis that CWE could relax ileal smooth muscle was confirmed. CWE concentration-dependently abolished the neurogenic contraction, which was not affected by atropine pre-treatment, thus suggesting that muscarinic receptor is not implicated. Notably, CWE reduced neurogenic contraction at a lower concentration, from 0.3 mg/ml onwards, compared to the augmented basal contraction, only at 1.0 mg/ml. This finding complemented the results on airways where CWE has induced concentration-dependent contraction. At high concentration of CWE, it is possible that the acetylcholine release from nerve terminals is reduced (causing diminished neurogenic contraction) while smooth muscle muscarinic receptors are activated (causing increased basal contraction) in parallel.

However, this conjecture was contrasted by the observation where CWE-induced basal contraction was augmented by atropine, suggesting that the basal contraction is not mediated by activation of smooth muscle muscarinic receptors. This led us to speculate that CWE might be compensating the contracting effect through muscarinic autoinhibition, and therefore explaining the augmented basal contractile response to atropine. To support this notion, Takeuchi et al. (2005) reported that in

mouse ileum, atropine increased electrical field stimulation-induced acetylcholine release due to blockade of muscarinic autoinhibition. We postulate that CWE might be acting on the muscarinic autoreceptors to inhibit basal contraction. As CWE comprises a mixture of components, it is possible that one of the components in CWE is counteracting the contraction through stimulating effect on inhibitory muscarinic autoreceptors, which are blocked by atropine, and thus causing the contracting component in CWE to override.

Subsequently, the reduced neurogenic contraction by CWE was slightly recovered by nifedipine, whilst basal contraction was unaffected, suggesting that the reduction in neurogenic contraction is mediated by increased Ca^{2+} influx through L-type calcium channels. The involvement of L-type calcium channels in electrically stimulated contractions of gastrointestinal smooth muscle have been shown in the literature. EFS of rat jejunum strips induced significantly lower contraction in L-type calcium channel-knockout mice, suggesting that Ca^{2+} influx through L-type calcium channels play a role (Wegener et al., 2006). This is supported by other studies in which EFS-induced contractile responses are sensitive to nifedipine in rat ileum (Sadraei, Asghari, & Poorkhosravi, 2011) and to verapamil in guinea pig ileum (Yokoyama & Yagasaki, 1990). Based on the assumption that opening of L-type calcium channels contributes to electrically evoked contraction, we speculate that CWE might act as an inverse agonist on L-type calcium channels and hence explaining the reversal of CWE-inhibited neurogenic contraction by nifedipine. Another explanation is that CWE may elevate $[Ca^{2+}]_i$ in specific cell type. It is proposed that NO released from nitrergic nerves triggers increase in $[Ca^{2+}]_i$ in ICC through L-type calcium channels, which in turn activate NO synthesis to cause relaxation of canine colon (Bennett, 1997).

However, given that NO pathway was not affected by CWE in airway and vascular smooth muscle, this hypothesis is less likely to be true.

Other mechanisms such as activation of NANC components or inhibitory sympathetic nerves that could directly relax the ileal smooth muscle were investigated. The outcome showed that rauwolscine did not influence the effects of CWE against these contractions, suggesting that presynaptic α_2-adrenoceptors are not implicated. Likewise, the presence of naloxone and propranolol did not affect the effects of CWE in ileal tissues, indicating that opioid receptors and β-adrenoceptors are unlikely to be involved.

L. rhinocerotis sclerotial powder contains adenosine and its derivatives (Section 2.3.3, **Chapter 2**). In gastrointestinal tissues, interpretation of adenosine-induced response is difficult due to concurrent activation of different adenosine receptors. At basal tone in rat ileum, exogenous adenosine induced contraction that was partially dependent on pre-junctional activation of adenosine receptors (Zoppellaro et al., 2013). By contrast, exogenous adenosine inhibited neurogenic contraction to electrical stimulation in guinea pig ileum through pre- and post-junctional adenosine receptor activation (Bornstein, 2008). Whether CWE modulates ileal smooth muscle contraction and relaxation via adenosine receptor remains undetermined with the current protocol, but we speculate that adenosine may partially contribute to its inhibitory effect on neurogenic contraction.

With the evidence gathered from the present study with ileal tissues, no conclusion can be drawn whether the components mediating the basal contraction evoked by CWE is due to activation of muscle fibre or nerves. To summarize the findings in guinea pig ileum, CWE evoked basal contraction, which is likely to be counteracted by activation of muscarinic autoinhibition, and attenuated electrically

stimulated neurogenic contraction, which is possibly mediated by inducing Ca^{2+} influx through L-type calcium channels. Opioid receptors, α_2-adrenoceptors, and β-adrenoceptors are unlikely to be involved.

Chapter 6. Fractionation of *Lignosus rhinocerotis* extract and the pharmacological effects on airways

6.1 Introduction

Observations in **Chapter 2 to Chapter 4** had underpinned the bronchodilator properties of *L. rhinocerotis*. To our knowledge, the airway relaxation effect of this mushroom is not reported elsewhere in the literature, and therefore the bioactive components responsible for this property remain poorly studied.

Polysaccharides, proteins, or polysaccharide-protein complex found in the high-molecular-weight fraction have been consistently proposed to be responsible for the bioactivities observed in a number of studies with *L. rhinocerotis* (Hu, Huang, Wong, & Yang, 2017; Lai et al., 2008; M. L. Lee et al., 2012; Sook Shien Lee et al., 2014; Liu et al., 2016). The first to make the proposition was Lai et al. (2008), who was also the first to report the antiproliferative effect of *L. rhinocerotis* against leukaemia cancer cell lines. In the same study, the hot water extract of *P. rhinocerus* sclerotia exhibited anti-apoptotic effect in human acute promyelocytic leukaemia cells (HL-60), whereas the cold alkaline extract was devoid of such inhibition. Given that the hot water extract and cold alkaline extract are characterized to be polysaccharide-protein complex and glucans respectively, the researchers proposed that polysaccharide-protein complex or proteins are responsible for the antiproliferative effects (Lai et al., 2008).

Besides, the high-molecular-weight fraction of *L. rhinocerotis* TM02 cultivar, which is rich in polysaccharide and proteins, exhibited antiproliferative activity in human breast and lung cancer cell lines (M. L. Lee et al., 2012). Additionally,

immunostimulating activity was displayed in a study showing that polysaccharide fractions of *L. rhinocerotis* sclerotia may confer protective effect over mice model of cyclophosphamide-induced immunosuppression by stimulating the proliferation of lymphocyte and release of serum TNF-α and INF-γ (Hu, Huang, Wong, & Yang, 2017). However, it is unknown whether the mushroom sample in the same study was cultivar or wild type. On the contrary, high-molecular-weight fraction containing the highest amount of polysaccharide and proteins has displayed anti-inflammatory effects by strongly inhibiting lipopolysaccharide-induced TNF-α production in RAW264.7 cells and carrageenan-induced paw oedema in Sprague Dawley rat model (Sook Shien Lee et al., 2014). Subsequently, the protein components derived from the high-molecular-weight fraction largely inhibited the TNF-α production, whilst non-protein components were inactive, strongly suggesting that the proteins are accountable for the anti-inflammatory effect (Sook Shien Lee et al., 2014). Taken together, these evidence indicates that the high-molecular-weight fraction containing polysaccharides, polysaccharide-protein complex, and proteins from the sclerotial part of *L. rhinocerotis* is medicinally important with immunomodulatory and anti-proliferative activities.

Components or purified compounds from medicinal mushrooms and plants have been reported to possess bronchodilator or antitussive effects. In mice model, airway hyperresponsiveness as characterized by increased lung resistance was induced by ovalbumin sensitization and challenge. Mice treated with polysaccharide fraction of *Ganoderma formosanum* intraperitoneally has largely attenuated methacholine-induced increased lung resistance (Pi et al., 2014). Oral application of a polysaccharide fraction with highly branched arabinogalactan protein derived from a medicinal plant, *Terminalia chebula*, displayed antitussive properties in TRIK strain guinea pigs

(Nosalova et al., 2013). Furthermore, a polysaccharide fraction isolated from *Ganoderma formosanum* attenuated methacholine-induced increased lung resistance in airway inflammation model of mice (Pi et al., 2014). Triterpenes from *Ganoderma tsugae,* FIP-fve from *Flammulina velutipes*, and cordycepin from *Cordyceps militaris* also elicited bronchodilator effects by significantly reducing the methacholine-induced airway hyperresponsiveness as characterized by reduced airflow limitation and pulmonary resistance, in ovalbumin-challenged mice model (M. L. Chen & Lin, 2007; Chu et al., 2017; Yang et al., 2015). The improvement in lung function of these mice was comparable to dexamethasone-treated control group (Yang et al., 2015). Two putative fungal immunomodulatory proteins, later named as FIP-Lrh, were revealed by genome sequencing (H. Y. Yap et al., 2014). Subsequent study by Pushparajah et al. (2016) isolated and characterized the cDNA of FIP-Lrh, indicating that FIP-Lrh shares similar predicted 3D-structure to FIP-fve, a fungal immunomodulatory protein isolated from *Flammulina velutipes.* Nevertheless, whether the fungal immunomodulatory protein present in *L. rhinocerotis* is responsible for the bronchodilator effect is yet to be elucidated.

The presence of various compounds in *L. rhinocerotis* represents the many possibilities contributing to the bronchodilator effect of *L. rhinocerotis*. Isolating and screening each of these compounds would be a laborious process. There is therefore a need to narrow down the list of candidate compounds responsible for the airway relaxation effect. This is achievable through fractionation of the CWE of *L. rhinocerotis* into different molecular weights and examination of their effects on isolated airways. There were several reasons that led us to investigate the fractions in this study. Firstly, given the array of bioactivities of polysaccharides, proteins, and polysaccharide-protein complex in medicinal mushrooms, it is therefore reasonable to

speculate that the components accountable for bronchodilator effect of CWE are also large-molecular-weight substances. Secondly by using fractionation technique, crude extracts can be separated based on the desired features, where in our case grouping by molecular weights is of interest, before subjecting them to qualitative and quantitative analyses and bioassays. With this technique, we could identify the most efficient fraction as well as eliminating the non-active fraction, and therefore providing a guide to future work in isolation of active compounds. A brief overview of the fractionation method was given in the following subsection.

6.1.1 Fractionation of natural products

Crude extracts from natural products can be subjected to fractionation method where extracts are separated into groups of compounds based on differences in their physicochemical properties. Fractionation technique is particularly useful to reduce the complexity of the extracts to assist in identification of the bioactive compounds (Simon, Lamoree, Hamers, & de Boer, 2015). The grouping can be based on solubility, size, shape, electrical charge or polarity (Houghton & Raman, 2012). A recent review revealed that the term "bioassay-directed fractionation" is the most commonly used nomenclature designated to the concept where extracts are subjected to fractionation and biological analysis, which led to cycles of further fractionation and biological analysis, iteratively (Weller, 2012). Once the candidate compounds are identified, subsequent chemical analysis including purification and structure elucidation of the chemical compounds are conducted (Simon et al., 2015).

Fractionation can be performed in many methods including chromatography, precipitation, solvent-solvent extraction, distillation, electrophoresis, and so on (Houghton & Raman, 2012). Among all, chromatography in various types are the most commonly used technique for fractionation. Recent advances in fractionation methods include multi-step solid phase extraction (Thiericke, Schmid, Moore, & Ebert, 2000), multi-channel counter-current chromatography (S. Wu, Yang, Gao, Liu, & Liu, 2008), high-speed counter-current chromatography, and preparative chromatography (X. Wang et al., 2011).

The choice of fractionation method can be influenced by several factors: (i) the nature of substances e.g. solubility, polarity, susceptibility to degradation (to pH, water, light and oxygen), (ii) the availability of equipment and cost, (iii) the procedure following the fractionation, and (iv) the safety (Houghton & Raman, 2012). Firstly, the extraction procedure prior to fractionation would affect the nature of constituents present in the extracts. For instance, if water is used as the solvent of extraction, the extract will contain mainly polar constituents and some compounds may have electrical charge (Houghton & Raman, 2012). In this case, precipitation method by cooling will be less than useful. Secondly, some fractionation instruments range from simple and inexpensive to sophisticated and expensive, and the choice of method therefore depend on the budget and availability of equipment (Conner et al., 2014). Thirdly, the purpose of the fraction will determine the fractionation method. For example, fraction to be subjected to biological test needs to be compatible with the test system in terms of their toxicity and solvent (Weller, 2012). Organic solvents are frequently undesirable due to toxicity in biological system and aqueous solvent is preferred in this aspect. By contrast, these would be of less concern if the fraction is subjected to chemical procedures such as further fractionation or isolation of active

constituents (Houghton & Raman, 2012). Lastly, usage of techniques and materials that will pose risk to the personnel should be minimized (Houghton & Raman, 2012).

6.1.2 Significance of study

The experiments conducted in the present chapter aimed to investigate the bronchodilator effect of the fractions of CWE. Gel permeation chromatography, which separates molecules based on their size, was of interest in the present chapter where the CWE of *L. rhinocerotis* could be separated into different molecular weights for organ bath experiments. We hypothesized that airway relaxation effect of CWE differs in these fractions. The chemical compositions in each fraction were characterized by their amounts of proteins and carbohydrate, and monosaccharide profile to reveal the important sugar residues. The specific objectives of this chapter were as follows:

(i) To fractionate the CWE into high-molecular-weight (HMW), medium-molecular-weight (MMW), and low-molecular-weight (LMW) fractions through gel permeation chromatography.

(ii) To characterize these fractions by the compositions of carbohydrate and protein, and monosaccharide profile.

(iii) To construct cumulative CRCs to these fractions on carbachol-pre-contracted isolated airway tissues using organ bath technique.

(iv) To assess the effect of pre-treatment with fractions against carbachol- and 5-HT-induced contractions in isolated airway tissues using organ bath technique.

(v) To assess the effect of pre-treatment with fractions against $CaCl_2$-induced contraction with calcium-free Krebs protocol using organ bath technique.

6.2 Materials and methods

Section 6.2.3 and 6.3.1 were performed and analyzed by Dr. Fung Shin Yee and her student, Alvin Chee Sum Yap, from Department of Molecular Medicine, University of Malaya. Section 6.2.4, 6.2.5 and 6.3.2 were performed and analyzed by Prof. Peter Cheung Chi Keung and his student, Xiaojie Li, from School of Life Sciences, Chinese University of Hong Kong. The fractions of CWE used in organ bath experiments were supplied by Dr. Fung Shin Yee.

6.2.1 Drugs and materials

CWE was prepared as described in Section 2.2.2, **Chapter 2.** With regards to organ bath experiments, normal and calcium-free Krebs solutions were prepared as per **Appendix A**. Calcium-free Krebs solution was used in Section 6.2.8 as specified**,** while other sections were conducted with normal Krebs solution (standard recipe with external Ca^{2+}). Drugs used in this chapter are prepared as per Section 3.2.1 and Section 4.2.1 **(Chapter 3 and 4)**.

6.2.2 Tissue preparation

Ethical approval was obtained from the University of Nottingham's Animal Welfare and Ethics Review Body (UNMC#2kn and UNMC12). All experiments were conducted with male Sprague Dawley rats (235-440 g; 2-3 months old) purchased from University Putra Malaysia or University Kebangsaan Malaysia. Rats were

sacrificed on the day of experiment by carbon dioxide. Steps as per Section 2.2.4.1 (**Chapter 2**) were repeated where tracheal and bronchial rings were isolated, mounted to organ bath set up, equilibrated to bath conditions, and exposed twice to 60 mM KCl to obtained the reference contracture. After the KCl was washed out and a stable basal tone was re-established, experiments were carried out as in following sections.

6.2.3 Preparation, extraction and fractionation of CWE

CWE was fractionated by gel permeation chromatography using a Sephadex G-50 column (212 ml). Aqueous elution was carried out at room temperature by gravity and 100 fractions of 2.5 ml volume each were collected. Aliquots from the tubes were sampled for testing the protein and carbohydrate content by measurement of its absorbance reading at 595 nm and 490 nm, respectively. Molecular weight of the pooled fractions was determined by comparing their ratio of eluent volume (Ve) and void volume (Vo) to the Ve/Vo of selected protein standards including carbonic anhydrase (29 kDa), soybean trypsin inhibitor (20 kDa), ribonuclease A (14 kDa), cardiotoxin (7 kDa), cobalamin (1.35 kDa), and riboflavin (0.376 kDa).

6.2.4 Determination of total carbohydrate and protein contents

Carbohydrate and protein contents in the different fractions were determined with phenol-sulfuric acid method as described by DuBois, Gilles K. A., Hamilton, A. J. Rebers, & Smith (1956) and Bradford method (Bradford, 1976), respectively. D-glucose and BSA were used as standards, respectively.

6.2.5 Determination of monosaccharide composition

The monosaccharide composition of the carbohydrate moiety in the CWE and its different molecular weight fractions were determined by the alditol acetate derivatives of the monosaccharides by gas chromatography (7890B, Agilent Technology, USA) equipped with an Alltech DB-225 capillary column (15 m x 0.25 mm i.d., 0.25 μm films). The oven temperature was increased from 150 ºC to 220 ºC at the rate of 2 ºC/min and kept at 220 ºC for 15 min. The carrier gas was helium. The monosaccharide standards consisted of D-fucose, L-rhamnose, D-ribose, L-arabinose, D-xylose, D-mannose, D-galactose, and D-glucose. D-allose was used as internal standard. All the monosaccharide standards were purchased from Sigma-Aldrich, USA.

6.2.6 Effect of CWE and fractions on pre-contracted airway segments

Tracheal and bronchial segments were pre-contracted with 1 μM carbachol. Once a stable contraction was established, cumulative concentrations of CWE, HMW, MMW or LMW fractions were added into the preparation every 15 minutes. The degree of response (tissue relaxation) was measured as a fraction of the contraction achieved by 1 μM carbachol. The tissue relaxation was expressed as a percentage of carbachol-induced tone. In another set of tissues, purified water was used as vehicle control.

6.2.7 Effect of CWE and fractions against contractions to carbachol and 5-HT

Our earlier results showed that pre-incubation with 3.5 mg/ml of CWE and HMW fraction completely abolished the contractile response to carbachol and 5-HT (data not shown). To express the differences between fractions and CWE explicitly, we therefore used lower concentration i.e. 2.5 mg/ml (concentration that CWE caused appx. 60-70% relaxation of airways) for pre-incubation. Tracheal rings were pre-incubated with 2.5 mg/ml CWE, 2.5 mg/ml HMW fraction, 2.5 mg/ml LMW fraction, 30 nM ipratropium, or purified water (vehicle control) for at least 30 minutes, prior to the construction of cumulative CRCs to carbachol or 5-HT. Tissue contraction to carbachol or 5-HT was expressed as a percentage of reference KCl-induced tone.

6.2.8 Effect of CWE and fractions against calcium-induced contraction

Tracheal segments were bathed in calcium-free Krebs solution and pre-incubated with the 2.5 mg/ml CWE, 2.5 mg/ml HMW fraction, 2.5 mg/ml LMW fraction, or 10 µM nifedipine for at least 30 minutes. KCl (60mM) was added to depolarize the cell membrane and left to incubate for 10 minutes before $CaCl_2$ was reintroduced cumulatively. Tissue contraction to $CaCl_2$ was expressed as a percentage of reference KCl-induced tone.

6.2.9 Statistical analysis

Data were analysed and graphs were drawn using PRISM v7.0 (Graph pad software). All data were expressed as mean ± SEM of *n* number of animals. Maximum tissue contraction or relaxation response (E_{max}) was derived from nonlinear regression analysis of the obtained CRC or from the response generated at the highest concentration tested (if response has not plateaued). Statistical analyses were performed using one-way ANOVA with Dunnett correction (Fig. 6.2 and 6.3) or two-way ANOVA followed by multiple comparison test with Bonferroni correction (Fig. 6.1). Results were considered statistically significant if p-value was less than 0.05.

6.3 Results

6.3.1 Fractionation of CWE by molecular weight

CWE of the sclerotial powder of *L. rhinocerotis* yielded 7.04 ± 0.69 g of freeze-dried solid. Further fractionation of the extract by Sephadex G-50 gel permeation chromatography yielded a broad protein peak and several carbohydrate peaks. The fraction tubes collected were pooled into three fractions based on their molecular weight range into HMW, MMW, and LMW fractions. The molecular weight range of each fraction was: HMW (> 29.9 kDa), MMW (7.1 kDa to 27.4 kDa) and LMW (0.8 kDa to 6.5 kDa). The fractionation profile is shown in **Appendix E**.

6.3.2 Chemical composition of CWE and its fractions

Table 6.1 shows that the majority of carbohydrate and protein present in CWE was present in the HMW fraction, indicating the existence of polysaccharides and polysaccharide-protein complex. There was a larger amount of non-protein and non-carbohydrate substances in the LMW and MMW fractions than the HMW fraction. These are low-molecular-weight molecules such as phenolic compounds found abundantly in CWE (Y. H. Y. Yap et al., 2013). According to the monosaccharides profile, different sugar composition was present in different molecular-weight carbohydrates. Among all, glucose was the most dominant sugar found in CWE and its fractions, indicating the presence of water-soluble glucans that are commonly found in mushrooms. Besides, there were small amounts of other heteroglycans containing arabinose, mannose and galactose in CWE and its fractions. Notably, the amount of galactose in the fractions correlated with the amount of protein in the fractions, suggesting the presence of galacto-glycoprotein linkages in polysaccharide-protein complexes.

Table 6.1: Chemical composition and monosaccharide profile of cold water extract and its fractions.

Sample	Protein %	Total Carbohydrate %	Monosaccharides (Normalized %)				
			Arabinose	Xylose	Mannose	Galactose	Glucose
TM02 sclerotial powder	1.38	7.76	-	2.39	2.52	1.73	93.37
CWE	2	68	0.39	-	1.25	2.29	96.08
LMW fraction	0.3	22	3.11	-	5.39	-	91.49
MMW fraction	1	35	-	-	-	1.25	98.74
HMW fraction	4	71	-	-	5.11	4.62	90.27

Abbreviations: CWE = Cold water extract; HMW = High-molecular-weight; LMW = Low-molecular-weight; MMW = Medium-molecular-weight

6.3.3 Unequivocal airway relaxation effects of CWE, HMW and MMW fractions

CWE, HMW and MMW fractions significantly relaxed tracheal segments pre-contracted with carbachol from 1.75, 1.25 and 1.50 mg/ml onwards, respectively (Fig. 6.1A). Similarly for bronchial segments, CWE, HMW and MMW fractions produced significant relaxant responses from 3.50 (CWE) and 2.00 mg/ml (HMW and MMW) onwards (Fig. 6.1B). Based on the maximum tissue response at 3.5 mg/ml, vehicle control tissues produced E_{max} of 39.68 ± 5.47% and 49.68 ± 11.85% in tracheal and bronchial tissues, respectively. The maximum responses of test samples were similar in trachea (T) and bronchus (B) and significantly different from vehicle control, where HMW fraction (T: 117.32 ± 11.01%, $p < 0.0001$; B: 101.67 ± 7.31%, $p < 0.001$) and MMW fraction (T: 105.84 ± 7.86%, $p < 0.0001$; B: 108.30 ± 8.16%, $p < 0.001$) produced the largest response followed by CWE (T: 79.45 ± 8.21%, $p = 0.0018$; B: 86.90 ± 7.21%, $p = 0.0119$) (Fig. 6.1C and D). The maximum relaxant responses produced by LMW fraction in trachea and bronchus were no different (T: 40.64 ± 17.51%; B: 65.80 ± 5.91%) from vehicle control with $p > 0.9999$. Fig. 6.1C shows that the bronchodilator effect of LMW fraction in tracheal rings was significantly lower compared to CWE ($p = 0.056$), HMW ($p < 0.0001$), and MMW ($p < 0.0001$) fractions. Similarly in Fig. 6.1D, the bronchodilator effect of LMW fraction in bronchial rings was significantly lower than HMW ($p = 0.0092$) and MMW ($p = 0.0005$) fractions, but not different from CWE.

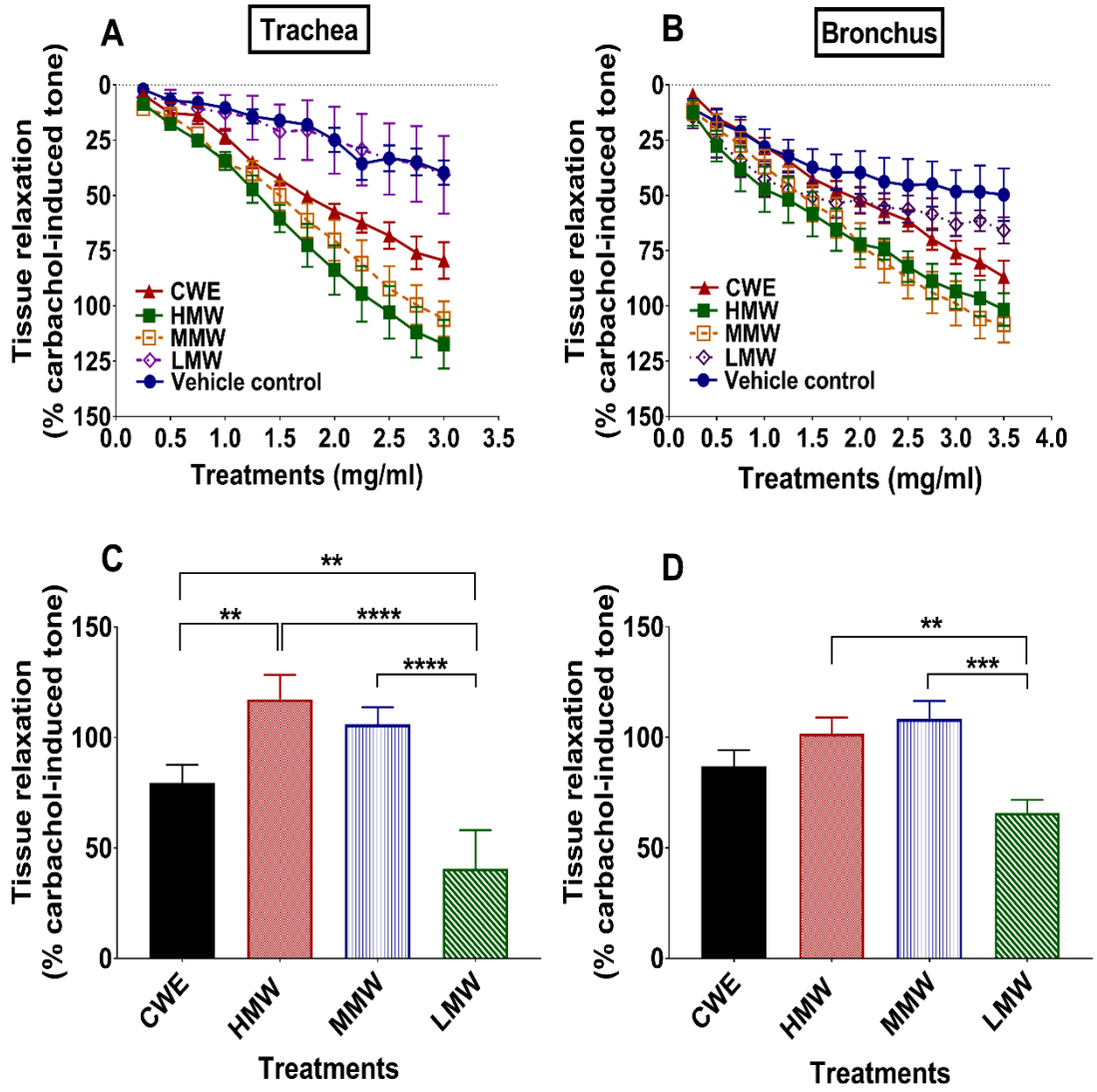

Figure 6.1: Effect of cold water extract and fractions on rat airways pre-contracted with carbachol. Concentration-response curves to CWE and its HMW, MMW and LMW fractions in (A) tracheal and (B) bronchial rings pre-contracted with 1 µM carbachol. Maximum tissue relaxation at the highest concentration tested in (C) tracheal at 3.0 mg/ml and in (D) bronchial tissues at 3.5 mg/ml. Tissue responses were expressed as a percentage of carbachol-induced contraction. Data were shown as means ± SEM of 4 to 6 animals. One-way ANOVA with Bonferroni correction where comparison of means among groups was made: $^{**}p < 0.01$; $^{***}p < 0.001$;$^{****}p < 0.0001$. (Abbreviations: CWE = Cold water extract; HMW= High-molecular-weight fraction; LMW = Low-molecular-weight fraction; MMW = Medium-molecular-weight fraction)

6.3.4 HMW fraction markedly prevented carbachol- and 5-HT-induced airway contraction

Based on the above findings (Section 6.3.3), subsequent experiments were carried out using 2.5 mg/ml of CWE, HMW and LMW fractions on tracheal rings. HMW fraction almost totally prevented carbachol- and 5-HT-induced contraction, respectively, compared to vehicle control in the airway segments (Fig. 6.2A and B). Although the effect of CWE was not as marked as HMW fraction, it also significantly attenuated the maximum response of carbachol. This was similar to ipratropium, which had reduced the carbachol-induced contraction. On the contrary, LMW fraction did not affect any of the tissue contractions induced by carbachol or 5-HT. Pre-treatment with CWE and its fractions did not affect the potencies of both carbachol and 5-HT CRC. The E_{max} and pEC_{50} values are summarized in Table 6.2.

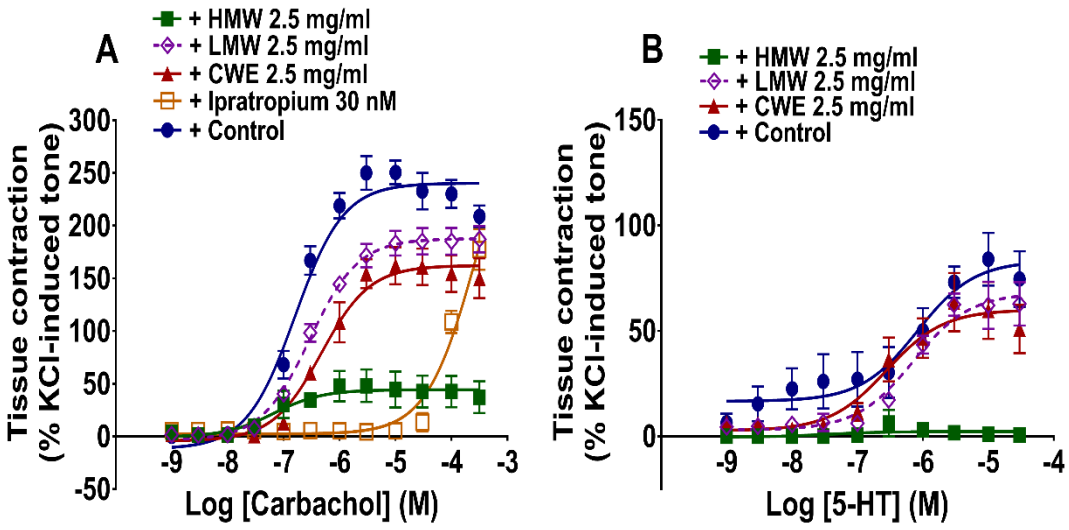

Figure 6.2: Effect of cold water extract and fractions against carbachol- and 5-hydroxytryptamine-induced contractions in rat trachea. Concentration-response curves to (A) carbachol and (B) 5-HT in tracheal rings pre-incubated with CWE, ipratropium, fractions, or purified water (vehicle control) for 30 minutes. Tissue responses were expressed as a percentage of reference KCl-induced contraction. Data were shown as means ± SEM of 5 to 6 animals. (Abbreviations: 5-HT = 5-hydroxytryptamine; CWE = Cold water extract; HMW= High-molecular-weight fraction; LMW = Low-molecular-weight fraction)

Table 6.2: The maximum responses (E_{max}) and pEC_{50} values of carbachol and 5-hydroxytryptamine derived from the respective concentration response curve in the presence of CWE and fractions. One-way ANOVA where comparison of the mean was made between vehicle control and the treatment groups; *$p < 0.05$, ****$p < 0.0001$. Individual p-value was stated. Data were shown as means ± SEM with 5 to 6 animals.

Treatments	Carbachol		5-HT	
	E_{max} (%)	pEC_{50}	E_{max} (%)	pEC_{50}
+ Vehicle (water)	241.20 ± 10.92	6.79 ± 0.09	85.24 ± 13.84	6.46 ± 0.48
+ HMW 2.5 mg/ml	44.52 ± 16.37**** ($p < 0.0001$)	6.70 ± 0.51 ($p > 0.999$)	2.48 ± 1.52*** ($p = 0.0002$)	-[a]
+ LMW 2.5 mg/ml	187.90 ± 12.02 ($p > 0.999$)	6.54 ± 0.06 ($p > 0.999$)	69.91 ± 9.89 ($p > 0.999$)	6.16 ± 0.13 ($p = 0.841$)
+ CWE 2.5 mg/ml	165.00 ± 18.52* ($p = 0.0129$)	6.38 ± 0.17 ($p > 0.958$)	60.28 ± 12.92 ($p = 0.3755$)	7.15 ± 0.55 ($p = 0.439$)
+ Ipratropium 30 nM	139.70 ± 13.20* ($p = 0.0447$)	-[b]	-	-

[a]pEC_{50} value was unable to be calculated by Prism software due to non-converged points.

[b]Unable to calculate as maximum response has not plateaued at the highest concentration tested.

Abbreviations: 5-HT = 5-hydroxytryptamine; CWE = Cold water extract; HMW = High-molecular-weight fraction; LMW = Low-molecular-weight fraction; MMW = Medium-molecular-weight fraction

6.3.5 HMW fraction significantly limited calcium-induced contraction

Fig. 6.3 shows that in vehicle control tissues, $CaCl_2$ induced a maximum response of 91.44 ± 12.70%. In comparison, HMW fraction significantly attenuated the contraction induced by $CaCl_2$ (E_{max}: 37.75 ± 3.95%, p = 0.0005), which was similar to nifedipine (E_{max}: 21.83 ± 5.61%, p = 0.0001). CWE also significantly reduced the maximum response of $CaCl_2$ CRC (E_{max}: 54.48 ± 5.27%, p = 0.0149), although to a lesser extent than HMW fraction and nifedipine. In contrast, LMW fraction was devoid of effect (E_{max}: 100.90 ± 8.09%, p = 0.829).

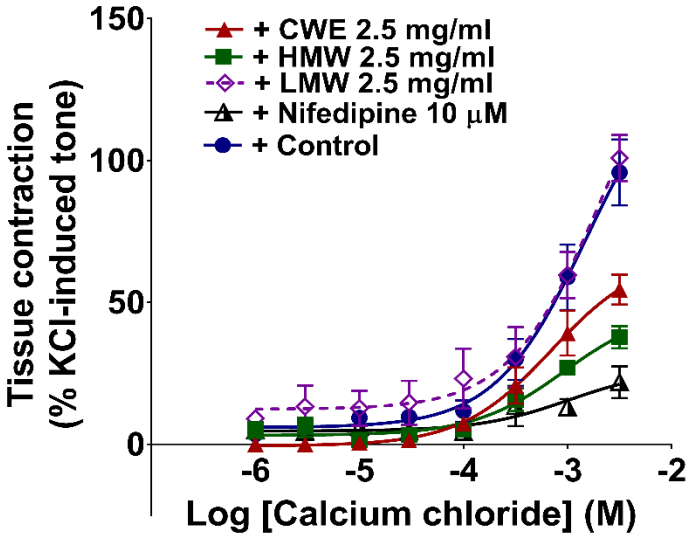

Figure 6.3: Effect of cold water extract and fractions against calcium chloride-induced contraction in rat trachea. In the absence of external Ca^{2+}, tracheal rings were pre-incubated with CWE, HMW fraction, LMW fraction, nifedipine, or purified water (vehicle control) for 30 minutes. Then, 60 mM KCl was added to depolarize the tissue prior to addition of increasing concentrations of calcium chloride to induce contraction. Tissue responses were expressed as a percentage of reference KCl-induced tone. Data were shown as means ± SEM of 5 to 7 animals. (Abbreviations: 5-HT = 5-hydroxytryptamine; CWE = Cold water extract; HMW= High-molecular-weight fraction; LMW = Low-molecular-weight fraction)

6.4 Discussions

This is the first study to elucidate the bioactive fractions accounting for the airway relaxation effect elicited by *L. rhinocerotis*. To identify the bronchodilator components, CWE was fractionated using Sephadex G-50 gel permeation chromatography into HMW, MMW and LMW fractions. Our hypothesis was that bronchodilator effect of CWE differs in fractions of different molecular weight. This is supported by the successful demonstration that both HMW and MMW fractions exhibited highest efficacy in relaxing the pre-contracted airways compared to CWE and LMW fraction. This infers that the bioactive components responsible for the airway relaxation effects are large-molecular-weight substances mostly present in the HMW and MMW fractions. Effect of the LMW fraction was similar to the vehicle control, thus indicating no significant bioactive component is present in this fraction.

Moreover, we showed that pre-incubation with the HMW fraction inhibited the contractions to both carbachol and 5-HT to a similar degree. The HMW fraction had abolished carbachol- and 5-HT-induced contractions in a non-competitive manner. This suggests that the HMW fraction non-selectively inhibits the downstream mechanism of $G_{\alpha q}$-coupled receptor activation. Our results also showed that the efficacies of CWE and HMW fraction were comparable to or even better than that of ipratropium in inhibition of carbachol-induced airway contraction. The difference in the effect of CWE from HMW fraction as observed in Fig. 6.2 also implies that the airway relaxation effect of *L. rhinocerotis* is not mediated via blockade of muscarinic receptors, unlike conventional antimuscarinic bronchodilator.

Following these observations, we subsequently investigated the effect of the CWE and its fractions on extracellular Ca^{2+} entry. Nifedipine was chosen as a positive

control in this study to confirm the involvement of these channels in $CaCl_2$-induced contraction. The effectiveness of the HMW fraction in blocking $CaCl_2$-induced contraction was similar to nifedipine, thus implying the HMW fraction may be blocking VOCC, especially L-type calcium channels. The degree of relaxation elicited by CWE and its fractions on carbachol- and 5-HT-induced contraction correlated well with the inhibitory effect on $CaCl_2$-induced contraction, suggesting that the effect is mainly mediated by inhibition of Ca^{2+} entry. This evidence strongly suggests that one of the mechanisms implicated by CWE-induced airway relaxation is linked to regulation of calcium signalling and $G_{\alpha q}$ protein-coupled receptor activation.

In this study, the largest amount of carbohydrate and protein was found in the HMW fraction (71% and 4% respectively), followed by the MMW fraction (35% and 1% respectively) and the LMW fraction (22% and 0.3% respectively). As the LMW fraction containing an insignificant amount of protein did not display any bronchodilator properties at the concentration tested, our results strongly suggest that the polysaccharide-protein complex or proteins found in HMW and MMW fractions are likely to contribute to the bronchorelaxation effect of CWE. This is in agreement with another published study where the HMW fraction of TM02 cultivar exhibited the greatest anti-inflammatory activities against human lung and breast cancer cells (Sook Shien Lee et al., 2014).

Gathered evidence from literature indicates that most of the mushroom polysaccharides are β-glucans (De Silva et al., 2013; Lai et al., 2008; Wong et al., 2011) which mainly consist of β-1,3 backbone and β-1,6-linked side branches (Cheung, 2013). An alkali-soluble polysaccharide isolated from sclerotia of *L. rhinocerotis* cultivar was characterized to be hyperbranched glucan with (1,3)-β-D-glucopyranose backbone and β-1,6-linked side branches that adopts compact coil conformation (Hu,

Huang, Wong, Yang, et al., 2017). The medicinal properties of polysaccharides are closely related to their monosaccharide composition, glycosidic linkages, branching, molecular weight, water solubility and chain conformation (Bohn & BeMiller, 1995; Q. Wang et al., 2017; Wong et al., 2011). An understanding of their structures is thus crucial for successful interpretation of their bioactivities.

In the present chapter, we had investigated the monosaccharide compositions in the CWE and its fractions. Our monosaccharide profile analysis revealed that glucose is the most abundant sugar in the CWE and its fractions. The amount of galactose and protein corresponded with the bronchorelaxation activities; this sugar was found in the highest amount in the bioactive HMW fraction, followed by CWE. Besides, high amount of mannose was present in HMW fraction. However, mannose did not seem to contribute to the bronchodilator effect as the MMW fraction was devoid of mannose, but was able to produce pronounced bronchorelaxation similar to the HMW fraction. Furthermore, mannose, but not galactose, was found in the LMW fraction. We postulate that the glucose and galactose consistently found in the HMW and MMW fractions and the CWE appear to be the important residues in the glycosidic linkages of polysaccharide-protein complex contributing to the bronchorelaxation activities. Recently, a novel polysaccharide-protein complex was isolated from the hot-water-soluble polysaccharide fraction of *P. rhinocerus* and chemically characterized, indicating that glucose and mannose are the predominant carbohydrate moieties in the polysaccharide-protein complex with antitumor activity (Liu et al., 2016). The slight variations in the sugar composition between our study and the previous report might be attributed to the differences in extraction method, cultivar and geographical origins. In addition, in contrast with the previous findings by Liu et al. (2016), our preliminary experiments with hot water extract of *L. rhinocerotis*

showed insignificant bronchorelaxation effect (**Appendix B**), suggesting that the manno-glycoprotein linkages in polysaccharide-protein complex are not likely to contribute to the bronchodilator effect.

As a whole, observations in the present chapter clearly indicate that the bronchodilator effect of CWE of *L. rhinocerotis* is attributed to constituents found in the HMW and MMW fractions. Polysaccharide, proteins, or polysaccharide-protein complexes, with glucose and galactose being the potentially important sugar residues in polysaccharide, are the candidate components accountable for the airway relaxation effect. On the contrary, the LMW fraction was devoid of any effect on airways, inferring that the LMW compounds are unlikely to be bioactive. This provides a theoretical basis for future work to concentrate on isolating and purifying the active compounds from HMW fraction of *L. rhinocerotis*.

Chapter 7. Effect of *Lignosus rhinocerotis* extract on mast cell degranulation

7.1 Introduction

Mast cell degranulation is a cardinal feature in the early phase of allergen-induced asthma. Mast cells originate from haematopoietic stem cells and are ubiquitous throughout the body (Moon, Dean Befus, & Kulka, 2014). The infiltration of large amount of mast cells within bronchial smooth muscle bundles of asthmatic patients indicates that mast cells may be a key factor in determining asthmatic phenotype (Peter Bradding et al., 2006; Christopher E Brightling et al., 2002).

Degranulation of mast cells initiates with binding of antigens (allergens) with IgE that leads to cross linking of mast cell surface high-affinity IgE receptors (FcεRI), followed by release of various pro-inflammatory mediators from mast cells (Toru et al., 1996). Upon exposure to antigen, IgE binding to the antigen causes crosslinking of FcεRI on mast cell surface. The crosslinking of FcεRI/IgE with antigen activates Lyn kinase, which, in turn, causes tyrosine phosphorylation of the immunoreceptor tyrosine-based activation motif (ITAM) (Siraganian, Castro, Barbu, & Zhang, 2011). Subsequent phosphorylation of Syk kinase leads to downstream signalling events which include activation of mitogen-activated protein kinase (MAPK) family and elevated Ca^{2+} mobilization through the activation of DAG/IP_3/PKC pathway (Sandig & Bulfone-Paus, 2012).

Mast cell activation recruits $PLC_{\gamma 1}$ to the membrane with tyrosine phosphorylation by Syk and Bruton's RK (Finn & Walsh, 2013). DAG and IP_3 are generated as a result of breakdown of PIP_2 catalysed by $PLC_{\gamma 1}$. Besides, activated Syk

also phosphorylates the Linker for Activation of T cells (LAT) which regulate downstream signalling events leading to cytokine gene transcription and degranulation. Consequently, these events lead to mast cell activation and degranulation with the release of a range of preformed mediators such as histamine, proteases and other enzymes from the secretory granules, and *de novo* synthesized phospholipid metabolites and cytokines (Moon et al., 2014).

In general, there are three groups of mediators based on their mode of generation and/or release from the mast cell granules. Firstly, mediators pre-formed and stored in mast cell granules are rapidly released through mast cell degranulation (Moon et al., 2014). Mast cell secretory granules, which is also termed secretory lysosomes, contain lysosomal enzymes including β-hexosaminidase (an acid hydrolase) and other mediators, such as histamine, serotonin, proteases, and carboxypeptidases (Moon et al., 2014). Common techniques measure the contents of these mediator components in medium or releasing buffer normalized to the total cellular pool in cell culture systems (Kuehn, Radinger, & Gilfillan, 2010). The most widely assessed components are histamine, serotonin, and β-hexosaminidase. Histamine is the major mediator released during activation of mast cell and basophil, which are both effector cells implicated in immediate allergic reactions and allergic diseases (Miyake & Karasuyama, 2017). The determination of histamine levels is generally performed by ELISA or fluorospectrophotometry. Nevertheless, the detection of histamine via these techniques are proved to be difficult due to short half-life of histamine (within minutes) and instability of fluorescent material (Stone, Prussin, & Metcalfe, 2010). The fluorometric assay might also interact with other amines e.g. 5-HT, rendering the assay to be non-selective to histamine (Passante, Ehrhardt, Sheridan, & Frankish, 2009).

As an alternative to histamine, β-hexosaminidase has become a popular degranulation marker in recent years as its measurement is relatively simpler and cheaper (Kuehn et al., 2010). Results from previous study comparing the release of β-hexosaminidase and histamine imply that β-hexosaminidase is a more suitable biomarker for degranulation in RBL-2H3 cells due to easy and rapid detection (Passante & Frankish, 2009). β-hexosaminidase is released concurrently with histamine during degranulation and is therefore a reproducible indicator well correlated with histamine release.

Secondly, mediators that are generated upon mast cell activation and released later than the first group is the phospholipid metabolites, such as PGD_2, LTB_4, LTC_4, LTD_4, LTE_4, and platelet-activating factor (Stone et al., 2010). These mediators are generated as a consequence of phospholipase A_2 activation following mast cell activation. Thirdly, cytokines and chemokines are synthesized due to enhanced gene expression induced by mast cell activation. Thus, mast cell degranulation can be qualitatively and quantitatively measured through the analysis of these mediators released from secretory granules. Techniques that monitor these events and assess the parameters of cell signalling are employed to study mast cell degranulation (Kuehn et al., 2010).

The proposed release mechanisms of preformed mediators from mast cells are categorized into piecemeal degranulation and anaphylactic degranulation. Piecemeal degranulation selectively releases portions of the granule contents without granule fusion to granule or to plasma membrane, probably via the budding of vesicles transported and fused to plasma membrane (Moon et al., 2014). On the other hand, anaphylactic degranulation is a complete release of the granule contents involving direct granule-to-granule and/or granule-to-membrane fusions. The stages of

anaphylactic degranulation are in the following order: swelling of the polymer gel matrix within granules, granule to granule membrane fusion, degranulation channel formation, pore formation, granule matrix extrusion, and lastly the shedding of extruded matrix materials (mast cell membranes and processes) (Dvorak et al., 1991).

Basophils, which is another granulocyte of white blood cells, share functional similarities with mast cells. Similarities between basophils and mast cells are, for example, the presence of secretory granules which release histamine and other mediators upon degranulation, expression of FcεRI, and secretion of Th2 cytokines, IL-4 and IL-13 (Obata et al., 2007; Stone et al., 2010). By contrast, the differences between basophils and mast cell include: (i) basophils circulate in peripheral blood while mast cells reside in tissues, and (ii) basophils release lesser amount of tryptase and narrower range of phospholipid metabolites (Stone et al., 2010). While most research interest lies on the mast cells and their central roles in asthma, the role of basophils is less well defined (Miyake & Karasuyama, 2017). In fact, emerging evidence points to the important role of basophils in allergic inflammation; however, their effects on airway inflammation in IgE-dependent asthma model remain elusive (Miyake & Karasuyama, 2017). Basophils also show importance in mediating lung eosinophilic inflammation induced by protease allergens (D. A. Hill et al., 2012; Motomura et al., 2014).

7.1.1 The suitability of RBL-2H3 cells as a model of degranulation

Cell culture is a useful technique for the examination of mast cell and basophil degranulation. Mast cells can be activated via immunogenic (IgE-dependent) mechanism or non-immunogenic (IgE-independent) mechanism (Seifert, 2015). IgE/antigen-dependent stimulation is normally performed by sensitizing the cells with IgE conjugated with chemical recognizable by the antigen. Frequently used antigens are ovalbumin (chicken egg albumin) and human serum albumin. The examples of broadly used IgE-independent mast cell activator and inducer of histamine release are compound 48/80 (a polymer produced by condensation of N-methyl-p-methoxyphenethylamine with formaldehyde), Ca^{2+} ionophores (Ca^{2+} carrier), and others (Seifert, 2015).

Rat basophil leukaemia (RBL) cells were first induced by injecting the rats with carcinogen β-chlorethylamine (B. Y. A. Kulczycki, Isersky, & Metzger, 1974). Subsequently, the leukemic cells isolated from tumour were adapted to suspension culture and termed RBL-1, which bind specifically to IgE (A. Kulczycki & Metzger, 1974). Although RBL-1 cells express cell surface FcεRI, it failed to release histamine in response to IgE/antigen trigger or chemical stimulation by a calcium ionophore, A-23187 (Siraganian, Kulczycki, Mendoza, & Metzger, 1975). It was until year 1981 when RBL-2H3, a subline isolated from the subclone RBL-IV (HR^{+}) cells with good histamine releasing capacity to IgE/antigen trigger, was created (Barsumian, Isersky, Petrino, & Siraganian, 1981). Since then, the RBL-2H3 cell line has been extensively used to study the properties of FcεRI.

Although RBL-2H3 cell line is generally regarded as mast cell line in many studies, it, in fact, showed similar characteristics of both mucosal mast cells and

basophils (Passante & Frankish, 2009). RBL-2H3 cells are commonly employed as a model to study IgE-mediated degranulation of mast cells and basophil due to its ease of maintenance, similar characteristics to mast cells in terms of histamine and mediators secretion, and expression of FcεRI (Kuehn et al., 2010; Passante & Frankish, 2009). It has also been frequently used to screen for degranulation inhibitors from natural products (Ikawati, Wahyuono, & Maeyama, 2001; Matsuda, Nakamura, & Yoshikawa, 2016). In light of this, we will use RBL-2H3 cells to investigate the effect of *L. rhinocerotis* CWE on degranulation throughout this study.

7.1.2 The role of natural products in inhibiting mast cell degranulation

Natural products exhibited inhibiting properties on mast cell and basophil degranulation. In fact, the isolation of a natural mast cell stabilizer from *Amni visnaga* inspired the synthesis of the first established mast cell stabilizer, namely disodium cromoglycate (Finn & Walsh, 2013). As for medicinal mushrooms, a few have reported anti-degranulation effect in the cell culture systems. For instance, dichloromethane extract and purified compounds, melleolide H and J, from *Armillaria ostoyae* (Merdivan, Jenett-Siems, Siems, Niedermeyer, Solis, et al., 2017) and dichloromethane extract from the fruiting body of *Tricholoma populinum* Lange (Merdivan, Jenett-Siems, Siems, Niedermeyer, Schultze, et al., 2017) have significant inhibitory effect on IgE/antigen-induced release of β-hexosaminidase in RBL-2H3 cells. Besides, the water extract of *Phellinus linteus* fruiting body greatly reduced compound 48/80-induced histamine release and Ca^{2+} uptake in rat peritoneal mast cells *in vitro* (Choi et al., 2006). *Sparassis crispa* extract was also revealed to significantly decrease compound 48/80- and A23187-induced histamine release as

well as Ca^{2+} uptake in mice and human mast cells (H. H. Kim et al., 2012). In addition, a number of natural product-derived compounds such as terpenoids, flavonoids, coumarins, phenols and amino acids exhibited mast cell stabilizing properties *in vitro* and *in vivo* (Finn & Walsh, 2013). Despite these pieces of evidence, the precise mechanism by which natural products mediate the anti-degranulation effect are poorly understood.

With regards to *L. rhinocerotis*, a recent study revealed that its hot water extract significantly attenuated eosinophil cell infiltration into lung tissues and reduced levels of serum IgE and Th2 cytokines such as IL-4, IL-5, and IL-13 in BALF of airway inflammation mice model (Johnathan et al., 2016). As mentioned earlier, the interleukins IL-4, IL-5, and IL-13 are mediators released from mast cells and basophils degranulation. This piece of evidence may allude to the inhibitory effect of *L. rhinocerotis* on mast cell degranulation.

7.1.3 Significance of study

In light of the traditional usage of *L. rhinocerotis* in treating asthma, we hypothesized that *L. rhinocerotis* may modulate mast cell degranulation and therefore hold potential to relieve allergic asthma. To our knowledge, the effect of *L. rhinocerotis* on mast cells were not reported yet. The main goal of the present chapter was to investigate the effect of CWE of *L. rhinocerotis* on degranulation in IgE/antigen-stimulated and unstimulated RBL-2H3 cells. The specific objectives of this chapter were as follows:

(i) To determine the non-cytotoxic concentrations of CWE through MTT (3-(4,5-dimethylthiazolyl-2)-2,5-diphenyltetrazolium bromide) assay.

(ii) To determine the optimum concentrations of IgE and antigen to induce submaximal release of β-hexosaminidase.

(iii) To examine the effect of CWE treatment alone on degranulation of unstimulated cells through β-hexosaminidase assay, Alcian blue staining, and annexin V binding assay.

(iv) To evaluate the effect of CWE treatment on degranulation of IgE/antigen-stimulated cells through β-hexosaminidase assay, Alcian blue staining, and annexin V binding assay.

7.2 Materials and methods

7.2.1 Drugs and materials

CWE was prepared as described in Section 2.2.2, **Chapter 2**. RBL-2H3 cell line was purchased from American Type Culture Collection (ATCC CRL-2256, USA). MTT reagent, sodium pyruvate, and Eagle's Minimum Essential Medium (EMEM) were purchased from Nacalai Tesque, Japan. PBS solution was purchase from Cellgro, USA. Fetal bovine serum (FBS) (South America origin) was purchased from iDNA Biotechnology, Malaysia. Dinitrophenyl-human serum albumin (DNP-HSA), Anti-dinitrophenyl Immunoglobulin E (Anti-DNP IgE, 1.1 mg/ml) , Trypsin-EDTA 0.25%, 4-Nitrophenyl N-acetyl-β-D-gluconide (PNAG), Alcian blue 8Gx, and piperazine-N,N'-bis(2-ethanesulfonic acid) (PIPES) were purchased from Sigma, US. Penicillin 10000 unit/ml-Streptomycin 10000 µg/ml and Tryptan blue stain were purchased from Invitrogen, USA. BSA was purchased from Affymetrix, USA. All ingredients from Siraganian buffer, citrate buffer and stop solution, and safranin O stain were purchased from R & M Chemicals, UK, except BSA and PIPES. Ketotifen fumarate was purchased from Tokyo Chemical Industry, Japan, while chlorpheniramine maleate was purchased from Santa Cruz, USA. Annexin-V-Fluos staining kit was purchased from Roche, Germany. Compositions of Siraganian buffer are listed in **Appendix A**.

Stop solution composed of 0.1 M Na_2CO_3/$NaHCO_3$ dissolved in purified water, with the pH adjusted to 10, whereas citrate buffer was made of citric acid (0.1 M) and sodium citrate (0.1 M) dissolved in purified water with the pH adjusted to 4.5. Chlorpheniramine and ketotifen were dissolved in purified water to make stock solutions of 1 to 2 mg/ml. The MTT reagent was dissolved in PBS to make stock solution of 5 mg/ml. DNP-HSA was dissolved in purified water to make stock

concentration of 0.256 mg/ml whilst anti-DNP IgE was dissolved in PBS to make stock solution of 0.05 to 0.1 mg/ml. Alcian blue stain was dissolved in 120 mM HCl, with the pH adjusted to 1.0 while safranin O stain was dissolved in purified water to make stock solutions of 1% and 0.1% (w/v), respectively.

7.2.2 Cell culture

RBL-2H3 cells were maintained as adherent cultures according to ATCC protocol (ATCC® CRL-2256™) in media containing EMEM supplemented with 15% FBS, 100 unit/ml Penicillin-100 µg/ml Streptomycin, and 1 mM sodium pyruvate. Cells were incubated in a humidified incubator with 95% O_2/5% CO_2 air atmosphere, and passaged every 2 to 4 days according to the manufacturer's instructions. Noteworthy, the histamine releasing capacity of RBL-2H3 cells appears to be gradually reduced with subcultures (Barsumian et al., 1981). Degranulation response was shown to decrease after > 8–10 passages in RBL-2H3 cells (Vines et al., 2002). Hence, all following assays were performed with cell passage number ranging from 4 to 5 to preserve the maximum degranulation response. Considering the time-dependent properties of CWE (see Section 2.3.5, **Chapter 2**), cells were treated with CWE over 2 and 5 hours in the following degranulation assays.

7.2.3 Cell viability assay

This subsection served to determine the optimum non-cytotoxic concentrations of CWE for RBL-2H3 cells to be used in following degranulation assays. Cell viability was determined by a colorimetric assay using MTT reagent. This assay relies on the reduction of water-soluble yellow MTT dye by metabolically active cells, mainly by the action of cellular dehydrogenase enzymes. The resulting insoluble purple formazan crystals formed within healthy cells are solubilized in DMSO, and the absorbance of the formazan solution is quantified spectrophotometrically. Our preliminary results showed that treatment with CWE > 62.5 µg/ml for 48 hours significantly reduced the cell viability (**Appendix D**). Therefore, we treated the cells with concentrations of CWE ≤ 62.5 µg/ml in this subsection. Firstly, RBL-2H3 cells were seeded into 96-well plate at 1 x 10^4 cells/well and incubated overnight. Medium in the wells was then replaced with FBS-free fresh medium for serum starvation, and cells were treated with CWE (3.9 to 62.5 µg/ml) or purified water (vehicle control) for 24 and 48 hours. At the end of incubation period, the medium was carefully removed, replaced with 200 µl fresh medium (containing MTT solution 0.15% v/v), and incubated for another 4 hours. Then, 170 µl of MTT-containing medium was aspirated from each well and replaced with 170 µl of DMSO. The plate was gently shaken to mix and dissolve the formazan crystals. Once all crystals dissolved, the plate was read on microplate spectrophotometer (Biotek instrument, USA) at 570 nm. The viability of treated cells was expressed as a percentage of absorbance values normalized to untreated cells from which blank control (only medium) was subtracted. Untreated cells represented 100% cell viability.

7.2.4 Optimization of IgE/antigen-stimulated degranulation using β-hexosaminidase assays

β-hexosaminidase cleaves PNAG molecule that contains terminal N-acetyl hexosamines, producing yellow 4-nitrophenoxide which can be quantified spectrophotometrically and represents the amount of β-hexosaminidase (Shibata & Yagi, 1996). Increased β-hexosaminidase levels in the environment represent an increased activity of degranulation. To determine the optimum concentrations of anti-DNP IgE and DNP-HSA (antigen) for degranulation, we first measured and compared the β-hexosaminidase activities between stimulated and unstimulated cells (spontaneous release) based on previous protocols with minor modification (Dearman, Skinner, Deakin, Shaw, & Kimber, 2005; Juckmeta, Thongdeeying, & Itharat, 2014).

Cells were seeded in 24-well plates and allowed to adhere. Upon reaching 60-70% confluency, medium was replaced with EMEM containing 2% FBS. Based on observation from Section 7.2.3 above, cells appeared rounded up after 24-hour serum starvation at 0% FBS. Therefore, a minimum concentration of FBS, 2%, was used to preserve the cell adherence as well as to minimize potential interference of serum on antibody and proteins present in CWE. Cells were sensitized with anti-DNP IgE at a final concentration of 0.5 µg/ml and incubated overnight (~18 hours). At the end of incubation, each well was first washed with PBS, followed by washing with 400 µl Siraganian buffer (releasing buffer). Cells were incubated with Siraganian buffer for 10 minutes before stimulated with DNP-HSA at concentrations 0.05 to 16 µg/ml (in 4-fold increment) and incubated at 37°C for 1 hour to stimulate degranulation. At the end of incubation, the plate was removed from incubator, chilled on ice for 10 minutes to stop the degranulation reaction, and then centrifuged at 250 xg for 5 minutes at 4°C.

The resulting supernatant (50 µl) was collected from each well and transferred to a 96-well plate. To lyse the remaining cell pellets on 24-well plate, 150 µl of 0.1% Triton X-100 (v/v in Siraganian buffer) was added into each well, mixed, and cooled on ice for 5 minutes. The cell lysate was then collected and transferred to the same 96-well plate that contained the supernatant. Subsequently, 50 µl of PNAG solution (4 mM in 0.1 M citrate buffer) was added into each well of 96-well plate (containing supernatant and cell lysates) and incubated for 90 minutes at 37°C. To stop the reaction, stop solution (200 µl) was added into each well and incubated for 10 minutes. Lastly, the plate was read on spectrophotometer at 405 nm and the absorbance values were taken. To estimate the spontaneous release of β-hexosaminidase, control cells untreated by anti-DNP IgE and DNP-HSA were similarly assayed.

Based on the results from experiments above, the concentration of DNP-HSA that gave submaximal β-hexosaminidase release was 0.25 µg/ml (with 0.5 µg/ml anti-DNP IgE). The experiments were then repeated with 0.25 µg/ml DNP-HSA and anti-DNP IgE at concentrations 0.1 to 0.8 µg/ml (in 2-fold increment). The concentration of anti-DNP IgE that produced maximal β-hexosaminidase release was determined to be 0.1 µg/ml. Therefore, following degranulation experiments with CWE treatment used 0.25 µg/ml DNP-HSA and 0.1 µg/ml anti-DNP IgE. Degranulation was expressed as a percentage of released β-hexosaminidase normalized to total β-hexosaminidase content (from cell lysate).

7.2.5 β-hexosaminidase assays

To examine the effect of CWE on IgE/antigen-induced β-hexosaminidase release, the experiments were repeated as per Section 7.2.4. After sensitization with anti-DNP IgE overnight, cells were treated with CWE (3.9 to 62.5 µg/ml) or purified water (vehicle control) in Siraganian buffer, and were incubated for 2 hours before the addition of DNP-HSA. The experiment was repeated with positive controls i.e. ketotifen (70 µM) (histamine H_1 receptor antagonist and mast cell stabilizer, Lian et al., 2015) and chlorpheniramine (70 µM) (histamine H_1 receptor antagonist, Juckmeta et al., 2014) replacing the CWE. β-hexosaminidase activity was assayed as described in Section 7.2.4.

In a different set of experiments to determine if CWE alone affects degranulation in the absence of antigen, the protocol was repeated as above with treatment of CWE (3.9 to 62.5 µg/ml) and vehicle control (purified water) in IgE-sensitized cells (without DNP-HSA). Cells were first sensitized overnight with anti-DNP IgE. Then, they were pre-incubated with CWE in Siraganian buffer for 2 hours, before subjected to β-hexosaminidase assay. In another set of experiments, cells were incubated with CWE (3.9 to 62.5 µg/ml) in FBS-free EMEM instead of Siraganian buffer for 2 hours, followed by the removal of medium and replacement with Siraganian buffer. Subsequently, β-hexosaminidase quantification was performed. To estimate the spontaneous degranulation, similar protocols were carried out in cells without stimulation by IgE and DNP-HSA. Degranulation was expressed as a percentage of released β-hexosaminidase from which spontaneous release was subtracted and normalized to total β-hexosaminidase content (from cell lysate). We

were unable to extend the CWE treatment for longer duration as cells tend to detach from the bottom of flask with more than 3 hours of incubation in Siraganian buffer.

7.2.6 Alcian blue staining

Mast cell granules contain proteoglycans which consist of a core protein (serglycin) and glycosaminoglycan (heparin and chondroitin sulfate) side chains linked to the core protein through glycosidic bonds (Moon et al., 2014). The high anionic charge of glycosaminoglycan allows binding of acidic dye to the basic secretory granules (Rönnberg, Melo, & Pejler, 2012). The acidic Alcian blue stain is one of the commonly used stains for basophil granules (Gilbert & Ornstein, 1975). In this subsection, Alcian blue staining experiments were carried out as described by Huang et al. (2010) with minor modification.

Firstly, RBL-2H3 cells were seeded into cover slips placed inside wells of 6-well plate (each well contains a slip). Upon reaching 70% confluency, the old medium was removed and cells were washed with PBS. After overnight sensitization of cells with anti-DNP IgE, old medium was removed and cells were washed with PBS. Treatments with CWE (3.9 to 62.5 µg/ml), ketotifen (70 µM), chlorpheniramine (70 µM), or vehicle control (purified water) in FBS-free EMEM were added accordingly and incubated for 2 or 5 hours. At the end of incubation, degranulation of cells was stimulated by adding DNP-HSA for 1 hour. Then, the plates were cooled on ice for 10 minutes to stop degranulation. Cover slips containing the cells were stained with 1% Alcian blue solution for approximately 10 to 13 minutes, then briefly rinsed with purified water. Subsequently, cells were stained with 0.1% safranin O solution, which

served as the counterstain (Thrasher, Scalfone, Holowka, & Appleton, 2013) for ~10 minutes, followed by brief rinsing with purified water and a quick dip in ethanol to dry the slides. Lastly, cells were mounted onto microscope slides to be viewed under light microscope (Nikon Eclipse 80i) and stained cell images were captured using Nikon DS-Ri1 camera. Total (unstained and stained with Alcian blue) and degranulated (unstained with Alcian blue) basophils were counted from four fields of view and averaged.

In a different experiment to determine if CWE affects degranulation in the absence of antigen, the protocol was repeated as above with treatment of CWE (3.9 to 62.5 µg/ml) or purified water (vehicle control) in IgE-sensitized cells (without DNP-HSA). Degranulation index was expressed as a percentage of unstained cells relative to total cells. Degranulation index was expressed as a percentage of degranulated cells relative to total cells in IgE/antigen-sensitized cells. To estimate the spontaneous degranulation, similar protocols were carried out in cells without stimulation by IgE and DNP-HSA.

7.2.7 Flow cytometry analysis

During early apoptosis, changes occur at the cell surface in which the cell plasma membrane "flips over", causing the phosphatidylserine on the inner part of plasma membrane exposed to the outer surface of cell. Annexin-V-fluorescein, a Ca^{2+}-dependent protein, specifically binds to the exposed phosphatidylserine on outer plasma membrane and has been widely used as early apoptosis marker (Istvan, Haanen, Steffens-Nakken, & Reutelingsperger, 1995). Mast cell degranulation resembles the

changes occurring in early apoptosis where secretory granules are externalized and phosphatidylserine is exposed to external surface during exocytosis (degranulation). This process is described to involve non-apoptotic phosphatidylserine externalization (Rysavy et al., 2014). It was shown that phosphatidylserine exposure is rather a direct consequence of exocytosis instead of an effect of FcεRI crosslinking (Martin et al., 2000). Given that, annexin V is considered an effective indicator for degranulation and the binding of annexin V to cell surface secretory granules has strong correlation with β-hexosaminidase release in literature (Demo et al., 1999; F. Huang et al., 2010; Martin et al., 2000; Windmiller & Backer, 2003). The binding site of annexin V is suggested to be located at or near sites of secretory granule fusion on cell membrane (Demo et al., 1999).

The application of propidium iodide (PI) allows for differentiation of necrotic/late apoptotic cells from degranulating/early apoptotic cells (Demo et al., 1999). Therefore in this experiment, cells that showed early apoptosis as characterized by positively stained with annexin V and negative for propidium iodide (Annexin V^+/PI^-), were quantified as the degree of degranulation. The fluorescence signal is detectable and measurable using flow cytometry. The following experimental procedures were performed according to the instructions in Annexin-V-Fluos staining kit (Roche, Germany).

Cells were first seeded into 6-well plate and grown until 70% confluent. Following overnight sensitization with anti-DNP IgE, cells were treated with CWE (3.9 to 62.5 µg/ml), ketotifen (70 µM), chlorpheniramine (70 µM), or purified water (vehicle control) in FBS-free EMEM for 2 or 5 hours. Degranulation was then stimulated with DNP-HSA for 1 hr. After the reaction was stopped by cooling on ice for 10 minutes, medium was removed and trypsin-EDTA 0.25% solution was added

into each well to trypsinize the cells. Cell suspension was collected into tubes, followed by spinning at 150 xg for 3.5 minutes. Supernatant was discarded to remove cell debris and dead cells, and cell pellets were resuspended in ice-cold PBS. The centrifuge and resuspension of cells were repeated twice. Cell pellets were resuspended in solution containing Fluorescein Isothiocyanate (FITC)-labelled annexin V, PI, and incubation buffer according to the kit instruction. Stained cells were then incubated in dark for 10 minutes before being analysed on a flow cytometer (BD Accuri^{TM} C6, USA). Annexin V and PI emissions were detected in the FL1 and FL2 channels, respectively. To estimate the spontaneous degranulation, similar protocols were carried out in cells without stimulation by IgE and DNP-HSA. Degranulation was expressed as a percentage of annexin V^+/PI^- cells relative to total cell population, and was calculated using BD Accuri^{TM} C6 software.

7.2.8 Statistical analysis

Data were analysed and graphs were drawn using PRISM v7.0 (Graph pad software). All data were expressed as mean ± standard error of mean (SEM) of independent experiments. Statistical analyses were performed using one-way ANOVA with Dunnett correction and Student's unpaired t-test. Results were considered statistically significant if p-value was less than 0.05.

7.3 Results

7.3.1 Concentrations of CWE ≤ 62.5 µg/ml did not affect viability of RBL-2H3 cells

Fig. 7.1 shows that concentrations of CWE ≤ 62.5 µg/ml treatment for 24 and 48 hours did not significantly affect the cell viability compared to vehicle control ($p > 0.05$). At 62.5 µg/ml of CWE, treatment for 24 hours ($p = 0.9831$) and 48 hours ($p = 0.8901$) were not significantly different from their respective vehicle control. Hence, concentration range of CWE between 3.9 to 62.5 µg/ml was used for the following assays. It is also noted that both treated and untreated cells incubated in FBS-free medium for 48 hours had greatly decreased cell viability, by ~2-fold compared to 24-hour incubation ($p < 0.001$).

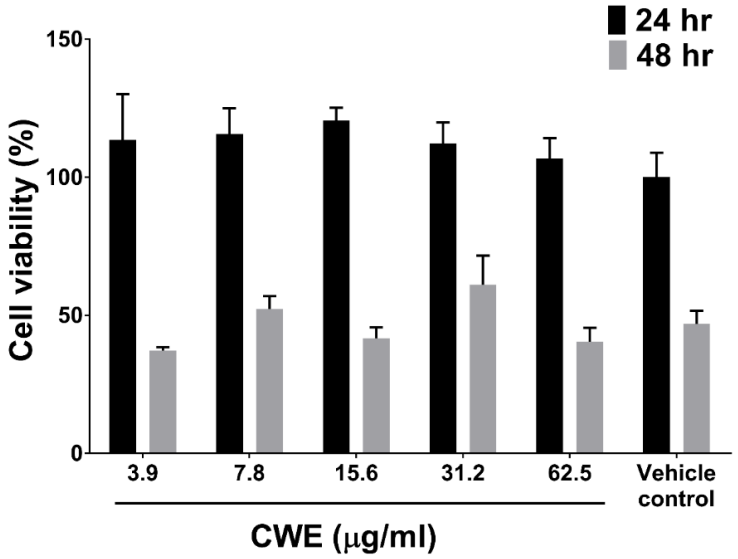

Figure 7.1: Effect of cold water extract on RBL-2H3 cell viability. RBL-2H3 cells were treated with various concentrations of CWE or purified water (vehicle control) for 48 hours (hr). Cell viability was examined by MTT assay. The cell viability was expressed as a percentage of viable cells in treated samples relative to the untreated cells from which blank control was subtracted. Untreated cells represent 100% cell viability. Data were shown as mean ± SEM of 3 independent experiments with 4 to 6 technical replicates in each run. (Abbreviations: CWE = cold water extract; MTT = 3-(4, 5-dimethylthiazolyl-2)-2, 5-diphenyltetrazolium bromide)

7.3.2 Concentrations of IgE and antigen for following degranulation assays were optimized

The following experiments served to optimize the concentrations of anti-DNP IgE and DNP-HSA for submaximal degranulation. Firstly, cells were sensitized with 0.5 µg/ml anti-DNP IgE while the concentration of DNP-HSA was varied. Fig. 7.2A shows that spontaneous release of β-hexosaminidase from RBL-2H3 cells was 4.67 ± 1.21%. In IgE-sensitized cells, 0.05 µg/ml of DNP-HSA stimulated highest β-hexosaminidase release (22.43 ± 6.81%), followed by 0.25 µg/ml of DNP-HSA (20.82 ± 10.84%). We therefore used the concentration that produced submaximal β-hexosaminidase release i.e. 0.25 µg/ml of DNP-HSA in subsequent experiments while varying the concentrations of IgE. 0.1 µg/ml of IgE produced highest amount of β-hexosaminidase release (39.88 ± 17.59%) when compared to other concentrations (Fig. 7.2B). The stimulated β-hexosaminidase release was ~11-fold higher than spontaneous release. Given that, the concentrations of anti-DNP IgE and DNP-HSA were determined to be 0.1 µg/ml and 0.25 µg/ml, respectively, for following assays.

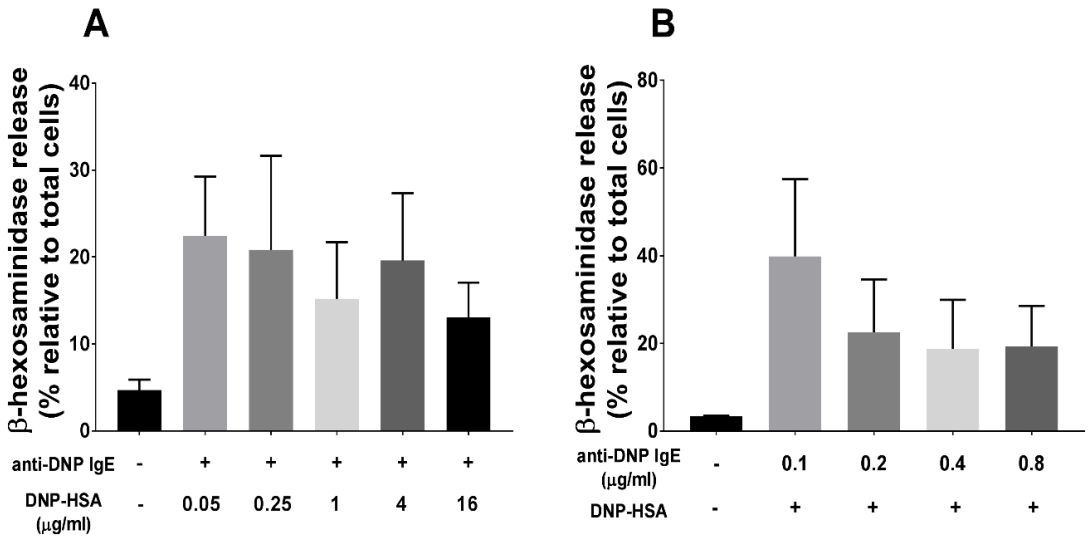

Figure 7.2: IgE/antigen-mediated degranulation as measured by β-hexosaminidase release. (A) Cells were sensitized with 0.5 µg/ml of anti-DNP IgE, before stimulated with various concentrations of DNP-HSA. Spontaneous release of β-hexosaminidase was measured in cells untreated by IgE and DNP-HSA (represented by double "-"). The concentration of DNP-HSA that produced submaximal release was determined as 0.25 µg/ml. Subsequently in (B), cells were sensitized with various concentrations of anti-DNP IgE, before stimulated with 0.25 µg/ml DNP-HSA. B-hexosaminidase release was expressed as a percentage relative to total β-hexosaminidase content in cell lysates. Data were shown as mean ± SEM of 3 independent experiments with 4 technical replicates in each run. (Abbreviations: anti-DNP IgE = Anti-dinitrophenyl immunoglobulin E; DNP-HSA = Dinitrophenyl-human serum albumin)

7.3.3 CWE triggered β-hexosaminidase release in unstimulated cells

In IgE/antigen-stimulated cells, statistical tests showed that pre-treatment with CWE in Siraganian buffer did not have significant effect on β-hexosaminidase activity (CWE 62.5 µg/ml vs vehicle: p = 0.186) (Fig. 7.3A). However, we observed a nonsignificant trend of increasing β-hexosaminidase release with higher concentrations of CWE in the stimulated cells (Fig. 7.3A) which correlated with the unstimulated cells (Fig. 7.3B). Pre-treatment with CWE slightly but nonsignificantly

increased the amount of β-hexosaminidase release by 18.70% (at 62.5 µg/ml CWE, p = 0.1861) compared to vehicle control (Fig. 7.3A). This coincided with Fig. 7.3B where 31.2 µg/ml and 62.5 µg/ml of CWE treatment alone in unstimulated cells significantly increased the β-hexosaminidase release by 17.16% (p = 0.0323) and 30.63% (p = 0.0005), respectively compared to vehicle control. These results suggest that CWE alone could stimulate degranulation in RBL-2H3 cells.

Next, we investigated if CWE-induced β-hexosaminidase release is an augmentation of stimulation with DNP-HSA. Cells were initially pre-treated with CWE in medium, and the medium containing treatment was then replaced with Siraganian buffer prior to stimulation with DNP-HSA. Statistical test showed no significant difference between treatments and vehicle control (CWE 62.5 µg/ml vs vehicle: p = 0.322) (Fig. 7.3C). Nevertheless, we observed a nonsignificant trend towards decreasing β-hexosaminidase release with increasing concentrations of CWE, by 13.01% (at 62.5 µg/ml CWE) lower than vehicle control. Ketotifen and chlorpheniramine did not have statistically significant effect on β-hexosaminidase release, but slight reduction of the release by both drugs was observed in Fig. 7.3A (by 21.94% and 19.30%, respectively) and in Fig 7.3C (by 10.99% and 6.5%, respectively). Our observations infer that CWE-induced β-hexosaminidase release is mainly accumulated during the incubation period. Pre-treatment with CWE may dampen subsequent allergen-stimulated degranulation.

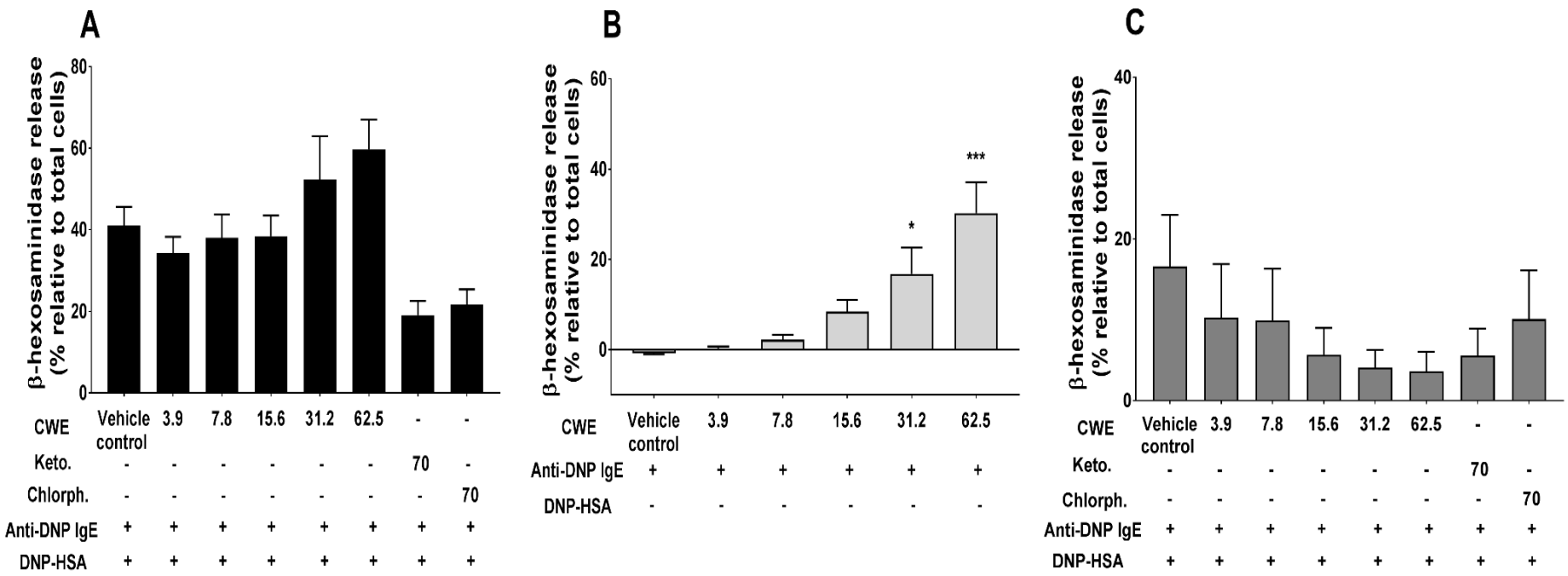

Figure 7.3: Effect of cold water extract on β-hexosaminidase release. (A) IgE/antigen-stimulated cells sensitized were treated with various concentrations of CWE, ketotifen, chlorpheniramine, or vehicle control (purified water) for 2 hours in Siraganian buffer. (B) Cells were sensitized by anti-DNP IgE, followed by incubation with CWE for 2 hours. DNP-HSA was not added in this experiment to investigate the effect of CWE alone on IgE-sensitized cells. Similar protocols in (A) were performed for (C), except that treatments were first incubated in FBS-free medium for 2 hours, and the medium containing the treatment was then replaced with Siraganian buffer. DNP-HSA was added in (A) and (C) to stimulate β-hexosaminidase release. Concentrations of CWE were expressed in μg/ml while ketotifen and chlorpheniramine were expressed in μM. Net β-hexosaminidase release (from which spontaneous release was subtracted) was expressed as a percentage relative to total β-hexosaminidase content in cell lysates. Data were shown as mean ± SEM of 3 to 4 independent experiments with 3 to 4 technical replicates in each run. One-way ANOVA with Dunnett correction between control and treatment: $*p < 0.05$, $***p < 0.001$. (Abbreviations: Anti-DNP IgE = Anti-dinitrophenyl immunoglobulin E; Chlorph. = Chlorpheniramine; CWE = Cold water extract; DNP-HSA = Dinitrophenyl-human serum albumin; Keto. = Ketotifen)

7.3.4 CWE decreased degranulation index in IgE/antigen-stimulated cells via Alcian blue staining

Fig. 7.4A shows that degranulation index was significantly increased in IgE/antigen-stimulated cells by 33.66% (p = 0.0301) higher than unstimulated cells, indicating an increased degranulation in stimulated cells with fading of Alcian blue stain. Representative figures of unstimulated and stimulated cells are shown in Fig. 7.4B and C, respectively where degranulated cells were characterized by vacuolated cytoplasm, faded purple red stain (Safranin O) in cytoplasm, absence of blue-stained granule and less distinct outer membrane outline.

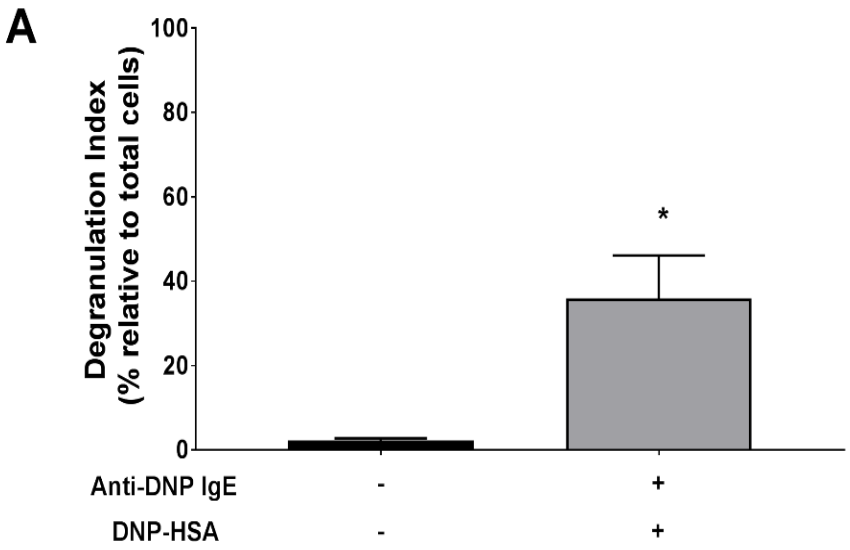

Figure 7.4: IgE/Antigen-induced degranulation characterized by Alcian blue staining. (A) Degranulation index was calculated in cells in the absence or presence of stimulation by anti-DNP IgE and DNP-HSA. Degranulation index was expressed as a percentage of degranulated cells (unstained) normalized to total number of cells (Alcian blue-stained and unstained) in four fields of view. Data were shown as mean ± SEM of 4 independent experiments. Unpaired T-test between groups: *p < 0.0001. (Abbreviations: anti-DNP HSA = Anti-dinitrophenyl immunoglobulin E; DNP-HSA = Dinitrophenyl-human serum albumin, IgE = Immunoglobulin E)

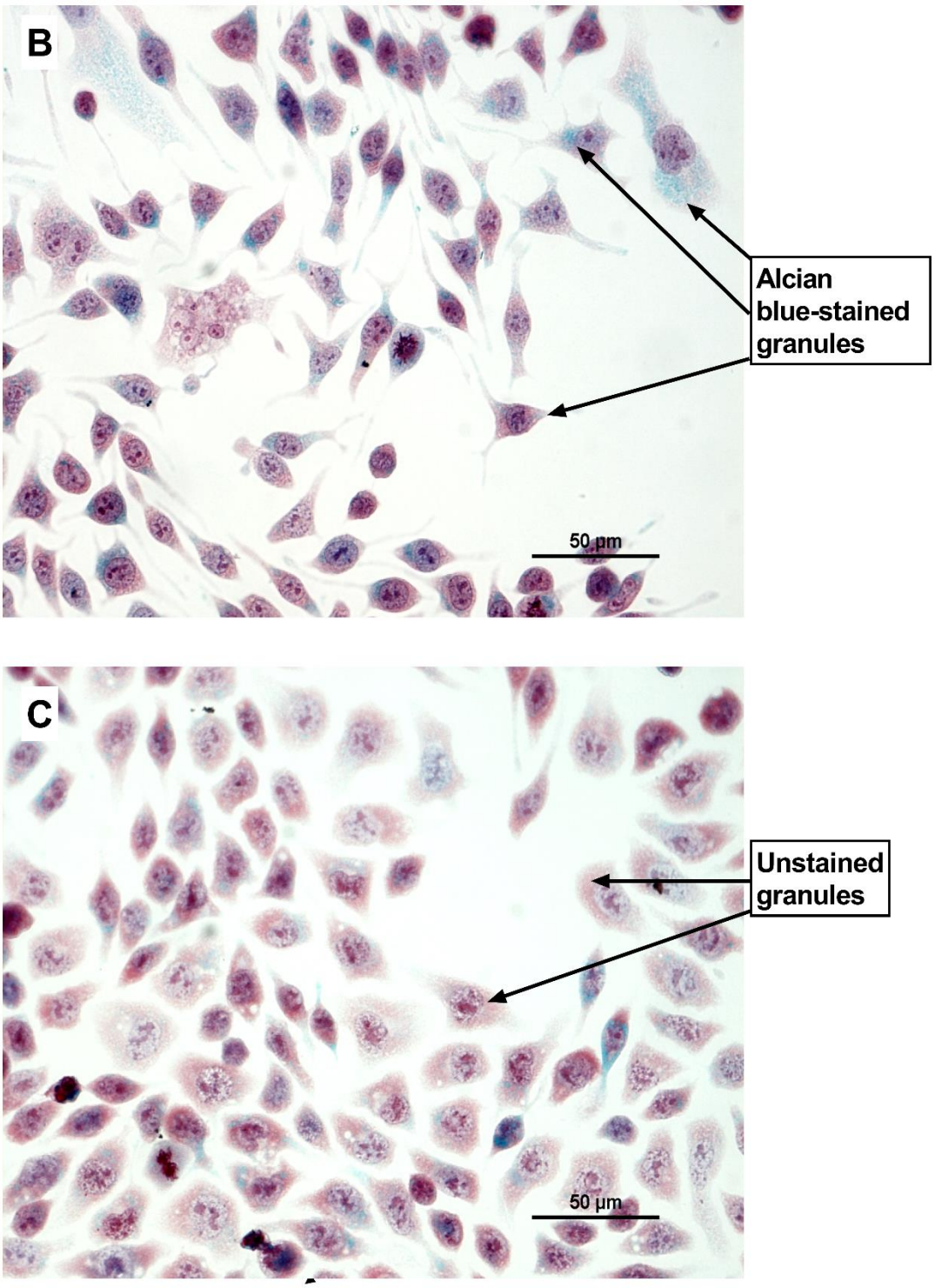

Figure 7.4: (B) and (C) are representative figures of cells characterized by Alcian blue staining. There was increased degranulation with faded blue stain in (C) stimulated cells compared to (B) unstimulated cells.

Subsequently, we investigated the effect of pre-treatment with CWE on stimulated cells for 2 hours and 5 hours. Fig. 7.5A and B show that pre-treatment with ketotifen for 2 hours and 5 hours significantly decreased the degranulation index in stimulated cells by 23.84% and 26.2%, respectively, when compared to respective vehicle control. Treatment with CWE from 3.9 µg/ml to 62.5 µg/ml for 5 hours significantly reduced the degranulation index, with maximum response 31.82% lower than vehicle control (Fig. 7.5B). Shorter duration of treatment with CWE i.e. 2 hours exhibited nonsignificant trend of decreasing degranulation index with higher concentrations of CWE, with maximum response 14.17% lower than vehicle control (Fig. 7.5A). Treatment with chlorpheniramine for 5 hours slightly decreased the degranulation index by 17.16% compared to vehicle control (Fig. 7.5B). Representative figures of untreated and treated cells are shown in Fig. 7.5C to F. Degranulation index and p-values are summarized in Table 7.1.

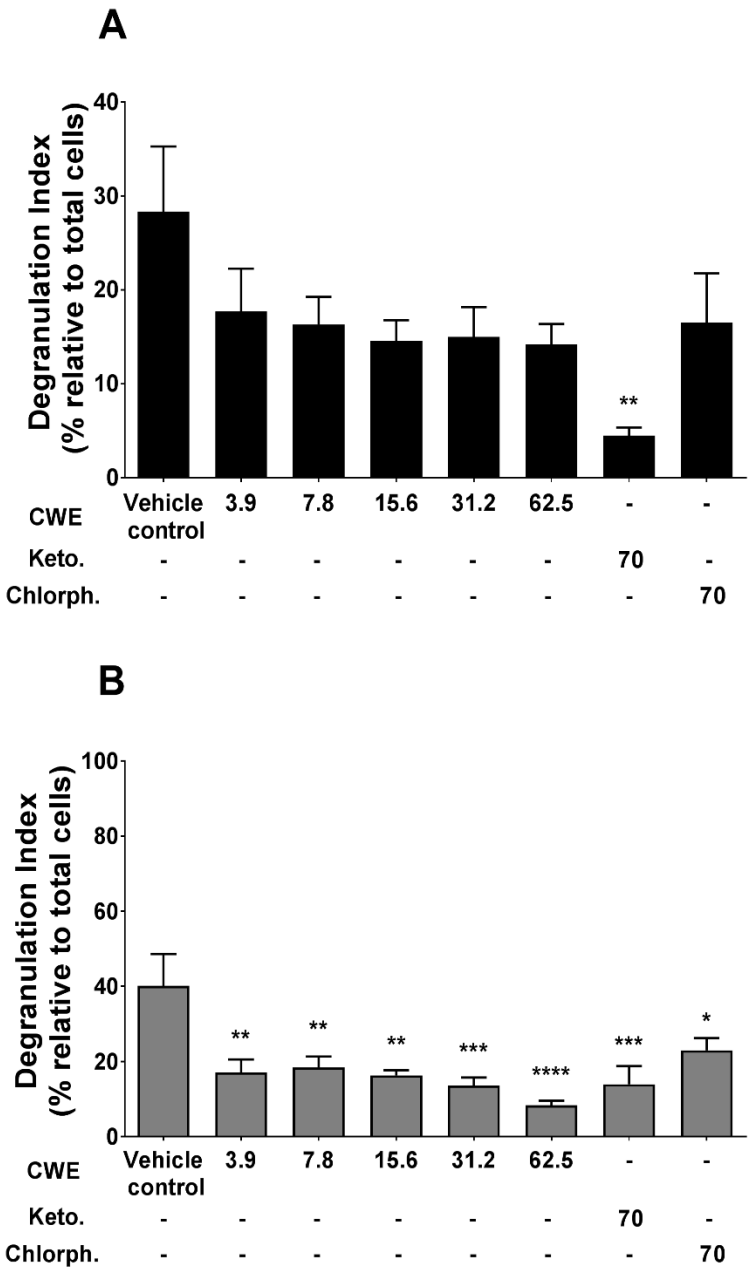

Figure 7.5: Effect of cold water extract on degranulation index of IgE/antigen-stimulated cells characterized by Alcian blue staining. IgE-sensitized cells were treated with CWE, ketotifen, chlorpheniramine, or vehicle control (purified water) for (A) 2 or (B) 5 hours, followed by stimulation with DNP-HSA. Concentrations of treatments were expressed in µg/ml while ketotifen and chlorpheniramine were expressed in µM. Degranulation index was expressed as a percentage of degranulated cells (unstained) normalized to total number of cells (unstained and Alcian blue-stained) in four fields of view. Data were shown as mean ± SEM of 3 to 4 independent experiments. One-way ANOVA with Dunnett correction was made between treatment and vehicle control: *$p < 0.05$, **$p < 0.01$, ***$p < 0.001$, ****$p < 0.0001$ (Abbreviations: Anti-DNP IgE: Anti-dinitrophenyl immunoglobulin E; Chlorph.: Chlorpheniramine; CWE: Cold water extract; DNP-HSA: Dinitrophenyl-human serum albumin, Keto.: Ketotifen)

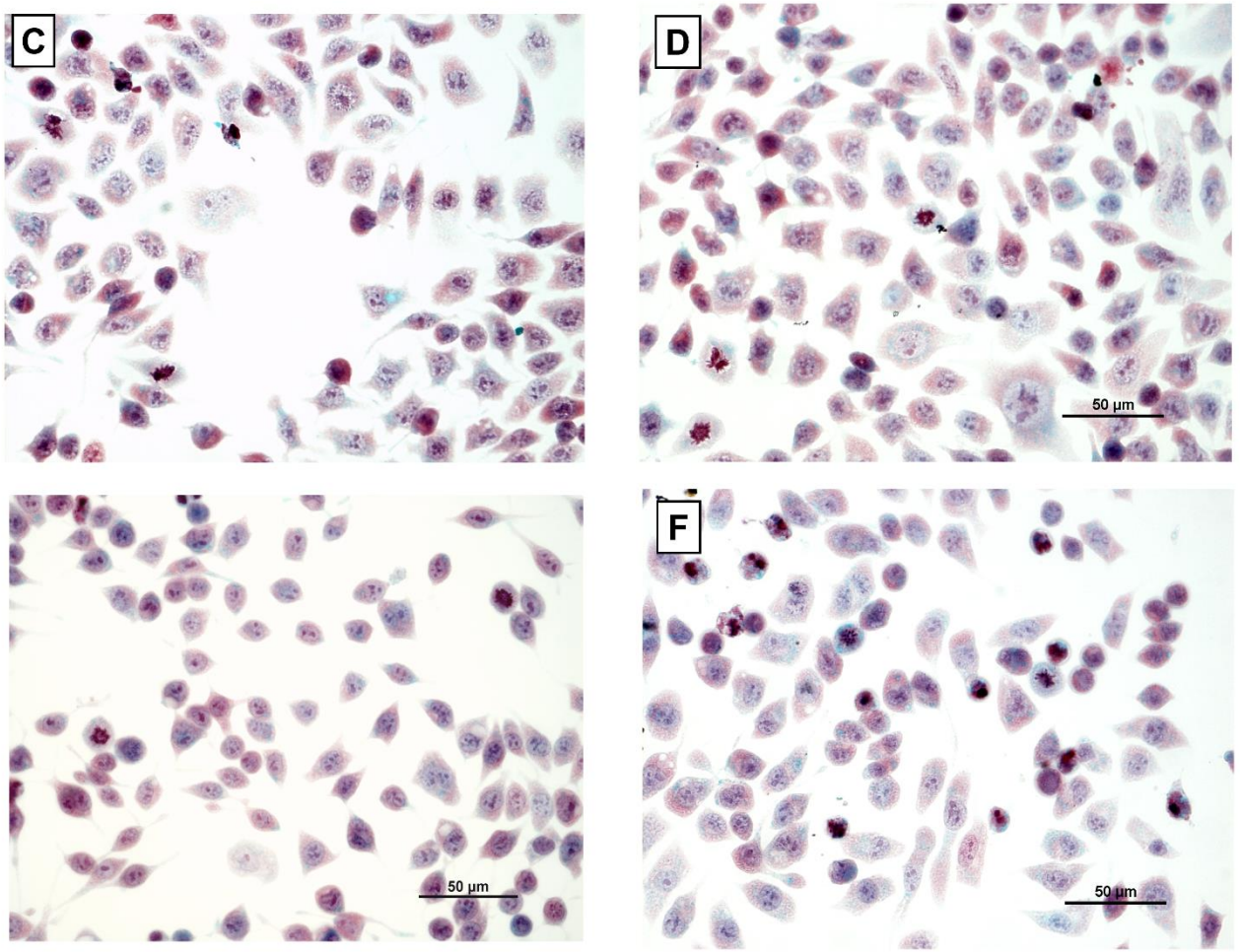

Figure 7.5: (C) to (F) are representative figures of IgE/antigen-stimulated cells characterized by Alcian blue staining with 5-hour treatment. (C): Vehicle control, (D): CWE 3.9 µg/ml, (E): CWE 62.5 µg/ml, (F): Ketotifen 70 µM.

Table 7.1: Degranulation index of RBL-2H3 cells treated with cold water extract. IgE/antigen-stimulated RBL-2H3 cells were treated for 2 or 5 hours with CWE before subjected to Alcian blue staining. One-way ANOVA with Dunnett correction where comparison of the means was made between vehicle control and the treatment groups (*p < 0.05, **p < 0.01, ***p < 0.001, ***p < 0.0001). Data represented the means ± SEM of 3 to 4 independent experiments.

Treatments	2-hour		5-hour	
	Degranulation index (%)	p-value	Degranulation index (%)	p-value
+ Vehicle (water)	28.33 ± 6.93	-	40.14 ± 8.50	-
+ CWE 3.9 µg/ml	17.68 ± 4.59	0.486	17.07 ± 3.48**	0.004
+ CWE 7.8 µg/ml	16.31 ± 2.95	0.296	18.44 ± 2.90**	0.007
+ CWE 15.6 µg/ml	14.59 ± 2.18	0.153	16.32 ± 1.34**	0.003
+ CWE 31.2 µg/ml	14.98 ± 3.18	0.178	13.62 ± 2.13***	0.001
+ CWE 62.5 µg/ml	14.16 ± 2.21	0.129	8.32 ± 1.25****	< 0.0001
+ Ketotifen 70 µM	4.49 ± 0.85**	0.002	13.94 ± 4.82***	0.001
+ Chlorpheniramine 70 µM	16.52 ± 5.24	0.3199	22.98 ± 3.21*	0.0475

Abbreviations: CWE = Cold water extract; RBL-2H3: Rat basophil leukaemia

To examine the effect of CWE alone on unstimulated cells, IgE-sensitized cells were incubated with CWE for 2 hours before subjected to Alcian blue staining. Fig. 7.6 shows that there was no significant difference between CWE treatment groups and vehicle control. We, however, observed a slight nonsignificant increasing trend of degranulation index with increasing concentrations of CWE. The degree of degranulation index induced by 62.5 µg/ml of CWE was 11.81% higher than vehicle control ($p > 0.9999$).

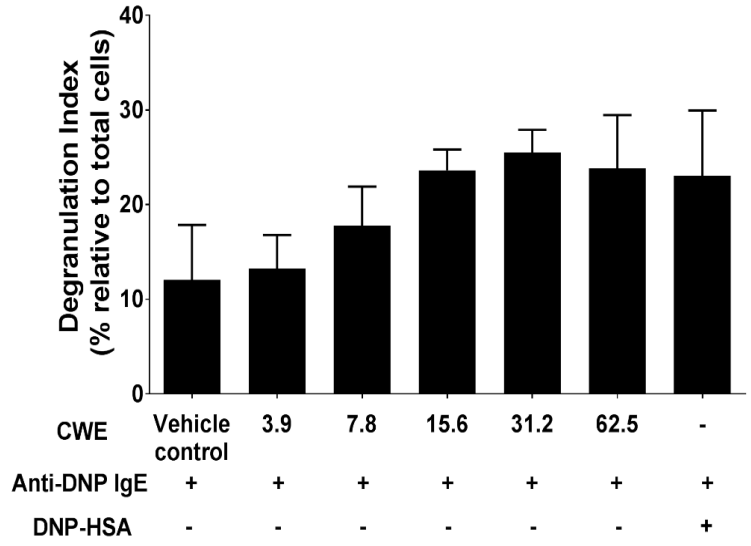

Figure 7.6: Effect of cold water extract on degranulation index of unstimulated cells characterized by Alcian blue staining. IgE-sensitized cells were treated with CWE or vehicle control (purified water) for 2 hours before subjected to Alcian blue staining. Concentrations of CWE were expressed in µg/ml. Degranulation index was expressed as a percentage of degranulated cells (unstained) relative to total number of cells (Unstained and stained with Alcian blue) in four fields of view. Data were shown as mean ± SEM of 3 independent experiments. (Abbreviation: CWE: Cold water extract; Anti-DNP IgE = Anti-dinitrophenyl immunoglobulin E; DNP-HSA = Dinitrophenyl-human serum albumin)

7.3.5 CWE increased phosphatidylserine externalization in unstimulated cells

Early apoptosis (annexin V^+/PI^- cells) is frequently used as an indicator for degranulation in RBL-2H3 cells. First, we investigated the effect of IgE/antigen stimulation on degranulation. Fig. 7.7A demonstrates that stimulation with DNP-HSA significantly increased the degranulation by 68.78% ($p < 0.0001$) compared to unstimulated cells. In IgE-sensitized cells (unstimulated with DNP-HSA), CWE treatment alone at all concentrations significantly increased the degranulation with maximum response of 74.18% higher than vehicle control ($p = 0.001$) (Fig. 7.7B).

In IgE/antigen-stimulated cells, treatments with CWE from 3.9 µg/ml to 62.5 µg/ml for 2 and 5 hours were devoid of effect on the degranulation in stimulated cells (2-hour treatment with CWE 62.5 µg/ml vs vehicle control: $p = 0.355$; 5-hour treatment with CWE 62.5 µg/ml vs vehicle control: $p = 0.9486$) (Fig. 7.7C and D). Treatment with ketotifen for 2 hours decreased the degree of degranulation in stimulated cells by 30.32% ($p = 0.0096$) lower than vehicle control (Fig. 7.7C). However, 5-hour treatment with ketotifen did not affect the degree of degranulation ($p = 0.7299$) (Fig. 7.7D). Representative density plots of flow cytometry are shown in Fig. 7.8.

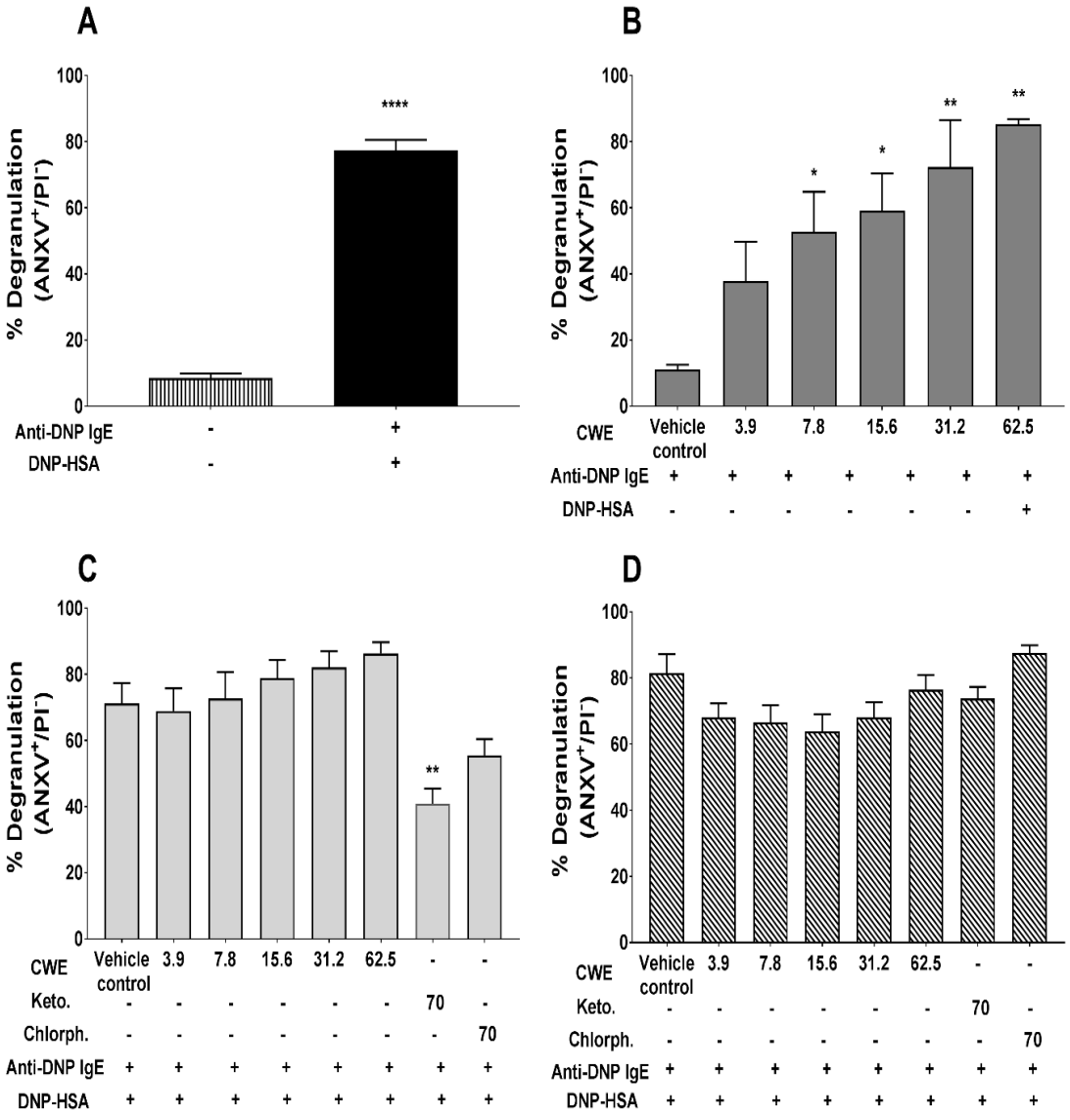

Figure 7.7: Flow cytometric analysis of the effect of cold water extract on cell degranulation. (A) Cells were analysed in the presence or absence of anti-DNP IgE sensitization and DNP-HSA stimulation. (B) Unstimulated cells were treated with different concentrations of CWE or purified water (vehicle control) for 2 hours. In a different set of experiments, IgE/antigen-treated cells were treated with different concentrations of CWE, ketotifen, chlorpheniramine, or purified water (vehicle control) for (C) 2 or (D) 5 hours. After the above treatments, cells were stained with FITC-labelled annexin V and propidium iodide followed by flow cytometric analysis. Concentrations of CWE were expressed in µg/ml while ketotifen and chlorpheniramine were expressed in µM. Degranulation was expressed as a percentage of annexin V^+/PI^- cells relative to total cell population. Data were shown as mean ± SEM of 3 to 4 independent experiments with 2 to 3 technical replicates in each run. (A) Unpaired t-test and (B) one-way ANOVA with Dunnett correction between treatment and vehicle control: $*p < 0.05$, $**p < 0.01$, $****p < 0.0001$. (Abbreviations: CWE = Cold water extract; Anti-DNP IgE = Anti-dinitrophenyl immunoglobulin E; Chlorph. = Chlorpheniramine; DNP-HSA = Dinitrophenyl-human serum albumin; Keto. = Ketotifen)

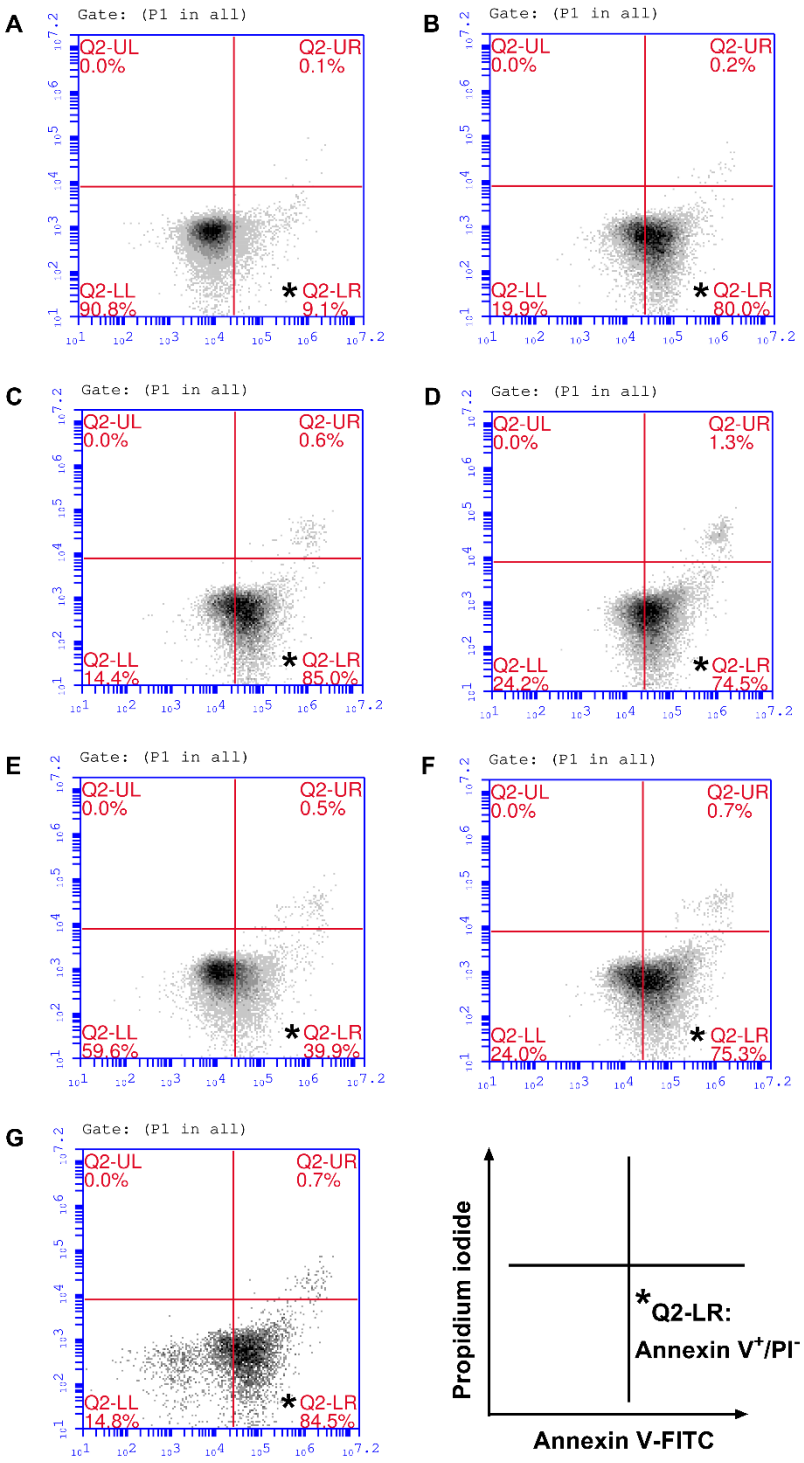

Figure 7.8: Representative density plots of flow cytometric analysis on RBL-2H3 cells stained with FITC-labelled annexin V and propidium iodide. (A) Unstimulated cells. In (B) to (F), IgE/antigen-stimulated cells were treated with (B) vehicle control for 2 hours, CWE 62.5 µg/ml for (C) 2 hours and (D) 5 hours, or ketotifen 70 µM for (E) 2 and (F) 5 hours. (G) IgE-sensitized cells treated with CWE 62.5 µg/ml alone for 2 hours. Annexin V^+/PI^- cells (phosphatidylserine exposure) was represented in Q2-LR and was shown as a percentage of total cell population. (Abbreviations: Anti-DNP IgE: Anti-dinitrophenyl immunoglobulin E; CWE: Cold water extract; DNP-HSA: Dinitrophenyl-human serum albumin, PI = Propidium iodide)

7.4 Discussions

MTT assay conducted in the present chapter showed that treatment with CWE concentrations from 3.9 to 62.5 µg/ml for 24 and 48 hours did not affect the viability of RBL-2H3 cells. When treated for 48 hours in FBS-free medium, the overall cell viability, including vehicle control, had largely decreased compared to 24-hour treatment. In following assays, the duration of cells incubated in FBS-free medium (from overnight IgE sensitization of RBL-2H3 cells to treatment) was performed within 24 hours, and the overall cell viability should not be affected.

Our results demonstrated that the extent of degranulation in unstimulated and untreated cells (spontaneous release) was less than 10% throughout all assays. IgE/antigen stimulation also consistently increased level of degranulation as measured with assays of β-hexosaminidase release, Alcian blue staining and annexin V binding. Through microscopic observation, reduced Alcian blue-stained granules and sparse intracellular particles were observed in IgE/antigen-stimulated cells, indicating a reduction of secretory granules during degranulation. The degree of IgE/antigen-induced degranulation in β-hexosaminidase and annexin V binding assays correlated with each other, with ~11-fold and ~9-fold increase from unstimulated cells, respectively. The consistency of results between β-hexosaminidase and annexin V binding assay is in accordance with the study by Demo et al. (1999). The release of β-hexosaminidase exhibited a bell-shaped CRC to increasing concentrations of anti-DNP IgE, which is in line with previous report by Dearman et al. (2005).

On the other hand, microscopic analysis with Alcian blue staining in IgE/antigen-stimulated cells showed distinct morphological changes in RBL-2H3 cells and faded blue stain, indicating secretory granules had reduced during

degranulation. IgE/antigen stimulation was also found to induce ~16-fold higher degranulation index as compared to unstimulated cells in Alcian blue assay. This suggests that the fading of Alcian blue stain is not in proportion to the levels of β-hexosaminidase release and annexin V binding, inferring that IgE/antigen stimulation triggers similar degree of phosphatidylserine exposure and β-hexosaminidase release, but a higher degree of loss in Alcian blue-stained secretory granules.

We then investigated the effect of CWE on degranulation in IgE/antigen-stimulated cells. In both β-hexosaminidase (2-hour treatment) and annexin V binding (2- and 5-hour treatment) assays, CWE did not significantly affect the degree of degranulation. Alcian blue staining results showed that treatment with CWE for 2 and 5 hours has retained stained granules in the cells. The inconsistencies across these assays imply that CWE at these treatment concentrations and durations inhibit the reduction of secretory granules, but do not inhibit the β-hexosaminidase release and phosphatidylserine exposure on cell membrane. These observations seem to diverge with previous study where marked reduction in cytokines such as IL-4, IL-5 and IL-13 was observed with *L. rhinocerotis* treatment in ovalbumin-challenged mice model (Johnathan et al., 2016). However, the mentioned study used different extract i.e. hot water extract, and therefore may explain the discrepancy. It was also not determined if other mediators such as histamine and leukotrienes, which are typically released by mast cells are affected (Johnathan et al., 2016).

In addition, pre-treatment with ketotifen for 2 hours largely reduced the degree of IgE/antigen-triggered degranulation in annexin V binding and Alcian blue stain assays. Intriguingly, 5-hour treatment with ketotifen inhibited the reduction in stained granules but did not decrease amount of annexin V^+/PI^- cells. The lack of effect of ketotifen (treated for 2 hours) on β-hexosaminidase release also cannot be explained.

These results suggest that ketotifen inhibits the loss of granules but does not inhibit immediate β-hexosaminidase release and phosphatidylserine externalization. Ketotifen possesses mast cell stabilizing properties with concomitant H_1 receptor antagonism (Cuss, 1999). Mast cell stabilizer mainly acts by stabilizing the mast cells against activation by IgE/antigen to inhibit degranulation, but the precise molecular mechanisms remain obscure (Finn & Walsh, 2013). This is in contrast other studies where ketotifen (20 μM) treated for 10 min (W. Wang, Zhou, Liu, & Zou, 2012) and 30 min (Lian et al., 2015) significantly decreased β-hexosaminidase release from RBL-2H3 cells. We speculate that the discrepancy might be due to the treatment duration of ketotifen, as the results in flow cytometry showed that ketotifen was ineffective in reducing degranulation with relatively longer duration of treatment. Another possibility is that higher concentration of ketotifen, up to 100 μM, is required for effective inhibitory effect (De Souza Santos et al., 2013). Besides, chlorpheniramine also lacked of anti-degranulation effect as measured by β-hexosaminidase release and annexin V binding, in contrast with other researchers (Juckmeta et al., 2014). In general, RBL-2H3 cells showed inconsistent responses to mast cell stabilizers among different studies (Passante et al., 2009).

In unstimulated cells, CWE treatment alone significantly increased β-hexosaminidase release (Fig. 7.3B) and annexin V^+/PI^- cells (Fig. 7.7B), which are comparable to the degree of degranulation in IgE/antigen-stimulated cells and in a concentration-dependent and proportional manner. The replacement of medium containing CWE prior to stimulation with antigen have slightly reduced β-hexosaminidase release subsequently (Fig. 7.3C), suggesting that CWE stimulates β-hexosaminidase release during the pre-incubation period. We speculate that β-hexosaminidase is maximally released during CWE pre-incubation, and hence

subsequent IgE/antigen-stimulated β-hexosaminidase release is limited. Similar to IgE/antigen-stimulated cells, the degree of increased annexin V^+/PI^- cells in unstimulated cells was in proportion to the increase in β-hexosaminidase release in CWE-treated cells.

In line with this, the amount of annexin V^+/PI^- cells was shown to be proportional to the degree of degranulation associated with β-hexosaminidase release (Demo et al., 1999), and to a lesser extent with histamine release in relative to β-hexosaminidase (Peng et al., 2011). However, the molecular mechanisms of phosphatidylserine exposure linked to granular secretion remain unclear. The above findings suggest that CWE is inducing degranulation by itself. In contrast to the above assays, CWE alone did not have significant effect in Alcian blue staining, suggesting that the amount of granules are not decreased or degranulated. This finding is however at odds with literature in which the outcome of Alcian blue staining frequently correlates with that in β-hexosaminidase release (F. Huang et al., 2010). We cannot explain this but postulate that CWE may stimulate β-hexosaminidase release and exposure of granules on cell membrane, but prevent the loss of secretory granules.

Factor contributing to the contrasting actions of CWE is not known yet, and this is complicated by the presence of mixed components in CWE. Since CWE pre-treatment had triggered β-hexosaminidase release and phosphatidylserine externalization, we speculate that CWE may "prime" the cells to be resistant to further degranulation with antigen stimulation. Furthermore, the evidence gathered above infers that phosphatidylserine externalization and β-hexosaminidase release, which are in good correlation, are early processes in degranulation. Reduced secretory granules as characterized by the fading of Alcian blue stain may occur in a later stage of

degranulation. Therefore, it is possible that CWE and ketotifen may exhibit inhibitory effects on different stages of degranulation.

Noteworthy, the annexin V^+/PI^- staining indicates early apoptotic cells in general, and therefore it was not possible to discriminate between non-apoptotic degranulated cells and early apoptotic cells (unrelated to degranulation). We cannot exclude if the stimulation with DNP-HSA will also induce early apoptosis without degranulation in RBL-2H3 cells. However, phosphatidylserine exposure in apoptosis and non-apoptosis have distinct differences in terms of their time course of action. It occurs over a time course of seconds to a few minutes in non-apoptosis and over hours in apoptosis respectively (Rysavy et al., 2014). IgE/antigen stimulation for 30 minutes markedly and rapidly increased annexin V-bound phosphatidylserine exposure (Martin et al., 2000). By 24 hours after the stimulation, no difference in apoptotic nuclei or phosphatidylserine exposure as measured by flow cytometric analysis was detected when compared to unstimulated cells, indicating that phosphatidylserine exposure in mast cell degranulation is a non-apoptotic and reversible process (Martin et al., 2000). In our studies, it is noted that the tested concentrations of CWE that caused increased annexin V^+/PI^- cells were not cytotoxic, as shown in MTT assay. This suggests that phosphatidylserine exposure is a reversible process in degranulation, in agreement with the literature.

In murine primary lung mast cells, treatment with adenosine moderately reduced the IgE/antigen-induced β-hexosaminidase release (Hua et al., 2008). RBL-2H3 cells express adenosine A_3 receptors as evidenced by RNA sequencing and ligand binding studies (Ramkumar, Stiles, Beaven, & Ali, 1993). Large body of *in vitro* and *in vivo* evidence shows that A_3 receptors, and to a lesser extent A_{2B} receptors, are the main receptor subtypes implicated in activation of murine mast cell and basophils

through stimulating degranulation and release of mediators (Rudich, Ravid, & Sagi-Eisenberg, 2012). Pronounced elevation of plasma and serum histamine concentrations and mast cell degranulation were also observed in Sprague Dawley rats receiving A_3 receptor agonist (Fozard, Pfannkuche, & Schuurman, 1996). The function of A_{2B} receptors is however complexed by evidence of enhanced IgE/antigen-induced β-hexosaminidase release along with increased extracellular Ca^{2+} influx in bone marrow-derived mast cells of A_{2B} receptor knockout mice (Hua et al., 2007). By contrast, adenine was reported with anti-degranulation activity. Hosoi et al. (2018) revealed that in RBL-2H3 cells, IgE/antigen-induced releases of β-hexosaminidase and histamine, Ca^{2+} influx and downstream activation of Syk/Akt/ERK were inhibited by adenine. Adenine also inhibited β-hexosaminidase release induced by thapsigargin and Ca^{2+} ionophores in relatively lesser extent (Hosoi et al., 2018). In the same study, adenosine enhanced β-hexosaminidase release in RBL-2H3 cells, which is in consistent with previous literature.

Apart from adenosine and adenine, polysaccharides exhibited inhibitory effects on mast cell degranulation. A low-molecular-weight β-glucan derived from *Aureobasidium pullulans*, a yeast-like fungus, was shown to inhibit IgE/antigen-induced β-hexosaminidase release from RBL-2H3 and bone marrow-derived cultured mast cells (Sato et al., 2012). However, high concentrations of β-glucan were required to exhibit a significant effect (500 to 1000 μg/ml in RBL-2H3 cells; 250 to 1000 μg/ml in cultured mast cells). The stimulatory effect of CWE on β-hexosaminidase release and phosphatidylserine exposure was not entirely unexpected because some mushroom polysaccharides also demonstrated immunostimulatory activities through activation of innate immune cells including macrophage, natural killer cells, and neutrophils (J. Y. Kim et al., 2008; Nandi et al., 2014; Wong et al., 2009). It is however

not known if the polysaccharides will exert direct stimulating effect on mast cells. Although the bioactive component contributing to the modulatory effect of CWE on RBL-2H3 cells degranulation is unclear yet, it is reasonable to speculate that adenosine, adenine, and β-glucan present in the *L. rhinocerotis* (Section 2.3.3, **Chapter 3**) might play a role.

Ca^{2+} plays a pivotal role in mast cell degranulation, in which entry of Ca^{2+} is essential for the activation and subsequent release of chemical mediators from secretory granule The exocytosis in mast cells can be evoked by Ca^{2+} ionophores, indicating a role of the elevated cytosolic Ca^{2+} concentration in the acceleration of exocytosis (Hong-Geller & Cerione, 2000). DNP-HSA was shown to induce Ca^{2+} mobilization in association with degranulation in RBL-2H3 cells (Hosoi et al., 2018). Increased $[Ca_{2+}]_i$ results in binding of Ca^{2+} to calmodulin that activates MLCK and subsequent signalling pathways. Interestingly, it was reported that a calmodulin antagonist, W-13, also exhibited contrasting effect on degranulation of RBL-2H3 cells (Funaba, Ikeda, & Abe, 2003). Treatment with W-13 alone slightly increased the release of β-hexosaminidase, but the subsequent ionomycin-induced β-hexosaminidase release was dampened. This resembles the action of CWE. In **Chapter 4**, CWE blocked extracellular Ca^{2+} entry into cells in isolated airways and DRG cells, possibly via inhibition of membrane calcium channels. Experiments herein do not allow further interpretation of the effect of CWE on Ca^{2+} entry into mast cells, but we speculate that CWE may regulate the Ca^{2+}-calmodulin pathway, contributing to the biphasic actions.

To summarize, the present chapter demonstrated that in unstimulated RBL-2H3 cells, treatment with CWE alone increased phosphatidylserine externalization and β-hexosaminidase release. On the other hand, no difference was observed on the

amount of Alcian blue-stained secretory granules in cells treated with CWE alone. In IgE/antigen-stimulated RBL-2H3 cells, CWE preserved the Alcian blue-stained granules, but had no statistically significant effect on phosphatidylserine externalization and β-hexosaminidase release. The tested concentrations of CWE were not cytotoxic as indicated in the MTT assay, implying that the increased phosphatidylserine exposure are presumably associated with degranulation. Overall results suggest that CWE has stimulatory effect on degranulation of unstimulated mast cells, but may inhibit the loss of secretory granules during degranulation process in IgE/antigen-stimulated cells.

Chapter 8. General discussions

Available records revealed that *L. rhinocerotis* is most commonly used for treating asthma and chronic cough. Although previous work had been conducted to examine the effect of *L. rhinocerotis* on inflammatory markers of asthma (Johnathan et al., 2016), a direct physiological evidence of the airway relaxation effect was still lacking. Thus, there is a compelling need to scientifically validate the traditional usage of *L. rhinocerotis* for treating these respiratory conditions and to bridge the gap in existing research literature.

In light of this, this research was initiated to evaluate the pharmacological actions of *L. rhinocerotis* on smooth muscles, especially airways, and effects on mast cells to substantiate their traditional usage as well as to explore its potential as alternative or adjunct treatment with conventional antiasthmatic therapies. We also investigated for the first time the effects of *L. rhinocerotis* extract on vascular and ileal smooth muscles to characterize the mechanisms of action of this mushroom in different tissues and to support its actions on airways.

To fulfil this, several research questions were set out in the introduction of this thesis (Section 1.5, **Chapter 1**): (1) What are the effects and mechanisms of action of the crude extracts of *L. rhinocerotis* on airway smooth muscle as well as other smooth muscles (blood vessels and ileum)? (2) How does fractionation of *L. rhinocerotis* by molecular weight affect the airway relaxation effect? (3) What are the effects of the crude extract of *L. rhinocerotis* on mast cell degranulation? These questions were addressed in the following subsections.

8.1 Pharmacological effects and mechanisms of action of crude extracts of *L. rhinocerotis*

Since traditional preparation methods of *L. rhinocerotis* for treating airway diseases are through dissolving in hot water or eaten raw, it was hypothesized that hot water and cold water extraction would exhibit bronchodilator effect. To test this hypothesis, hot water extract (HWE), cold water extract (CWE) and methanol extract (ME) of *L. rhinocerotis* were prepared based on extraction methods adapted from literature. The relaxation effects of these extracts were examined on pre-contracted rat tracheal and bronchial segments using organ bath technique. Our results demonstrated that CWE has time-dependent and concentration-dependent airway relaxation effect, supporting our hypothesis. Unexpectedly, HWE and ME were devoid of effect. We thus postulated that the bioactive substances may be heat-labile or water-soluble, or the traditional benefit in hot water preparation is due to synergism with other herbs. To our knowledge, this is the first report of direct bronchodilator activities of *L. rhinocerotis* extract. Findings deduced from this study set a basis for subsequent investigations of the most active extract, CWE, as described below.

8.1.1 Airway smooth muscle

The main focus of this thesis is to investigate the pharmacological and mechanisms of action of *L. rhinocerotis* on airways. The effect of CWE on rat isolated airways contracted by different contractile agonists was examined using organ bath set up. Results showed that CWE remarkably reduced carbachol-induced pre-contraction in a time-dependent and concentration-dependent manner. Pre-treatment with CWE also

showed pronounced non-competitive antagonistic effects on carbachol- and 5-HT-induced contractions. Activations of M_3 receptors and 5-HT, especially 5-HT_{2A}, receptors associated with airway contraction are presumably coupled to $G_{\alpha q}$ protein (Hazelwood & Sanders-Bush, 2004; Kurrasch-Orbaugh et al., 2003)**.** The above observations suggest that the relaxation effect of CWE is not mediated through direct blockade of muscarinic receptor, but possibly through inhibition of components downstream of $G_{\alpha q}$-coupled signaling pathway. Another possibility is that CWE may activate independent relaxing mechanisms such as cAMP and cGMP pathways. In support of this, CWE significantly inhibited KCl-induced pre-contraction, in a similar degree of response against carbachol-induced pre-contraction. KCl is known to depolarize cell membrane, causing smooth muscle contraction primarily through opening of L-type calcium channels (Sanderson et al., 2008). We thus deduced two hypotheses about the mechanisms of action mediated by CWE and tested them subsequently: (1) CWE activates either cAMP or cGMP pathways, or (2) CWE blocks membrane calcium channels, especially L-type calcium channels.

The first hypothesis was refuted by subsequent experiments, as both inhibitors of PDE4 (which selectively degrades cAMP) and NO synthase did not affect CWE-induced relaxation. Further investigations showed that CWE did not affect β-adrenoceptors and TEA-sensitive K^+ channels. It is generally accepted that β-adrenoceptor activation leads to elevated levels of cAMP that in turn activate PKA. One of the actions of PKA is believed to trigger the opening of BK_{Ca} channels (Barisione et al., 2010), which is sensitive to blockade by TEA (Kotlikoff, 1993), leading to membrane hyperpolarization and smooth muscle relaxation. Hence, the above findings further support that cAMP pathway may not be implicated. However,

we cannot completely rule out the involvement of cAMP and cGMP pathways as CWE-induced relaxation was slightly augmented by non-selective PDE inhibition.

In support of the second hypothesis, the role of CWE on membrane calcium channels was confirmed in subsequent investigations. In the absence of external Ca^{2+} (Ca^{2+}-free Krebs solution) protocol, CWE was shown to block Ca^{2+}-induced contraction, in which the effect was mirrored by nifedipine, a L-type calcium channel blocker. Besides, CWE did not affect the initial peak of carbachol-induced contraction (contributed by both intracellular and extracellular Ca^{2+}) but had attenuated the sustained phase of carbachol-induced contraction (predominantly depend on extracellular Ca^{2+} influx) in calcium-free Krebs solution. This was further validated by the observation that contractions induced by carbachol, 5-HT, and KCl almost completely depended on the presence of external Ca^{2+}, and intracellular Ca^{2+} only played an insignificant role. Subsequently, we revealed that carbachol-induced contraction was partially inhibited by nifedipine, SKF96365 and 2-APB, implying that muscarinic receptors couple to TRPC and L-type calcium channels in airway smooth muscle. Since pre-exposure of airway tissues to Pyr3, a TRPC3 channel inhibitor, did not affect carbachol-induced contraction, TRPC3 channel may play a minor role. Taken together, CWE may exert inhibitory effect on membrane calcium channels, especially L-type calcium channels and TRPC channels.

The above results of CWE in rat airways paralleled the findings in porcine bronchioles, strongly suggesting that the airway relaxation effect is not species-specific. Similar to rat airways, CWE exhibited concentration-dependent relaxation on porcine bronchioles contracted by carbachol, in which the contraction was sensitive to blockade of TRPC and L-type calcium channels. This is consistent with earlier study by Flores-Soto et al. (2013) where L-type calcium channels and SOCC are the primary

channels of extracellular Ca^{2+} influx for carbachol-induced contraction in guinea pig trachea. CWE also significantly inhibited Ca^{2+}-induced contraction in calcium-free Krebs solution, confirming that it blocks extracellular Ca^{2+} influx.

Unexpectedly, non-cumulative CRCs to CWE, but not cumulative CRCs, elicited contractile response on basal tone of both rat and porcine airways. CWE also potentiated KCl-induced contraction in calcium-free environment in porcine bronchioles, but not in rat airways. This contraction is unlikely to be due to immediate increase in $[Ca^{2+}]_i$ and we postulate that CWE may enhance the Ca^{2+} sensitivity of smooth muscle. Muscarinic receptor activation stimulates downstream DAG/PKC pathway that increases Ca^{2+} sensitivity of contractile apparatus in smooth muscle (Girolamo Pelaia et al., 2008). This hypothesis is in line with the results that CWE-induced contraction is mediated through muscarinic receptor activation (see Section 3.3.7, **Chapter 3**).

There are several speculations to CWE-induced contraction. Firstly, if the bronchodilator and bronchoconstricter effects are mediated through a single component in CWE, this component may act as a partial agonist that activates muscarinic receptors in the absence of muscarinic agonist but inhibits muscarinic receptors in the presence of muscarinic agonist. Secondly, the bronchodilator and bronchoconstricter effects are possibly induced by different components in CWE through different mechanisms. The first speculation challenges our previous proposition that CWE does not directly inhibit muscarinic receptors to relax carbachol-contracted airways, whereas the second speculation supports it.

Composition analysis of *L. rhinocerotis* sclerotial powder revealed the presence of polysaccharides (mainly β-glucans), glycoproteins, adenosine and its derivatives. Mixed actions of adenosine on airways had been reported in literature

(Burnstock et al., 2012; Spicuzza et al., 2006). Our results, however, had precluded the possibility that adenosine is the bioactive component responsible for the bronchodilator as well as bronchoconstricter effects.

8.1.2 Vascular smooth muscle

The mechanisms of action mediated by CWE as proposed in airway smooth muscle are backed by findings in vascular smooth muscle. Similar relaxant responses were elicited by CWE in rat aorta pre-contracted with phenylephrine and porcine coronary artery pre-contracted with U46619. Both phenylephrine and U46619 are known to activate $G_{\alpha q}$-coupled receptors, and extracellular Ca^{2+} influx through membrane calcium channels play an important role in causing smooth muscle contraction (Ding & Muray, 2005). The non-selective vasodilator effects of CWE on contractions induced by different contractile agonists support that the relaxation effect of CWE is mainly mediated through blockade of extracellular Ca^{2+} influx. CWE also decreased Ca^{2+}-induced contraction in calcium-free Krebs solution, in agreement with the results in airway smooth muscle. Furthermore, both phenylephrine- (Govindaraju et al., 2018) and U46619-induced contractions (see Section 5.3.5, **Chapter 5**) were blocked by inhibitors of L-type calcium channels and TRPC channels, supporting that both of these channels may be blocked by CWE. The role of TRPC channels in CWE-mediated relaxation is evidenced by the expression of their subtypes in airway smooth muscle of porcine, human, rat, and mice (Ay et al., 2004; Gosling, Poll, & Li, 2005; Sweeney et al., 2002; Xiao et al., 2010). Despite that our functional data herein point to the involvement of TRPC channels on airway and vascular smooth muscles, we failed to induce prominent airway contraction in rat with Hyp9 (TRPC6 activator) and

OAG (DAG and TRPC3/6/7 activator) in earlier experiments (data not shown). This challenged our hypothesis that CWE may inhibit TRPC channels in causing airway relaxation. In addition, the precise TRPC channel subtypes related to the relaxation effect remains elusive. Hence, the evidence of TRPC channels expression is clearly warranted. It should also be noted that the exact TRPC channel subtypes contributing to smooth muscle contraction are not fully defined yet, therefore the role of TRPC channels remains inconclusive.

Noteworthy, a higher concentration of CWE was required to achieve full relaxation in phenylephrine-contracted aorta when compared to carbachol-contracted airway smooth muscle. This may be explained by our earlier publication in which intracellular Ca^{2+} plays relatively bigger role in $G_{\alpha q}$-coupled receptor-mediated contraction in rat aorta compared to trachea (Govindaraju et al., 2018). Based on our interpretation above, the airway relaxation effect of CWE is mostly mediated via inhibition of extracellular Ca^{2+} influx, and hence it may have a relatively bigger impact on airway smooth muscle.

In addition, the involvement of EDRFs and NO pathway in CWE-induced relaxation of aorta was ruled out, indicating that NO/cGMP pathway is unlikely to be involved and supporting the results in airway smooth muscle. Carbachol-induced relaxation (presumably through endothelial M_3 receptor activation) in aorta was unaffected in the presence of CWE. This further refuted our previous hypothesis of CWE acting as a partial agonist that inhibits the muscarinic receptors in the presence of muscarinic agonist. In contrast to airway tissues, CWE did not elicit contractile response on aorta and coronary artery at basal tone. This may support previous hypothesis that CWE induces contraction through muscarinic receptor activation and

relaxation through inhibition of calcium channels or other components downstream of $G_{\alpha q}$-coupled signaling pathway.

8.1.3 Ileal smooth muscle

To examine the effect of CWE on endogenous acetylcholine release, contraction of ileal tissues was evoked by electrical field stimulation. CWE abolished electrically evoked neurogenic contraction but increased the basal tone in the same tissue. These responses apparently coincided with the results in airway smooth muscle, but subsequent mechanistic studies showed opposing outcomes. The reduction in neurogenic contraction was not mediated via muscarinic, α_2-adrenergic and opioid receptors. Unexpectedly, CWE-attenuated neurogenic contraction may be mediated via Ca^{2+} influx through activation of L-type calcium channels, as evidenced by a slightly enhanced inhibition of neurogenic contraction by CWE in the presence of nifedipine. This finding is at odds with previous results in airway and vascular smooth muscle where CWE was demonstrated to block L-type calcium channels. Evidence supports the role of L-type calcium channels in electrically stimulated contraction of guinea pig ileum (Y Ito, Kuriyama, & Parker, 1988; Sadraei et al., 2011; Yokoyama & Yagasaki, 1990). Based on the assumption that opening of L-type calcium channels on smooth muscle and cholinergic nerve endings results in neurogenic contraction of ileum, CWE might act as an inverse agonist on L-type calcium channels.

Moreover, the increased basal tension elicited by CWE was potentiated by muscarinic receptor blockade, suggesting that CWE may counteract its contracting effect by activating muscarinic receptors through another component. From these

observations, we speculate that while one component in CWE stimulates ileal contraction, another component counteracts the contracting effect through activation of muscarinic autoreceptors. This contrasted with the observations in airway and vascular smooth muscles. Further investigations showed that CWE-induced basal contraction was not mediated via L-type calcium channels, α_2-adrenoceptors, and opioid receptors. Given that adenosine had been shown to relax and contract ileal tissues through activation of pre- and post-junctional adenosine receptors by other researchers (Bornstein, 2008), it is therefore reasonable to speculate that it may partly contribute to the inhibitory effect of CWE on neurogenic contraction.

8.1.4 Summary of findings on smooth muscles

Relaxation effects of CWE of *L. rhinocerotis* were explicitly shown in different types of smooth muscles of different species. In all tissues, the efficacies of CWE-induced relaxation were near to or $\geq 100\%$. Gathered functional evidence from different tissues strongly suggests that β-adrenoceptors, K^+ channels, cAMP and NO/cGMP pathways are possibly not involved. Overall findings strongly support that the potential mechanisms of action of CWE–induced relaxation is through inhibition of membrane calcium channels as well as $G_{\alpha q}$-coupled signaling pathway. The association of calcium channel antagonism with smooth muscle relaxation is seen in a number of medicinal plants (Estrada-Soto et al., 2007; Gilani et al., 2010; Perez-Hernandez, Ponce-Monter, Medina, & Joseph-Nathan, 2008; Ventura-Martínez, Rivero-Osorno, Gómez, & González-Trujano, 2011). However, due to the controversial role of L-type calcium channel blockers in asthma, whether the traditional use of *L. rhinocerotis* as antiasthmatic is attributed to its calcium channel blocking effect is not conclusive yet.

While the vascular data largely fit those from airways, ileum demonstrated similar responses to vascular and airway tissues but opposing observation for some mechanisms, possibly due to its existence of complex enteric nervous system. Therefore, different mechanisms may be implicated by CWE in ileum. In the case of extrapolating these *in vitro* data to *in vivo* antiasthmatic potential, the relative potencies of CWE in rat tissues (regardless of other species) would rank as: bronchus > trachea > aorta, indicating a higher selectivity for airway tissues. This comparison of potencies was, however, regardless of the different contractile agents used to contract these tissues. The evident contrasting effects of CWE implies that in healthy human CWE may induce airway contraction, whereas in asthmatic patients, chronic application of CWE may prevent airway contraction during EAR and LAR. *In vivo* data is warranted to confirm this hypothesis.

The present study also revealed contracting responses of CWE in airway and ileal smooth muscles at basal tone. This was however not seen in vascular smooth muscle. Most evidence points to the possibility that the contracting and relaxing effects are attributed to different components through different mechanisms in CWE. We deduce that the contracting effect is mediated via muscarinic receptor activation, whereas the relaxing effect is mediated via inhibition of $G_{\alpha q}$-coupled receptor signaling pathway and membrane calcium channels. It is also reasonable to speculate that when the smooth muscle tone is increased (through contractile agonists), the relaxing component in CWE counteracts and predominates over the contracting component. This might partly contribute to the phenomenon where longer exposure time to CWE leads to greater relaxation effect (Section 2.3.5, **Chapter 2**). While one may think the contracting effect alone is deleterious, together with the relaxing

component they might provide an extended protection against airway contraction, thus explaining the benefit of traditional preparation of *L. rhinocerotis*.

The contractile mechanisms elicited by contractile agonists and proposed relaxation mechanisms mediated by CWE in airway and vascular smooth muscles are illustrated in Fig. 8.1 below.

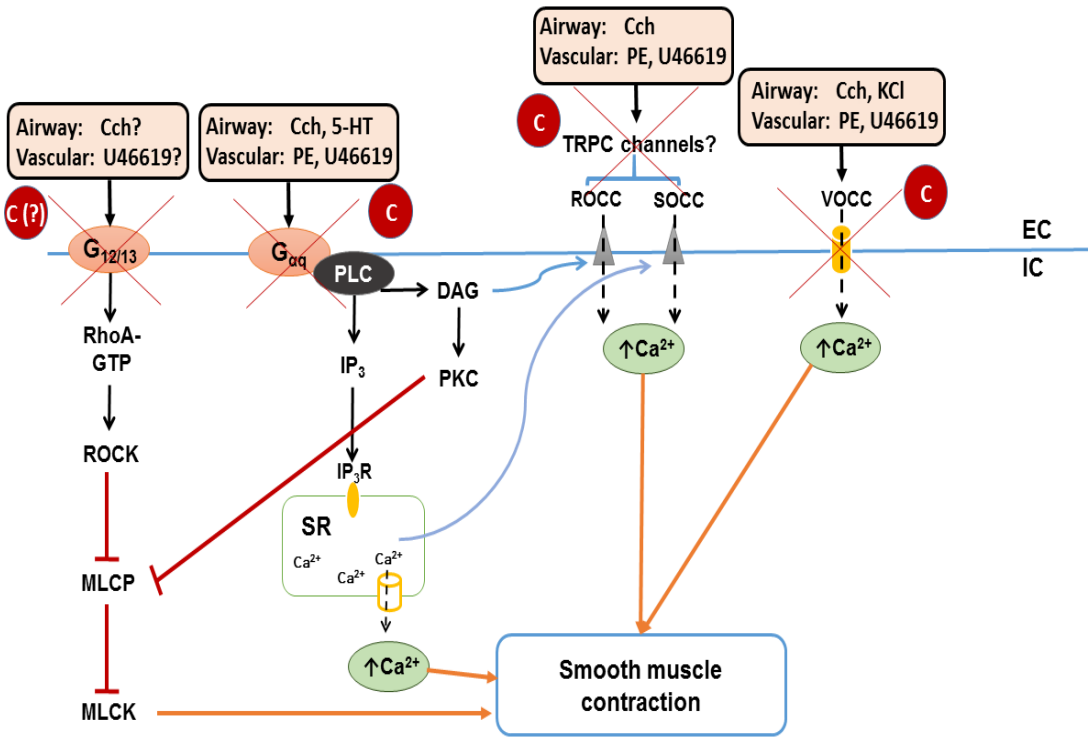

Figure 8.1: Schematic diagram of the proposed mechanisms mediated by cold water extract of *Lignosus rhinocerotis* in airway and vascular smooth muscle relaxation. Cold water extract of *L. rhinocerotis* is represented as 'C' in red circle in the diagram. Cold water extract inhibits activation of $G_{\alpha q}$ protein-coupled pathway by Cch, 5-HT, PE, and U46619. Indirect evidence shows that cold water extract may inhibit TRPC channels (candidates of ROCC and SOCC) and VOCC (especially L-type calcium channels). Although carbachol and U46619 are commonly known to activate $G_{\alpha q}$ protein-coupled receptors, there is evidence pointing to their coupling to $G_{12/13}$ (Wirth et al., 2008; Yoo et al., 2017). Hence, cold water extract may potentially inhibit the $G_{12/13}$-mediated RhoA/ROCK pathway. (Abbreviations: Cch = Carbachol; DAG = Diacylglycerol; EC = Extracellular; IC = Intracellular; IP_3 = Inositol triphosphate; IP_3R = IP_3 receptor; KCl = Potassium chloride; 5-HT = 5-hydroxytryptamine; MLCK = Myosin light chain kinase; MLCP = Myosin light chain phosphatase; PE = Phenylephrine; PKC = Protein kinase C; PLC = Phospholipase C; RhoA-GTP = RhoA-GTPase; ROCC = Receptor-operated calcium channels; ROCK = Rho-associated protein serine/threonine kinase; SOCC = Store-operated calcium channels; SR = Sarcoplasmic reticulum; VOCC = Voltage-operated calcium channels)

8.1.5 Effects of CWE on dorsal root ganglion cells and calcium chelation

The effect of CWE on inhibition of Ca^{2+} influx was substantiated by visualization of the calcium dynamics in rat DRG cells using calcium imaging technique. Evidence indicates that the exposure of DRG cells to KCl triggers cell depolarization and elevates calcium transients, which depend mostly on extracellular Ca^{2+} influx through L-type and N-type calcium channels (Fuchs et al., 2007; L. Zhao et al., 2016). CWE pre-treatment successfully inhibited KCl-induced elevation in $[Ca^{2+}]_i$, suggesting that CWE could inhibit extracellular Ca^{2+} influx through these calcium channels. However, due to unexpected spectroscopic interference from CWE, we were unable to interpret the immediate changes in calcium dynamics induced by CWE. Besides, complexometric titration study showed that CWE did not exhibit Ca^{2+}-chelating effect, and hence the relaxation effect is unlikely to be due to chelation of Ca^{2+}. Overall findings corroborate results in airway smooth muscle to support the role of CWE in inhibiting extracellular Ca^{2+} influx through membrane calcium channels, especially L-type calcium channels.

8.1.6 Fractionation of CWE and their effects on airways

In an attempt to identify the bioactive components of *L. rhinocerotis* contributing to bronchodilator effect, fractionation of the CWE by molecular weight was performed. We hypothesized that the bronchodilator effect of CWE on rat isolated airways differs in different fractions. In support of this hypothesis, HMW and MMW fractions demonstrated equally pronounced bronchodilator effects, whereas LMW fraction was devoid of effect, indicating that the bioactive component is not LMW compound. Subsequently, the effects of HMW fraction, LMW fraction and CWE on carbachol-, 5-HT-, and Ca^{2+}-induced contractions were compared.

As a result, HMW fraction exhibited highest inhibitory effects, followed by CWE and LMW fraction, inferring that the bronchodilator effect of CWE is in good correlation with the molecular weight of fractions. Analysis of carbohydrate and protein contents strongly suggests that polysaccharide-protein complex or proteins are likely to be the bioactive components. The medicinal properties of polysaccharides are closely related to their monosaccharide composition, glycosidic linkages, branching, molecular weight, water solubility and chain conformation (Bohn & BeMiller, 1995; Q. Wang et al., 2017). Glucose and galactose consistently found in HMW and MMW fractions are likely to be the important residues responsible for bronchodilator effects. Given that the HMW and MMW fractions possessed more pronounced bronchodilator effect than the CWE and LMW fraction, it is possible that the bronchoconstricter component in CWE may lie in the LMW fraction.

8.2 Effects of CWE on mast cell degranulation

To examine the effect of CWE on mast cell degranulation, cell culture technique with RBL-2H3 cell line was used. IgE sensitization and antigen stimulation had stimulated the release of β-hexosaminidase, and increased the degree of phosphatidylserine externalization (unrelated to cell death) and degranulation index (Alcian blue staining), indicating ongoing degranulation process. CWE treatment on IgE/antigen-stimulated cells showed slight but nonsignificant increasing trend of β-hexosaminidase release and early apoptotic cell numbers. In accord with this, CWE treatment alone in unstimulated cells significantly increased the degree of β-hexosaminidase release and phosphatidylserine externalization. In marked contrast, CWE treatment on IgE/antigen-stimulated cells had reduced the degranulation index by Alcian blue staining, suggesting that it prevents complete loss of stained secretory granules.

Further experiments showed that CWE stimulated β-hexosaminidase release during pre-incubation period, and it effectively dampened subsequent β-hexosaminidase release upon antigen stimulation. Overall evidence denotes that phosphatidylserine externalization and β-hexosaminidase release occur in the early stage of degranulation, which may be stimulated by CWE. We postulate that the loss of stained secretory granules happens in a later stage of degranulation, and this may be inhibited by CWE.

8.3 Limitations and future studies

The findings of this study focused on isolated airway segments in an *in vitro* environment using organ bath technique. This method is useful for direct measurement of smooth muscle contractility and highly reproducible. However, it failed to provide insight into responses in fully integrated multi-cell type system and dynamic mechanical environment as it cannot entirely mimic the natural physiological conditions. In addition, the airway tissues were isolated from non-asthmatic animals. We cannot exclude the possibility that different responses may be observed for *L. rhinocerotis* in asthmatic animal model. Our attempt to minimize the variation was by using carbachol and 5-HT to contract the airways to mimic the overactivation of muscarinic receptors, which is one of the features of asthma.

In addition, the current analysis was restricted to functional data on smooth muscles. Although this is useful in elucidating the pharmacological effects of CWE, we lack of molecular evidence to confirm the mechanisms. We also did not elucidate the effect of CWE on RhoA/ROCK pathway. To complement the organ bath data, future research should include protein expression study such as western blot analysis to monitor the key phosphorylation effectors downstream of $G_{\alpha q}$ and $G_{12/13}$ protein-coupled pathways such as PKC and ROCK, and to confirm the existence of TRPC channels in airway and vascular smooth muscles. The expression of TRPC channels can also be proven through studies using calcium channel knockout mice and gene silencing approaches. Unfortunately, the calcium imaging study was unable to show the immediate effect of CWE on calcium dynamics due to interference. In future studies, patch clamp electrophysiology technique can be employed to measure the effect of CWE on currents through potential calcium ion channels, such as TRPC and

L-type calcium channels, in smooth muscle cell membrane to support its inhibitory role on extracellular Ca^{2+} influx.

One subject that remains to be explored is the exact substances responsible for the pronounced bronchodilator effect. This study had narrowed down the possible bioactive components to be polysaccharide-protein complex or proteins. However, one of the limitations of this study is that the mechanistic studies should have been performed with fractions of CWE to confirm the identity of the bioactive components and minimize interference from other components. Purification of these compounds and investigating their effects on airways are crucial. On the other hand, it is undetermined in this study whether the bronchoconstricter and bronchodilator effects are elicited by the same large-molecular-weight bioactive components. This can be confirmed in future investigations by testing these fractions on basal tone of airway smooth muscle to help identifying the bioactive components.

As for cell culture studies, Alcian blue staining assay was quantified through microscopic observation in which the data analysis may be subjective. Despite the fact that RBL-2H3 cells are useful in study of IgE-mediated mast cell degranulation, in the aspect of certain mediator release it is significantly influenced by the releasing media composition (Passante et al., 2009). There also exists inconsistencies as different responses to mast cell stabilizers and mediator release were reported by different researchers using the same cell line (Passante et al., 2009). Future studies may focus on examining the key phosphorylation effectors by which CWE affects mast cell degranulation including Syk, LAT, MAPK, and Lyn using western blot analysis. Experiments that visualize the calcium dynamics in RBL-2H3 cells, for instance by using labelled calcium indicator dyes and fluorometric assay, can help to support the effect of CWE on degranulation.

Last but not the least, future studies should also move on to investigate if *L. rhinocerotis* exhibits similar responses on airway contraction and mast cell degranulation using *in vivo* asthmatic animal models or human subjects to provide better extrapolation to human situation.

8.4 Concluding statements

This study reported novel findings of *L. rhinocerotis* on smooth muscles and on mast cell degranulation, filling the knowledge gap in scientific literature. We conclude with compelling evidence that CWE of *L. rhinocerotis* presented unequivocal relaxation effect in airway contraction, supporting the traditional usage of *L. rhinocerotis* for treating asthma and chronic cough. The objectives as outlined in Section 1.5 (**Chapter 1**) in this thesis were met. In answering the research questions, we conclude that:

(i) The CWE exhibited airway relaxation effect in pre-contracted airway smooth muscle (rat and porcine), whist HWE and ME were devoid of effect. Similar relaxation effect was observed for CWE in pre-contracted vascular smooth muscle (rat and porcine) and neurogenic contraction of ileal smooth muscle (guinea pig), indicating a non-species-specific effect observed in many types of smooth muscle tissues.

(ii) Gathered evidence from airway and vascular smooth muscle showed that the relaxation effect is unlikely to involve β-adrenoceptors, K^+ channels, and NO pathways. The cAMP and cGMP pathways are possibly not implicated.

(iii) One of the mechanisms of action mediating CWE-induced relaxation was via inhibition of membrane calcium channels, particularly L-type calcium

channels. This is supported by findings from airway and vascular smooth muscle, and dorsal root ganglion cells.

(iv) The CWE elevated basal tone of airways and ileum, but slightly relaxed porcine coronary artery. The basal tone of rat aorta was not affected. Most evidence from airways and blood vessels points to conjecture that the relaxing and contracting effects of CWE are mediated through different components and mechanisms.

(v) In IgE/antigen-stimulated RBL-2H3 cells, CWE stimulated β-hexosaminidase release and phosphatidylserine exposure, which are possibly in early processes of degranulation processes, and inhibited secretory granule reduction, which is possibly in later stage of degranulation.

(vi) Bioactive components responsible for the bronchodilator effect of CWE are possibly large-molecular-weight components such as polysaccharide-protein complexes and proteins.

(vii) Future directions should include characterization of the effects of CWE on individual calcium ion channels and isolation of bioactive components as proposed in Section 8.3.

References

Abdullah, N., Haimi, M. Z. D., Lau, B. F., & Annuar, M. S. M. (2013). Domestication of a wild medicinal sclerotial mushroom, *Lignosus rhinocerotis* (Cooke) Ryvarden. *Industrial Crops and Products*, *47*, 256–261. https://doi.org/10.1016/j.indcrop.2013.03.012

Abramov, A. Y., Zamaraeva, M. V., Hagelgans, A. I., Azimov, R. R., & Krasilnikov, O. V. (2001). Influence of plant terpenoids on the permeability of mitochondria and lipid bilayers. *Biochimica et Biophysica Acta - Biomembranes*, *1512*(1), 98–110. https://doi.org/10.1016/S0005-2736(01)00307-8

Abramowitz, J., & Birnbaumer, L. (2009). Physiology and pathophysiology of canonical transient receptor potential channels. *The FASEB Journal*, *23*(2), 297–328. https://doi.org/10.1096/fj.08-119495

Adcock, I. M., Caramori, G., & Chung, K. F. (2008). New targets for drug development in asthma. *Lancet*, *372*(9643), 1073–1087. https://doi.org/10.1016/S0140-6736(08)61449-X

Adcock, J. J. (2009). TRPV1 receptors in sensitisation of cough and pain reflexes. *Pulmonary Pharmacology and Therapeutics*, *22*(2), 65–70. https://doi.org/10.1016/j.pupt.2008.12.014

Adner, M., Rose, A. C., Zhang, Y., Swärd, K., Benson, M., Uddman, R., … Cardell, L. O. (2002). An assay to evaluate the long-term effects of inflammatory mediators on murine airway smooth muscle: Evidence that TNF_{α} up-regulates 5-HT_{2A}-mediated contraction. *British Journal of Pharmacology*, *137*(7), 971–982. https://doi.org/10.1038/sj.bjp.0704928

Ahmad, M. S., Noor, Z. M., & Ariffin, Z. Z. (2013). New Thrombolytic Agent from Endophytic Fungi and Lignosus rhinocerus. *The Open Conference Proceedings Journal*, *4*(Suppl-2, M22), 95–98. https://doi.org/10.2174/2210289201304020095

Ahmed, F., Foster, R. W., Small, R. C., & Weston, A. H. (1984). Some features of the spasmogenic actions of acetylcholine and histamine in guinea-pig isolated trachealis. *British Journal of Pharmacology*, *83*(1), 227–233.

Ahmed, T., Brot, J. D., & Abraham, W. (1988). The role of calcium antagonists in bronchial reactivity. *Journal of Allergy and Clinical Immunology*, *81*(1), 133–144.

Alangari, A. A. (2014). Corticosteroids in the treatment of acute asthma. *Annals of Thoracic Medicine*, *9*(4), 187–192. https://doi.org/10.4103/1817-1737.140120

Alexander, S. P. H., Kelly, E., Marrion, N., Peters, J. A., Benson, H. E., Faccenda, E., … Zajac, J. (2015). The Concise Guide to PHARMACOLOGY 2015/16: Overview. *British Journal of Pharmacology*, *172*(24), 5729–5743. https://doi.org/10.1111/bph.13347

Alfieri, A., Parisi, A., Maione, F., Grassia, G., Morello, S., Ialenti, A., … Cicala, C. (2012). Hyperresponsiveness to adenosine in sensitized Wistar rats over-expressing A_1 receptor. *European Journal of Pharmacology*, *695*(1–3), 120–125.

https://doi.org/10.1016/j.ejphar.2012.09.002

Amberg, G. C., & Navedo, M. F. (2013). Calcium dynamics in vascular smooth muscle. *Microcirculation*, *20*(4), 281–289. https://doi.org/10.1111/micc.12046

An, W. F., & Tolliday, N. J. (2009). *Introduction: cell-based assays for high-throughput screening.* (P. A. Clemons, N. J. Tolliday, & B. K. Wagner, Eds.), *Methods in Molecular Biology* (Vol. 486). New York: Humana Press. https://doi.org/10.1007/978-1-60327-545-3_1

Andrè, E., Gatti, R., Trevisani, M., Preti, D., Baraldi, P. G., Patacchini, R., & Geppetti, P. (2009). Transient receptor potential ankyrin receptor 1 is a novel target for pro-tussive agents. *British Journal of Pharmacology*, *158*(6), 1621–1628. https://doi.org/10.1111/j.1476-5381.2009.00438.x

Andreasen, D., Friis, U. G., Uhrenholt, T. R., Jensen, B. L., Skøtt, O., & Hansen, P. B. (2006). Coexpression of voltage-dependent calcium channels $Ca_{v1.2}$, $_{2.1a}$, and $_{2.1b}$ in vascular myocytes. *Hypertension*, *47*, 735–741. https://doi.org/10.1161/01.HYP.0000203160.80972.47

Arch, J. R., Buckle, D. R., Bumstead, J., Clarke, G. D., Taylor, J. F., & Taylor, S. G. (1988). Evaluation of the potassium channel activator cromakalim (BRL 34915) as a bronchodilator in the guinea-pig: comparison with nifedipine. *British Journal of Pharmacology*, *95*(3), 763–770.

Arrieta, J., Siles-Barrios, D., García-Sánchez, J., Reyes-Trejo, B., & Sánchez-Mendoza, M. E. (2010). Relaxant effect of the extracts of *Crataegus mexicana* on guinea pig tracheal smooth muscle. *Pharmacognosy Journal*, *2*(17), 40–46. https://doi.org/10.1016/S0975-3575(10)80008-2

Ay, B., Prakash, Y. S., Pabelick, C. M., & Sieck, G. C. (2004). Store-operated Ca^{2+} entry in porcine airway smooth muscle. *American Journal of Physiology. Lung Cellular and Molecular Physiology*, *286*, L909-917. https://doi.org/10.1152/ajplung.00317.2003

Azevedo, M. F., Faucz, F. R., Bimpaki, E., Horvath, A., Levy, I., De Alexandre, R. B., … Stratakis, C. A. (2014). Clinical and molecular genetics of the phosphodiesterases (PDEs). *Endocrine Reviews*, *35*(2), 195–233. https://doi.org/10.1210/er.2013-1053

Azliza, M. A., Ong, H. C., Vikineswary, S., Noorlidah, A., & Haron, N. W. (2012). Ethno-medicinal resources used by the Temuan in Ulu Kuang village. *Studies on Ethno-Medicine*, *6*(1), 17–22. https://doi.org/10.1080/09735070.2012.11886415

Azmir, J., Zaidul, I. S. M., Rahman, M. M., Sharif, K. M., Mohamed, A., Sahena, F., … Omar, A. K. M. (2013). Techniques for extraction of bioactive compounds from plant materials: A review. *Journal of Food Engineering*, *117*(4), 426–436. https://doi.org/10.1016/j.jfoodeng.2013.01.014

Baba, K., Kawanishi, M., Satake, T., & Tomita, T. (1985). Effects of verapamil on the contractions of guinea-pig tracheal muscle induced by Ca, Sr and Ba. *British Journal of Pharmacology*, *84*(1), 203–211.

Baba, K., Satake, T., Takagi, K., & Tomita, T. (1986). Effects of verapamil on the response of the guinea- pig tracheal muscle to carbachol. *British Journal of Pharmacology*, *88*(2), 441–449. https://doi.org/10.1111/j.1476-5381.1986.tb10222.x

Barisione, G., Baroffio, M., Crimi, E., & Brusasco, V. (2010). Beta-adrenergic agonists. *Pharmaceuticals*, *3*(4), 1016–1044. https://doi.org/10.3390/ph3041016

Barnes, P. J. (1989). Mechanisms of disease: Airway receptors. *Postgraduate Medical Journal*, *65*, 532–542.

Barnes, P. J. (1998). Pharmacology of airway smooth muscle. *American Journal of Respiratory and Critical Care Medicine*, *158*(5 Pt 3), S123-32. https://doi.org/10.1164/ajrccm.158.supplement_2.13tac800

Barnes, P. J. (2012). Chapter 41 - Autonomic Control of the Lower Airways. In I. Biaggioni, G. Burnstock, P. A. Low, & J. F. R. B. T.-P. on the A. N. S. (Third E. Paton (Eds.), *Primer on the Autonomic Nervous System* (3rd ed., pp. 201–204). San Diego: Academic Press. https://doi.org/https://doi.org/10.1016/B978-0-12-386525-0.00041-X

Barros, L., Cruz, T., Baptista, P., Estevinho, L. M., & Ferreira, I. C. F. R. (2008). Wild and commercial mushrooms as source of nutrients and nutraceuticals. *Food and Chemical Toxicology*, *46*(8), 2742–2747. https://doi.org/10.1016/j.fct.2008.04.030

Barsumian, E. L., Isersky, C., Petrino, M. G., & Siraganian, R. P. (1981). IgE-induced histamine release from rat basophilic leukemia cell lines: isolation of releasing and nonreleasing clones. *European Journal of Immunology*, *11*(4), 317–323. https://doi.org/10.1002/eji.1830110410

Bartlett, D., Jeffery, P., Ambrogio, G. S., & Wise, J. C. M. (1976). Location of stretch receptors in the trachea and bronchi of the dog. *J Physiol.*, *258*(2), 409–420.

Bastin, G., & Heximer, S. P. (2011). Intracellular regulation of heterotrimeric G-protein signaling modulates vascular smooth muscle cell contraction. *Archives of Biochemistry and Biophysics*, *510*(2), 182–189. https://doi.org/10.1016/j.abb.2011.05.008

Batbayar, S., Lee, D. H., & Kim, H. W. (2012). Immunomodulation of fungal β-glucan in host defense signaling by dectin-1. *Biomolecules and Therapeutics*, *20*(5), 433–445. https://doi.org/10.4062/biomolther.2012.20.5.433

Baumgarten, H. G., Bennette, A., Bertaccini, G., Buffa, R., Capella, C., Caprilli, R., … Corriaziari, E. (1982). *Mediators and Drugs in Gastrointestinal Motility I: Morphological Basis and Neurophysiological Control*. (G. Bertaccini, Ed.). New York: Springer-Verlag Berlin Heidelberg. https://doi.org/10.1007/978-3-642-68437-1

Ben-Jebria, A., Marthan, R., Rossetti, M., & Savineau, J. (1993). Effect of passive sensitization on the mechanical activity of human isolated bronchial smooth muscle induced by substance P, neurokinin A and VIP. *British Journal of Pharmacology*, *109*(1), 131–136. https://doi.org/10.1111/j.1476-5381.1993.tb13542.x

Bennett, M. R. (1997). Non-adrenergic non-cholinergic (NANC) transmission to smooth muscle: 35 years on. *Progress in Neurobiology*, *52*(3), 159–195. https://doi.org/10.1016/S0301-0082(97)00012-9

Berair, R., Hollins, F., & Brightling, C. (2013). Airway smooth muscle hypercontractility in asthma. *Journal of Allergy*, *2013*, 1–7. https://doi.org/10.1146/annurev.pathmechdis.1.110304.100213

Billington, C. K., Ojo, O. O., Penn, R. B., & Ito, S. (2013). cAMP Regulation of airway smooth muscle function. *Pulmonary Pharmacology & Therapeutics*, *26*(1), 112–120. https://doi.org/10.1016/j.pupt.2012.05.007

Billington, C. K., & Penn, R. B. (2003). Signaling and regulation of G protein-coupled receptors in airway smooth muscle. *Respiratory Research*, *4*(1), 23. https://doi.org/10.1186/1465-9921-4-2

Birrell, M. A., Belvisi, M. G., Grace, M., Sadofsky, L., Faruqi, S., Hele, D. J., … Morice, A. H. (2009). TRPA1 agonists evoke coughing in guinea pig and human volunteers. *American Journal of Respiratory and Critical Care Medicine*, *180*(11), 1042–1047. https://doi.org/10.1164/rccm.200905-0665OC

Birring, S. S. (2011). Controversies in the evaluation and management of chronic cough. *American Journal of Respiratory and Critical Care Medicine*, *183*(6), 708–715. https://doi.org/10.1164/rccm.201007-1017CI

Black, J., Armour, C., Johnson, P., & Vincenc, K. (1986). The calcium dependence of histamine, carbachol and potassium chloride-induced contraction in human airways *in vitro*. *European Journal of Pharmacology*, *125*, 159–168.

Black, J. L., & Barnes, P. J. (1990). Potassium channels and airway function: new therapeutic prospects. *Thorax*, *45*, 213–218.

Black, J. L., Marthan, R., Armour, C. L., & Johnson, P. R. A. (1989). Sensitization alters contractile responses and calcium influx in human airway smooth muscle. *J Allergy Clin Immunol*, *84*(4 Pt 1), 440–447.

Bohn, J. A., & BeMiller, J. N. (1995). (1→3)-β-d-Glucans as biological response modifiers: a review of structure-functional activity relationships. *Carbohydrate Polymers*, *28*(1), 3–14. https://doi.org/10.1016/0144-8617(95)00076-3

Boonsong, S., Klaypradit, W., & Wilaipun, P. (2016). Antioxidant activities of extracts from five edible mushrooms using different extractants. *Agriculture and Natural Resources*, *50*(2), 89–97. https://doi.org/10.1016/j.anres.2015.07.002

Bornstein, J. C. (2008). Purinergic mechanisms in the control of gastrointestinal motility. *Purinergic Signalling*, *4*(3), 197–212. https://doi.org/10.1007/s11302-007-9081-z

Brackett, L. E., & Daly, J. W. (1991). Relaxant effects of adenosine analogs on guinea pig trachea *in vitro*: xanthine-sensitive and xanthine-insensitive mechanisms. *The Journal of Pharmacology and Experimental Therapeutics*, *257*(1), 205–213.

Bradding, P. (2007). Mast cell regulation of airway smooth muscle function in asthma. *European Respiratory Journal*, *29*(5), 827–830. https://doi.org/10.1183/09031936.00017707

Bradding, P., Walls, A. F., & Holgate, S. T. (2006). The role of the mast cell in the pathophysiology of asthma. *Journal of Allergy and Clinical Immunology*, *117*(6), 1277–1284. https://doi.org/10.1016/j.jaci.2006.02.039

Bradford, M. M. (1976). A rapid and sensitive method for the quantitation of microgram quantities of protein utilizing the principle of protein-dye binding. *Analytical Biochemistry*, *72*(1), 248–254. https://doi.org/https://doi.org/10.1016/0003-2697(76)90527-3

Brar, M. K. S. (2004). Glucocorticoid-resistant bronchial asthma. *Medical Journal*

Armed Forces India, *60*(2), 186–187. https://doi.org/10.1016/S0377-1237(04)80119-9

Brightling, C. E. (2011). Eosinophils, bronchitis and asthma: Pathogenesis of cough and airflow obstruction. *Pulmonary Pharmacology and Therapeutics*, *24*(3), 324–327. https://doi.org/10.1016/j.pupt.2010.11.001

Brightling, C. E., Bradding, P., Symon, F. a, Holgate, S. T., Wardlaw, A. J., & Pavord, I. D. (2002). Mast-cell infiltration of airway smooth muscle in asthma. *The New England Journal of Medicine*, *346*(22), 1699–1705. https://doi.org/10.1056/NEJMoa012705

Brightling, C. E., Ward, R., Goh, K. L., Wardlaw, A. J., & Pavord, I. D. (1999). Eosinophilic bronchitis is an important cause of chronic cough. *American Journal of Respiratory and Critical Care Medicine*, *160*(2), 406–410. https://doi.org/https://doi.org/10.1164/ajrccm.160.2.9810100

Brown, G. D., & Gordon, S. (2003). Fungal beta-glucans and mamalian immunity. *Immunity*, *19*, 311–315.

Brown, R., Spina, D., & Page, C. (2008). Adenosine receptors and asthma. *British Journal of Pharmacology*, *153*, S446-456. https://doi.org/10.1007/978-3-540-89615-9_11

Brozovich, F. V, Nicholson, C. J., Degen, C. V, Gao, Y. Z., Aggarwal, M., & Morgan, K. G. (2016). Mechanisms of vascular smooth muscle contraction and the basis for pharmacologic treatment of smooth muscle disorders. *Pharmacological Reviews*, *68*(2), 476–532. https://doi.org/10.1124/pr.115.010652

Buckner, C. K., Dea, D., Liberati, N., & Krell, R. D. (1991). A pharmacologic examination of receptors mediating serotonin-induced bronchoconstriction in the anesthetized guinea pig. *Journal of Pharmacology and Experimental Therapeutics*, *257*(1), 26 LP-34.

Burdette, S. C., & Lippard, S. J. (2003). Meeting of the minds: metalloneurochemistry. *Proceedings of the National Academy of Sciences of the United States of America*, *100*(7), 3605–3610. https://doi.org/10.1073/pnas.0637711100

Burkill, I. H. (1966). *A Dictionary of the Economic Products of the Malay Peninsula. Vol. I & II*. Kuala Lumpur: Ministry of Agriculture Malaysia.

Burnstock, G., Brouns, I., Adriaensen, D., & Timmermans, J.-P. (2012). Purinergic signaling in the airways. *Pharmacological Reviews*, *64*(4), 834–868. https://doi.org/10.1124/pr.111.005389

Camacho, P., Fan, H., Liu, Z., & He, J.-Q. (2016). Small mammalian animal models of heart disease. *American Journal of Cardiovascular Disease*, *6*(3), 70–80. https://doi.org/10.3390/jcdd3040030

Campos-Bedolla, P., Vargas, M. H., Segura, P., Carbajal, V., Calixto, E., Figueroa, A., … Montaño, L. M. (2008). Airway smooth muscle relaxation induced by 5-HT_{2A} receptors: Role of Na^+/K^+-ATPase pump and Ca^{2+}-activated K^+ channels. *Life Sciences*, *83*(11–12), 438–446. https://doi.org/10.1016/j.lfs.2008.07.006

Cazzola, M., & Matera, M. G. (2000). 5-HT modifiers as a potential treatment of asthma. *Trends in Pharmacological Sciences*, *21*(1), 13–16. https://doi.org/10.1016/S0165-6147(99)01408-X

Cazzola, M., Matera, M. G., D'Amato, G., & Rossi, F. (1995). Effects of serotonin on airways: recent developments. *Allergy*, *50*(1), 1–10. https://doi.org/10.1111/j.1398-9995.1995.tb02476.x

Chang, Y. S., & Lee, S. S. (2004). Utilisation of macrofungi species in Malaysia. *Fungal Diversity*, *15*, 15–22.

Chen, M. L., & Lin, B. F. (2007). Effects of triterpenoid-rich extracts of Ganoderma tsugae on airway hyperreactivity and Th2 responses *in vivo*. *International Archives of Allergy and Immunology*, *143*(1), 21–30. https://doi.org/10.1159/000098222

Chen, S., Yin, D.-K., Yao, W.-B., Wang, Y.-D., Zhang, Y.-R., & Gao, X.-D. (2009). Macrophage receptors of polysaccharide isolated from a marine filamentous fungus *Phoma herbarum* YS4108. *Acta Pharmacologica Sinica*, *30*(7), 1008–1014. https://doi.org/10.1038/aps.2009.93

Chen, Y., & Huang, L.-Y. M. (2017). A simple and fast method to image calcium activity of neurons from intact dorsal root ganglia using fluorescent chemical Ca^{2+} indicators. *Molecular Pain*, *13*, 1–9. https://doi.org/10.1177/1744806917748051

Cherubini, E., Morita, K., & North, R. A. (1985). Opioid inhibition of synaptic transmission in the guinea- pig myenteric plexus. *British Journal of Pharmacology*, *85*(4), 805–817. https://doi.org/10.1111/j.1476-5381.1985.tb11079.x

Cherubini, E., & North, R. A. (1985). Mu and kappa opioids inhibit transmitter release by different mechanisms. *Proc Natl Acad Sci U S A*, *82*(6), 1860–1863. https://doi.org/10.1073/pnas.82.6.1860

Cheung, P. C. K. (2013). Mini-review on edible mushrooms as source of dietary fiber: Preparation and health benefits. *Food Science and Human Wellness*, *2*(3–4), 162–166. https://doi.org/10.1016/j.fshw.2013.08.001

Chiou, W. F., Chang, P. C., Chou, C. J., & Chen, C. F. (2000). Protein constituent contributes to the hypotensive and vasorelaxant activities of *Cordyceps sinensis*. *Life Sciences*, *66*(14), 1369–1376. https://doi.org/10.1016/S0024-3205(00)00445-8

Choi, Y. H., Yan, G. H., Chai, O. H., Lim, J. M., Sung, S. Y., Zhang, X., … Song, C. H. (2006). Inhibition of anaphylaxis-like reaction and mast cell activation by water extract from the fruiting body of *Phellinus linteus*. *Biol Pharm Bull*, *29*(7), 1360–1365. https://doi.org/JST.JSTAGE/bpb/29.1360 [pii]

Chu, P. Y., Sun, H. L., Ko, J. L., Ku, M. S., Lin, L. J., Lee, Y. T., … Lue, K. H. (2017). Oral fungal immunomodulatory protein-*Flammulina velutipes* has influence on pulmonary inflammatory process and potential treatment for allergic airway disease: A mouse model. *Journal of Microbiology, Immunology and Infection*, *50*(3), 297–306. https://doi.org/10.1016/j.jmii.2015.07.013

Chung, K. F., & Pavord, I. D. (2008). Prevalence, pathogenesis, and causes of chronic cough. *The Lancet*, *371*, 1364–1374. https://doi.org/10.1016/S0140-6736(08)60595-4

Clague, R. U., Eglen, R. M., Strachan, A. C., & Whiting, R. L. (1985). Action of agonists and antagonists at muscarinic receptors present on ileum and atria *in*

vitro. *British Journal of Pharmacology*, *86*(1), 163–170. https://doi.org/10.1111/j.1476-5381.1985.tb09446.x

Conner, J., Wuchterl, D., Lopez, M., Minshall, B., Prusti, R., Boclair, D., … Allen, C. (2014). *Chapter 26: The Biomanufacturing of Biotechnology Products*. (C. Shimasaki, Ed.), *Biotechnology Entrepreneurship: Starting, Managing, and Leading Biotech Companies*. Waltham, USA: Elsevier. https://doi.org/10.1016/B978-0-12-404730-3.00026-9

Cör, D., Knez, Ž., & Hrnčič, M. K. (2018). Antitumour, antimicrobial, antioxidant and antiacetylcholinesterase effect of *Ganoderma Lucidum* terpenoids and polysaccharides: A review. *Molecules*, *23*(3), 649. https://doi.org/10.3390/molecules23030649

Corteling, R. L., Li, S., Giddings, J., Westwick, J., Poll, C., & Hall, I. P. (2004). Expression of transient receptor potential C6 and related transient receptor potential family members in human airway smooth muscle and lung tissue. *American Journal of Respiratory Cell and Molecular Biology*, *30*(2), 145–154. https://doi.org/10.1165/rcmb.2003-0134OC

Crichton, R. R. (2008). 18 - Metals in brain and their role in various neurodegenerative diseases. In *Biological Inorganic Chemistry: An Introduction* (pp. 297–320). Amsterdam: Elsevier. https://doi.org/https://doi.org/10.1016/B978-044452740-0.50018-1

Crick, S. J., Sheppard, M. N., Ho, S. Y., Gebstein, L., & Anderson, R. H. (1998). Anatomy of the pig heart : comparisons with normal human cardiac structure. *Journal of Anatomy*, (193), 105–119.

Cui, B. K., Tang, L. P., & Dai, Y. C. (2011). Morphological and molecular evidences for a new species of Lignosus (Polyporales, Basidiomycota) from tropical China. *Mycological Progress*, *10*(3), 267–271. https://doi.org/10.1007/s11557-010-0697-y

Cushley, M., Tattersfield, A., & Holgate, S. (1983). Inhaled adenosine and guanosine on airway resistance in normal and asthmatic subjects. *British Journal of Clinical Pharmacology*, *15*(2), 161–165. https://doi.org/10.1111/j.1365-2125.1983.tb01481.x

Cushley, M., Wee, L., & Holgate, S. (1986). The effect of inhaled 5-hydroxytryptamine (5- HT, serotonin) on airway calibre in man. *British Journal of Clinical Pharmacology*, *22*(4), 487–490. https://doi.org/10.1111/j.1365-2125.1986.tb02923.x

Cuss, F. M. (1999). Beyond the histamine receptor: effect of antihistamines on mast cells. *Clinical and Experimental Allergy*, *29*(Supplement 3), 54–59. https://doi.org/10.1046/j.1365-2222.1999.00013.x

Dai, J. M., Kuo, K.-H., Leo, J. M., van Breemen, C., & Lee, C.-H. (2006). Mechanism of ACh-induced asynchronous calcium waves and tonic contraction in porcine tracheal muscle bundle. *American Journal of Physiology. Lung Cellular and Molecular Physiology*, *290*(3), L459-469. https://doi.org/10.1152/ajplung.00092.2005

Dai, J. M., Kuo, K. H., Leo, J. M., Paré, P. D., Van Breemen, C., & Lee, C. H. (2007). Acetylcholine-induced asynchronous calcium waves in intact human bronchial

muscle bundle. *American Journal of Respiratory Cell and Molecular Biology*, *36*(5), 600–608. https://doi.org/10.1165/rcmb.2006-0096OC

Darmani, N. A., & Broadley, K. J. (1986). Actions and interactions of adenosine, theophylline and enprofylline on the guinea-pig spirally cut trachea. *European Journal of Pharmacology*, *125*(3), 353–362. https://doi.org/10.1016/0014-2999(86)90791-0

De Silva, D. D., Rapior, S., Hyde, K. D., & Bahkali, A. H. (2012). Medicinal mushrooms in prevention and control of diabetes mellitus. *Fungal Diversity*, *56*(1), 1–29. https://doi.org/10.1007/s13225-012-0187-4

De Silva, D. D., Rapior, S., Sudarman, E., Stadler, M., Xu, J., Aisyah Alias, S., & Hyde, K. D. (2013). Bioactive metabolites from macrofungi: Ethnopharmacology, biological activities and chemistry. *Fungal Diversity*, *62*(1), 1–40. https://doi.org/10.1007/s13225-013-0265-2

De Souza Santos, M., Jonis Andrioli, W., Freire De Morais Del Lama, M. P., Kenupp Bastos, J., Nanayakkara, N. P. D., & Zumstein Georgetto Naal, R. M. (2013). *In vitro* anti-allergic activity of the fungal metabolite pyridovericin. *International Immunopharmacology*, *15*(3), 532–538. https://doi.org/10.1016/j.intimp.2013.01.017

Dearman, R. J., Skinner, R. A., Deakin, N., Shaw, D., & Kimber, I. (2005). Evaluation of an *in vitro* method for the measurement of specific IgE antibody responses: The rat basophilic leukemia (RBL) cell assay. *Toxicology*, *206*(2), 195–205. https://doi.org/10.1016/j.tox.2004.08.007

DeHaven, W. I., Smyth, J. T., Boyles, R. R., Bird, G. S., & Putney, J. W. (2008). Complex actions of 2-aminoethyldiphenyl borate (2-APB) on store-operated calcium entry. *Journal of Biological Chemistry*, *283*(28), 19265–19273. https://doi.org/10.1074/jbc.M801535200

Dellipizzi, A., Pucci, M. L., Mosny, A. Y., Deseyn, K., & Nasjletti, A. (1997). Contribution of constrictor prostanoids to the calcium-dependent basal tone in the aorta from rats with aortic coarctation-induced hypertension: Relationship to nitric oxide. *The Journal of Pharmacology and Experimental Therapeutics*, *283*(1), 75–81.

Demo, S. D., Masuda, E., Rossi, A. B., Throndset, B. T., Gerard, A. l., Chan, E. H., … Fisher, J. M. (1999). Quantitative measurement of mast cell degranulation using a novel flow cytometric annexin-V binding assay. *Cytometry*, *36*(4), 340–348. https://doi.org/10.1002/(SICI)1097-0320(19990801)36:4<340::AID-CYTO9>3.0.CO;2-C

Di Maria, G. U., Spicuzza, L., Mistretta, a, & Mazzarella, G. (2000). Role of endogenous nitric oxide in asthma. *Allergy*, *55 Suppl 6*, 31–35.

Dias, D. A., Urban, S., & Roessner, U. (2012). A historical overview of natural products in drug discovery. *Metabolites*, *2*(4), 303–336. https://doi.org/10.3390/metabo2020303

Dietrich, C., & Kilbinger, H. (1995). Prejunctional M1 and postjunctional M3 muscarinic receptors in the circular muscle of the guinea-pig ileum. *Naunyn-Schmiedeberg's Archives of Pharmacology*, *351*(3), 237–243. https://doi.org/10.1007/BF00233242

Ding, X., & Muray, P. A. (2005). Cellular mechanisms of thromboxane A2-mediated contraction in pulmonary veins. *American Journal of Physiology: Lung Cellular and Molecular Physiology*, *289*(5), L825–L833. https://doi.org/10.1152/ajplung.00177.2005

Dinwiddie, R., & Müller, W. G. (2002). Adolescent treatment compliance in asthma. *Journal of the Royal Society of Medicine*, *95*(2), 68–71. https://doi.org/10.1258/jrsm.95.2.68

Doeing, D. C., & Solway, J. (2013). Airway smooth muscle in the pathophysiology and treatment of asthma. *Journal of Applied Physiology*, *114*(7), 834–843. https://doi.org/10.1152/japplphysiol.00950.2012

Drummond, G. R., & Cocks, T. M. (1996). Evidence for mediation by endothelium-derived hyperpolarizing factor of relaxation to bradykinin in the bovine isolated coronary artery independently of voltage-operated Ca^{2+} channels. *British Journal of Pharmacology*, *117*(6), 1035–1040. https://doi.org/10.1111/j.1476-5381.1996.tb16693.x

DuBois, M., Gilles K. A., E., Hamilton, J. K., A. J. Rebers, P., & Smith, F. (1956). Calorimetric method for determination of sugars and related substances. *Analytical Chemistry*, *28*, 350–356.

Dubuis, E., Wortley, M. A., Grace, M. S., Maher, S. A., Adcock, J. J., Birrell, M. A., & Belvisi, M. G. (2014). Theophylline inhibits the cough reflex through a novel mechanism of action. *Journal of Allergy and Clinical Immunology*, *133*(6), 1588–1598. https://doi.org/10.1016/j.jaci.2013.11.017

Dürk, T., Duerschmied, D., Müller, T., Grimm, M., Reuter, S., Vieira, R. P., … Idzko, M. (2013). Production of serotonin by tryptophan hydroxylase 1 and release via platelets contribute to allergic airway inflammation. *American Journal of Respiratory and Critical Care Medicine*, *187*(5), 476–485. https://doi.org/10.1164/rccm.201208-1440OC

Dvorak, A. M., Massey, W., Warner, J., Kissell, S., Kagey-Sobotka, A., & Lichtenstein, L. M. (1991). IgE-mediated anaphylactic degranulation of isolated human skin mast cells. *Blood*, *77*(3), 569–578.

Earley, S., & Brayden, J. E. (2015). Transient receptor potential channels in the vasculature. *Physiological Reviews*, *95*(2), 645–690. https://doi.org/10.1152/physrev.00026.2014

Edwards, G., Dora, K. A., Gardener, M. J., Garland, C. J., & Weston, A. H. (1998). K^+ is an endothelium-derived hyperpolarizing factor in rat arteries. *Nature*, *396*, 269. Retrieved from http://dx.doi.org/10.1038/24388

Eglen, R. M., & Harris, G. C. (1993). Selective inactivation of muscarinic M_2 and M_3 receptors in guinea-pig ileum and atria *in vitro*. *British Journal of Pharmacology*, *109*(4), 946–952. https://doi.org/10.1111/j.1476-5381.1993.tb13712.x

Eglen, R. M., Hegde, S. S., & Watson, N. (1996). Muscarinic receptor subtypes and smooth muscle function. *Pharmacological Reviews*, *48*(4), 531—565. Retrieved from http://europepmc.org/abstract/MED/8981565

Eichler, I., Wibawa, J., Grgic, I., Knorr, A., Brakemeier, S., Pries, A. R., … Köhler, R. (2003). Selective blockade of endothelial Ca^{2+}-activated small- and intermediate-conductance K^+-channels suppresses EDHF-mediated vasodilation.

British Journal of Pharmacology, *138*(4), 594–601. https://doi.org/10.1038/sj.bjp.0705075

Eik, L. F., Naidu, M., David, P., Wong, K. H., Tan, Y. S., & Sabaratnam, V. (2012). *Lignosus rhinocerus* (Cooke) ryvarden: A medicinal mushroom that stimulates neurite outgrowth in PC-12 cells. *Evidence-Based Complementary and Alternative Medicine*, *2012*. https://doi.org/10.1155/2012/320308

El Enshasy, H. A., & Hatti-Kaul, R. (2013). Mushroom immunomodulators: Unique molecules with unlimited applications. *Trends in Biotechnology*, *31*(12), 668–677. https://doi.org/10.1016/j.tibtech.2013.09.003

Erle, D. J., & Sheppard, D. (2014). The cell biology of asthma. *Journal of Cell Biology*, *205*(5), 621–631. https://doi.org/10.1083/jcb.201401050

Estrada-Soto, S., Rodríguez-Avilez, A., Castañeda-Ávila, C., Castillo-España, P., Navarrete-Vázquez, G., Hernández, L., & Aguirre-Crespo, F. (2007). Spasmolytic action of *Lepechinia caulescens* is through calcium channel blockade and NO release. *Journal of Ethnopharmacology*, *114*(3), 364–370. https://doi.org/10.1016/j.jep.2007.08.023

Etter, E. F., Eto, M., Wardle, R. L., Brautigan, D. L., & Murphy, R. A. (2001). Activation of myosin light chain phosphatase in intact arterial smooth muscle during nitric oxide-induced relaxation. *The Journal of Biological Chemistry*, *276*(37), 34681–34685. https://doi.org/10.1074/jbc.M104737200

Fabricant, D. S., & Farnsworth, N. R. (2001). The value of plants used in traditional medicine for drug discovery. *Environmental Health Perspectives*, *109*(Suppl. 1), 69–75. https://doi.org/10.1289/ehp.01109s169

Fang, Z., Hwang, J. H., Kim, J. S., Jung, S. J., & Oh, S. B. (2010). R-type calcium channel isoform in rat dorsal root ganglion neurons. *Korean Journal of Physiology and Pharmacology*, *14*(1), 45. https://doi.org/10.4196/kjpp.2010.14.1.45

Faruqi, S., Murdoch, R. D., Allum, F., & Morice, A. H. (2014). On the definition of chronic cough and current treatment pathways: an international qualitative study. *Cough*, *10*(1), 5. https://doi.org/10.1186/1745-9974-10-5

Fastier, F. N., & Reid, C. S. W. (1949). "Constant flow" organ-bath techniques. *British Journal of Pharmacology and Chemotherapy*, *4*(1), 109–110. Retrieved from http://www.ncbi.nlm.nih.gov/pmc/articles/PMC1509897/

Félétou, M., & Vanhoutte, P. M. (2000). Endothelium-dependent hyperpolarization of vascular smooth muscle cells. *Acta Pharmacol Sin.*

Finn, D. F., & Walsh, J. J. (2013). Twenty-first century mast cell stabilizers. *British Journal of Pharmacology*, *170*(1), 23–37. https://doi.org/10.1111/bph.12138

Firth, A. L., Remillard, C. V., & Yuan, J. X. J. (2007). TRP channels in hypertension. *Biochimica et Biophysica Acta*, *1772*(8), 895–906. https://doi.org/10.1016/j.bbadis.2007.02.009

Fisslthaler, B., Popp, R., Kiss, L., Potente, M., Harder, D. R., Fleming, I., & Busse, R. (1999). Cytochrome P450 2C is an EDHF synthase in coronary arteries. *Nature*, *401*, 493. https://doi.org/10.1038/46816

Flores-Soto, E., Reyes-García, J., Sommer, B., & Montaño, L. M. (2013).

Sarcoplasmic reticulum Ca^{2+} refilling is determined by L-type Ca^{2+} and store operated Ca^{2+} channels in guinea pig airway smooth muscle. *European Journal of Pharmacology*, *721*(1–3), 21–28. https://doi.org/10.1016/j.ejphar.2013.09.060

Forstermann, U., Schmidt, H. H. H. W., Pollock, J. S., Sheng, H., Mitchell, J. A., Warner, T. D., … Murad, F. (1991). Isoforms of nitric oxide synthase characterization and purification from different cell types. *Biochemical Pharmacology*, *42*(10), 1849–1857.

Fosbraey, P., & Johnson, E. S. (1980). Release-modulating acetylcholine receptors on cholinergic neurones of the guinea pig ileum. *British Journal of Pharmacology*, *68*(2), 289–300. https://doi.org/10.1111/j.1476-5381.1980.tb10418.x

Fozard, J. R., Pfannkuche, H. J., & Schuurman, H. J. (1996). Mast cell degranulation following adenosine A_3 receptor activation in rats. *European Journal of Pharmacology*, *298*(3), 293–297. https://doi.org/10.1016/0014-2999(95)00822-5

Frigo, G. M., & Lecchini, S. (1970). An improved method for studying the peristaltic reflex in the isolated colon. *British Journal of Pharmacology*, *39*(2), 346–356. Retrieved from http://www.ncbi.nlm.nih.gov/pmc/articles/PMC1702850/

Fryer, A. D., & Jacoby, D. B. (1998). Muscarinic receptors and control of airway smooth muscle. *American Journal of Respiratory and Critical Care Medicine*, *158*(5 Pt 3), S154–S160. https://doi.org/10.1164/ajrccm.158.supplement_2.13tac120

Fuchs, A., Rigaud, M., Sarantopoulos, C. D., Filip, P., & Hogan, Q. H. (2007). Contribution of calcium channel subtypes to the intracellular calcium signal in sensory neurons: the effect of injury. *Anesthesiology*, *107*(1), 117–127. https://doi.org/10.1097/01.anes.0000267511.21864.93

Funaba, M., Ikeda, T., & Abe, M. (2003). Degranulation in RBL-2H3 cells: Regulation by calmodulin pathway. *Cell Biology International*, *27*(10), 879–885. https://doi.org/10.1016/S1065-6995(03)00177-X

Furchgott, R. F. (1999). Endothelium-derived relaxing factor: Discovery, early studies, and identifcation as nitric oxide (nobel lecture). *Angewandte Chemie International Edition*, *38*(13/14), 1870–1880. https://doi.org/10.1002/(SICI)1521-3773(19990712)38:13/14<1870::AID-ANIE1870>3.3.CO;2-#

Furuya, T., Hirotani, M., & Matsuzawa, M. (1983). N6-(2-hydroxyethyl)adenosine, a biologically active compound from cultured mycelia of *Cordyceps* and *Isaria* species. *Phytochemistry*, *22*(11), 2509–2512.

Gaddum, J. H. (1953). The technique of superfusion. *British Journal of Pharmacology and Chemotherapy*, *8*(3), 321–326. https://doi.org/10.1111/j.1476-5381.1953.tb00801.x

Galligan, J. J., & Akbarali, H. I. (2014). Molecular physiology of enteric opioid receptors. *American Journal of Gastroenterology*, *2*, 17–21. https://doi.org/10.1038/ajgsup.2014.5

Ganitkevich, B., & Isenberg, G. (1990). Contribution of two types of calcium channels to membrane conductance of single myocytes from guinea-pig coronary artery. *Physiology*, *426*, 19–42.

Gashaw, I., Ellinghaus, P., Sommer, A., & Asadullah, K. (2011). What makes a good drug target? *Drug Discovery Today*, *16*(23/24), 1037–1043. https://doi.org/10.1016/j.drudis.2011.09.007

Gemes, G., Rigaud, M., Koopmeiners, A. S., Poroli, M. J., Zoga, V., & Hogan, Q. H. (2010). Calcium signaling in intact dorsal root ganglia: new observations and the effect of injury. *Anesthesiology*, *113*(1), 134–146. https://doi.org/10.1097/ALN.0b013e3181e0ef3f

Gerevich, Z., Borvendeg, Sebestyen J. Schröder, W., Heike, F., Kerstin, W., Nörenberg, W., Fürst, S., … Peter, I. (2004). Inhibition of N-Type voltage-activated calcium channels in rat dorsal root ganglion neurons by P2Y receptors is a possible mechanism of ADP-induced analgesia. *Journal of Neuroscience*, *24*(4), 797–807. https://doi.org/10.1523/JNEUROSCI.4019-03.2004

Gilani, A. H., Mandukhail, S. U. R., Iqbal, J., Yasinzai, M., Aziz, N., Khan, A., & Najeeb-ur-Rehman. (2010). Antispasmodic and vasodilator activities of *Morinda citrifolia* root extract are mediated through blockade of voltage dependent calcium channels. *BMC Complementary and Alternative Medicine*, *10*, 2. https://doi.org/10.1186/1472-6882-10-2

Gilbert, H. S., & Ornstein, L. (1975). Basophil counting with a new staining method using alcian blue. *Blood*, *46*(2), 279–286.

Ginsburg, R., Bristow, M. R., Harrison, D. C., & Stinson, E. B. (1980). Studies with isolated human coronary arteries: some general observations, potential mediators of spasm, role of calcium antagonists. *Chest*, *78*(1, Supplement), 180–186. https://doi.org/https://doi.org/10.1378/chest.78.1_Supplement.180

Goldie, R. G., Paterson, J. W., & Wale, J. L. (1982). Pharmacological responses of human and porcine lung parenchyma, bronchus and pulmonary artery. *British Journal of Pharmacology*, *76*(4), 515–521. https://doi.org/10.1111/j.1476-5381.1982.tb09248.x

Gosens, R., Zaagsma, J., Meurs, H., & Halayko, A. J. (2006). Muscarinic receptor signaling in the pathophysiology of asthma and COPD. *Respiratory Research*, *7*, 73. https://doi.org/10.1186/1465-9921-7-73

Gosling, M., Poll, C., & Li, S. (2005). TRP channels in airway smooth muscle as therapeutic targets. *Naunyn-Schmiedeberg's Archives of Pharmacology*, *371*(4), 277–284. https://doi.org/10.1007/s00210-005-1058-2

Govindaraju, K., Lee, M. K., Mbaki, Y., & Nee, T. K. (2018). Intracellular stored calcium plays a minor role in G_q-coupled receptor-mediated contraction in rat airway smooth muscle. *Life Sciences, Medicine and Biomedicine*, *2*(2), 1–6.

Grassby, P. F., & Broadley, K. J. (1984). Characterization of β-adrenoceptors mediating relaxation of the guinea-pig ileum. *Journal of Pharmacy and Pharmacology*, *36*(9), 602–607. https://doi.org/10.1111/j.2042-7158.1984.tb04906.x

Grienberger, C., & Konnerth, A. (2012). Imaging calcium in neurons. *Neuron*, *73*(5), 510–517. https://doi.org/10.4161/chan.4.6.12869

Grienke, U., Zöll, M., Peintner, U., & Rollinger, J. M. (2014). European medicinal polypores - A modern view on traditional uses. *Journal of Ethnopharmacology*, *154*(3), 564–583. https://doi.org/10.1016/j.jep.2014.04.030

Griffith, T. M. (2004). Endothelium-dependent smooth muscle hyperpolarization: Do gap junctions provide a unifying hypothesis? *British Journal of Pharmacology*, *141*(6), 881–903. https://doi.org/10.1038/sj.bjp.0705698

Griffith, T. M., Henderson, A. H., Edwards, D. H., & Lewis, M. J. (1984). Isolated perfused rabbit coronary artery and aortic strip preparations: the role of endothelium-derived relaxant factor. *The Journal of Physiology*, *351*(1), 13–24. https://doi.org/10.1113/jphysiol.1984.sp015228

Guan, Y. Y., Kwan, C. Y., & Daniel, E. E. (1988). The effects of EGTA on vascular smooth muscle contractility in calcium-free medium. *Canadian Journal of Physiology and Pharmacology*. https://doi.org/10.1139/y88-172

Guo, C., Wong, K. H., & Cheung, P. C. K. (2011). Hot water extract of the sclerotium of *Polyporus rhinocerus* Cooke enhances the immune functions of murine macrophages. *International Journal of Medicinal Mushrooms*, *13*(3), 237–244. https://doi.org/10.1615/IntJMedMushr.v13.i3.30

H, P., & Paramesh, R. C. (2018). Overview in the management of persistent cough in paediatric practice. *MOJ Current Research and Reviews*, *1*(4), 154–157. https://doi.org/10.15406/mojcrr.2018.01.00024

Hanani, M. (2005). Satellite glial cells in sensory ganglia: From form to function. *Brain Research Reviews*, *48*(3), 457–476. https://doi.org/10.1016/j.brainresrev.2004.09.001

Hanania, N. A. (2008). Targeting airway inflammation in asthma: Current and future therapies. *Chest*, *133*(4), 989–998. https://doi.org/10.1378/chest.07-0829

Hannon, J. P., Tigani, B., Wolber, C., Williams, I., Mazzoni, L., Howes, C., & Fozard, J. R. (2002). Evidence for an atypical receptor mediating the augmented bronchoconstrictor response to adenosine induced by allergen challenge in actively sensitized Brown Norway rats. *British Journal of Pharmacology*, *135*(3), 685–696. https://doi.org/10.1038/sj.bjp.0704516

Harding, S. D., Sharman, J. L., Faccenda, E., Southan, C., Pawson, A. J., Ireland, S., … Davies, J. A. (2018). NC-IUP: The IUPHAR/BPS Guide to PHARMACOLOGY in 2018: updates and expansion to encompass the new guide to IMMUNOPHARMACOLOGY. *Nucl. Acids Res.*, *46*(D1), D1091–D1106. https://doi.org/10.1093/nar/gkx1121

Harteneck, C., & Gollasch, M. (2011). Pharmacological modulation of diacylglycerol-sensitive TRPC3/6/7 channels. *Current Pharmaceutical Biotechnology*, *12*(1), 35–41. https://doi.org/10.2174/138920111793937943

Harvey, A. L., Edrada-Ebel, R., & Quinn, R. J. (2015). The re-emergence of natural products for drug discovery in the genomics era. *Nature Reviews Drug Discovery*, *14*(2), 111–129. https://doi.org/10.1038/nrd4510

Hazelwood, L. a, & Sanders-Bush, E. (2004). His452Tyr polymorphism in the human 5-HT_{2A} receptor destabilizes the signaling conformation. *Molecular Pharmacology*, *66*(5), 1293–1300. https://doi.org/10.1124/mol.66.5.

He, X., Li, S., Liu, B., Susperreguy, S., Formoso, K., Yao, J., … Liao, Y. (2017). Major contribution of the 3/6/7 class of TRPC channels to myocardial ischemia/reperfusion and cellular hypoxia/reoxygenation injuries. *Proceedings of the National Academy of Sciences*, *114*(23), E4582–E4591.

https://doi.org/10.1073/pnas.1621384114

Heim, N., & Griesbeck, O. (2004). Genetically encoded indicators of cellular calcium dynamics based on troponin C and green fluorescent protein. *Journal of Biological Chemistry*, *279*(14), 14280–14286. https://doi.org/10.1074/jbc.M312751200

Henry Nicholas Ridley. (1890). On the so-called Tiger's Milk, "susu rimau" of the Malays. *Journal of the Straits Branch of the Royal Asiatic Society*, 341.

Hill, D. A., Siracusa, M. C., Abt, M. C., Kim, B. S., Kobuley, D., Kubo, M., … Artis, D. (2012). Commensal bacteria-derived signals regulate basophil hematopoiesis and allergic inflammation. *Nature Medicine*, *18*(4), 538–546. https://doi.org/10.1038/nm.2657

Hill, J. A., Olson, E. N., & Griendling, K. K. (Eds.). (2012). *Muscle: Fundamental biology and mechanisms of disease*. Amsterdam; Boston: Elsevier Science.

Hirota, K., Hashiba, E., Yoshioka, H., Kabara, S., & Matsuki, A. (2003). Effects of three different L-type Ca^{2+} entry blockers on airway constriction induced by muscarinic receptor stimulation. *British Journal of Anaesthesia*, *90*(5), 671–675. https://doi.org/10.1093/bja/aeg118

Hirota, S., & Janssen, L. J. (2007). Store-refilling involves both L-type calcium channels and reverse-mode sodium-calcium exchange in airway smooth muscle. *European Respiratory Journal*, *30*(2), 269–278. https://doi.org/10.1183/09031936.00008507

Hirst, G. D. S., & Ward, S. M. (2003). Interstitial cells: Involvement in rhythmicity and neural control of gut smooth muscle. *Journal of Physiology*, *550*(2), 337–346. https://doi.org/10.1113/jphysiol.2003.043299

Hobbs, C. (2002). *Medicinal mushrooms: An exploration of tradition, healing, and culture*. Canada: Botanica Press, Book Publishing Company. Retrieved from https://books.google.com.my/

Holgate, S., & Polosa, R. (2006). The mechanisms, diagnosis, and management of severe asthma in adults. *Lancet*, *368*(9537), 780–793. https://doi.org/https://doi.org/10.1016/S0140-6736(06)69288-X

Holt, P. G., & Sly, P. D. (2007). Th2 cytokines in the asthma late-phase response. *Lancet*, *370*(9596), 1396–1398. https://doi.org/10.1016/S0140-6736(07)61587-6

Hong-Geller, E., & Cerione, R. A. (2000). Cdc42 and Rac stimulate exocytosis of secretory granules by activating the IP_3/calcium pathway in RBL-2H3 mast cells. *The Journal of Cell Biology*, *148*(3), 481–493. https://doi.org/10.1083/jcb.148.3.481

Horinouchi, T., & Koike, K. (2000). Functional identification of b_3-adrenoceptors in the guinea-pig ileum using the non-selective b-adrenoceptor antagonist (+/-)-bupranolol. *Journal of Autonomic Pharmacology*, *20*, 253–258.

Hosoe, T., Iizuka, T., Chiba, Y., Itabashi, T., Morita, H., Ishizaki, T., & Kawai, K. (2006). Relaxing effects of Phellinus gilvus extract and purified ebricoic acid on rat aortic rings. *Journal of Natural Medicines*, *60*(2), 130–134. https://doi.org/10.1007/s11418-006-0030-x

Hosoi, T., Ino, S., Ohnishi, F., Todoroki, K., Yoshii, M., Kakimoto, M., … Ozawa, K.

(2018). Mechanisms of the action of adenine on anti-allergic effects in mast cells. *Immunity, Inflammation and Disease*, *6*(1), 97–105. https://doi.org/10.1002/iid3.200

Houghton, P. J., & Raman, A. (2012). *Laboratory handbook for the fractionation of natural extracts*. Springer Science & Business Media B.V. https://doi.org/10.1007/978-1-4615-5809-5

Hu, T., Huang, Q., Wong, K., & Yang, H. (2017). Structure, molecular conformation, and immunomodulatory activity of four polysaccharide fractions from *Lignosus rhinocerotis* sclerotia. *International Journal of Biological Macromolecules*, *94*, 423–430. https://doi.org/10.1016/j.ijbiomac.2016.10.051

Hu, T., Huang, Q., Wong, K., Yang, H., Gan, J., & Li, Y. (2017). A hyperbranched β-D-glucan with compact coil conformation from *Lignosus rhinocerotis* sclerotia. *Food Chemistry*, *225*, 267–275. https://doi.org/10.1016/j.foodchem.2017.01.034

Hua, X., Chason, K. D., Fredholm, B. B., Deshpande, D. A., Penn, R. B., & Tilley, S. L. (2008). Adenosine induces airway hyperresponsiveness through activation of A_3 receptors on mast cells. *J Allergy Clin Immunol*, *122*(1), 107–113.e7. https://doi.org/10.1038/nchembio.1527.A

Hua, X., Kovarova, M., Chason, K. D., Nguyen, M., Koller, B. H., & Tilley, S. L. (2007). Enhanced mast cell activation in mice deficient in the A_{2b} adenosine receptor. *The Journal of Experimental Medicine*, *204*(1), 117–128. https://doi.org/10.1084/jem.20061372

Huang, F., Zhang, X., Zhang, L., Li, Q., Ni, B., Zheng, X., & Chen, A. (2010). Mast cell degranulation induced by chlorogenic acid. *Acta Pharmacologica Sinica*, *31*(7), 849–854. https://doi.org/10.1038/aps.2010.63

Huang, N. L. (1999). Identification of the scientific name of Hurulingzhi. *Acta Edulis Fungi*, *6*, 30–32.

Hughes, J. P., Rees, S. S., Kalindjian, S. B., & Philpott, K. L. (2011). Principles of early drug discovery. *British Journal of Pharmacology*, *162*(6), 1239–1249. https://doi.org/10.1111/j.1476-5381.2010.01127.x

Hutchinson, D. S., Evans, B. A., & Summers, R. J. (2001). Beta(1)-adrenoceptors compensate for beta(3)-adrenoceptors in ileum from beta(3)-adrenoceptor knock-out mice. *British Journal of Pharmacology*, *132*(2), 433–442. https://doi.org/10.1038/sj.bjp.0703828

Ikawati, Z., Wahyuono, S., & Maeyama, K. (2001). Screening of several Indonesian medicinal plants for their inhibitory effect on histamine release from RBL-2H3 cells. *Journal of Ethnopharmacology*, *75*, 249–256. https://doi.org/10.1016/S0378-8741(01)00201-X

Imaizumi, Y., & Watanabe, M. (1981). The effect of tetraethylammonium chloride on potassium permeability in the smooth muscle cell membrane of canine trachea. *The Journal of Physiology*, *316*(Jul), 33–46.

Ina, K., Kataoka, T., & Ando, T. (2013). The use of lentinan for treating gastric cancer. *Anti-Cancer Agents in Medicinal Chemistry*, *13*(5), 681–688. https://doi.org/10.2174/1871520611313050002

Inoue, R., Jensen, L. J., Shi, J., Morita, H., Nishida, M., Honda, A., & Ito, Y. (2006).

Transient receptor potential channels in cardiovascular function and disease. *Circulation Research*, *99*(2), 119–131. https://doi.org/10.1161/01.RES.0000233356.10630.8a

Inoue, R., Okada, T., Onoue, H., Hara, Y., Shimizu, S., Naitoh, S., … Mori, Y. (2001). The transient receptor potential protein homologue TRP6 is the essential component of vascular α_1-adrenoceptor–activated ca^{2+}-permeable cation channel. *Circulation Research*, *88*(3), 325–332. https://doi.org/10.1161/01.RES.88.3.325

Istvan, V., Haanen, C., Steffens-Nakken, H., & Reutelingsperger, C. (1995). A novel assay for apoptosis: Flow cytometric detection of phosphatidylserine early apoptotic cells using fluorescein labelled Annexin V. *Journal of Immunological Methods*, *184*(1), 39–51. https://doi.org/10.1016/0022-1759(95)00072-I

Ito, Y., & Itoh, T. (1984). The roles of stored calcium in contractions of cat tracheal smooth muscle produced by electrical stimulation, acetylcholine and high K^+. *British Journal of Pharmacology*, *83*(3), 667–676. https://doi.org/10.1111/j.1476-5381.1984.tb16220.x

Ito, Y., Kuriyama, H., & Parker, I. (1988). Calcium transients evoked by electrical stimulation of smooth muscle from guinea-pig ileum recorded by the use of Fura-2. *The Journal of Physiology*, *407*, 117–134.

Jeong, S. C., Koyyalamudi, S. R., Jeong, Y. T., Song, C. H., & Pang, G. (2012). Macrophage immunomodulating and antitumor activities of polysaccharides isolated from agaricus bisporus white button mushrooms. *Journal of Medicinal Food*, *15*(1), 58–65. https://doi.org/doi: 10.1089/jmf.2011.1704

Jespersen, B., Tykocki, N. R., Watts, S. W., & Cobbett, P. J. (2015). Measurement of smooth muscle function in the isolated tissue bath-applications to pharmacology research. *Journal of Visualized Experiments*, *95*(e52324), 1–9. https://doi.org/10.3791/52324

Johnathan, M., Gan, S. H., Ezumi, M. F. W., Faezahtul, A. H., & Nurul, A. A. (2016). Phytochemical profiles and inhibitory effects of Tiger Milk mushroom (*Lignosus rhinocerus*) extract on ovalbumin-induced airway inflammation in a rodent model of asthma. *BMC Complementary and Alternative Medicine*, *16*(167). https://doi.org/10.1186/s12906-016-1141-x

Juckmeta, T., Thongdeeying, P., & Itharat, A. (2014). Inhibitory effect on β-hexosaminidase release from RBL-2H3 cells of extracts and some pure constituents of Benchalokawichian, a Thai Herbal Remedy, used for allergic disorders. *Evidence-Based Complementary and Alternative Medicine*, *2014*, 1–8. https://doi.org/10.1155/2014/828760

Jude, J. A., Wylam, M. E., Walseth, T. F., & Kannan, M. S. (2008). Calcium signaling in airway smooth muscle. *Proceedings of the American Thoracic Society*, *5*(1), 15–22. https://doi.org/10.1513/pats.200704-047VS

Judge, E. P., Hughes, J. M. L., Egan, J. J., Maguire, M., Molloy, E. L., & O'Dea, S. (2014). Anatomy and bronchoscopy of the porcine lung: A model for translational respiratory medicine. *American Journal of Respiratory Cell and Molecular Biology*, *51*(3), 334–343. https://doi.org/10.1165/rcmb.2013-0453TR

Kanae, Y., Takagi, T., & Hotta, K. (1977). Mobilization of cellular calcium and contraction-relaxation of vascular smooth muscle. *The Japanese Journal of*

Physiology, *27*, 551–564.

Kang, K.-T. (2014). Endothelium-derived relaxing factors of small resistance arteries in hypertension. *Toxicological Research*, *30*(3), 141–148. https://doi.org/10.5487/TR.2014.30.3.141

Kerr, P. M., Hillier, K., Wallis, R. M., & Garland, C. J. (1995). Characterization of muscarinic receptors mediating contractions of circular and longitudinal muscle of human isolated colon. *British Journal of Pharmacology*, *115*(8), 1518–1524. https://doi.org/10.1111/j.1476-5381.1995.tb16645.x

Keyhanmanesh, R., Gholamnezhad, Z., & Boskabady, M. H. (2014). The relaxant effect of *Nigella sativa* on smooth muscles, Its possible mechanisms and clinical applications. *Iranian Journal of Basic Medical Sciences*, *17*(12), 939–949.

Khan, T., Ali, S., Qayyum, R., Hussain, I., Wahid, F., & Shah, A. J. (2016). Intestinal and vascular smooth muscle relaxant effect of *Viscum album* explains its medicinal use in hyperactive gut disorders and hypertension. *BMC Complementary and Alternative Medicine*, *16*, 251. https://doi.org/10.1186/s12906-016-1229-3

Khazdair, M. R., & Boskabady, M. H. (2015). The relaxant effect of *Ferula assafoetida* on smooth muscles and the possible mechanisms. *Journal of HerbMed Pharmacology*, *4*(2), 40–44.

Kim, H. H., Lee, S., Singh, T. S. K., Choi, J. K., Shin, T. Y., & Kim, S. H. (2012). *Sparassis crispa* suppresses mast cell-mediated allergic inflammation: Role of calcium, mitogen-activated protein kinase and nuclear factor-κB. *International Journal of Molecular Medicine*, *30*(2), 344–350. https://doi.org/10.3892/ijmm.2012.1000

Kim, J. Y., Byeon, S. E., Lee, Y. G., Lee, J. Y., Park, J., Hong, E. K., & Cho, J. Y. (2008). Immunostimulatory activities of polysaccharides from liquid culture of pine-mushroom *Tricholoma matsutake*. *Journal of Microbiology and Biotechnology*, *18*(1), 95–103.

Kiyonaka, S., Kato, K., Nishida, M., Mio, K., Numaga, T., Sawaguchi, Y., … Mori, Y. (2009). Selective and direct inhibition of TRPC3 channels underlies biological activities of a pyrazole compound. *Proceedings of the National Academy of Sciences*, *106*(13), 5400–5405. https://doi.org/10.1073/pnas.0808793106

Kobayashi, H., Matsunaga, K., & Oguchi, Y. (1995). Antimetastatic effects of PSK (Krestin), a protein-bound polysaccharide obtained from basidiomycetes: An overview. *Cancer Epidemiology Biomarkers and Prevention*, *4*(3), 275–281. https://doi.org/PMID: 7606203

Kohda, H., Tokumoto, W., Sakamoto, K., Fujii, M., Hirai, Y., Yamasaki, K., … Uchida, M. (1985). The biologically active constituents of *Ganoderma lucidum* (FR.) KARST. histamine release-inhibitory triterpenes. *Chemical & Pharmaceutical Bulletin*, *33*(4), 1367–1374. https://doi.org/10.1248/cpb.33.1367

Kojima, Y., Takahashi, T., Fujina, M., & Owyang, C. (1994). Inhibition of cholinergic transmission by opiates in ileal myenteric plexus is mediated by kappa receptor. Involvement of regulatory inhibitory G protein and calcium N-channels. *Journal of Pharmacology and Experimental Therapeutics*, *268*(2), 965–970.

Kotlikoff, M. I. (1993). Potassium channels in airway smooth muscle: A tale of two

channels. *Pharmacology & Therapeutics*, *58*(1), 1–12.

Kuehn, H. S., Radinger, M., & Gilfillan, A. M. (2010). Measuring mast cell mediator release. *Current Protocols in Immunology*, *91*(1), 7.38.1-7.38.9. https://doi.org/10.1002/0471142735.im0738s91

Kuga, T., Sadoshima, J., Tomoike, H., Kanaide, H., Akaike, N., & Nakamura, M. (1990). Actions of Ca^{2+} antagonists on two types of Ca^{2+} channels in rat aorta smooth muscle cells in primary culture. *Circulation Research*, *67*(2), 469–480. https://doi.org/10.1161/01.RES.67.2.469

Kulczycki, A., & Metzger, H. (1974). The interaction of IgE with rat basophilic leukemia cells. II. Quantitative aspects of the binding reaction. *The Journal of Experimental Medicine*, *140*, 1676–1695. https://doi.org/10.1084/jem.140.6.1676

Kulczycki, B. Y. A., Isersky, C., & Metzger, H. (1974). The interaction of IgE with rat basophilic leukemia cells. I. Evidence for specific binding of IgE. *The Journal of Experimental Medicine*, *139*, 600–616.

Kunichika, N., Yu, Y., Remillard, C. V, Platoshyn, O., Zhang, S., & Yuan, J. X.-J. (2004). Overexpression of TRPC1 enhances pulmonary vasoconstriction induced by capacitative Ca^{2+} entry. *American Journal of Physiology: Lung Cellular and Molecular Physiology*, *287*(5), L962–L969. https://doi.org/10.1152/ajplung.00452.2003

Kurrasch-Orbaugh, D. M., Parrish, J. C., Watts, V. J., & Nichols, D. E. (2003). A complex signaling cascade links the serotonin2A receptor to phospholipase A2 activation: The involvement of MAP kinases. *Journal of Neurochemistry*, *86*(4), 980–991. https://doi.org/10.1046/j.1471-4159.2003.01921.x

Lai, C. K. M., Wong, K. H., & Cheung, P. C. K. (2008). Antiproliferative effects of sclerotial polysaccharides from *Polyporus rhinocerus* Cooke (Aphyllophoromycetideae) on different kinds of leukemic cells. *International Journal of Medicinal Mushrooms*, *10*(3), 255–264. https://doi.org/10.1615/IntJMedMushr.v10.i3.60

Lau, B. F., Abdullah, N., Aminudin, N., & Lee, H. B. (2013). Chemical composition and cellular toxicity of ethnobotanical-based hot and cold aqueous preparations of the tiger's milk mushroom (*Lignosus rhinocerotis*). *Journal of Ethnopharmacology*, *150*(1), 252–262. https://doi.org/10.1016/j.jep.2013.08.034

Lau, B. F., Abdullah, N., Aminudin, N., Lee, H. B., & Tan, P. J. (2015). Ethnomedicinal uses, pharmacological activities, and cultivation of *Lignosus* spp. (tigeŕs milk mushrooms) in Malaysia - A review. *Journal of Ethnopharmacology*, *169*, 441–458. https://doi.org/10.1016/j.jep.2015.04.042

Lau, B. F., Abdullah, N., Aminudin, N., Lee, H. B., Yap, K. C., & Sabaratnam, V. (2014). The potential of mycelium and culture broth of *Lignosus rhinocerotis* as substitutes for the naturally occurring sclerotium with regard to antioxidant capacity, cytotoxic effect, and low-molecular-weight chemical constituents. *PloS One*, *9*(7), e102509. https://doi.org/10.1371/journal.pone.0102509

Lechin, F., Van Der Dijs, B., Orozco, B., Lechin, M., & Lechin, A. E. (1996). Increased levels of free serotonin in plasma of symptomatic asthmatic patients. *Annals of Allergy, Asthma and Immunology*, *77*(3), 245–253.

https://doi.org/10.1016/S1081-1206(10)63263-2

Lee, C. H., Poburko, D., Sahota, P., Sandhu, J., Ruehlmann, D. O., & van Breemen, C. (2001). The mechanism of phenylephrine-mediated $[Ca^{2+}]_i$ oscillations underlying tonic contraction in the rabbit inferior vena cava. *Journal of Physiology*, *534*(3), 641–650. https://doi.org/10.1111/j.1469-7793.2001.t01-1-00641.x

Lee, M. L., Tan, N. H., Fung, S. Y., Tan, C. S., & Ng, S. T. (2012). The antiproliferative activity of sclerotia of *Lignosus rhinocerus* (tiger milk mushroom). *Evidence-Based Complementary and Alternative Medicine*, *2012*, 5–9. https://doi.org/10.1155/2012/697603

Lee, S. S., Chang, Y. S., & Noraswati, M. N. R. (2009). Utilization of macrofungi by some indigenous communities for food and medicine in Peninsular Malaysia. *Forest Ecology and Management*, *257*, 2062–2065. https://doi.org/10.1016/j.foreco.2008.09.044

Lee, S. S., Tan, N. H., Fung, S. Y., Sim, S. M., Tan, C. S., & Ng, S. T. (2014). Anti-inflammatory effect of the sclerotium of L*ignosus rhinocerotis* (Cooke) Ryvarden, the Tiger Milk mushroom. *BMC Complementary and Alternative Medicine*, *14*, 359. https://doi.org/10.1186/1472-6882-14-359

Lee, S. Y., Cho, J. Y., Shim, J. J., Kim, H. K., Kang, K. H., Yoo, S. H., & In, K. H. (2001). Airway inflammation as an assessment of chronic nonproductive cough. *Chest*, *120*(4), 1114–1120. https://doi.org/10.1378/chest.120.4.1114

Lewis, M. J., Short, A. L., & Lewis, K. E. (2006). Autonomic nervous system control of cardiovascular and respiratory systems in asthma. *Respiratory Medicine*, *100*(10), 1688–1705.

Lian, Q., Cheng, Y., Zhong, C., & Wang, F. (2015). Inhibition of the IgE-mediated activation of RBL-2H3 cells by TIPP, a novel thymic immunosuppressive pentapeptide. *International Journal of Molecular Sciences*, *16*(1), 2252–2268. https://doi.org/10.3390/ijms16012252

Lievremont, J., Bird, G. S., & Putney, J. W. (2005). Mechanism of inhibition of TRPC cation channels by 2-aminoethoxydiphenylborane. *Molecular Pharmacology*, *68*(3), 758–762. https://doi.org/10.1124/mol.105.012856.1

Lin, J.-Y., Chen, M.-L., Chiang, B.-L., & Lin, B.-F. (2006). *Ganoderma tsugae* supplementation alleviates bronchoalveolar inflammation in an airway sensitization and challenge mouse model. *International Immunopharmacology*, *6*(2), 241–251. https://doi.org/10.1016/j.intimp.2005.08.009

Lincoln, T. M. (1989). Cyclic GMP and mechanisms of vasodilation. *Pharmacology and Therapeutics*, *41*(3), 479–502. https://doi.org/10.1016/0163-7258(89)90127-7

Lindsay, R. M. (1988). Nerve growth factors (NGF, BDNF) enhance axonal regeneration but are not required for survival of adult sensory neurons. *Journal of Neuroscience*, *8*(7), 2394–2405.

Liu, C., Chen, J., Chen, L., Huang, X., & Cheung, P. C. K. (2016). Immunomodulatory activity of polysaccharide–protein complex from the mushroom sclerotia of *Polyporus rhinocerus* in murine macrophages. *Journal of Agricultural and Food Chemistry*, *64*(16), 3206–3214. https://doi.org/10.1021/acs.jafc.6b00932

Löfdahl, A., Wenglén, C., Rydell-Törmänen, K., Westergren-Thorsson, G., & Larsson-Callerfelt, A. K. (2018). Effects of 5-Hydroxytryptamine class 2 receptor antagonists on bronchoconstriction and pulmonary remodeling processes. *The American Journal of Pathology*, *188*(5), 1113–1119. https://doi.org/10.1016/j.ajpath.2018.01.006

Loong, B. J., Tan, J. H., Lim, K. H., Mbaki, Y., & Ting, K. N. (2015). Contractile function of smooth muscle retained after overnight storage. *Naunyn-Schmiedeberg's Archives of Pharmacology*, *388*(10), 1061–1067. https://doi.org/10.1007/s00210-015-1140-3

Losinski, A., & Alexander, S. P. H. (1995). Adenosine receptor-mediated relaxation of guinea-pig precontracted, isolated trachea. *British Journal of Pharmacology*, *116*, 2425–2428.

Ma, H.-T., Venkatachalam, K., Parys, J. B., & Gill, D. L. (2002). Modification of store-operated channel coupling and inositol trisphosphate receptor function by 2-aminoethoxydiphenyl borate in DT40 lymphocytes. *The Journal of Biological Chemistry*, *277*(9), 6915–6922. https://doi.org/10.1074/jbc.M107755200

Majed, B. H., & Khalil, R. A. (2012). Molecular mechanisms regulating the vascular prostacyclin pathways and their adaptation during pregnancy and in the newborn. *Pharmacological Reviews*, *64*(3), 540–582. https://doi.org/10.1124/pr.111.004770

Martin, S., Pombo, I., Poncet, P., David, B., Arock, M., & Blank, U. (2000). Immunologic stimulation of mast cells leads to the reversible exposure of phosphatidylserine in the absence of apoptosis. *International Archives of Allergy and Immunology*, *123*(3), 249–258. Retrieved from https://www.karger.com/DOI/10.1159/000024451

Martinovic, M. (2013). News in the pathophysiology of asthma. *Vojnosanitetski Pregled*, *70*(8), 768–772. https://doi.org/10.2298/VSP1308768M

Matsuda, H., Nakamura, S., & Yoshikawa, M. (2016). Degranulation inhibitors from medicinal plants in antigen-stimulated rat. *Chemical and Pharmaceutical Bulletin*, *64*(2), 96–103.

Matsui, M., Motomura, D., Fujiwara, T., Jiang, J., Takahashi, S., Manabe, T., & Taketo, M. M. (2002). Mice lacking M_2 and M_3 muscarinic acetylcholine receptors are devoid of cholinergic smooth muscle contractions but still viable. *The Journal of Neuroscience*, *22*(24), 10627–10632. https://doi.org/10.1016/j.eururo.2006.10.028

McCorry, L. K. (2009). *Essentials of human physiology for pharmacy* (2nd ed.). Boca Raton, Fla; London: CRC Press.

McKenzie, C., MacDonald, A., & Shaw, A. M. (2009). Mechanisms of U46619-induced contraction of rat pulmonary arteries in the presence and absence of the endothelium. *British Journal of Pharmacology*, *157*(4), 581–596. https://doi.org/10.1111/j.1476-5381.2008.00084.x

Meera, P., Wallner, M., & Toro, L. (2000). A neuronal beta subunit (KCNMB4) makes the large conductance, voltage- and Ca^{2+}-activated K_+ channel resistant to charybdotoxin and iberiotoxin. *Proceedings of the National Academy of Sciences*, *97*(10), 5562–5567. https://doi.org/10.1073/pnas.100118597

Meldolesi, J. (2004). The development of Ca^{2+} indicators: A breakthrough in pharmacological research. *Trends in Pharmacological Sciences*, *25*(4), 172–174. https://doi.org/10.1016/j.tips.2004.02.004

Merdivan, S., Jenett-Siems, K., Siems, K., Niedermeyer, T. H. J., Schultze, N., Steinborn, C., … Lindequist, U. (2017). Effects of extracts and compounds from *Tricholoma populinum* Lange on degranulation and IL-2/IL-8 secretion of immune cells. *Zeitschrift Fur Naturforschung - Section C Journal of Biosciences*, *72*(7–8), 277–283. https://doi.org/10.1515/znc-2016-0247

Merdivan, S., Jenett-Siems, K., Siems, K., Niedermeyer, T., Solis, M. J., Unterseher, M., & Lindequist, U. (2017). Inhibition of degranulation of RBL-2H3 cells by extracts and compounds from *Armillaria ostoyae*. *Planta Medica International Open*, *4*(01), e1–e7. https://doi.org/10.1055/s-0042-121608

Merkus, D., Houweling, B., Mirza, A., Boomsma, F., van den Meiracker, A. H., & Duncker, D. J. (2003). Contribution of endothelin and its receptors to the regulation of vascular tone during exercise is different in the systemic, coronary and pulmonary circulation. *Cardiovascular Research*, *59*(3), 745–754. https://doi.org/Doi 10.1016/S0008-6363(03)00479-6

Meurs, H., Gosens, R., & Zaagsma, J. (2008). Airway hyperresponsiveness in asthma: Lessons from *in vitro* model systems and animal models. *European Respiratory Journal*, *32*(2), 487–502. https://doi.org/10.1183/09031936.00023608

Michel, J.-B., Li, Z., & Lacolley, P. (2012). Smooth muscle cells and vascular diseases. *Cardiovascular Research*, *95*(2), 135–137. https://doi.org/10.1093/cvr/cvs172

Millqvist, E. (2016). TRPV1 and TRPM8 in treatment of chronic cough. *Pharmaceuticals*, *9*(3), 45. https://doi.org/10.3390/ph9030045

Mitchell, J. A., Ali, F., Bailey, L., Moreno, L., & Harrington, L. S. (2008). Role of nitric oxide and prostacyclin as vasoactive hormones released by the endothelium. *Experimental Physiology*, *93*(1), 141–147. https://doi.org/10.1113/expphysiol.2007.038588

Mitchelson, F., & Ziegler, A. (1984). The effect of gallamine, gallopamil and nifedipine on responses to acetylcholine and carbachol in the taenia of the guinea-pig caecum. *British Journal of Pharmacology*, *83*, 145–155.

Miyake, K., & Karasuyama, H. (2017). Emerging roles of basophils in allergic inflammation. *Allergology International*, *66*(3), 382–391. https://doi.org/10.1016/j.alit.2017.04.007

Miyawaki, A., Griesbeck, O., Heim, R., & Tsien, R. Y. (1999). Dynamic and quantitative Ca^{2+} measurements using improved cameleons. *Proceedings of the National Academy of Sciences*, *96*(5), 2135–2140. https://doi.org/10.1073/pnas.96.5.2135

Mizuno, M., Shiomi, Y., Minato, K. I., Kawakami, S., Ashida, H., & Tsuchida, H. (2000). Fucogalactan isolated from *Sarcodon aspratus* elicits release of tumor necrosis factor-α and nitric oxide from murine macrophages. *Immunopharmacology*, *46*(2), 113–121. https://doi.org/10.1016/S0162-3109(99)00163-0

Mizuta, K., Zhang, Y., Xu, D., Masaki, E., Panettieri, R. A., & Emala, C. W. (2012). The dopamine D2 receptor is expressed and sensitizes adenylyl cyclase activity

in airway smooth muscle. *American Journal of Physiology: Lung Cellular and Molecular Physiology*, *302*(3), L316–L324. https://doi.org/10.1152/ajplung.00130.2011

Mohanarji, S., Dharmalingam, S., Kalusalingam, A., & Science, A. (2012). Screening of *Lignosus rhinocerus* extracts as antimicrobial agents against selected human pathogens. *Journal of Pharmaceutical and Biomedical Sciences*, *18*(18), 1–4.

Moon, T. C., Dean Befus, A., & Kulka, M. (2014). Mast cell mediators: Their differential release and the secretory pathways involved. *Frontiers in Immunology*, *5*(NOV), 1–18. https://doi.org/10.3389/fimmu.2014.00569

Moraes, E. R. de, Kushmerick, C., & Naves, L. A. (2017). Morphological and functional diversity of first-order somatosensory neurons. *Biophysical Reviews*, *9*(5), 847–856. https://doi.org/10.1007/s12551-017-0321-3

Morita, K., & North, R. A. (1982). Opiate activation of potassium conductance in myenteric neurons: inhibition by calcium ion. *Brain Research*, *242*(1), 145–150. https://doi.org/10.1016/0006-8993(82)90504-2

Morris, S. M., & Billiar, T. R. (1994). New insights into the regulation nitric oxide synthesis of inducible nitric oxide synthesis. *American Journal of Physiology*, *266*(6 Pt 1), E829-839.

Motomura, Y., Morita, H., Moro, K., Nakae, S., Artis, D., Endo, T. A., … Kubo, M. (2014). Basophil-derived interleukin-4 controls the function of natural helper cells, a member of ILC2s, in lung inflammation. *Immunity*, *40*(5), 758–771. https://doi.org/10.1016/j.immuni.2014.04.013

Murphy, D. M., & Byrne, P. M. (2010). Recent advances in the pathophysiology of asthma. *Chest*, *137*(6), 1417–1426. https://doi.org/10.1378/chest.09-1895

Nandi, A. K., Samanta, S., Maity, S., Sen, I. K., Khatua, S., Devi, K. S. P., … Islam, S. S. (2014). Antioxidant and immunostimulant β-glucan from edible mushroom *Russula albonigra* (Krombh.) Fr. *Carbohydrate Polymers*, *99*, 774–782. https://doi.org/10.1016/j.carbpol.2013.09.016

Nasser, Y., Ho, W., & Sharkey, K. A. (2006). Distribution of adrenergic receptors in the enteric nervous system of the guinea pig, mouse, and rat. *The Journal of Comparative Neurology*, *495*(5), 529–553. https://doi.org/10.1002/cne.20898

Nau, F., Miller, J., Saravia, J., Ahlert, T., Yu, B., Happel, K. I., … Nichols, C. D. (2015). Serotonin 5-HT_2 receptor activation prevents allergic asthma in a mouse model. *American Journal of Physiology - Lung Cellular and Molecular Physiology*, *308*(2), L191–L198. https://doi.org/10.1152/ajplung.00138.2013

Newman, D. J., & Cragg, G. M. (2012). Natural products as sources of new drugs over the 30 years from 1981 to 2010. *Journal of Natural Products*, *75*(3), 311–335. https://doi.org/10.1021/np200906s

Ng, L. C., & Gurney, A. M. (2001). Store-operated channels Mediate Ca^{2+} influx and contraction in rat pulmonary artery. *Circulation Research*, *89*, 923–929. https://doi.org/10.1161/hh2201.100315

Ng, T. P., Wong, M. L., Hong, C. Y., Koh, K. T. C., & Goh, L. G. (2003). The use of complementary and alternative medicine by asthma patients. *QJM: An International Journal of Medicine*, *96*(10), 747–754.

https://doi.org/10.1093/qjmed/hcg121

Niimi, A. (2011). Cough and asthma. *Current Respiratory Medicine Reviews*, *7*, 47–54. https://doi.org/10.1016/j.pupt.2013.06.003

Niimi, A., Torrego, A., Nicholson, A. G., Cosio, B. G., Oates, T. B., & Chung, K. F. (2005). Nature of airway inflammation and remodeling in chronic cough. *Journal of Allergy and Clinical Immunology*, *116*(3), 565–570. https://doi.org/10.1016/j.jaci.2005.07.010

Nijkamp, F. P., Linde, H. J. Van Der, & Folkerts, G. (1993). Nitric oxide synthesis inhibitors induce airway hyperresponsiveness in the guinea pig *in vivo* and *in vitro*: Role of the epithelium. *American Review of Respiratory Disease*, *148*(3). https://doi.org/https://doi.org/10.1164/ajrccm/148.3.727

Nishiwaki, H., Saitoh, N., Nishio, H., Takeuchi, T., & Hata, F. (1998). Relationship between inhibitory effect of endogenous opioid via Mu-receptors and muscarinic autoinhibition in acetylcholine release from myenteric plexus of guinea pig ileum. *The Japanese Journal of Pharmacology*. https://doi.org/10.1254/jjp.77.279

North, R. A., Williams, J. T., Surprenant, A., & Christie, M. J. (1987). Mu and delta receptors belong to a family of receptors that are coupled to potassium channels. *Proceedings of the National Academy of Sciences of the United States of America*, *84*(August), 5487–5491. https://doi.org/10.1073/PNAS.84.15.5487

Nosalova, G., Jurecek, L., Chatterjee, U. R., Majee, S. K., Nosal, S., & Ray, B. (2013). Antitussive activity of the water-extracted carbohydrate polymer from *Terminalia chebula* on citric acid-induced cough. *Evidence-Based Complementary and Alternative Medicine*, *2013*. https://doi.org/10.1155/2013/650134

Nunes, C., Pereira, A. M., & Morais-Almeida, M. (2017). Asthma costs and social impact. *Asthma Research and Practice*, *3*, 1. https://doi.org/10.1186/s40733-016-0029-3

O'Byrne, P. M., Gauvreau, G. M., & Brannan, J. D. (2009). Provoked models of asthma: What have we learnt? *Clinical and Experimental Allergy*, *39*(2), 181–192. https://doi.org/10.1111/j.1365-2222.2008.03172.x

Obata, K., Mukai, K., Tsujimura, Y., Ishiwata, K., Kawano, Y., Minegishi, Y., … Karasuyama, H. (2007). Basophils are essential initiators of a novel type of chronic allergic inflammation. *Blood*, *110*(3), 913–920. https://doi.org/10.1182/blood-2007-01-068718

Ogishima, M., Kaibara, M., Ueki, S., Kurimoto, T., & Taniyama, K. (2000). Z-338 facilitates acetylcholine release from enteric neurons due to blockade of muscarinic autoreceptors in guinea pig stomach. *The Journal of Pharmacology And Experimental Therapeutics*, *294*(1), 33–37. Retrieved from http://jpet.aspetjournals.org/content/294/1/33.abstract

Oh, J. Y., Choi, W. S., Lee, C. H., & Park, H. J. (2011). The ethyl acetate extract of *Cordyceps militaris* inhibits IgE-mediated allergic responses in mast cells and passive cutaneous anaphylaxis reaction in mice. *Journal of Ethnopharmacology*, *135*(2), 422–429. https://doi.org/10.1016/j.jep.2011.03.030

Okada, T., Inoue, R., Yamazaki, K., Maeda, A., Kurosaki, T., Yamakuni, T., … Mori, Y. (1999). Molecular and functional characterization of a novel mouse transient

receptor potential protein homologue TRP7. *The Journal of Biological Chemistry*, *274*(39), 27359–27370.

Ouedraogo, N., & Roux, E. (2014). Physiology of airway smooth muscle contraction: An overview. *Pulmonary and Respiratory Medicine*, *4*(6), 6. https://doi.org/10.4172/2161-105X.1000221

Ouyang, K., Zheng, H., Qin, X., Zhang, C., Yang, D., Wang, X., … Cheng, H. (2005). Ca^{2+} sparks and secretion in dorsal root ganglion neurons. *Proceedings of the National Academy of Sciences of the United States of America*, *102*(34), 12259–12264. https://doi.org/10.1073/pnas.0408494102

Palmer, A. E., Giacomello, M., Kortemme, T., Hires, S. A., Lev-Ram, V., Baker, D., & Tsien, R. Y. (2006). Ca^{2+} indicators based on computationally redesigned calmodulin-peptide pairs. *Chemistry and Biology*, *13*(5), 521–530. https://doi.org/10.1016/j.chembiol.2006.03.007

Palmer, A. E., Qin, Y., Park, J. G., & McCombs, J. E. (2011). Design and application of genetically encoded biosensors. *Trends in Biotechnology*, *29*(3), 144–152. https://doi.org/10.1016/j.tibtech.2010.12.004

Paredes, R. M., Etzler, J. C., Watts, L. T., Zheng, W., & Lechleiter, J. D. (2008). Chemical calcium indicators. *Methods*, *46*(3), 143–151. https://doi.org/10.1016/j.ymeth.2008.09.025

Park, J. F., & Luo, Z. D. (2010). Calcium channel functions in pain processing. *Channels*, *4*(6), 510–517. https://doi.org/10.4161/chan.4.6.12869

Passante, E., Ehrhardt, C., Sheridan, H., & Frankish, N. (2009). RBL-2H3 cells are an imprecise model for mast cell mediator release. *Inflammation Research*, *58*(9), 611–618. https://doi.org/10.1007/s00011-009-0028-4

Passante, E., & Frankish, N. (2009). The RBL-2H3 cell line: Its provenance and suitability as a model for the mast cell. *Inflammation Research*, *58*(11), 737–745. https://doi.org/10.1007/s00011-009-0074-y

Patel, S., & Goyal, A. (2012). Recent developments in mushrooms as anti-cancer therapeutics: a review. *3 Biotech*, *2*(1), 1–15. https://doi.org/10.1007/s13205-011-0036-2

Patel, S., Shi, Y., Niculescu, R., Chung, E. H., Martin, J. L., & Zalewski, A. (2000). Characteristics of coronary smooth muscle cells and adventitial fibroblasts. *Circulation*, *101*(5), 524–532. https://doi.org/10.1165/ajrcmb.22.1.f172

Paton, W. D. M., & Vane, J. R. (1963). An analysis of the responses of the isolated stomach to electrical stimulation and to drugs. *The Journal of Physiology*, *165*(1), 10–46. Retrieved from http://www.ncbi.nlm.nih.gov/pmc/articles/PMC1359254/

Pelaia, G., Gallelli, L., Vatrella, A., Grembiale, R. D., Maselli, R., De Sarro, G. B., & Marsico, S. A. (2002). Potential role of potassium channel openers in the treatment of asthma and chronic obstructive pulmonary disease. *Life Sciences*, *70*, 977–990. https://doi.org/10.1016/S0024-3205(01)01487-4

Pelaia, G., Renda, T., Gallelli, L., Vatrella, A., Busceti, M. T., Agati, S., … Marsico, S. a. (2008). Molecular mechanisms underlying airway smooth muscle contraction and proliferation: Implications for asthma. *Respiratory Medicine*, *102*(8), 1173–1181. https://doi.org/10.1016/j.rmed.2008.02.020

Peng, B., He, R., Xu, Q.-H., Gao, J., Lu, Y.-L., & Li, J.-R. (2011). Comparison of RBL-2H3 and P815 cell lines for establishing *in vitro* model of mast cell degranulation. *Chinese Journal of Natural Medicines*, *9*(3), 227–231. https://doi.org/http://dx.doi.org/10.3724/SP.J.1009.2011.00227

Perez-Hernandez, N., Ponce-Monter, H., Medina, J. A., & Joseph-Nathan, P. (2008). Spasmolytic effect of constituents from *Lepechinia caulescens* on rat uterus. *Journal of Ethnopharmacology*, *115*(1), 30–35. https://doi.org/10.1016/j.jep.2007.08.044

Perez-Zoghbi, J. F., Bai, Y., & Sanderson, M. J. (2010). Nitric oxide induces airway smooth muscle cell relaxation by decreasing the frequency of agonist-induced Ca^{2+} oscillations. *The Journal of General Physiology*, *135*(3), 247–259. https://doi.org/10.1085/jgp.200910365

Pérez Koldenkova, V., & Nagai, T. (2013). Genetically encoded Ca^{2+} indicators: Properties and evaluation. *Biochimica et Biophysica Acta - Molecular Cell Research*, *1833*(7), 1787–1797. https://doi.org/10.1016/j.bbamcr.2013.01.011

Petrova, R. D., Wasser, S. P., Mahajna, J. A., Denchev, C. M., & Nevo, E. (2005). Potential role of medicinal mushrooms in breast cancer treatment: current knowledge and future perspectives. *International Journal of Medicinal Mushrooms*, *7*(1–2), 141–155. https://doi.org/10.1615/IntJMedMushr.v7.i12.140

Phan, C., David, P., Naidu, M., Wong., K.-H., & Sabaratnam, V. (2013). Neurite outgrowth stimulatory effects of culinary- medicinal mushrooms and their toxicity assessment using differentiating Neuro-2a and embryonic fibroblast BALB/3T3. *BMC Complementary and Alternative Medicine*, *13*, 261. https://doi.org/10.1186/1472-6882-13-261

Pi, C., Wang, H., Lu, C., Lu, F. L., & Chen, C. (2014). Ganoderma formosanum polysaccharides attenuate Th2 inflammation and airway hyperresponsiveness in a murine model of allergic asthma. *SpringerPlus*, *3*(297), 1–11.

Plant, T. D., & Schaefer, M. (2003). TRPC4 and TRPC5: Receptor-operated Ca^{2+}-permeable nonselective cation channels. *Cell Calcium*, *33*(5–6), 441–450. https://doi.org/10.1016/S0143-4160(03)00055-1

Polverino, M., Polverino, F., Fasolino, M., Andò, F., Alfieri, A., & De Blasio, F. (2012). Anatomy and neuro-pathophysiology of the cough reflex arc. *Multidisciplinary Respiratory Medicine*, *7*, 5. https://doi.org/10.1186/2049-6958-7-5

Poucheret, P., Fons, F., & Rapior, S. (2006). Biological and pharmacological activit of higher fungi: A 20-year retrospective analysis. *Cryptogamie, Mycologie*, *27*(4), 311–333.

Prado, C. M., Martins, M. a., & Tibério, I. F. L. C. (2011). Nitric oxide in asthma physiopathology. *ISRN Allergy*, *2011*, 1–13. https://doi.org/10.5402/2011/832560

Price, J. (1985). An immunohistochemical and quantitative examination of dorsal root ganglion neuronal subpopulations. *The Journal of Neuroscience*, *5*(8), 2051–2059.

Proskocil, B. J., & Fryer, A. D. (2005). B_2-agonist and anticholinergic drugs in the treatment of lung disease. *Proceedings of the American Thoracic Society*, *2*(4),

305–310. https://doi.org/10.1513/pats.200504-038SR

Pucci, M. L., Tong, X., Miller, K. B., Guan, H., & Nasjletti, A. (1995). Calcium- and protein kinase C–dependent basal tone in the aorta of hypertensive rats. *Hypertension*, *25*(4), 752–757.

Pushparajah, V., Fatima, A., Chong, C. H., Gambule, T. Z., Chan, C. J., Ng, S. T., … Lim, R. L. H. (2016). Characterisation of a new fungal immunomodulatory protein from tiger milk mushroom, *Lignosus rhinocerotis*. *Scientific Reports*, *6*(January), 1–12. https://doi.org/10.1038/srep30010

Raemdonck, K., de Alba, J., Birrell, M. a, Grace, M., Maher, S. a, Irvin, C. G., … Belvisi, M. G. (2012). A role for sensory nerves in the late asthmatic response. *Thorax*, *67*(1), 19–25. https://doi.org/10.1136/thoraxjnl-2011-200365

Rameshrad, M., Babaei, H., Azarmi, Y., & Fouladi, D. F. (2016). Rat aorta as a pharmacological tool for *in vitro* and *in vivo* studies. *Life Sciences*, *145*, 190–204. https://doi.org/10.1016/j.lfs.2015.12.043

Ramkumar, V., Stiles, G. L., Beaven, M. A., & Ali, H. (1993). The A_3 adenosine receptor is the unique adenosine receptor which facilitates release of allergic mediators in mast cells. *Journal of Biological Chemistry*, *268*(23), 16887–16890.

Rang, H. P., Dale, M. M., Ritter, J. M., Flower, R. J., Henderson, G., & Henderson, G. (2015). *Rang & Dale's Pharmacology* (8th ed.). London, England: Elsevier Churchill Livingstone.

Reese, D. E., Mikawa, T., & Bader, D. M. (2002). Development of the coronary vessel system. *Circulation Research*, *91*(9), 761–768. https://doi.org/10.1161/01.RES.0000038961.53759.3C

Ren, L., Perera, C., & Hemar, Y. (2012). Antitumor activity of mushroom polysaccharides: a review. *Food & Function*, *3*(11), 1118. https://doi.org/10.1039/c2fo10279j

Reynolds, S. D., Pinkerton, K. E., & Mariassy, A. T. (2015). Chapter 6: Epithelial Cells of Trachea and Bronchi. In *Comparative Biology of the Normal Lung: Second Edition* (Second Edi, pp. 61–81). Elsevier Inc. https://doi.org/10.1016/B978-0-12-404577-4.00006-0

Ricciardolo, F. L. M. (2003). Multiple roles of nitric oxide in the airways. *Thorax*, *58*(2), 175–182.

Riccio, A., Mattei, C., Kelsell, R. E., Medhurst, A. D., Calver, A. R., Randall, A. D., … Pangalos, M. N. (2002). Cloning and functional expression of human short TRP7, a candidate protein for store-operated Ca^{2+} influx. *Journal of Biological Chemistry*, *277*(14), 12302–12309. https://doi.org/10.1074/jbc.M112313200

Rivera, J. O., Hughes, H. W., & Stuart, A. G. (2004). Herbals and Asthma: Usage Patterns among a Border Population. *Annals of Pharmacotherapy*, *38*(2), 220–225. https://doi.org/10.1345/aph.1D319

Robinson, D. S. (2010). The role of the T cell in asthma. *Journal of Allergy and Clinical Immunology*, *126*(6), 1081–1091. https://doi.org/10.1016/j.jaci.2010.06.025

Rodrigues, M., Silva, a C., Águas, a P., & Grande, N. R. (2005). The coronary circulation of the pig heart : Comparison with the human heart. *European Journal*

Of Anatomy, *9*(2), 67–87.

Romoser, V. A., Hinkle, P. M., & Persechini, A. (1997). Detection in living cells of Ca^{2+}-dependent changes in the fluorescence emission of an indicator composed of two green fluorescent protein variants linked by a calmodulin binding sequence - A new class of fluorescent indicators. *Journal of Biological Chemistry*, *272*(20), 13270–13274.

Rönnberg, E., Melo, F. R., & Pejler, G. (2012). Mast cell proteoglycans. *Journal of Histochemistry and Cytochemistry*, *60*(12), 950–962. https://doi.org/10.1369/0022155412458927

Rubanyi, G., & Paul, R. J. (1985). Two distinct effects of oxygen on vascular tone in isolated porcine coronary arteries. *Circulation Research*, *56*(1), 1–10. https://doi.org/https://doi.org/10.1161/01.RES.56.1.1

Rudich, N., Ravid, K., & Sagi-Eisenberg, R. (2012). Mast cell adenosine receptors function: A focus on the A_3 adenosine receptor and inflammation. *Frontiers in Immunology*, *3*, 134. https://doi.org/10.3389/fimmu.2012.00134

Rysavy, N. M., Shimoda, L. M. N., Dixon, A. M., Speck, M., Stokes, A. J., Umemoto, E. Y., … Turner, H. (2014). Beyond apoptosis: The mechanism and function of phosphatidylserine asymmetry in the membrane of activating mast cells. *BioArchitecture*, *4*(4–5), 127–137. https://doi.org/10.1080/19490992.2014.995516

Sadraei, H., Asghari, G., & Poorkhosravi, R. (2011). Spasmolytic effect of root and aerial parts extract of *Pycnocycla spinosa* on neural stimulation of rat ileum. *Research in Pharmaceutical Sciences*, *6*(1), 43–50.

Sahni, D., Kaur, G. D., Harjeet, & Jit, I. (2008). Anatomy & distribution of coronary arteries in pig in comparison with man. *Indian Journal of Medical Research*, *127*(6), 564–570.

Salido, G. M., Sage, S. O., & Rosado, J. a. (2009). TRPC channels and store-operated Ca^{2+} entry. *Biochimica et Biophysica Acta - Molecular Cell Research*, *1793*(2), 223–230. https://doi.org/10.1016/j.bbamcr.2008.11.001

Sanderson, M. J., Delmotte, P., Bai, Y., & Perez-Zogbhi, J. F. (2008). Regulation of airway smooth muscle cell contractility by Ca^{2+} signaling and sensitivity. *Proceedings of the American Thoracic Society*, *5*(1), 23–31. https://doi.org/10.1513/pats.200704-050VS

Sandig, H., & Bulfone-Paus, S. (2012). TLR signaling in mast cells: Common and unique features. *Frontiers in Immunology*, *3*(JUL), 1–13. https://doi.org/10.3389/fimmu.2012.00185

Sasidharan, S., Chen, Y., Saravanan, D., Sundram, K. M., & Yoga Latha, L. (2011). Extraction, isolation and characterization of bioactive compounds from plants' extracts. *African Journal of Traditional, Complementary and Alternative Medicines*, *8*(1), 1–10. https://doi.org/10.4314/ajtcam.v8i1.60483

Sato, H., Kobayashi, Y., Hattori, A., Suzuki, T., Shigekawa, M., & Jippo, T. (2012). Inhibitory effects of water-soluble low-molecular-weight β-(1,3-1,6) D-glucan isolated from *Aureobasidium pullulans* 1A1 strain black yeast on mast cell degranulation and passive cutaneous anaphylaxis. *Bioscience, Biotechnology, and Biochemistry*, *76*(1), 84–88. https://doi.org/10.1271/bbb.110536

Schachter, E. N., Zuskin, E., Goswami, S., Castranova, V., Arumugam, U., Whitmer, M., … Fainberg, J. (2005). Pharmacological study of oyster mushroom (*Pleurotus ostreatus*) extract on isolated guinea pig trachea smooth muscle. *Lung*, *183*(1), 63–71. https://doi.org/10.1007/s00408-004-2527-y

Scheibner, J., Trendelenburg, A.-U., Hein, L., Starke, K., & Blandizzi, C. (2002). Alpha2-adrenoceptors in the enteric nervous system: A study in alpha2A-adrenoceptor-deficient mice. *British Journal of Pharmacology*, *135*(3), 697–704. https://doi.org/10.1038/sj.bjp.0704512

Schmidt, D., Ruehlmann, E., Branscheid, D., Magnussen, H., & Rabe, K. F. (1999). Passive sensitization of human airways increases responsiveness to leukotriene C4. *European Respiratory Journal*, *14*(2), 315–319. https://doi.org/10.1034/j.1399-3003.1999.14b13.x

Schmidt, T. F., Pavinatto, F. J., Caseli, L., Gonzaga, M. L. C., Soares, S. A., Ricardo, N. M. P. S., & Oliveira, O. N. (2009). Interaction of polysaccharide-protein complex from *Agaricus blazei* with Langmuir and Langmuir-Blodgett films of phospholipids. *Journal of Colloid and Interface Science*, *330*(1), 84–89. https://doi.org/10.1016/j.jcis.2008.10.024

Scroggs, R. S., & Fox, A. P. (1992). Calcium current variation between acutely isolated adult rat dorsal root ganglion neurons of different size. *The Journal of Physiology*, *445*(1), 639–658. https://doi.org/10.1113/jphysiol.1992.sp018944

Seifert, R. (2015). How do basic secretagogues activate mast cells? *Naunyn-Schmiedeberg's Archives of Pharmacology*, *388*(3), 279–281. https://doi.org/10.1007/s00210-015-1093-6

Selig, W. M., Bloomquist, M. A., Cohen, M. L., & Fleisch, J. H. (1988). Serotonin-induced pulmonary responses in the perfused guinea pig lung: Evidence for $5HT_2$ receptor-mediated pulmonary vascular and airway smooth muscle constriction. *Pulmonary Pharmacology*, *1*(2), 93–99. https://doi.org/10.1016/S0952-0600(88)80005-X

Semenov, I., Herlihy, J. T., & Brenner, R. (2012). *In vitro* measurements of tracheal constriction using mice. *Journal of Visualized Experiments*, *64*(e3703), 1–7. https://doi.org/10.3791/3703

Seow, C. Y., Schellenberg, R. R., & Pare, P. D. (1998). Structural and functional changes in the airway smooth muscle of asthmatic subjects. *American Journal of Respiratory and Critical Care Medicine*, *158*, S179–S186.

Seow, S. L. S., Eik, L. F., Naidu, M., David, P., Wong, K. H., & Sabaratnam, V. (2015). *Lignosus rhinocerotis* (Cooke) Ryvarden mimics the neuritogenic activity of nerve growth factor via MEK/ERK1/2 signaling pathway in PC-12 cells. *Scientific Reports*, *5*(November), 1–13. https://doi.org/10.1038/srep16349

Shibata, H., & Yagi, T. (1996). Rate assay of N-acetyl-β-D-hexosaminidase with 4-nitrophenyl N-acetyl-β-D-glucosaminide as an artificial substrate. *Clinica Chimica Acta*, *251*(1), 53–64. https://doi.org/10.1016/0009-8981(96)06292-4

Shimokawa, H., Yasutake, H., Fujii, K., Owada, M. K., Nakaike, R., Fukumoto, Y., … Takeshita, A. (1996). The importance of the hyperpolarizing mechanism increases as the vessel size decreases in endothelium-dependent relaxations in rat mesenteric circulation. *Journal of Cardiovascular Pharmacology*, *28*(5), 703–

711.

Shore, S. a., & Moore, P. E. (2003). Regulation of β-adrenergic responses in airway smooth muscle. *Respiratory Physiology and Neurobiology*, *137*(2–3), 179–195. https://doi.org/10.1016/S1569-9048(03)00146-0

Siddiqui, S., Redhu, N. S., Ojo, O. O., Liu, B., Irechukwu, N., Billington, C., … Moir, L. M. (2013). Emerging airway smooth muscle targets to treat asthma. *Pulmonary Pharmacology and Therapeutics*, *26*(1), 132–144. https://doi.org/10.1016/j.pupt.2012.08.008

Simon, E., Lamoree, M. H., Hamers, T., & de Boer, J. (2015). Challenges in effect-directed analysis with a focus on biological samples. *Trends in Analytical Chemistry*, *67*, 179–191. https://doi.org/10.1016/j.trac.2015.01.006

Singh, S. S., Wang, H., Chan, Y. S., Pan, W., Dan, X., Yin, C. M., … Ng, T. B. (2015). Lectins from edible mushrooms. *Molecules*, *20*(1), 446–469. https://doi.org/10.3390/molecules20010446

Siraganian, R. P., Castro, R. O. De, Barbu, E. A., & Zhang, J. (2011). Mast cell signaling: the role of protein tyrosine kinase Syk, its activation and screening methods for new pathway participants. *FEBS Lett.*, *584*(24), 4933–4940. https://doi.org/10.1016/j.febslet.2010.08.006.Mast

Siraganian, R. P., Kulczycki, A., Mendoza, G., & Metzger, H. (1975). Ionophore A-23187 induced histamine release from rat mast cells and rat basophil leukemia (RBL-1) cells. *The Journal of Immunology*, *115*(6), 1599–1602.

Smyth, J. T., Hwang, S. Y., Tomita, T., DeHaven, W. I., Mercer, J. C., & Putney, J. W. (2010). Activation and regulation of store-operated calcium entry. *Journal of Cellular and Molecular Medicine*, *14*(10), 2337–2349. https://doi.org/10.1111/j.1582-4934.2010.01168.x

So, I., Yang, D. K., Kim, H. J., Min, K. W., Kang, T. M., Kim, S. J., … Kim, I.-G. (2003). Five subtypes of muscarinic receptors are expressed in gastric smooth muscles of guinea pig. *Experimental & Molecular Medicine*, *35*(1), 46–52. https://doi.org/10.1038/emm.2003.7

Soejima, O., Katsuragi, T., & Furukawa, T. (1993). Opposite modulation by muscarinic M_1 and M_3 receptors of acetylcholine release from guinea pig ileum as measured directly. *European Journal of Pharmacology*, *249*(1–2), 1–6. https://doi.org/10.1016/0014-2999(93)90654-Z

Song, W.-J., Chang, Y.-S., Faruqi, S., Kim, J.-Y., Kang, M.-G., Kim, S., … Morice, A. H. (2015). The global epidemiology of chronic cough in adults: a systematic review and meta-analysis. *European Respiratory Journal*, *45*(5), 1479–1481. https://doi.org/10.1183/09031936.00218714

Spencer, N. J., Smith, C. B., & Smith, T. K. (2001). Role of muscle tone in peristalsis in guinea-pig small intestine. *Journal of Physiology*, *530*(2), 295–306. https://doi.org/10.1111/j.1469-7793.2001.0295l.x

Spicuzza, L., Maria, G. Di, & Polosa, R. (2006). Adenosine in the airways : Implications and applications. *European Journal of Pharmacology*, *533*, 77–88. https://doi.org/10.1016/j.ejphar.2005.12.056

Stathopulos, P. B., Schindl, R., Fahrner, M., Zheng, L., Gasmi-Seabrook, G. M., Muik,

M., … Ikura, M. (2013). STIM1/Orai1 coiled-coil interplay in the regulation of store-operated calcium entry. *Nature Communications*, *4*, 2963. https://doi.org/10.1038/ncomms3963

Stengel, P. W., & Cohen, M. L. (2003). M_1 receptor-mediated nitric oxide-dependent relaxation unmasked in stomach fundus from M_3 receptor knockout mice. *The Journal of Pharmacology and Experimental Therapeutics*, *304*(2), 675–682. https://doi.org/10.1124/jpet.102.042283.M

Stone, K. D., Prussin, C., & Metcalfe, D. D. (2010). IgE, mast cells, basophils, and eosinophils. *Journal of Allergy and Clinical Immunology*, *125*(2 SUPPL. 2), S73–S80. https://doi.org/10.1016/j.jaci.2009.11.017

Striessnig, J., Grabner, M., Mitterdorfer, J., Hering, S., Sinnegger, M. J., & Glossmann, H. (1998). Structural basis of drug binding to L-type Ca^{2+} channels. *Trends in Pharmacological Sciences*, *19*(3), 108–115. https://doi.org/10.1016/S0165-6147(98)01171-7

Sweeney, M., McDaniel, S. S., Platoshyn, O., Zhang, S., Yu, Y., Lapp, B. R., … Yuan, J. X.-J. (2002). Role of capacitative Ca^{2+} entry in bronchial contraction and remodeling. *Journal of Applied Physiology*, *92*(4), 1594–1602. https://doi.org/10.1152/japplphysiol.00722.2001

Swindle, M. M., Makin, A., Herron, A. J., Clubb, F. J., & Frazier, K. S. (2012). Swine as models in biomedical research and toxicology testing. *Veterinary Pathology*, *49*(2), 344–356. https://doi.org/10.1177/0300985811402846

Szarek, J. L., Zhang, J. Z., & Gruetter, C. A. (1995). Mechanisms of 5-hydroxytryptamine-induced contraction of isolated rat intrapulmonary bronchi. *Pulmonary Pharmacology*, *8*(6), 273–281. https://doi.org/10.1006/pulp.1995.1037

Szymański, P., Markowicz, M., & Mikiciuk-Olasik, E. (2012). Adaptation of high-throughput screening in drug discovery—toxicological screening tests. *International Journal of Molecular Sciences*, *13*(1), 427–452. https://doi.org/10.3390/ijms13010427

Takahashi, A., Camacho, P., Lechleiter, J. D., & Herman, B. (1999). Measurement of intracellular calcium. *Physiological Reviews*, *79*(4), 1089–1125. https://doi.org/10.1152/physrev.1999.79.4.1089

Takemoto, M., Ito, Y., Takagi, K., Ogino, K., & Tomita, T. (1998). Effects of excess K^+ on carbachol-induced contractions in the guinea-pig tracheal muscle. *Journal of Smooth Muscle Research*, *34*, 45–55.

Takemoto, M., Takagi, K., Ogino, K., & Tomita, T. (1998). Comparison of contractions produced by carbachol, thapsigargin and cyclopiazonic acid in the guinea-pig tracheal muscle. *British Journal of Pharmacology*, *124*(7), 1449–1454. https://doi.org/10.1038/sj.bjp.0701993

Takeuchi, T., Fujinami, K., Goto, H., Fujita, A., Taketo, M. M., Manabe, T., … Hata, F. (2005). Roles of M_2 and M_4 muscarinic receptors in regulating acetylcholine release from myenteric neurons of mouse ileum. *Journal of Neurophysiology*, *93*, 2841–2848. https://doi.org/10.1152/jn.00986.2004.

Tan, C. S. (2009). *Setting-up pilot-plant for up-scaling production of 'Tiger-Milk'-mushroom as dietary functional food. Government of Malaysia: MOA*

TF0109M004.

Tan, C. S., Ng, S. T., Vikneswary, S., Lo, F. P., & Tee, C. S. (2010). Genetic marker for the identification of a malaysian mushroom, *Lignosus rhinocerus* (Cendawan Susu Rimau). *Acta Hortic*, (859), 161–167.

Tan, C. S., Ng, S. T., Yap, Y. H. Y., Lee, H. Y., Lee, S. S., Lee, M. L., … Sim, S. M. (2012). Breathing new life to a Malaysia lost national treasure—the Tiger Milk mushroom (*Lignosus rhinocerotis*). In M. Zhang, J. Wang, H. Chen (Ed.), *Mushroom Science XVIII: Proceedings of the 18th Congress of the International Society for Mushroom Science* (pp. 66–71). Beijing, China.

The Global Asthma Report 2014. Auckland, New Zealand: Global Asthma Network, (2014)

Thiericke, R., Schmid, I., Moore, T., & Ebert, G. (2000). Drug discovery from nature: A device for automated sample preparation. *American Biotechnology Laboratory*, *18*(10), 66.

Thrasher, S. M., Scalfone, L. K., Holowka, D., & Appleton, J. A. (2013). *In vitro* modeling of rat mucosal mast cell function in Trichinella spiralis infection Seana. *Parasite Immunology*, *35*(1), 21–31. https://doi.org/10.1016/j.pestbp.2011.02.012.Investigations

Ting, N., Thambyraja, A., Sugden, D., Scalbert, E., Delagrange, P., & Wilson, V. G. (2000). Pharmacological studies on the inhibitory action of melatonin and putative melatonin analogues on porcine vascular smooth muscle. *Naunyn-Schmiedeberg's Archives of Pharmacology*, *361*(3), 327–333. https://doi.org/10.1007/s002109900198

Togias, A. (2003). H1-Receptors: Localization and role in airway physiology and in immune functions. *Journal of Allergy and Clinical Immunology*, *112*(4), S60–S68. https://doi.org/10.1016/S0091-6749(03)01878-5

Toru, H., Ra, C., Nonoyama, S., Suzuki, K., Yata, J., & Nakahata, T. (1996). Induction of the high-affinity IgE receptor (Fc epsilon RI) on human mast cells by IL-4. *International Immunology*, *8*(9), 1367–1373.

Tuli, H. S., Sandhu, S. S., & Sharma, A. K. (2014). Pharmacological and therapeutic potential of Cordyceps with special reference to Cordycepin. *3 Biotech*, *4*(1), 1–12. https://doi.org/10.1007/s13205-013-0121-9

Unno, T., Matsuyama, H., Izumi, Y., Yamada, M., Wess, J., & Komori, S. (2006). Roles of M_2 and M_3 muscarinic receptors in cholinergic nerve-induced contractions in mouse ileum studied with receptor knockout mice. *British Journal of Pharmacology*, *149*(8), 1022–1030. https://doi.org/10.1038/sj.bjp.0706955

Unno, T., Matsuyama, H., Sakamoto, T., Uchiyama, M., Izumi, Y., Okamoto, H., … Komori, S. (2005). M_2 and M_3 muscarinic receptor-mediated contractions in longitudinal smooth muscle of the ileum studied with receptor knockout mice. *British Journal of Pharmacology*, *146*(1), 98–108. https://doi.org/10.1038/sj.bjp.0706300

Vane, J. R. (1964). The use of isolated organs for detecting active substances in the circulating blood. *British Journal of Pharmacology*, *23*, 360–373. https://doi.org/10.1111/j.1476-5381.1997.tb06805.x

Vanhoutte, P. M. (1989). Endothelium and control of vascular function. *Hypertension.*, *13*, 658–667.

Venkatachalam, K., & Montell, C. (2007). TRP channels. *Annu Rev Biochem.*, *76*, 387–417. https://doi.org/10.1146/annurev.biochem.75.103004.142819.TRP

Venkatachalam, K., van Rossum, D. B., Patterson, R. L., Ma, H.-T., & Gill, D. L. (2002). The cellular and molecular basis of store-operated calcium entry. *Nature Cell Biology*, *4*(11), E263–E272. https://doi.org/10.1038/ncb1102-e263

Ventura-Martínez, R., Rivero-Osorno, O., Gómez, C., & González-Trujano, M. E. (2011). Spasmolytic activity of *Rosmarinus officinalis L.* involves calcium channels in the guinea pig ileum. *Journal of Ethnopharmacology*, *137*(3), 1528–1532. https://doi.org/10.1016/j.jep.2011.08.047

Vines, C. M., Xue, M., Maestas, D. C., Cimino, D. F., & Prossnitz, E. R. (2002). Regulation of N-formyl peptide-mediated degranulation by receptor phosphorylation. *Journal of Immunology*, *169*(12), 6760–6766. https://doi.org/10.4049/jimmunol.169.12.6760

Wachtel-Galor, S., Yuen, J., Buswell, J. A., & Benzie, I. F. F. (2011). *Herbal medicine: Biomolecular and clinical aspects.* (B. IFF & W.-G. S, Eds.) (2nd ed.). Boca Raton (FL): CRC Press/Taylor & Francis. Retrieved from https://www.ncbi.nlm.nih.gov/books/NBK92757/

Waller, B. F., Orr, C. M., Slack, J. D., Pinkerton, C. A., Tassel, J. Van, & Peters, T. (1992). Anatomy, histology , and pathology of coronary arteries : A review relevant to new interventional and imaging techniques-Part I. *Clinical Pathoiogic Correlations*, *15*, 451–457.

Wang, N., Li, J., Huang, X., Chen, W., & Chen, Y. (2016). Herbal medicine Cordyceps sinensis improves health-related quality of life in moderate-to-severe asthma. *Evidence-Based Complementary and Alternative Medicine*, 1–8. https://doi.org/10.1155/2016/6134593

Wang, Q., Sheng, X., Shi, A., Hu, H., Yang, Y., Liu, L., … Liu, H. (2017). β-Glucans: Relationships between modification, conformation and functional activities. *Molecules*, *22*(2), 1–13. https://doi.org/10.3390/molecules22020257

Wang, W., Zhou, Q., Liu, L., & Zou, K. (2012). Anti-allergic activity of emodin on IgE-mediated activation in RBL-2H3 cells. *Pharmacological Reports*, *64*(5), 1216–1222. https://doi.org/10.1016/S1734-1140(12)70917-9

Wang, X., Liang, Y., Peng, C., Xie, H., Pan, M., Zhang, T., & Ito, Y. (2011). Preparative isolation and purification of chemical constituents of Belamcanda by MPLC, HSCCC and prep-HPLC. *Journal of Liquid Chromatography Related Technology*, *34*(4), 241–257. https://doi.org/10.1080/10826076.2011.547058

Ward, J. K., Belvisi, M. G., Fox, A. J., Miura, M., Tadjkarimi, S., Yacoub, M. H., & Barnes, P. J. (1993). Modulation of cholinergic neural bronchoconstriction by endogenous nitric oxide and vasoactive intestinal peptide in human airways *in vitro*. *Journal of Clinical Investigation*, *92*(2), 736–742.

Wegener, J. W., Schulla, V., Koller, A., Klugbauer, N., Feil, R., & Hofmann, F. (2006). Control of intestinal motility by the $Ca_{v1.2}$ L-type calcium channel in mice. *The FASEB Journal*, *20*(8), 1260–1262. https://doi.org/10.1096/fj.05-5292fje

Weller, M. G. (2012). A unifying review of bioassay-guided fractionation, effect-directed analysis and related techniques. *Sensors*, *12*(7), 9181–9209. https://doi.org/10.3390/s120709181

Willetts, H. J., & Bullock, S. (1992). Developmental biology of sclerotia. *Mycological Research*, *96*(10), 801–816. https://doi.org/10.1016/S0953-7562(09)81027-7

William, B., & Russell, G. W. E. (1907). *The diary of John Evelyn* (Vol. 1). M. Walter Dunne.

Windmiller, D. A., & Backer, J. M. (2003). Distinct Phosphoinositide 3-kinases mediate mast cell degranulation in response to G-protein-coupled versus FceRI receptors. *The Journal of Biological Chemistry*, *278*(14), 11874–11878. https://doi.org/doi: 10.1074/jbc.M211787200

Wirth, A., Benyó, Z., Lukasova, M., Leutgeb, B., Wettschureck, N., Gorbey, S., … Offermanns, S. (2008). G12-G13-LARG-mediated signaling in vascular smooth muscle is required for salt-induced hypertension. *Nature Medicine*, *14*(1), 64–68. https://doi.org/10.1038/nm1666

Wohlsen, A., Martin, C., Vollmer, E., Branscheid, D., Magnussen, H., Becker, W. M., … Uhlig, S. (2003). The early allergic response in small airways of human precision-cut lung slices. *European Respiratory Journal*, *21*(6), 1024–1032. https://doi.org/10.1183/09031936.03.00027502

Wohlsen, A., Uhlig, S., & Martin, C. (2001). Immediate allergic response in small airways. *American Journal of Respiratory and Critical Care Medicine*, *163*(6), 1462–1469. https://doi.org/10.1164/ajrccm.163.6.2007138

Wong, K. H., Lai, C. K. M., & Cheung, P. C. K. (2009). Stimulation of human innate immune cells by medicinal mushroom sclerotial polysaccharides. *International Journal of Medicinal Mushrooms*, *11*(3), 215–223. https://doi.org/10.1615/IntJMedMushr.v11.i3.10

Wong, K. H., Lai, C. K. M., & Cheung, P. C. K. (2011). Immunomodulatory activities of mushroom sclerotial polysaccharides. *Food Hydrocolloids*, *25*(2), 150–158. https://doi.org/10.1016/j.foodhyd.2010.04.008

World Health Organization (WHO) (31 August 2017). Retrieved 30 June 2018, from: http://www.who.int/news-room/fact-sheets/detail/asthma

Wright, D. B., Tripathi, S., Sikarwar, a., Santosh, K. T., Perez-Zoghbi, J., Ojo, O. O., … Schaafsma, D. (2013). Regulation of GPCR-mediated smooth muscle contraction: Implications for asthma and pulmonary hypertension. *Pulmonary Pharmacology and Therapeutics*, *26*(1), 121–131. https://doi.org/10.1016/j.pupt.2012.06.005

Wright, D., Sharma, P., Ryu, M.-H., Rissé, P.-A., Ngo, M., Maarsingh, H., … West, A. R. (2012). Models to study airway smooth muscle contraction *in vivo*, *ex vivo* and *in vitro*: Implications in understanding asthma. *Pulmonary Pharmacology & Therapeutics*, *26*, 24–36. https://doi.org/10.1016/j.pupt.2012.08.006

Wu, L., Sweet, T., & Clapham, D. E. (2010). International union of basic and clinical pharmacology. LXXVI. Current progress in the mammalian TRP ion channel family. *Pharmocological Reviews*, *62*(3), 381–404. https://doi.org/10.1124/pr.110.002725.Abbreviations

Wu, S., Yang, L., Gao, Y., Liu, X., & Liu, F. (2008). Multi-channel counter-current chromatography for high-throughput fractionation of natural products for drug discovery. *Journal of Chromatography A*, *1180*, 99–107. https://doi.org/10.1016/j.chroma.2007.12.024

Wu, Z., Chen, S., & Pan, H. (2004). Differential sensitivity of N- and P/Q-Type Ca2+ channel currents to a μ opioid in isolectin B4-positive and -negative dorsal root ganglion neurons. *Journal of Pharmacology and Experimental Therapeutics*, *311*(3), 939–947. https://doi.org/10.1124/jpet.104.073429.central

Xiao, J. H., Zheng, Y. M., Liao, B., & Wang, Y.-X. (2010). Functional role of canonical transient receptor potential 1 and canonical transient receptor potential 3 in normal and asthmatic airway smooth muscle cells. *American Journal of Respiratory Cell and Molecular Biology*, *43*(1), 17–25. https://doi.org/10.1165/rcmb.2009-0091OC

Yahaya, N. F. M., Rahman, M. A., & Abdullah, N. (2014). Therapeutic potential of mushrooms in preventing and ameliorating hypertension. *Trends in Food Science and Technology*, *39*(2), 104–115. https://doi.org/10.1016/j.tifs.2014.06.002

Yang, X., Li, Y., He, Y., Li, T., Wang, W., Zhang, J., … Lin, R. (2015). Cordycepin alleviates airway hyperreactivity in a murine model of asthma by attenuating the inflammatory process. *International Immunopharmacology*, *26*(2), 401–408. https://doi.org/10.1016/j.intimp.2015.04.017

Yap, H. Y., Chooi, Y. H., Firdaus Raih, M., Fung, S. Y., Ng, S. T., Tan, C. S., & Tan, N. H. (2014). The genome of the Tiger Milk mushroom, *Lignosus rhinocerotis*, provides insights into the genetic basis of its medicinal properties. *BMC Genomics*, *15*(1), 1–12. https://doi.org/10.1186/1471-2164-15-635

Yap, H. Y. Y., Chooi, Y. H., Fung, S. Y., Ng, S. T., Tan, C. S., & Tan, N. H. (2015). Transcriptome analysis revealed highly expressed genes encoding secondary metabolite pathways and small cysteine-rich proteins in the sclerotium of lignosus rhinocerotis. *PLoS ONE*, *10*(11), e0143549. https://doi.org/10.1371/journal.pone.0143549

Yap, H. Y. Y., Fung, S. Y., Ng, S. T., Tan, C. S., & Tan, N. H. (2015a). Genome-based proteomic analysis of *Lignosus rhinocerotis* (Cooke) Ryvarden sclerotium. *International Journal of Medical Sciences*, *12*(1), 23–31. https://doi.org/10.7150/ijms.10019

Yap, H. Y. Y., Fung, S. Y., Ng, S. T., Tan, C. S., & Tan, N. H. (2015b). Shotgun proteomic analysis of tiger milk mushroom (*Lignosus rhinocerotis*) and the isolation of a cytotoxic fungal serine protease from its sclerotium. *Journal of Ethnopharmacology*, *174*, 437–451. https://doi.org/10.1016/j.jep.2015.08.042

Yap, H. Y. Y., Muria-Gonzalez, M. J., Kong, B. H., Stubbs, K. A., Tan, C. S., Ng, S. T., … Chooi, Y. H. (2017). Heterologous expression of cytotoxic sesquiterpenoids from the medicinal mushroom *Lignosus rhinocerotis* in yeast. *Microbial Cell Factories*, *16*, 103. https://doi.org/10.1186/s12934-017-0713-x

Yap, Y. H. Y., Tan, N. H., Fung, S. Y., Aziz, A. A., Tan, C. S., & Ng, S. T. (2013). Nutrient composition, antioxidant properties, and anti-proliferative activity of *Lignosus rhinocerus* Cooke sclerotium. *Journal of the Science of Food and Agriculture*, *93*(12), 2945–2952. https://doi.org/10.1002/jsfa.6121

Yokogawa, T., Kim, S. U., Krieger, C., & Puil, E. (2001). Analysis of GABA A- and GABA B-receptor mediated effects on intracellular Ca^{2+} in DRG hybrid neurones. *British Journal of Pharmacology*, *134*, 98–107.

Yokoyama, K., & Yagasaki, O. (1990). Effects of Ca^{2+} blockers on the various types of stimuli-induced acetylcholine release from guinea pig ileum myenteric plexus. *The Japanese Journal of Pharmacology*, *52*(1), 109–114. https://doi.org/10.1254/jjp.52.109

Yoo, E. J., Cao, G., Koziol-White, C. J., Ojiaku, C. A., Sunder, K., Jude, J. A., … Panettieri, R. A. (2017). $G_{\alpha 12}$ facilitates shortening in human airway smooth muscle by modulating phosphoinositide 3-kinase-mediated activation in a RhoA-dependent manner. *British Journal of Pharmacology*, *174*(23), 4383–4395. https://doi.org/10.1111/bph.14040

Zaila, C. F. S., Zuraina, M. Y. F., Norfazlina, M. N., Mun, L. L., Nurshahirah, N., & Rajab, N. F. (2013). Antiproliferative effect of *Lignosus rhinocerotis*, the tiger milk mushroom on HCT 116 human colorectal cancer cells. *The Open Conference Proceedings Journal*, *4*(Suppl-2, M16), 65–70. https://doi.org/10.2174/2210289201304020065

Zang, R., Li, D., Tang, I.-C., Wang, J., & Yang, S.-T. (2012). Cell-based assays in high-throughput screening for drug discovery. *International Journal of Biotechnology for Wellness Industries*, *1*, 31–51. https://doi.org/10.6000/1927-3037.2012.01.01.02

Zeng, W., Yuan, J. P., Kim, M. S., Choi, Y. J., Huang, G. N., Worley, P. F., & Muallem, S. (2008). STIM1 gates TRPC channels but not Orai1 by electrostatic interaction. *Molecular Cell*, *32*(3), 439–448. https://doi.org/10.1016/j.molcel.2008.09.020.STIM1

Zhang, T., Srivastava, K., Wen, M. C., Yang, N., Cao, J., Busse, P., … Li, X. M. (2010). Pharmacology and immunological actions of a herbal medicine ASHMI^{TM} on allergic asthma. *Phytotherapy Research*, *24*(7), 1047–1055. https://doi.org/10.1002/ptr.3077

Zhang, Y., Kong, H., Fang, Y., Nishinari, K., & Phillips, G. O. (2013). Schizophyllan: A review on its structure, properties, bioactivities and recent developments. *Bioactive Carbohydrates and Dietary Fibre*, *1*(1), 53–71. https://doi.org/10.1016/j.bcdf.2013.01.002

Zhang, Z. C., Lian, B., Huang, D. M., & Cui, F. J. (2009). Compare activities on regulating lipid-metabolism and reducing oxidative stress of diabetic rats of *Tremella aurantialba* broth's extract (TBE) with its mycelia polysaccharides (TMP). *Journal of Food Science*, *74*(1). https://doi.org/10.1111/j.1750-3841.2008.00989.x

Zhao, L., Li, L., Ma, K.-T., Wang, Y., Li, J., Shi, W.-Y., … Si, J.-Q. (2016). NSAIDs modulate GABA-activated currents via Ca^{2+}-activated Cl^{-} channels in rat dorsal root ganglion neurons. *Experimental and Therapeutic Medicine*, *11*(5), 1755–1761. https://doi.org/10.3892/etm.2016.3158

Zhao, Z., Vavrusova, M., & Skibsted, L. H. (2018). Antioxidant activity and calcium binding of isomeric hydroxybenzoates. *Journal of Food and Drug Analysis*, *26*(2), 591–598. https://doi.org/10.1016/j.jfda.2017.07.001

Zholos, A. V., & Bolton, T. B. (1997). Muscarinic receptor subtypes controlling the cationic current in guinea-pig ileal smooth muscle. *British Journal of Pharmacology*, *122*(5), 885–893. https://doi.org/10.1038/sj.bjp.0701438

Zoppellaro, C., Bin, A., Brun, P., Banzato, S., Macchi, V., Castagliuolo, I., & Giron, M. C. (2013). Adenosine-mediated enteric neuromuscular function is affected during Herpes Simplex virus type 1 infection of rat enteric nervous system. *PLoS ONE*, *8*(8). https://doi.org/10.1371/journal.pone.0072648

Appendix A. Composition of buffers

1. Organ bath experiments

Krebs-Henseleit bicarbonate solution (also termed as "normal Krebs solution" in **Chapter 4**), at pH 7.4.

Compounds	Concentration (in mM)
Sodium chloride (NaCl)	120
Potassium chloride (KCl)	5.4
Magnesium sulfate heptahydrate ($MgSO_4.7H_2O$)	1.2
Potassium dihydrogen phosphate (KH_2PO_4)	1.2
Sodium bicarbonate ($NaHCO_3$)	25
Glucose (D-glucose, anhydrous)	11.7
Calcium chloride ($CaCl_2$)	1.26[a,b]

All above ingredients were purchased from R & M chemicals, UK.
[a]Omitted in "calcium-free Krebs solution" (**Chapter 4**).
[b]Doubled the concentration for use in guinea pig ileum experiments (**Chapter 5**).

2. Calcium imaging experiments

Superfusion buffer at pH 7.4 (**Chapter 4**)

Compounds	Concentration (in mM)
Sodium chloride (NaCl)	145
Potassium chloride (KCl)	5
Magnesium sulfate ($MgSO_4$)	1
Hydroxyethylpiperazine ethane sulfonic acid (HEPES, $C_8H_{18}N_2O_4S$)	10
Bovine serum albumin (BSA)	0.1 (%)
Glucose (D-glucose, anhydrous)	10
Calcium chloride ($CaCl_2$)	2

All above ingredients were purchased from Sigma, UK.

3. Cell culture experiments (β-hexosaminidase assay)

Siraganian buffer (releasing buffer), at pH 7.2 (**Chapter 7**)

Compounds	Concentration (in mM)
Sodium chloride (NaCl)	119
Potassium chloride (KCl)	5
Magnesium chloride ($MgCl_2$)	0.4
Piperazine-N,N'-bis(2-ethanesulfonic acid) (PIPES)	25
Sodium hydroxide (NaOH)	40
Bovine serum albumin (BSA)	0.1 (%)
Glucose (D-glucose, anhydrous)	5.6
Calcium chloride ($CaCl_2$)	1

Appendix B. Effect of hot water extract of *Lignosus rhinocerotis* on rat trachea pre-contracted with carbachol

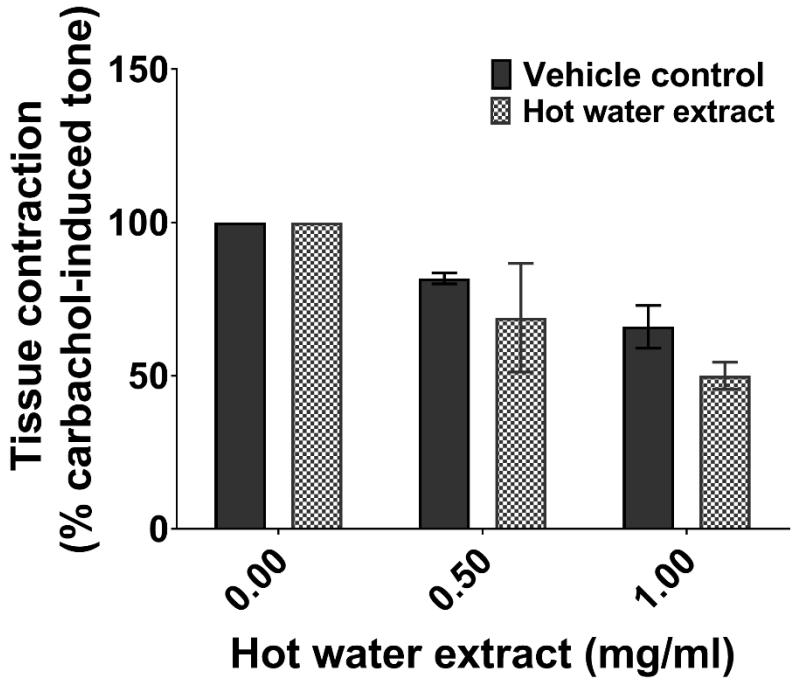

Appendix B: Hot water extract of *Lignosus rhinocerotis* was added in cumulative concentrations to rat tracheal rings pre-contracted with 1µM carbachol. Tissue response was expressed as a percentage of the carbachol-induced tone. Data were shown as mean ± SEM of 3 animals.

Appendix C. Representative trace recordings of cold water extract treatment on potassium chloride-induced tone and concentration-response curves to calcium chloride

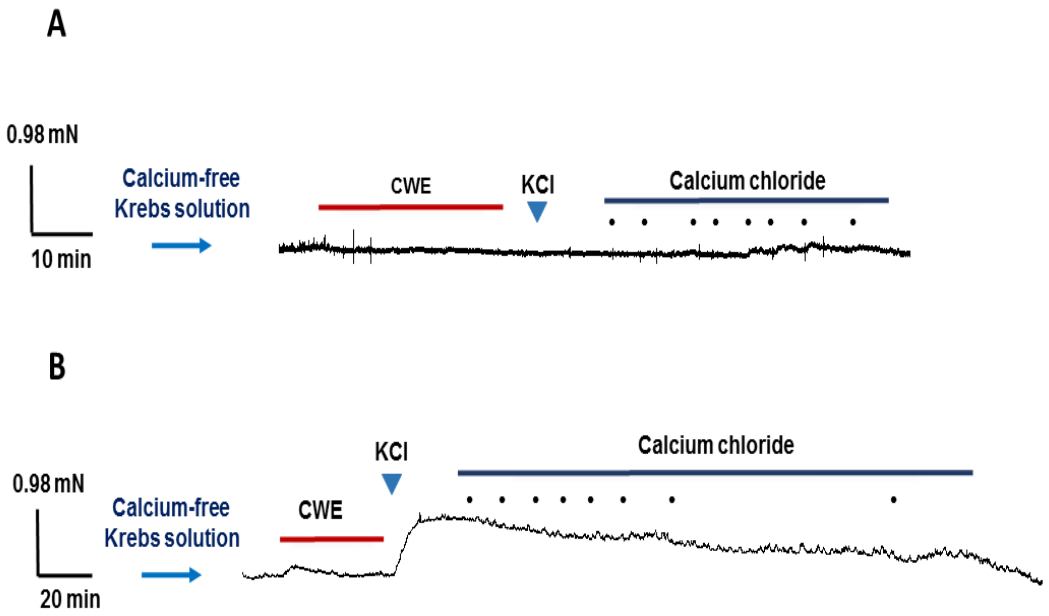

Appendix C: Representative trace recordings of the effect of cold water extract treatment against KCl-induced tone in the absence of external Ca^{2+}. After obtaining the reference KCl-induced tone, (A) rat tracheal and (B) porcine bronchiole rings were bathed in Ca^{2+}-free Krebs solution prior to incubation with CWE 3.5 mg/ml for at least 30 minutes (represented by red bar). Trace (A) shows that KCl (60 mM) added prior to cumulative concentration-response curves to calcium chloride did not induce any tone in rat trachea. Subsequent addition of calcium chloride induced slight contractions with increasing concentrations. In contrast, trace (B) shows that KCl (60 mM) has evoked contraction in CWE-treated bronchiole. The contraction decreased slowly over time and subsequent addition of calcium chloride did not induce further tone. Addition of each concentration of calcium chloride was represented by •. (Abbreviations: CWE = Cold water extract; KCl = Potassium chloride; mN = miliNewton; min = minutes)

Appendix D. Effect of cold water extract treatment on RBL-2H3 cell viability

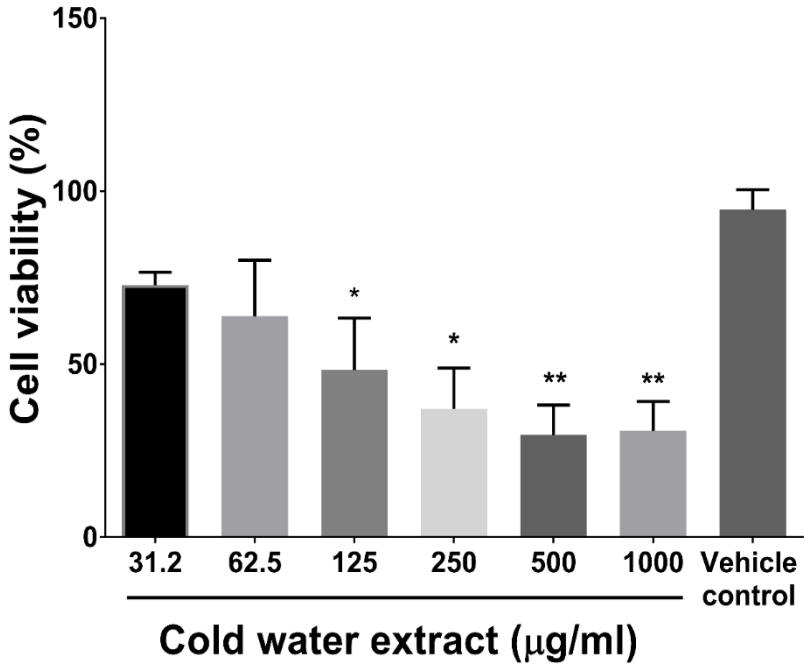

Appendix D: RBL-2H3 cells were treated with various concentrations of cold water extract or purified water (vehicle control) for 48 hr. Cell viability was examined by MTT assay as described in Section 7.2.3 (Chapter 7). The cell viability was expressed as a percentage relative to the untreated control. Data was shown as mean ± SEM of 3 to 4 independent experiments with 4 to 6 technical repeats in each run. (*$p < 0.05$, **$p < 0.01$; one-way ANOVA with Dunnett correction between treatment and vehicle control group)

Appendix E. Fractionation of cold water extract with Sephadex G-50 gel permeation chromatography

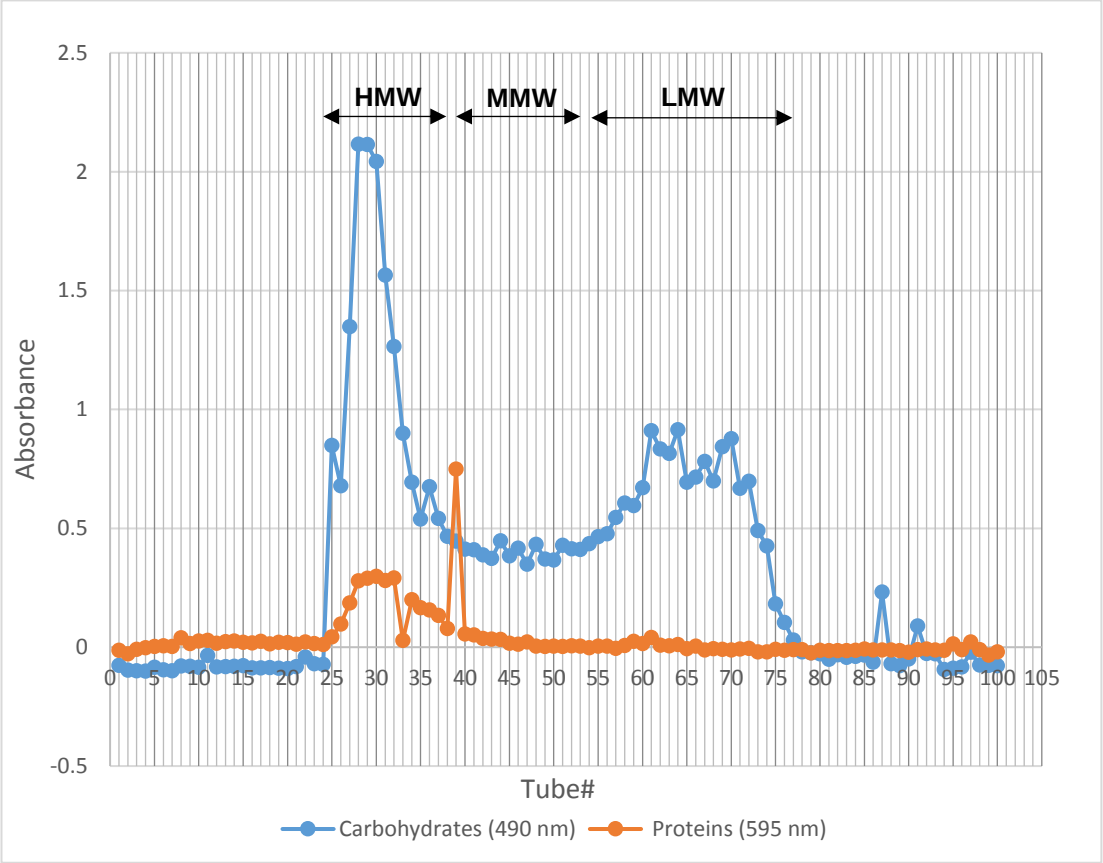

Appendix E: Fractionation of 100 tubes were collected with each tubes containing 2.5 mL of fraction. Proteins and carbohydrates content were measured as absorbance reading in 595 nm and 490 nm, respectively. The fractionation of the CWE was separated into three molecular weight range: HMW, MMW, and LMW fractions. Protein standard used for determining the molecular mass of pooled fraction were carbonic anhydrase (29 kDa), soybean trypsin inhibitor (20 kDa), ribonuclease A (14 kDa), cardiotoxin (7 kDa), cobalamin (1.35 kDa), and riboflavin (0.376 kDa) as indicated as x in the colour of blue, black, gold, orange, grey and green, respectively. Abbreviation: CWE = Cold water extract of *L. rhinocerotis*. (Abbreviations: CWE = Cold water extract; HMW = High-molecular-weight, MMW = Medium-molecular-weight; LMW = Low-molecular-weight)